



UNIVERSITÉ LIBRE DE BRUXELLES
École polytechnique de Bruxelles



Thèse

présentée en vue de l'obtention du grade de

DOCTEUR EN SCIENCES DE L'INGÉNIEUR

présentée et soutenue par

JOACHIM SCHÄFER

INFORMATION TRANSMISSION THROUGH
BOSONIC GAUSSIAN QUANTUM CHANNELS

ANNÉE ACADÉMIQUE 2012-2013

PROMOTEUR: NICOLAS J. CERF
CENTRE FOR QUANTUM INFORMATION AND COMMUNICATION

Joachim Schäfer
Université Libre de Bruxelles
École polytechnique de Bruxelles
50 av. F.D. Roosevelt - CP165/59
1050 Bruxelles
Belgique
Email: mail@joachimschaefer.de

Thèse de doctorat présentée en séance publique le 20 septembre 2013 à l'Université Libre de Bruxelles.

Jury: Jean-Marc Sparenberg, Président du jury, ULB
Nicolas J. Cerf, Promoteur, ULB
Jérémie Roland, ULB
Evgueni Karpov, ULB
Edouard Brainis, Universiteit Gent
Gerardo Adesso, University of Nottingham, Royaume-Uni
Vittorio Giovannetti, Scuola Normale Superiore di Pisa, Italie

Acknowledgements

First, and foremost I would like to thank Nicolas J. Cerf for giving me the opportunity to do a PhD in his research group. Thank you, Nicolas, for all your support and guidance during my PhD. I am very grateful to Evgueni Karpov, who was like a mentor to me. Thank you, Evgueni, for listening and replying with great patience to all my questions during our joint research.

My dear friend and colleague Ludovic Arnaud I thank for all our scientific and non-scientific discussions, which not necessarily were always fruitful, but every time entertaining. I would like to thank Raúl García-Patrón for his support and guidance, in particular during my research visit at the Max-Planck-Institute of Quantum Optics. I appreciated very much the rigorous mathematical approach of Oleg Pilyavets which was of great importance to solve our common problems. The entire research group QuIC receives my gratitude for their help during my stay in Brussels. In particular, I am thankful to Louis-Philippe Lamoureux who became a good friend of mine and introduced me to the martial art Taekwondo. I am also grateful to Arno Rauschenbeutel for supporting my decision to write my master's thesis at the ULB, as well as his support for my PhD studies. I thank the Belgian FRIA foundation for my research fellowship, which was essential for pursuing the PhD program and visiting conferences.

Last but not least I want to thank all my friends and my family. Without your constant support this would not have been possible.

To my mother Marion, my father Eugen, and my brothers Jan and Marc.

Abstract

In this thesis we study the information transmission through Gaussian quantum channels. Gaussian quantum channels model physical communication links, such as free space communication or optical fibers and therefore, may be considered as the most relevant quantum channels. One of the central characteristics of any communication channel is its capacity. In this work we are interested in the classical capacity, which is the maximal number of bits that can be reliably transmitted per channel use. An important lower bound on the classical capacity is given by the Gaussian capacity, which is the maximal transmission rate with the restriction that only Gaussian encodings are allowed: input messages are encoded in so-called Gaussian states for which the mean field amplitudes are Gaussian distributed.

We focus in this work mainly on the Gaussian capacity for the following reasons. First, Gaussian encodings are easily accessible experimentally. Second, the difficulty of studying the classical capacity, which arises due to an optimization problem in an infinite dimensional Hilbert space, is greatly reduced when considering only Gaussian input encodings. Third, the Gaussian capacity is conjectured to coincide with the classical capacity, even though this longstanding conjecture is unsolved until today.

We start with the investigation of the capacities of the single-mode Gaussian channel. We show that the most general case can be reduced to a simple, fiducial Gaussian channel which depends only on three parameters: its transmissivity (or gain), the added noise variance and the squeezing of the noise. Above a certain input energy threshold, the optimal input variances are given by a *quantum water-filling* solution, which implies that the optimal modulated output state is a thermal state. This is a quantum extension (or generalization) of the well-known classical water-filling solution for parallel Gaussian channels. Below the energy threshold the solution is given by a transcendental equation and only the less noisy quadrature is modulated. We characterize in detail the dependence of the Gaussian capacity on its channel parameters. In particular, we show that the Gaussian capacity is a non-monotonous function of the noise squeezing and analytically specify the regions where it exhibits one maximum, a maximum and a minimum, a saddle point or no extrema.

Then, we investigate the case of n -mode channels with noise correlations (i.e. memory), where we focus in particular on the classical additive noise channel. We consider memory models for which the noise correlations can be unraveled by a passive symplectic transformation. Therefore, we can simplify the problem to the study of the Gaussian capacity in an uncorrelated basis, which corresponds to the Gaussian capacity of n single-mode channels with a common input energy constraint. Above an input energy threshold the solutions is given by a *global quantum water-filling* solution, which implies that all modulated single-mode output states are thermal states with the same temper-

ature. Below the threshold the channels are divided into three sets: i) those that are excluded from information transmission, ii) those for which only the less noisy quadrature is modulated, and iii) those for which the quantum water-filling solution is satisfied. As an example we consider a Gauss-Markov correlated noise, which in the uncorrelated basis corresponds to a collection of single-mode classical additive noise channels. When rotating the collection of optimal single-mode input states back to the original, correlated basis the optimal multi-mode input state becomes a highly entangled state. We then compare the performance of the optimal input state with a simple coherent state encoding and conclude that one gains up to 10% by using the optimal encoding.

Since the preparation of the optimal input state may be very challenging we consider sub-optimal Gaussian-matrix product states (GMPS) as input states as well. GMPS have a known experimental setup and, though being heavily entangled, can be generated sequentially. We demonstrate that for the Markovian correlated noise as well as for a non-Markovian noise model in a wide range of channel parameters, a nearest-neighbor correlated GMPS achieves more than 99.9% of the Gaussian capacity. At last, we introduce a new noise model for which the GMPS is the exact optimal input state. Since GMPS are known to be ground states of quadratic Hamiltonians this suggests a starting point to develop links between optimization problems of quantum communication and many body physics.

Contents

Acknowledgements	I
Abstract	VI
List of Figures	XI
List of Tables	XIII
1. Motivation: Why Quantum Channels?	1
1.1. Preview of the thesis and our contributions	2
1.2. List of Publications	5
I. Mathematical Background	7
2. Shannon Information Theory	9
2.1. Shannon entropy	9
2.2. Channel capacity	11
2.3. Classical Gaussian channel	13
2.3.1. Single variate channel	13
2.3.2. Parallel uncorrelated channels	14
2.3.3. Parallel correlated channels	15
2.3.4. Markovian correlated channels	16
2.4. Limitations of Shannon Information Theory	21
3. Quantum Information Theory	23
3.1. Von Neumann entropy	24
3.2. Quantum channels	25
3.2.1. Memoryless channels	28
3.2.2. Memory channels	28
3.3. Holevo bound	29
3.4. Classical capacity	30
3.5. Quantum capacity	33
4. Quantum Optics	35
4.1. Quantization of the electromagnetic field	35
4.2. Quadrature operators	36

4.3. Quantum states of the electromagnetic field	38
4.3.1. Fock states	38
4.3.2. Coherent states and displacement operator	39
4.3.3. Squeezed states	40
4.4. Optical transformations	41
4.4.1. Phase shift	41
4.4.2. Beamsplitter	42
4.4.3. Displacement	43
4.4.4. One-mode squeezing	43
4.5. Phase-space Representation	44
5. Gaussian states and operations	47
5.1. Gaussian states	47
5.2. Gaussian operations	51
5.2.1. Gaussian unitary operations	51
5.2.2. General symplectic transformation	53
5.2.3. Partial trace	56
5.3. Gaussian channels	62
5.3.1. One-mode Gaussian channels	64
5.3.2. Multi-mode Gaussian channels	68
5.4. Generation of Gaussian matrix product states	69
5.5. Encoding and decoding in phase space	70
5.6. Classical capacity of Gaussian channels	73
5.6.1. Minimum output entropy conjecture	75
5.7. Gaussian classical capacity	76
II. Capacities of bosonic Gaussian channels	81
6. One-mode Gaussian channel	83
6.1. General thermal channel	83
6.2. Fiducial channel	86
6.3. Equivalence relations for capacities	93
6.4. Gaussian capacity	94
6.4.1. Quantum water-filling solution	97
6.4.2. Additivity of the Gaussian capacity	102
6.4.3. Solution in the full input energy domain	106
6.4.4. Limiting cases	112
6.4.5. Frequency parametrization	119
6.4.6. Dependency on channel parameters	122
6.4.7. Non-thermal canonical channels	132
6.5. Bounds on the classical capacity	139

7. Multi-mode Gaussian channels	145
7.1. Multi-mode Gaussian memory channel	145
7.2. Global quantum water-filling solution	146
7.3. Full solution for the classical additive noise channel ($\tau = 1$)	150
7.4. Classical additive channel with Gauss-Markov correlated noise	159
7.4.1. Two modes	160
7.4.2. Infinite number of modes	163
7.4.3. Optimal quantum input state	164
7.4.4. Full correlations	170
7.4.5. Classical limit	171
7.4.6. Symmetric correlations	173
7.4.7. How useful are the optimal input states?	173
8. Gaussian matrix-product states for coding	177
8.1. Optical scheme for nearest-neighbor GMPS	177
8.2. Transmission rates using GMPS	181
8.3. Optimal input state and ground state of quadratic Hamiltonian	187
9. Conclusions & Outlook	189
9.1. Single-mode Gaussian channel	189
9.2. Multi-mode Gaussian memory channels	191
9.3. Gaussian matrix-product states as input states	192
A. Toeplitz matrices	193
B. Entropy of Gaussian states	197
C. Gaussian Operations and Choi-Jamiolkowski Isomorphism	199
D. Calculations with Lagrange multiplier method	201
D.1. Solution below input energy threshold	201
D.2. Solution for frequency parametrization	202
D.3. Proofs for the one-mode fiducial channel with $\tau = 1$	205
D.3.1. Bounds below the threshold	205
D.3.2. Monotonicity of μ	206
D.3.3. Concavity of the Holevo χ^G -quantity in λ	210
D.3.4. Optimal noise distribution for one-mode	211
Bibliography	213
Index	226

List of Figures

2.1. Relationships of entropies (Venn diagram)	10
2.2. Classical communication system	12
2.3. Binary symmetric channel	13
2.4. Classical water-filling solution	15
2.5. Classical Gaussian memory channel with Markov correlated noise	17
2.6. Water-filling solution for Markov correlated noise	19
3.1. Quantum communication system	25
3.2. Quantum channel: Stinespring dilation	27
3.3. Quantum memory channels	29
4.1. Optical transformations: beamsplitter, displacement, “photon splitting”	42
5.1. Wigner functions of Gaussian states	48
5.2. Schematic plot of Wigner functions in phase space	49
5.3. Bloch-Messiah decomposition	54
5.4. Scheme of a two-mode squeezer given by the Bloch-Messiah decomposition	54
5.5. Schematic scheme of the continuous variable quantum non-demolition gate	55
5.6. Creation of a thermal state	56
5.7. Homodyne and heterodyne detection	58
5.8. Quantum teleportation	60
5.9. Physical schemes of thermal Gaussian channels	63
5.10. Physical schemes of non-thermal canonical channels	66
5.11. Gaussian quantum memory channels	68
5.12. Generation of a Gaussian matrix-product state	69
5.13. Encoding and action of a thermal channel in phase space	71
5.14. Two-state and four-state encoding in phase-space	72
5.15. Thermal Gaussian channel acting on a modulated Gaussian input state	79
6.1. Physical schemes of the thermal channel Φ^{TH}	84
6.2. Admissible regions in (τ, y) -plane for one-mode Gaussian quantum channels	86
6.3. Physical schemes of the fiducial channel Φ^{TH}	87
6.4. Equivalence relations of classical capacities of Gaussian channels	92
6.5. Quantum water-filling solution	100
6.6. Bloch-Messiah decomposition of Gaussian input state	102
6.7. Threshold function y_{thr} vs. τ for different values of s and fixed input energy	106
6.8. Solution for input energies below energy threshold, $\bar{N} < \bar{N}_{\text{thr}}$	109

LIST OF FIGURES

6.9. Optimal eigenvalues vs. input energy \bar{N} for $\tau = 1$	110
6.10. C_χ^G (one-mode) vs. τ	113
6.11. C_χ^G (one-mode) vs. τ (Limiting behavior)	117
6.12. C_χ^G (one-mode) vs. channel parameters	118
6.13. “Frequencies” and C_χ^G (one-mode) vs. environment “frequency” ω_{env}	123
6.14. C_χ^G (one-mode) vs. environment “frequency” ω_{env} for different domains of τ	124
6.15. Extremality properties of C_χ^G (one-mode) with respect to environment “frequency” ω_{env}	127
6.16. Parameter \tilde{y} vs. input energy \bar{N} and τ	128
6.17. Value of squeezing for which C_χ^G is extremal	130
6.18. C_χ^G vs. ζ (channel Φ^{SQ})	135
6.19. C_χ^G vs. $\tilde{\zeta}$ (channel Φ^{CS})	139
6.20. Dominant upper bounds (to the classical capacity) and C_χ^G (one-mode)	142
7.1. Global quantum water-filling solution	146
7.2. Solution (with $\tau = 1$) for input energies $\bar{N} < \bar{N}_{\text{glthr}}$ and five noisy channels	155
7.3. Solution for input energies below global energy threshold: “thermal equilibrium”	158
7.4. C_χ^G (two-modes) of Markov correlated noise vs. correlation parameter ϕ	161
7.5. Optimal input/modulation spectra (infinite number of uses) of Markov correlated noise	165
7.6. Functions $\mu_0(x)$ and $\mu_{\text{thr}}(x)$ vs. spectral parameter	166
7.7. Functions $\mu_{\text{thr}}(x)$, $\mu_0(x)$ and values of μ for different input energies	167
7.8. Optimal input and modulation spectra vs. spectral parameter	168
7.9. C^G (infinite number of uses) vs. correlation parameter ϕ and vs. noise variance N of Markov correlated noise	169
7.10. C^G (infinite number of uses) vs. noise variance N for fixed SNR for Markov correlated noise	172
7.11. Gain vs. input energy for two-modes and infinite number of modes	173
7.12. Contour plot of the maximal gain vs. correlation parameter ϕ and SNR	175
8.1. Optical scheme of Gaussian matrix-product state	178
8.2. Sequential generation of a 1D-Gaussian matrix-product state	179
8.3. Full optical scheme of 1D-Gaussian matrix-product state	179
8.4. GMPS rate vs. channel parameters for Markov and non-Markovian correlated noise	185
8.5. Optimal input correlation and input squeezing (GMPS) vs. correlation parameter for Markov and non-Markovian correlated noise	186

List of Tables

6.1. Canonical channels Φ^C and new representation in terms of thermal channel Φ^{TH} and non-thermal channels Φ^{CS} and Φ^{SQ}	85
6.2. Extremality properties of C_χ^G (one-mode) with respect to environment “frequency” ω_{env}	131
9.1. Summary of results and open questions for one-mode Gaussian channels .	190

1. Motivation: Why Quantum Channels?

Today's society is in permanent communication: we exchange messages via the phone, the internet, the radio and in many other ways. Conventionally, messages are encoded in sequences of bits. Each message is sent through a *channel*, which physically may correspond to a telephone line, an optical fibre or simply the air. Usually, the signals which carry the information correspond to voltages or strong light pulses and the physical channel is modeled by a *classical channel*. If however, a few photons or atoms are used as information carriers then laws of quantum mechanics dictate the behavior of the signals, and the underlying channel is modeled by a *quantum channel*. The central question of any communication scenario is: what is the maximal amount of bits that can be transmitted reliably per use of the channel? For classical channels Claude Shannon formulated in 1948 in his "Mathematical Theory of Communication" [Sha48] the answer to this question: the *classical capacity*. Though the classical capacity of classical channels was well defined, for classical Gaussian channels, which model telephone cables or satellite links, the definition lead to a contradicting result: despite a finite power at the input, in the limit of a small noise energy the capacity diverges. Since however, in this limit quantum effects dominate the noise cannot become arbitrarily small, and one has to consider a quantum channel instead. The classical capacity of quantum channels was formalized in [HJS⁺96, SW97, Hol98c] and corresponds to a maximization over all possible input encodings of the Holevo- χ -quantity, defined by Alexander Holevo in 1973 [Hol73]. The χ -quantity takes the quantum nature of the input signals and the noise into account, and therefore, is finite for small noise energy. However, the calculation of the classical capacity of quantum channels remains up to today a very challenging task and despite great efforts was only obtained for a few cases (see detailed discussion in Sec. 3.4).

Notwithstanding the fact that any channel is ultimately a quantum channel, one may wonder what is the advantage of a quantum channel over a classical channel? The answers in short are *privacy* and *security*. In order to explain this in detail we first lay out concepts to exploit quantum mechanics for security purposes. In 1970 Stephen Wiesner introduced his idea of *quantum money* (though published 13 years later [Wie83]), which, together with Holevo's definition of the χ -quantity, may be considered as the beginning of *Quantum Information Theory*. Essentially, by encoding the serial number of a banknote in non-orthogonal quantum states one is assured by the *no-cloning theorem* that there is no possibility to duplicate the banknote without introducing errors. The same idea was used in 1984 by Bennett and Brassard in their *BB84-protocol*: a secret key is encoded in a sequence of non-orthogonal quantum states [BB84] and sent through a quantum channel. Any eavesdropper will introduce errors when he or she wiretaps the signal and therefore, can be detected by the communicating parties. This may be the essential difference

1. Motivation: Why Quantum Channels?

between a classical channel and a quantum channel. Once a key is securely transmitted through the quantum channel it can be used with the encryption method *one-time pad*: the key is added to the encoded message, which is as long as the key. If for each message a new key is generated then this method is provably secure. Classical channels in contrary to quantum channels are vulnerable to wiretapping and for this reason a lot of the exchanged information is encrypted with algorithms such as RSA, developed 1977 by Ronald L. Rivest, Adi Shamir and Leonard Adleman [RSA78]. Such algorithms rely on the fact that up to today there is no efficient method to factor large numbers, as the underlying key is given by a product of large prime factors. However, there is up to now no proof for the non-existence of an efficient algorithm¹ for factoring numbers. Furthermore, a *quantum computer*, i.e. a machine which operates on quantum states and executes *quantum algorithms*, may pose a threat to encryption methods such as RSA. An example is Shor’s factorizing quantum algorithm which terminates in polynomial time [Sho94]. Current technology which is known to the public cannot realize a quantum computer that can run Shor’s algorithm at a scale large enough to threaten conventional encryption methods. A private company, however, may develop a quantum computer of sufficient scale. An example is the company D-Wave which recently released the 128-qubit quantum computer “D-Wave One”². The quantum computer of D-Wave however, cannot realize general quantum operations and as a consequence, cannot execute Shor’s algorithm.

Protocols such as the BB84 protocol are called *quantum key distribution* protocols and are one important application of a quantum channel. Generally speaking, a quantum channel describes any operation on a *quantum system* which outputs a quantum state. Therefore, quantum channels can model the actual transmission of photons or, for example, the manipulation of the state of a trapped ion.

1.1. Preview of the thesis and our contributions

In this thesis we focus on *bosonic Gaussian quantum channels* which model most optical quantum channels, such as optical fibers or free space communication [CD94, EW05, WPGP⁺12]. Their action is completely defined by transformations of the mean field amplitude and the covariances of the field’s quadratures. Furthermore, the underlying noise is fully characterized by a Gaussian distribution which is why their mathematical description is fairly simple. They map however, arbitrary input states to output states that live in an infinite dimensional Hilbert space. Since one has to maximize over all possible encodings that furthermore have to satisfy a physical input energy constraint, the calculation of the classical capacity becomes a challenging optimization problem.

Until today, strictly speaking, only the classical capacity of one particular Gaussian channel was obtained: the lossy channel with vacuum noise³ [GGL⁺04a]. This channel

¹Efficient means here that the algorithm terminates in polynomial time.

²Though there is a debate whether the “D-Wave One” really executes quantum algorithms, see e.g. [BAS⁺12, BRI⁺13, SS13].

³This result was extended to a multi-mode channel with particular noise correlations [LGM10].

corresponds to a beamsplitter which reduces the amplitude of the input signal and mixes the latter with vacuum. This model, however, cannot be considered as a model for the transmission through an optical fiber, because an optical fibre generally adds thermal noise.

For the lossy channel with vacuum noise it was shown that coherent states with Gaussian distributed mean field amplitudes provide the encoding that achieves the capacity [GGL⁺04a]. Coherent states describe very well the state of the electromagnetic field that is emitted by a laser and therefore, are very easy to generate experimentally. They are in the class of *Gaussian states*, i.e. quantum states whose field quadratures are Gaussian distributed in phase-space [EW05, Bra05b, WPGP⁺12]. Since these states can be easily generated and are furthermore very conveniently described by Gaussian distributions one may focus on the classical capacity restricted to Gaussian input encodings. This quantity is called the *Gaussian classical capacity*, or simply Gaussian capacity, and is of central interest in this work.

We begin the thesis with Part I which provides all definitions that are needed for the analysis of capacities of bosonic Gaussian channels. We first give an introduction to Shannon Information Theory and Quantum Information Theory, outlining the basis of information transmission through classical and quantum channels. Then we present a brief introduction to Quantum Optics and discuss all optical elements that are needed for this thesis. Afterwards, we introduce the encoding of information in phase-space, in particular in Gaussian states. Finally, we define the action of Gaussian channels, the definition of the classical capacity and Gaussian capacity.

Our results are presented in Part II.

We begin with the single-mode channel and study its Gaussian capacity in full generality in Chapter 6. Our starting point is the known classification of all single-mode Gaussian channels in terms of a set of seven *canonical* channels defined in [Hol07]. It was shown that any single-mode Gaussian channel is equivalent to a canonical one up to unitaries preceding and following the channel, which is also called *canonical decomposition*. Five of the seven canonical channels are *thermal channels*: they map thermal states to thermal states, such as the thermal lossy channel which models the transmission through an optical fiber. The canonical decomposition is not very useful for calculating capacities, since despite the preceding unitary does not change the Holevo χ -quantity, in general it changes the energy of the input state. Therefore, the problem of calculating the capacities cannot be reduced to calculating the capacity of the canonical channels. This is the starting point and motivation for the introduction of a newly defined *fiducial channel* and corresponding *fiducial decomposition* that overcomes this problem. We study in detail the properties of the fiducial channel and in particular its dependency on the noise squeezing. At last, we investigate how far the classical capacity of an arbitrary single-mode Gaussian channel is from its Gaussian capacity. The results of Chapter 6 have been partly published in Refs. (D), (E), (H) and (G)

In Chapter 7 we treat multi-mode Gaussian memory channels. The reason to consider memory channels is simply that “real-world communication channels often have memory” [AF97]. We focus on channels for which the noise correlations can be un-

1. Motivation: Why Quantum Channels?

raveled by a passive symplectic transformation. Effectively, this rotates the correlated noise into a basis where it becomes uncorrelated. In this uncorrelated basis one only has to consider a collection of single-mode channels, where in general each of the channels has different parameters, in particular different noise squeezing. As we shall see, the problem of finding the Gaussian capacity of such a collection of channels is related to the calculation of the capacity of multivariate classical Gaussian channels. The solution to the capacity of correlated classical Gaussian channels is given by rotating the noise covariance matrix into the basis where it is diagonal and by applying the *water-filling solution*. This solution realizes an equal distribution of output powers, i.e. the variance of each Gaussian distributed output random variable is equal. If the input power is high enough one realizes a *global water-filling solution*. Otherwise the channels which are too noisy are excluded from information transmission and one obtains a *local water-filling solution*. For bosonic Gaussian quantum channels, we will see that in the basis where the noise is uncorrelated, an equal distribution of energy at the output is optimal, as well. The solution however, has one significant difference: one has to take into account the input energy spent on the squeezing of the states. As a consequence we will obtain a *quantum water-filling solution* which becomes a *global quantum water-filling solution* if the input energy is above a certain threshold. Below this input energy the solution becomes more complicated and will lead to a division of channels into different sets, where some of the channels will be excluded from information transmission.

We apply our solution to the concrete example of a Gauss-Markov noise, which may be regarded as a good approximation of any naturally arising memory. For two uses of a such a channel it is known that entanglement at the input helps to increase the transmission rate [CCMR05, CCRM06]. We investigate in detail the optimal input encoding and the Gaussian capacity in the limit of an infinite number of uses. In particular, we compare the performance of the optimal input encoding with a non-entangled coherent state encoding. The reason to consider a simpler encoding is that the optimal input state is generally expected to be entangled (as in the two mode case), and therefore may be very difficult to generate experimentally. Several results of Chapter 7 have been published in Refs. (A) and (B).

Chapter 8 is devoted to the study of sub-optimal *Gaussian matrix-product states* as input states, where in particular we focus on nearest-neighbor correlated GMPS. Such states have the great advantage that though being heavily entangled, they can be generated sequentially. We compare the resulting transmission rates with the Gaussian capacity and with the transmission rate when using coherent states as input states. In addition, we study the similarities between the optimization problem of the Holevo quantity and the energy minimization in many body physics. The starting point here is the fact that GMPS are known to be ground states of quadratic Hamiltonians [SWC08]. Most of the results of this Chapter were published in Ref. (C).

Finally, we summarize our results and give a list of open questions in Chapter 9.

1.2. List of Publications

Peer-reviewed scientific journals

- (A) *Capacity of a bosonic memory channel with Gauss-Markov noise*, Joachim Schäfer, David Daems, Evgueni Karpov and Nicolas J. Cerf, Phys. Rev. A **80**, 062313 (2009), [doi:10.1103/PhysRevA.80.062313](https://doi.org/10.1103/PhysRevA.80.062313), [arXiv:0907.0982](https://arxiv.org/abs/0907.0982)
- (B) *Gaussian capacity of the quantum bosonic memory channel with additive correlated Gaussian noise*, Joachim Schäfer, Evgueni Karpov and Nicolas J. Cerf, Phys. Rev. A **84**, 032318 (2011), [doi:10.1103/PhysRevA.84.032318](https://doi.org/10.1103/PhysRevA.84.032318), [arXiv:1011.4118](https://arxiv.org/abs/1011.4118)
- (C) *Gaussian matrix-product states for coding in bosonic communication channels*, Joachim Schäfer, Evgueni Karpov and Nicolas J. Cerf, Phys. Rev. A **85**, 012322 (2012), [doi:10.1103/PhysRevA.85.012322](https://doi.org/10.1103/PhysRevA.85.012322), [arXiv:1201.0200](https://arxiv.org/abs/1201.0200)
- (D) *Equivalence Relations for the Classical Capacity of Single-Mode Gaussian Quantum channels*, Joachim Schäfer, Evgueni Karpov, Raúl García-Patrón, Oleg V. Pilyavets and Nicolas J. Cerf, Phys. Rev. Lett. **111**, 030503 (2013), [doi:10.1103/PhysRevLett.111.030503](https://doi.org/10.1103/PhysRevLett.111.030503), [arXiv:1303.4939](https://arxiv.org/abs/1303.4939)

Non-peer-reviewed conference proceedings

- (E) *Quantum water-filling solution for the capacity of Gaussian information channels*, Joachim Schäfer, Evgueni Karpov and Nicolas J. Cerf, Proceedings of SPIE, **7727**, 77270J (2010), [doi:10.1117/12.854641](https://doi.org/10.1117/12.854641)
- (F) *Information transmission in bosonic memory channels using Gaussian matrix-product states as near-optimal symbols*, Joachim Schäfer, Evgueni Karpov and Nicolas J. Cerf, 11th International Conference on Quantum Communication, Measurement and Computing (2012, in press)
- (G) *Gaussian classical capacity of Gaussian quantum channels*, Joachim Schäfer, Evgueni Karpov, Raúl García-Patrón, Oleg V. Pilyavets and Nicolas J. Cerf, Nanosystems: Physics, Chemistry, Mathematics **4**, 496 (2013)

In preparation

- (H) *Gaussian capacity of the single-mode Gaussian quantum channel*, Joachim Schäfer, Evgueni Karpov, Oleg V. Pilyavets and Nicolas J. Cerf, to be submitted to Phys. Rev. A

Part I.

Mathematical Background

2. Shannon Information Theory

We begin with a brief review of *Shannon Information Theory* (also called “Classical Information Theory”) which was developed by Claude E. Shannon in 1948 [Sha48]. The central quantity of information theory is the *entropy*. This physical quantity, which in thermodynamics is often regarded as the “disorder” of a system can as well be associated with the amount of information generated by a random source. We shall see in this chapter that the entropy is a central part of the definitions which we need throughout this thesis.

The definitions and formulas presented from section 2.1 up to subsection 2.3.3 are taken from [CT05].

2.1. Shannon entropy

Let X be a random variable that takes discrete values $x \in \mathcal{X}$ and is drawn according to a probability distribution $p(x)$. The *Shannon entropy* $H(X)$ is defined as

$$H(X) = H(p) = - \sum_{x \in \mathcal{X}} p(x) \log_2 p(x), \quad (2.1)$$

where the logarithm is taken to the base 2 (the entropy is measured in bits). We observe that the Shannon entropy is equivalent to the Gibbs entropy of a thermodynamic system (up to the missing Boltzmann constant), which is described by a mixture of micro states ρ_i associated to a probability p_i .

The entropy $H(X)$ has at the same time two equivalent meanings: it is the average amount of bits gained by measuring X and the amount of bits needed to obtain the outcome of X . For this reason the entropy is often referred to as the *uncertainty* of X . A random variable associated to an (unbiased) coin flip is a standard example to illustrate the concept of entropy. In this case the probabilities for $X = 0$ (“head”) and $X = 1$ (“tail”) are equal, i.e. $p(X = 0) = p(X = 1)$. Equation (2.1) yields $H(X) = 1$ bit of information that is gained by the flip, or needed to obtain its outcome.

The definition of the Shannon entropy stated in Eq. (2.1) can be generalized to two (and more) variables. Suppose that $\{X, Y\}$ are two random variables that take discrete values x and y and have the joint probability distribution $p(x, y)$. Then, their *joint entropy* is defined as

$$H(X, Y) = - \sum_{x \in \mathcal{X}} \sum_{y \in \mathcal{Y}} p(x, y) \log_2 p(x, y), \quad (2.2)$$

2. Shannon Information Theory

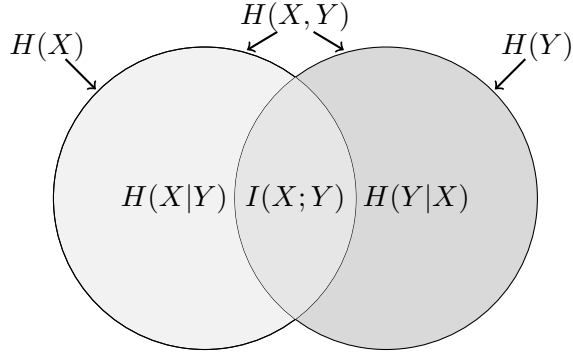


Figure 2.1.: Venn diagram: Relationships between (individual) entropies $H(X)$, $H(Y)$, joint entropy $H(X, Y)$, conditional entropy $H(X|Y)$ and the mutual information $I(X; Y)$.

which may be regarded as a joint measure of uncertainty. An important inequality is the subadditivity of the joint entropy, i.e.

$$H(X, Y) \leq H(X) + H(Y). \quad (2.3)$$

Clearly, the joint uncertainty can only be lower than the uncertainties of the individual systems, because X and Y may be correlated. This brings us to the definition of the *conditional entropy*, which may be regarded as the uncertainty of a random variable Y given the outcome of X . It is defined as

$$\begin{aligned} H(Y|X) &= \sum_{x \in \mathcal{X}} p(x) H(Y|X = x) \\ &= - \sum_{x \in \mathcal{X}} p(x) \sum_{y \in \mathcal{Y}} p(y|x) \log_2 p(y|x) \\ &= H(X, Y) - H(X), \end{aligned} \quad (2.4)$$

with $p(y|x) = p(x, y)/p(x)$. As seen from the last line in Eq. (2.4) $H(Y|X)$ can be calculated by the total uncertainty of X and Y reduced by the number of bits gained by measuring X . With the above definitions we can define the *mutual information* $I(X; Y)$ between X and Y , i.e.

$$\begin{aligned} I(X; Y) &= H(X) + H(Y) - H(X, Y) \\ &= H(X) - H(X|Y). \end{aligned} \quad (2.5)$$

We observe that the mutual information is the uncertainty of X that remains after knowing Y . The relations between the different entropies are depicted in a Venn diagram in Fig. 2.1.

The above definitions can be straightforwardly extended to the case when the alphabet of X and Y are continuous and the distribution functions $p(x)$ and $p(y)$ become

probability densities. The entropy and conditional entropy then read

$$\begin{aligned} H(X) &= - \int_{\mathbb{R}} dx p(x) \log_2 p(x), \\ H(X|Y) &= - \int_{\mathbb{R}} dx dy p(x, y) \log_2 p(x|y). \end{aligned} \tag{2.6}$$

The other definitions are extended equivalently, where essentially in all definitions sums have to be replaced by integrals (see [CT05] for details).

2.2. Channel capacity

Consider two parties, commonly referred to as Alice (the sender) and Bob (the receiver), that would like to communicate to each other. Alice encodes her message and sends it through a noisy *channel* to Bob, who tries to decode the message, i.e. to reconstruct the original message. An immediate question that is risen: what is the maximal amount of information (i.e. bits) Alice can transmit reliably to Bob per channel use. In other words: what is the *capacity* of the channel? Before we can define the capacity, we first need to define the action of the channel itself.

A *time-discrete channel* is a system composed of an input alphabet \mathcal{X} , an output alphabet \mathcal{Y} and a probability transition matrix $\mathbf{P}(y|x) \geq 0$ which is the probability that Bob successfully receives y when x was sent, with $\sum_y \mathbf{P}(y|x) = 1, \forall x \in \mathcal{X}$. We consider in the following only time-discrete channels, i.e. all messages are sent in discrete time steps. A channel is *memoryless* if the output of the k -th use of the channel only depends on the k -th input; otherwise the channel is a *memory channel*. Suppose Alice now uses a channel n times, or equivalently transmits sequences $\mathbf{x} = (x_1, x_2, \dots, x_n)^\top$ of length n . The channel is then defined by

$$(\mathcal{X}^n, \mathbf{P}(\mathbf{y}|\mathbf{x}), \mathcal{Y}^n), \tag{2.7}$$

where $\mathbf{x} \in \mathcal{X}^n, \mathbf{y} \in \mathcal{Y}^n$. We define a (M, n) -code for the channel $(\mathcal{X}^n, \mathbf{P}(\mathbf{y}|\mathbf{x}), \mathcal{Y}^n)$ as a system containing:

- An index set $\mathcal{I} = \{1, 2, \dots, M\}$, where each index stands for a message W .
- An encoding function $E^n : \mathcal{I} \rightarrow \mathcal{X}^n$, which assigns to each message W an input string \mathbf{x} with length n .
- A decoding function $D^n : \mathcal{Y}^n \rightarrow \mathcal{I}$, which returns an estimated message $W' = D^n(\mathbf{y})$ from the received output \mathbf{y} ,
with a probability of error $\epsilon_i = P(W' \neq W) = P(D^n(\mathbf{y}) \neq W | \mathbf{x} = E^n(W))$.

The communication system including the encoder, the channel, and the decoder is sketched in figure 2.2. The important question which emerges from previous defini-

2. Shannon Information Theory



Figure 2.2.: Classical communication system.

tions is how many bits can Alice maximally transmit to Bob per channel use? In order to answer this question we first define the *rate* of an (M, n) code, i.e.

$$R = \frac{\log_2 M}{n} \text{ bits per transmission}^1. \quad (2.8)$$

A rate R is *achievable* if there exists a sequence of $(2^{nR}, n)$ codes such that the maximal probability of error $\max_{i \in \mathcal{I}} \epsilon_i \rightarrow 0$, as $n \rightarrow \infty$. The *Shannon capacity* (or “channel capacity”) of a memoryless channel is the supremum of all achievable rates. In terms of the mutual information between Alice and Bob, the capacity is defined as

$$C_{\text{Sh}} = \max_{p(x)} I(X; Y), \quad (2.9)$$

where $I(X; Y)$ is maximized over all possible input distributions $p(x)$ and C_{Sh} is quantified in bits. Finally, we state *the channel coding theorem*: All rates below the capacity C_{Sh} are achievable. Specifically, for every rate $R < C_{\text{Sh}}$, there exists a sequence of $(2^{nR}, n)$ codes with maximum probability of error $\max_i \epsilon_i \rightarrow 0$ as $n \rightarrow \infty$. Conversely, any sequence of $(2^{nR}, n)$ codes with $\max_i \epsilon_i \rightarrow 0$ must have $R \leq C_{\text{Sh}}$. The proof of the channel coding theorem can be found in [CT05]. In summary, the capacity is the maximum amount of bits Alice can send reliably to Bob.

Let us study an example in order to better understand the notion of the capacity. Consider the binary symmetric channel or “bit-flip” channel depicted in Fig. 2.3. Alice’s input bit is flipped with probability p and is transmitted without error to Bob with probability $1 - p$. This implies that Bob does not know with certainty which was Alice’s input bit. It follows immediately that $H(Y|X) = H(p)$, and therefore

$$I(X : Y) = H(Y) - H(p). \quad (2.10)$$

Since the parameter p is fixed by the channel one has to maximize the output entropy $H(Y)$ over all input distributions in order to achieve the capacity. $H(Y)$ is a concave function with respect to $p(y)$ and maximized for a uniform distribution for which $H(Y) = 1$ bit (this distribution was given in the case of the unbiased coin flip mentioned above). Choosing the input distribution to be uniform, i.e. $p(x) = \{\frac{1}{2}, \frac{1}{2}\}$ leads to a uniform distribution $p(y) = \{\frac{1-p}{2} + \frac{p}{2}, \frac{1-p}{2} + \frac{p}{2}\} = \{\frac{1}{2}, \frac{1}{2}\}$ and therefore achieves the capacity

$$C_{\text{Sh}} = 1 - H(p) \text{ bits}. \quad (2.11)$$

Note that in the following we mostly omit the unit “bits”.

¹In most definitions the unit “bits” will be omitted.

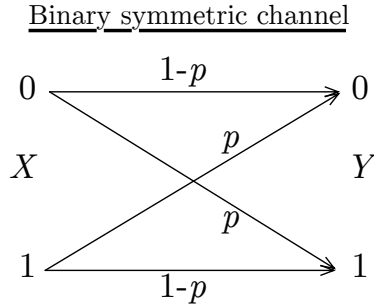


Figure 2.3.: Binary symmetric channel:

2.3. Classical Gaussian channel

We treat in the following the capacity of a *classical Gaussian channel*². Such channels are widely used to model conventional communication links, such as wireless telephone channels or satellite links. We discuss here only the most common classical Gaussian channel, i.e. the *additive channel*, and define first the general, multi-variate case.

Most generally, one is given a system of n parallel, *a priori* not independent Gaussian channels, that act as follows. The n output variables $\mathbf{Y} = \{Y_1, \dots, Y_n\}$ are given by the sum of n input variables $\mathbf{X} = \{X_1, \dots, X_n\}$ and n noise random variables $\mathbf{Z} = \{Z_1, \dots, Z_n\}$, drawn from a Gaussian distribution with a covariance matrix (CM) \mathbf{V}_Z , i.e.

$$\mathbf{Y} = \mathbf{X} + \mathbf{Z}, \quad \mathbf{Z} \sim \mathcal{N}(0, \mathbf{V}_Z). \quad (2.12)$$

Without any additional constraint at the input the capacity of this channel system is infinite, because Alice could separate her symbols at infinite distance ensuring that Bob receives them without error. Therefore, we need to impose a power constraint at the input of Alice. Namely, we restrict the sum of variances of the input symbols, i.e.

$$\frac{1}{n} \sum_{i=1}^n \text{Var}(X_i) \leq P, \quad (2.13)$$

where P corresponds to the average input power. We treat now several cases of covariances \mathbf{V}_Z and state briefly the corresponding solutions. For the definitions stated in subsections 2.3.1-2.3.3 more detailed derivations can be found in [CT05].

2.3.1. Single variate channel

The simplest scenario is the case of a single Gaussian channel, where the noise covariance matrix becomes simply a real variable N , i.e.

$$Y = X + Z, \quad Z \sim \mathcal{N}(0, N). \quad (2.14)$$

²We underline here the word “classical” because the main part of this work deals with quantum channels.

2. Shannon Information Theory

Since the input X and noise variable Z are independent we have

$$I(X; Y) = H(Y) - H(Z). \quad (2.15)$$

Because it is known that the entropy of a classical random variable with fixed variance is maximized by a Gaussian distribution (see [CT05]) it is optimal to choose a Gaussian distribution for the input variable X , i.e. the optimal input is $X \sim \mathcal{N}(0, P)$. Then the capacity is straightforwardly calculated and reads

$$C_{\text{Sh}} = \max_{\substack{p(x) \\ \text{Var}(X) \leq P}} I(X; Y) = \frac{1}{2} \log_2 \left(1 + \frac{P}{N} \right), \quad (2.16)$$

where $\frac{P}{N} \equiv \text{SNR}$ is called the *signal-to-noise* ratio.

2.3.2. Parallel uncorrelated channels

Let us now suppose that the n -parallel channels are independent. This means that $\mathbf{V}_Z = \text{diag}(N_1, N_2, \dots, N_n)$. Due to the subadditivity of the joint entropy [see Eq. (2.3)] and the fact that for the single variate case a Gaussian distribution for the input is optimal we straightforwardly obtain

$$\begin{aligned} I(\mathbf{X}; \mathbf{Y}) &= H(\mathbf{Y}) - \sum_i H(Z_i) \\ &\leq \sum_i (H(Y_i) - H(Z_i)) \\ &\leq \frac{1}{2} \sum_i \log_2 \left(1 + \frac{P_i}{N_i} \right), \end{aligned} \quad (2.17)$$

where $P_i = \text{Var}(X_i)$ is the variance of the individual Gaussian distributed random variable X_i . The problem that is left to solve is to determine the optimal power distribution $\{P_1, P_2, \dots, P_n\}$ with the constraint

$$\frac{1}{n} \sum_i P_i \leq P. \quad (2.18)$$

The method to find the solution of this problem is given by the Karush–Kuhn–Tucker conditions (KKT), which is an extension of the method of Lagrange multipliers (by adding inequality constraints). It follows that the input powers are given by the *water-filling* solution, i.e.

$$P_i = (w - N_i)^+, \quad \forall i, \quad (2.19)$$

where

$$(x)^+ = \begin{cases} x, & x \geq 0, \\ 0, & x < 0, \end{cases} \quad (2.20)$$

and w is the *water-filling* level satisfying $\frac{1}{n} \sum_i P_i = P$. We conclude that no energy is allocated to channels with noise variances that lay above the water-filling level. As a

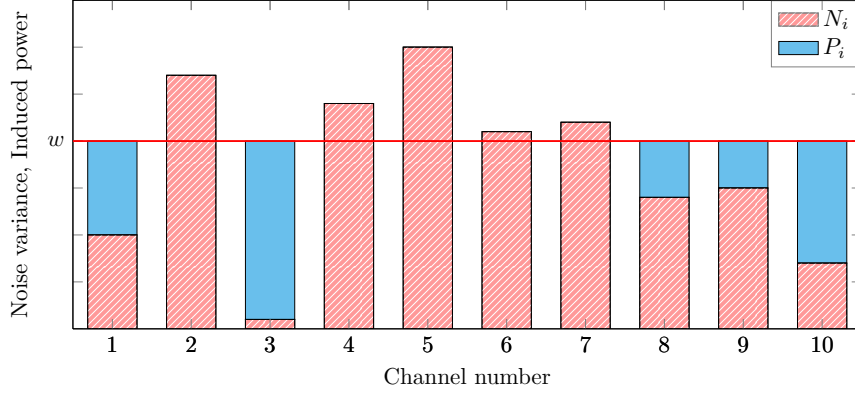


Figure 2.4.: Water-filling solution: Noise variance N_i , induced power P_i and water-filling level w vs. channel number i ; equation (2.19) is fulfilled for all i .

consequence they are excluded from information transmission. We depict the solution for an example in Fig. 2.4. With Eqs. (2.17) and (2.19) we determine the capacity for the system of parallel uncorrelated channels, that is

$$C = \frac{1}{2n} \sum_i \log_2 \left(1 + \frac{(w - N_i)^+}{N_i} \right), \quad (2.21)$$

where w satisfies Eq. (2.19) together with constraint (2.18).

2.3.3. Parallel correlated channels

In general, one has to consider a system of parallel correlated channels, i.e. the case when $\mathbf{V}_Z \neq \text{diag}(N_1, N_2, \dots, N_n)$. As mentioned before, in order to maximize the mutual information

$$I(\mathbf{X}; \mathbf{Y}) = H(\mathbf{Y}) - H(\mathbf{Z}), \quad (2.22)$$

the output \mathbf{Y} should be Gaussian distributed, which implies the input \mathbf{X} has to be Gaussian distributed with covariance matrix \mathbf{V}_X . Then, the action of the additive Gaussian channel expressed in terms of the covariance matrices reads

$$\mathbf{V}_Y = \mathbf{V}_X + \mathbf{V}_Z, \quad (2.23)$$

where \mathbf{V}_Y is the CM of the Gaussian distributed output \mathbf{Y} . For the output entropy we have

$$H(\mathbf{Y}) \propto \det(\mathbf{V}_X + \mathbf{V}_Z). \quad (2.24)$$

The determinant is invariant under rotation, and furthermore, for a matrix \mathbf{M} with entries M_{ij} the Hadamard inequality holds, i.e.

$$\det \mathbf{M} \leq \prod_i M_{ii}, \quad (2.25)$$

2. Shannon Information Theory

with equality if \mathbf{M} is diagonal. Then it is straightforward to show that \mathbf{V}_X and \mathbf{V}_Z have to be diagonal in the same basis in order to maximize Eq. (2.24) [which then maximizes (2.22)]. Then, the problem can be treated in the rotated basis where \mathbf{V}_Z is diagonal. For the given spectrum of \mathbf{V}_Z denoted $\lambda^{(Z)} = \{\lambda_1^{(Z)}, \dots, \lambda_n^{(Z)}\}$ the problem is simplified to a system of parallel uncorrelated channel. Hence, the solution is given by the water-filling solution over the spectrum of \mathbf{V}_Z . Once the optimal input covariance matrix is obtained it may contain correlations when rotated back to the original basis.

2.3.4. Markovian correlated channels

Let us study an example of correlated channels, namely, n -channels with noise correlations arising from a Gauss-Markov process. Markov processes are used e.g. to model processes in finance, climate research [SZ99], earthquakes or to approximate the random motion of particles suspended in a fluid (Brownian motion³). For Gaussian channels the underlying process is therefore a Gauss-Markov process, which we furthermore require to be stationary such that the channel is shift (or translationally) invariant⁴. A Gauss-Markov process of order \mathcal{P} (also called autoregressive (AR) process with white Gaussian noise) is defined as [SZ99]

$$Z_t = \sum_{k=1}^{\mathcal{P}} \phi_k Z_{t-k} + W_t, \quad t = 1, \dots, \infty, \quad (2.26)$$

where $\phi_1, \phi_2, \dots, \phi_{\mathcal{P}}$ are the correlation parameters and W_t are identically and independently Gaussian distributed random variables. We set the mean values of all random variables to zero, i.e. $E[Z_t] = E[W_t] = 0, \forall t$. This process is stationary (shift invariant) iff all roots of the characteristic polynomial

$$p(x) = 1 - \sum_{k=1}^{\mathcal{P}} \phi_k x^k \quad (2.27)$$

lie outside the unit circle $|x| = 1$. If the process is stationary, then the covariance matrix \mathbf{V}_{MK} of the stochastic process (2.26) is Toeplitz (see Appendix A). The latter implies that all variances of Z_t are equal, i.e.

$$\text{Var}(Z_1) = \text{Var}(Z_2) = \dots = \text{Var}(Z_n). \quad (2.28)$$

In the limit $n \rightarrow \infty$ the spectrum of \mathbf{V}_{MK} becomes [DC01, SZ99]

$$\lambda^{(\mathbf{V}_{\text{MK}})}(x) = \frac{\text{Var}(Z_t)}{|1 - \sum_{k=1}^{\mathcal{P}} \phi_k e^{ikx}|^2}. \quad (2.29)$$

The Gauss-Markov process of order \mathcal{P} satisfies a very strong property: Let $\{Z_t\}_{t=1}^{\infty}$ be

³We remark that Brownian motion in general is not a Markov process.

⁴This may be regarded more physical, as no channel use i is favored over another use k .

Additive Gaussian channel with Markov correlated noise

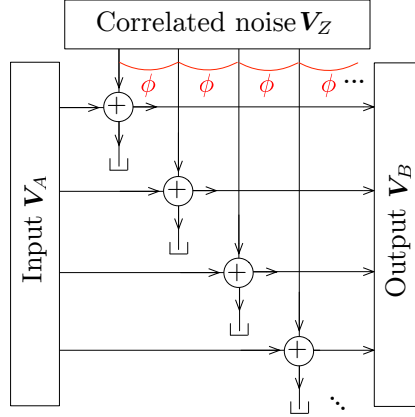


Figure 2.5.: Memory model for a classical Gaussian additive channel: The noise is given by a first-order Markov process, i.e. it exhibits a nearest-neighbor correlation with correlation parameter ϕ .

a stochastic process with zero mean $E[Z_t] = 0, \forall t$ and \mathcal{P} lag covariance constraints

$$E[Z_t, Z_{t+k}] = R_k, \quad k = 0, 1, \dots, \mathcal{P}. \quad (2.30)$$

Then the *entropy rate*

$$\lim_{n \rightarrow \infty} \frac{1}{n} H(X_1, X_2, \dots, X_n) \quad (2.31)$$

is maximized if the stochastic-process is given by a Gauss-Markov process of order \mathcal{P} satisfying the constraint stated in Eq. (2.30) [CC84]. This leads to the following conclusions for the additive noise channel $\mathbf{Y} = \mathbf{X} + \mathbf{Z}$: among all multi-variate noise processes \mathbf{Z} satisfying the correlation constraints given in Eq. (2.30) the Gauss-Markov process of order \mathcal{P} is the one that *is the worst* [DC01]. This means the Gauss-Markov process of order \mathcal{P} defines the noise that minimizes the capacity of the additive noise channel.

For simplicity, we focus now on the case $\mathcal{P} = 1$, i.e. the case of *nearest-neighbor correlations* modeled by the process

$$Z_t = \phi Z_{t-1} + W_t, \quad (2.32)$$

We fix $\text{Var}(Z_t) = N$ implying $\text{Var}(W_t) = (1 - \phi^2)N$. The covariance matrix then reads

$$\mathbf{V}_{\text{MK}} = N \begin{pmatrix} 1 & \phi & \phi^2 & \phi^3 & \dots & \dots & \phi^n \\ \phi & 1 & \phi & \phi^2 & \dots & \dots & \phi^{n-1} \\ \phi^2 & \phi & 1 & \phi & \dots & \dots & \phi^{n-2} \\ \phi^3 & \phi^2 & \phi & 1 & \dots & \dots & \phi^{n-3} \\ \vdots & \vdots & & \ddots & \ddots & & \vdots \\ \phi^{n-1} & \phi^{n-2} & \dots & & & 1 & \phi \\ \phi^n & \phi^{n-1} & \dots & \dots & \phi^2 & \phi & 1 \end{pmatrix}. \quad (2.33)$$

2. Shannon Information Theory

Then Eq. (2.29) simplifies to

$$\lambda^{(\mathbf{V}_{\text{MK}})}(x) = N \frac{1 - \phi^2}{1 + \phi^2 - 2\phi \cos(x)}, \quad N \geq 0, \phi \in [0, 1), x \in [0, 2\pi]. \quad (2.34)$$

Let us now study the capacity C_{Sh} of a system of n parallel channels, with noise CM \mathbf{V}_{MK} with eigenvalue spectrum $\lambda^{(\text{MK})}(x) \equiv \lambda^{(\mathbf{V}_{\text{MK}})}(x)$. Though the following results can be straightforwardly derived for the given spectrum $\lambda^{(\text{MK})}(x)$ we have not found any reference where they have been stated.

According to Eq. (2.23) the action of the channel may be written as

$$\mathbf{V}_Y = \mathbf{V}_X + \mathbf{V}_{\text{MK}}. \quad (2.35)$$

Since the process is stationary, the water-filling solution presented above translates to a water-filling solution in the spectral domain [CT05]. Therefore, in order to find the capacity we need to consider the noise spectrum in the limit $n \rightarrow \infty$ which is stated in Eq. (2.29). Again, the solution is given by the water-filling solution, which is now applied to a continuous spectrum, that is

$$\frac{1}{\pi} \int_0^\pi dx \left(w - \lambda^{(\text{MK})}(x) \right)^+ = P, \quad (2.36)$$

where one only needs to integrate from 0 to π due to the mirror symmetry of $\lambda^{(\text{MK})}(x)$ around $x = \pi$. Then, the capacity (2.21) becomes

$$C = \frac{1}{2\pi} \int_0^\pi dx \log_2 \left(1 + \frac{(w - \lambda^{(\text{MK})}(x))^+}{\lambda^{(\text{MK})}(x)} \right). \quad (2.37)$$

Since the function $\lambda^{(\text{MK})}(x)$ is monotonically decreasing in the interval $x \in [0, \pi]$, we can simplify the left hand side of (2.36), i.e.

$$\frac{1}{\pi} \int_0^\pi dx \left(w - \lambda^{(\text{MK})}(x) \right)^+ = \frac{1}{\pi} \int_\kappa^\pi dx \left(w - \lambda^{(\text{MK})}(x) \right) = \frac{1}{\pi} (\pi - \kappa) w - \frac{1}{\pi} \int_\kappa^\pi dx \lambda^{(\text{MK})}(x). \quad (2.38)$$

The primitive of $\lambda^{(\text{MK})}(x)$ reads

$$\int dx \lambda^{(\text{MK})}(x) = 2N \arctan \left(\frac{1 + \phi}{1 - \phi} \tan \left(\frac{x}{2} \right) \right) \equiv L^{(\text{MK})}(\phi, x), \quad (2.39)$$

where

$$\lim_{x \rightarrow \pi} L^{(\text{MK})}(\phi, x) = \pi N. \quad (2.40)$$

Then, Eq. (2.38) simplifies to

$$(\pi - \kappa) w + L^{(\text{MK})}(\phi, \kappa) = \pi (P + N). \quad (2.41)$$

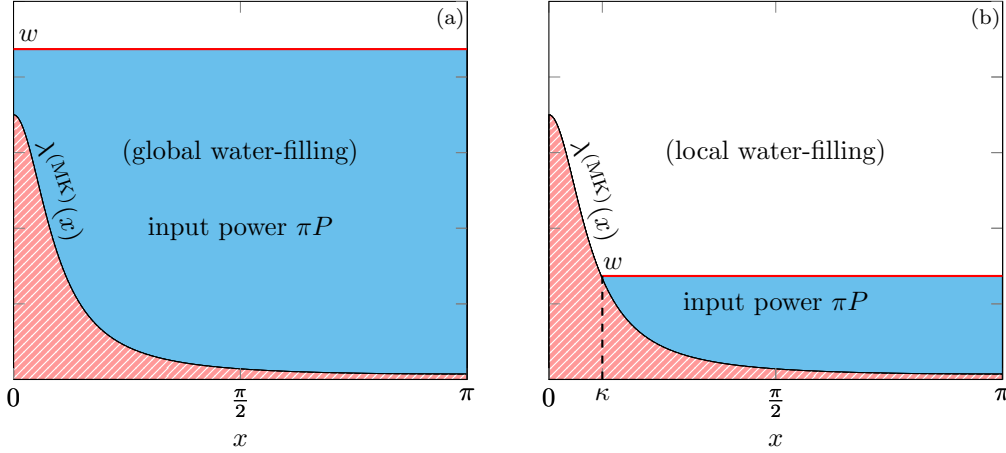


Figure 2.6.: Water-filling for Markovian correlated noise (stack plot): The solid line and the area underneath corresponds to $\lambda^{(\text{MK})}(x)$, the horizontal bar is the water-filling level w and the area underneath is the optimal input power distribution satisfying the water-filling solution. (a) Global water-filling: the power is sufficient to “fill” the whole spectrum. (b) Local water-filling: the power distribution “fills” only the spectrum in the domain $x \in [\kappa, \pi]$.

The solution of Eq. (2.41) leads to the position κ and the water-filling level w . Then the capacity (2.37) is given by

$$C_{\text{Sh}} = \frac{1}{2\pi} \int_{\kappa}^{\pi} dx \log_2 \left(\frac{w}{\lambda^{(\text{MK})}(x)} \right). \quad (2.42)$$

Let us briefly study the solution to Eq. (2.41). We know that if $\kappa = 0$ then the entire noise spectrum will be “filled”, i.e. $w - \lambda^{(\text{MK})}(x) \geq 0, \forall x$. In this case we speak of a *global water-filling* solution. Injecting $\kappa = 0$ in Eq. (2.41) yields the *power threshold*

$$P_{\text{thr}} = N \left(\frac{1 + \phi}{1 - \phi} - 1 \right). \quad (2.43)$$

This means a global water-filling solution is only achieved if $P \geq P_{\text{thr}}$. In this case Eq. (2.41) leads to the water-filling level $w = P + N$, i.e. the sum of average input variance and average noise variance. Then, using Eqs. (2.39) and (2.42) the solution to the capacity becomes

$$C_{\text{Sh}} = \frac{1}{2} \log_2 \left(\frac{1}{1 - \phi^2} \left(1 + \frac{P}{N} \right) \right), \quad P \geq P_{\text{thr}}. \quad (2.44)$$

We depict an example for this case in Fig. 2.6 (a). Equation (2.44) coincides with the single variate capacity (2.16) in the uncorrelated case ($\phi = 0$). The limit $\phi \rightarrow 1$ leads

2. Shannon Information Theory

to a divergence of C_{Sh} which is compensated by the divergence of the power threshold P_{thr} . Therefore, the solution stated in Eq. (2.44) is not achievable in this limit.

Now we discuss the solution when the global water-filling can no longer be satisfied, i.e. the solution for $P < P_{\text{thr}}$. In this case a *local water-filling* solution will be optimal. This means that a part of the spectrum is excluded from information transmission, namely, the part of the spectrum for which $x \in [0, \kappa]$. Due to the monotonicity of the noise spectrum the water-filling level is given by $w = \lambda^{(\text{MK})}(\kappa)$ where κ is obtained by solving Eq. (2.41). The capacity then reads

$$C_{\text{Sh}} = \frac{1}{2\pi} \left((\pi - \kappa) \log_2 \lambda^{(\text{MK})}(\kappa) - L^{(\text{MK})}(\phi, \pi) + L^{(\text{MK})}(\phi, \kappa) \right), \quad P \leq P_{\text{thr}}. \quad (2.45)$$

In Fig. 2.6 (b) we have plotted an example for a local water-filling. Equation (2.45) allows us to explicitly evaluate the limit $\phi \rightarrow 1$ (since in this limit $P < P_{\text{thr}}$).

Let us evaluate the behavior of the noise spectrum $\lambda^{(\text{MK})}(x)$ in this limit. Recall that the integral over the spectrum is independent of ϕ , i.e. its norm is given by the noise variance N :

$$\frac{1}{\pi} \int_0^\pi dx \lambda^{(\text{MK})}(x) = N. \quad (2.46)$$

In the limit $\phi \rightarrow 1$ we find that $\lambda^{(\text{MK})}(x)$ tends to zero everywhere except for $x = 0$ where it diverges to infinity, i.e.

$$\lim_{\phi \rightarrow 1} \lambda^{(\text{MK})}(0) = \lim_{\phi \rightarrow 1} N \frac{1 + \phi}{1 - \phi} \rightarrow \infty. \quad (2.47)$$

Then the optimal position κ will tend to 0 and the water-filling w will tend to the power constraint P . This is due to the following reasoning: in $L^{(\text{MK})}(\phi, x)$ [see (2.39)] the function $\frac{1+\phi}{1-\phi}$ tends stronger to infinity (with $\phi \rightarrow 1$) than $\tan \frac{x}{2}$ to zero (with $x \rightarrow 0$). Using Eqs. (2.40) and (2.41) we conclude that

$$\lim_{\phi \rightarrow 1} w = P. \quad (2.48)$$

2.4. Limitations of Shannon Information Theory

The behavior of the capacity (2.45) in this limit can be computed in several steps:

$$\begin{aligned}
\lim_{\phi \rightarrow 1} C_{\text{Sh}} &= \lim_{\phi \rightarrow 1} \frac{1}{2\pi} (\pi - \kappa) \log_2 w - \lim_{\phi \rightarrow 1} \frac{1}{2\pi} \int_{\kappa}^{\pi} dx \log_2 \lambda^{(\text{MK})}(x) \\
&= - \lim_{\epsilon \rightarrow 0} \frac{1}{2\pi} \int_0^{\pi} dx \log_2 \frac{1 - (1 - \epsilon)^2}{1 + (1 - \epsilon)^2 - 2(1 - \epsilon) \cos(x)} + c_w \\
&= - \lim_{\epsilon \rightarrow 0} \frac{1}{2\pi} \int_0^{\pi} dx \log_2 \frac{\epsilon}{(1 - \epsilon)(1 - \cos(x))} + c_w \\
&= \frac{1}{2} \lim_{\epsilon \rightarrow 0} \log_2 \frac{\epsilon}{1 - \epsilon} - \underbrace{\frac{1}{2\pi} \int_0^{\pi} dx \log_2 (1 - \cos(x))}_{=1/2} + c_w \rightarrow \infty.
\end{aligned} \tag{2.49}$$

where all terms of order ϵ^2 are neglected and $c_w = \frac{1}{2} \log_2 P$. Physically this is clear because the Shannon capacity of a noiseless channel diverges even for finite input powers.

2.4. Limitations of Shannon Information Theory

Shannon provided the maximal transmission rate of classical communication channels and proved that it is achievable when the number of uses tends to infinity. In the case of the single-variate Gaussian channel it was found to be

$$C_{\text{Sh}} = \frac{1}{2} \log_2 \left(1 + \frac{P}{N} \right), \tag{2.50}$$

where P is the average input power (i.e. the variance of the input distribution) and N the variance of the Gaussian distributed noise. One immediately concludes that equation (2.50) cannot be always valid. For a fixed input power and very small noise variances, i.e. when $N \rightarrow 0$, the capacity diverges. The same non-physical divergence was found for the Gauss-Markov channel in the limit $\phi \rightarrow 1$ (for arbitrary input powers and noise variances). This shows the limitation of Shannon Information Theory and the necessity for a larger theory that does not lead to this divergence, namely *Quantum Information Theory*. We shall see in the next chapter that we need to take into account the quantum nature of the input symbols (i.e. input *states*). In Shannon Information Theory the input symbols correspond to random variables which do not carry any intrinsic energy and do not lead to any noise in the channel. This assumption however is not physical. Ultimately, any information carrier requires a finite amount of energy and therefore, leads to noise. For this reason, the noise cannot become arbitrarily small which will be taken into account in *Quantum Information Theory*. Finally, this “physical” condition shall lead to the “true” equation for the classical capacity, which in the classical limit tends to C_{Sh} .

3. Quantum Information Theory

The previous section highlighted the incompleteness of Shannon Information Theory when reducing the noise of the system, or equivalently, reducing its size. Due to progressive downscaling of modern hardware elements the treatment of small system sizes is inevitable. Gordon E. Moore predicted in 1965 that every year the number of components in integrated circuits doubles [Moo65]. Surprisingly, up to today this trend was confirmed [Con13]. Since the size of the processors does not increase the individual transistors decrease in size and eventually scale down to sizes of a few atoms. Thus, communication and computation are ultimately subject to the laws of quantum mechanics. Therefore, *Quantum Information Theory* (or “Quantum Information Science”) was introduced, where now atoms, ions and photons are used as carriers of information.

Quantum information can be quantified in *quantum bits* (or “qubits”). The qubit is the quantum analogue of the classical bit. Unlike a classical bit which can only take the value 0 or 1, a qubit $|\psi\rangle$ corresponds to a pure quantum state that is given by an arbitrary superposition of two basis vectors $|0\rangle$ and $|1\rangle$ that span a two-dimensional Hilbert space \mathcal{H} , i.e.

$$|\psi\rangle = \alpha |0\rangle + \beta |1\rangle, \tag{3.1}$$

where α and β are complex numbers satisfying the normalization constraint $|\alpha|^2 + |\beta|^2 = 1$. The basis vectors $\{|0\rangle, |1\rangle\}$ may correspond to the polarization of a single photon or the spin of a single ion. When a qubit $|\psi\rangle$ is measured in an orthonormal basis $\{|0\rangle, |1\rangle\}$ it will yield one classical bit of information. More generally, one can consider *qudits*, that live in a d -dimensional Hilbert space, spanned by d basis vectors. When measured in a chosen basis a qudit yields a *discrete* outcome; in the case of a qubit 0 or 1. However, there also exist quantum systems that live in an infinite dimensional Hilbert space and physically correspond to a collection of particles, e.g. the coherent state $|\alpha\rangle$ which will be introduced in Sec. 4.3.2. In this example, the information is encoded in the amplitude of the state and can take continuous values. Therefore, as opposed to systems with a discrete number of basis states we speak in this case of *continuous variable* quantum information. We will discuss this in more details in Sec. 5.5 and first introduce properly the quantum equivalence to the Shannon entropy and classical channels.

In this chapter we define the necessary tools in order to study transmission rates of quantum communication channels, where all definitions are taken from [NC00], [KW05] and [Man06] unless explicitly stated otherwise.

3.1. Von Neumann entropy

The extension of the Shannon entropy and the Gibbs entropy to quantum mechanics is given by the *von Neumann entropy*. Let $\hat{\rho}$ be a density operator given by the composition of an ensemble $\{|x\rangle\}$ spanning the Hilbert space \mathcal{H} and drawn with probability $p(x)$, i.e.

$$\hat{\rho} = \sum_x p(x) |x\rangle \langle x|. \quad (3.2)$$

A density operator $\hat{\rho}$ is Hermitian, i.e. $\hat{\rho}^\dagger = \hat{\rho}$ (where “ \dagger ” denotes transposition and complex conjugation), positive-semidefinite and satisfies $\text{Tr}[\hat{\rho}] = 1$. Furthermore, a quantum state $\hat{\rho}$ is *pure* if $\text{Tr}[\hat{\rho}^2] = 1$ and *mixed* if $\text{Tr}[\hat{\rho}^2] < 1$. The von Neumann entropy of a state $\hat{\rho}$ is defined as

$$S(\hat{\rho}) = -\text{Tr}[\hat{\rho} \log_2 \hat{\rho}], \quad (3.3)$$

where we use in this work the logarithm to the base two (in order to express it in bits). If a density operator $\hat{\rho}$ is given in its eigenbasis $\{|j\rangle\}$, i.e.

$$\hat{\rho} = \sum_j \lambda_j |j\rangle \langle j|, \quad (3.4)$$

then the von Neumann entropy is simply given by

$$S(\hat{\rho}) = -\sum_j \lambda_j \log_2 \lambda_j = H(\lambda), \quad (3.5)$$

where $H(\lambda)$ is the Shannon entropy of a random variable with outcomes associated to probabilities λ_j . For a pure state $\hat{\rho} = |k\rangle \langle k|$, i.e. a state that is with probability $\lambda_k = 1$ in state $|k\rangle$, we conclude from Eq. (3.5) that $S(|k\rangle \langle k|) = 0$. In contrary, the state that maximizes the von Neumann entropy (in a d -dimensional Hilbert space) is the maximally mixed state

$$\hat{\rho} = \frac{1}{d} \sum_{j=1}^d |j\rangle \langle j|, \quad (3.6)$$

which has a uniform probability distribution $\lambda_j = \frac{1}{d}$, $\forall j$, which is known to maximize the Shannon entropy.

Let $\hat{\rho}_{AB} \in \mathcal{H}_{AB}$ be a state composed by two systems A and B . Then, its *joint von Neumann entropy* reads

$$S(\hat{\rho}_{AB}) = -\text{Tr}[\hat{\rho}_{AB} \log_2 \hat{\rho}_{AB}], \quad (3.7)$$

and equivalently to definitions of the Shannon entropy, the *conditional von Neumann entropy* and *mutual information* read

$$S(\hat{\rho}_A | \hat{\rho}_B) = S(\hat{\rho}_{AB}) - S(\hat{\rho}_B), \quad (3.8)$$

$$I(\hat{\rho}_A; \hat{\rho}_B) = S(\hat{\rho}_B) - S(\hat{\rho}_B | \hat{\rho}_A). \quad (3.9)$$

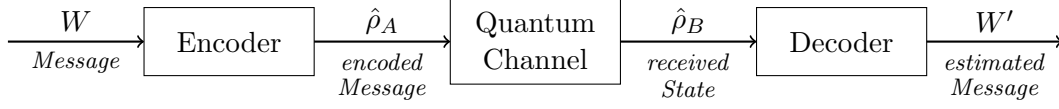


Figure 3.1.: Quantum communication system.

As in the case of the joint Shannon entropy the von Neumann entropy is subadditive:

$$S(\hat{\rho}_{AB}) \leq S(\hat{\rho}_A) + S(\hat{\rho}_B), \quad (3.10)$$

where $\hat{\rho}_A$, $\hat{\rho}_B$, are given by the *partial trace*:

$$\text{Tr}_A[\hat{\rho}_{AB}] = \hat{\rho}_B. \quad (3.11)$$

The partial trace of a bipartite system is defined as

$$\text{Tr}_B[|a_1\rangle\langle a_2| \otimes |b_1\rangle\langle b_2|] = |a_1\rangle\langle a_2| \text{Tr}[|b_1\rangle\langle b_2|]. \quad (3.12)$$

Note that equality in (3.10) holds if and only if $\hat{\rho}_{AB} = \hat{\rho}_A \otimes \hat{\rho}_B$, i.e. if the state $\hat{\rho}_{AB}$ is separable.

We now show that some properties that hold for the Shannon entropy do not hold for the von Neumann entropy. For instance, given two random variables X and Y , the uncertainty of X can never be higher than the joint entropy of X and Y , that is $H(X) \leq H(X, Y)$. In general, this does not hold for quantum states. Consider the pure state $\rho_{AB} = |\psi_{AB}\rangle\langle\psi_{AB}|$ with

$$|\psi_{AB}\rangle = \frac{1}{\sqrt{2}}(|00\rangle + |11\rangle), \quad (3.13)$$

where we used the notation $|00\rangle = |0\rangle \otimes |0\rangle$. Here, both subsystems are in a superposed state, which when measured (in the basis $\{|0\rangle, |1\rangle\}$) either leads to both subsystems being in the state $|0\rangle$ or both being in the state $|1\rangle$. Such a state is called an *entangled state*, and in this case is even maximally entangled: when tracing over one of the two systems the remaining state will be maximally mixed [as in Eq. (3.6)], i.e.

$$\text{Tr}_A[\rho_{AB}] = \frac{1}{2}(|0\rangle\langle 0| + |1\rangle\langle 1|). \quad (3.14)$$

As mentioned above, this state maximizes the von Neumann entropy. Thus, we find that $S(\hat{\rho}_{AB}) = 0$ and $S(\hat{\rho}_A) > 0$, which implies by Eq. (3.8) that $S(\hat{\rho}_A|\hat{\rho}_B) < 0$.

3.2. Quantum channels

In Shannon Information Theory a (classical) communication system consists of an input message W that is encoded in a random variable A (in general a random vector \mathbf{A}), sent through a classical channel that leads to the output random variable B which is

3. Quantum Information Theory

then decoded to obtain the output message W' . In a quantum communication system the message W is now encoded in a quantum state $\hat{\rho}_A$ that is sent through a *quantum channel* Ψ which outputs a quantum state $\hat{\rho}_B$ which when measured leads to the message W' (see Fig. 3.1). In general, a quantum channel may describe any physical process a quantum system undergoes. This can be the actual sending of e.g. photons, or the operation on the state of an atom. Formally, a quantum channel Ψ is a completely positive trace-preserving (CPTP) map

$$\Psi : \mathcal{B}(\mathcal{H}_A) \rightarrow \mathcal{B}(\mathcal{H}_B), \quad (3.15)$$

where $\mathcal{B}(\mathcal{H}_A)$ and $\mathcal{B}(\mathcal{H}_B)$ are Hilbert spaces containing bounded linear operators¹. We use equivalently the shorter notation

$$\hat{\rho}_B = \Psi[\hat{\rho}_A], \quad (3.16)$$

where $\hat{\rho}_A \in \mathcal{B}_*(\mathcal{H}_A)$ is an input state and $\hat{\rho}_B \in \mathcal{B}_*(\mathcal{H}_B)$ the corresponding output state. Note that the ‘‘trace-preserving’’ property of Ψ is implied by the definition that $\Psi[\hat{\rho}_A]$ is a density operator which has by definition $\text{Tr}[\Psi[\hat{\rho}_A]] = 1$. Complete positivity requires furthermore that $(\mathbb{I} \otimes \Psi)[\hat{\rho}_A]$ is positive for any operator $\hat{\rho}_A$, where \mathbb{I} is the identity operator. As a final property we state that Ψ is a *convex-linear map* on the set of density matrices, i.e. for probabilities p_i

$$\Psi \left[\sum_i p_i \hat{\rho}_i \right] = \sum_i p_i \Psi[\hat{\rho}_i]. \quad (3.17)$$

A quantum channel Ψ can always be represented as the unitary evolution of an input quantum system with state $\hat{\rho}_A$ coupled to an (ancillary) *environment state* $\hat{\rho}_E \in \mathcal{B}(\mathcal{H}_E)$. The final state $\hat{\rho}_B = \Psi[\hat{\rho}_A]$ is then obtained by taking the partial trace over the environment:

$$\Psi[\hat{\rho}_A] = \text{Tr}_E \left[\hat{U}_{AE}(\hat{\rho}_A \otimes \hat{\rho}_E) \hat{U}_{AE}^\dagger \right]. \quad (3.18)$$

We underline that \hat{U}_{AE} is a unitary operation that acts on the joint state $\hat{\rho}_A \otimes \hat{\rho}_E$. The decomposition stated in Eq. (3.18) is called *Stinespring dilation* and visualized in Fig. 3.2. Throughout this thesis we impose an intuitive physical constraint on quantum channels, namely, we assume all channels to be *causal channels*: outputs at some time step t do not depend on inputs at $t' > t$.

There exists an additional possibility to represent a completely positive map (we relax the trace-preserving property), namely the *Choi-Jamiołkowski isomorphism* [Jam72, Cho75] (for detailed explanations see e.g. [LS11]). We define the positive operator

$$\hat{P}_{AB} \equiv (\Psi_{B|A'} \otimes \mathbb{I}_A)(|\Phi^+\rangle \langle \Phi^+|_{AA'}), \quad (3.19)$$

¹Observables of a system are given by bounded linear operators on the Hilbert space \mathcal{H} , denoted by $\mathcal{B}_*(\mathcal{H})$; the quantum states $\hat{\rho}$ of the system are therefore elements of the dual space $\mathcal{B}(\mathcal{H})$ [KW05].

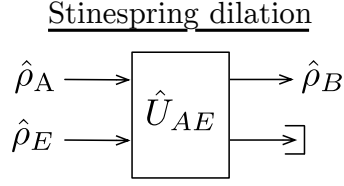


Figure 3.2.: Stinespring dilation: A quantum channel corresponds to the unitary evolution of the total state $\hat{\rho}_A \otimes \hat{\rho}_E$ and tracing out the environment.

defined on $\mathcal{B}(\mathcal{H}_A) \otimes \mathcal{B}(\mathcal{H}_B)$, where $\Psi_{B|A'}$ is a CPTP map $\Psi_{B|A'} : \mathcal{B}(\mathcal{H}_{A'}) \rightarrow \mathcal{B}(\mathcal{H}_B)$, \mathbb{I}_A is the identity operator acting on system A and

$$|\Phi^+\rangle_{AA'} = \sum_j |j\rangle_A |j\rangle'_{A'}, \quad (3.20)$$

is a (non-normalized) maximally entangled state living in $\mathcal{B}(\mathcal{H}'_A)$ where $\dim(\mathcal{H}'_A) = \dim(\mathcal{H}_A)$. This means the operator \hat{P}_{AB} is obtained by acting with Ψ on the system A' of the maximally entangled state and doing nothing to the system A . Then, the map $\Psi = \Psi_{B|A}$ is *Choi-isomorphic* to the operator \hat{P}_{AB} , i.e.

$$\Psi_{B|A}[\hat{\rho}_A] = \langle \Phi^+ |_{AA'} \hat{\rho}_{A'} \otimes \hat{P}_{AB} | \Phi^+ \rangle_{AA'}, \quad (3.21)$$

where $\hat{\rho}'_A$ is the same state as $\hat{\rho}_A$ but lives in $\mathcal{B}(\mathcal{H}'_A)$. Equivalently, the map Ψ is *Jamiolkowski-isomorphic* to the operator

$$\Psi_{B|A}[\hat{\rho}_A] = \langle \Phi^+ |_{AA'} \hat{\rho}_{A'} \otimes \hat{O}_{AB} | \Phi^+ \rangle_{AA'}, \quad (3.22)$$

where the positive operator \hat{O}_{AB} reads

$$\hat{O}_{AB} \equiv (\Psi \otimes \mathbb{I}_A)(|\Phi^+\rangle \langle \Phi^+|^{\text{T}_A}_{AA'}), \quad (3.23)$$

where T_A denotes the partial transpose in the basis used to define $|\Phi^+\rangle$.

The physical interpretation of the isomorphism is as follows: Given the state $\hat{P}_{AB} \in \mathcal{B}(\mathcal{H}_A) \otimes \mathcal{B}(\mathcal{H}_B)$ (or \hat{O}_{AB} equivalently) and a state $\hat{\rho}_A \in \mathcal{B}(\mathcal{H}_A)$, if we perform a measurement of the second subsystem of \hat{P}_{AB} and of $\hat{\rho}_A$ in the basis spanned by the maximally entangled states $|\Phi^+\rangle_{AA'}$ (also called “Bell measurement”, explained in Sec. 5.2.3) then the resulting state is $\Psi(\hat{\rho}_A)$. Equivalently, the right hand side of Eq. (3.21) can be understood as the *teleportation*² of the input state living in system A' to A conditioned on the outcome of the Bell measurement. As a consequence, given the state \hat{P}_{AB} the map Ψ can always be implemented if Bell measurements are available. However, the implementation may be probabilistic as it depends on the outcome of the measurement.

²The quantum teleportation protocol is not treated here for discrete quantum systems but explained for continuous variables in Sec. 5.2.3.

3. Quantum Information Theory

3.2.1. Memoryless channels

Suppose a given quantum channel Ψ is used n times. Note that n subsequent uses of a channel may be equivalently regarded as n parallel channels acting once on an n -partite system. An important question that arises: are the different uses of the channel affecting each other? If each channel use is independent from the others then we speak of a *memoryless channel*. A memoryless channel $\Psi^{(n)}$ acting on an n -partite (possibly entangled) input state $\hat{\rho}_A^{(n)}$ is defined as

$$\Psi^{(n)}[\hat{\rho}_A^{(n)}] = \text{Tr}_E \left[\hat{U}_{A_n E_n} \cdot \hat{U}_{A_{n-1} E_{n-1}} \cdots \hat{U}_{A_1 E_1} (\hat{\rho}_A^{(n)} \otimes \hat{\rho}_E^{(n)}) \hat{U}_{A_1 E_1}^\dagger \cdot \hat{U}_{A_2 E_2}^\dagger \cdots \hat{U}_{A_n E_n}^\dagger \right], \quad (3.24)$$

where the unitary operations $\hat{U}_{A_i E_i}$ are all identical and the ancillary environment state is given by a product state

$$\hat{\rho}_E^{(n)} = \hat{\rho}_{E_1} \otimes \hat{\rho}_{E_2} \otimes \cdots \otimes \hat{\rho}_{E_n}. \quad (3.25)$$

Therefore, one may write

$$\Psi^{(n)}[\hat{\rho}_A^{(n)}] = \Psi^{\otimes n}[\hat{\rho}_A^{(n)}], \quad (3.26)$$

i.e. the channel is equivalent to the tensor product of n identical channels.

3.2.2. Memory channels

In full generality, we need to take correlations between the different uses of a channel into account. A quantum channel $\Psi^{(n)}$ acting on an n -partite state is called a *memory channel* if it cannot be decomposed as in Eq. (3.26), i.e. if

$$\Psi^{(n)}[\hat{\rho}_A^{(n)}] \neq \Psi^{\otimes n}[\hat{\rho}_A^{(n)}]. \quad (3.27)$$

There are different models for memory channels [KW05, Man06]. A simple way to introduce a memory \mathcal{M} to the channel is to replace the previously separable environment state $\hat{\rho}_E^{(n)}$ by an entangled one, i.e.

$$\hat{\rho}_E^{(n)} \neq \hat{\rho}_{E_1} \otimes \hat{\rho}_{E_2} \otimes \cdots \otimes \hat{\rho}_{E_n}. \quad (3.28)$$

The corresponding Stinespring dilation reads as in Eq. (3.24), where the different unitary operations $\hat{U}_{A_i E_i}$ still act identically, but due to the correlations in the environment the channel is no longer factorizable. Such a model is depicted in Fig. 3.3 (a).

A more general memory model considers the memory \mathcal{M} to be given by an initial *memory state* $\hat{\rho}_M$. This state may affect each input state $\hat{\rho}_{A_i}$ and environment state $\hat{\rho}_{E_i}$ as it is passed on from channel use to channel use and thus creates correlation between the different channels. The total environment state $\hat{\rho}_E^{(n)}$ for this memory model is separable and each unitary acts now on the input, the environment and the memory state. The dilation for this model reads

$$\begin{aligned} & \Psi^{(n)}[\hat{\rho}_A^{(n)}] \\ &= \text{Tr}_E \left[\hat{U}_{A_n M E_n} \cdot \hat{U}_{A_{n-1} M E_{n-1}} \cdots \hat{U}_{A_1 M E_1} (\hat{\rho}_A^{(n)} \otimes \hat{\rho}_E^{(n)} \otimes \hat{\rho}_M) \hat{U}_{A_1 M E_1}^\dagger \cdots \hat{U}_{A_n M E_n}^\dagger \right]. \end{aligned} \quad (3.29)$$

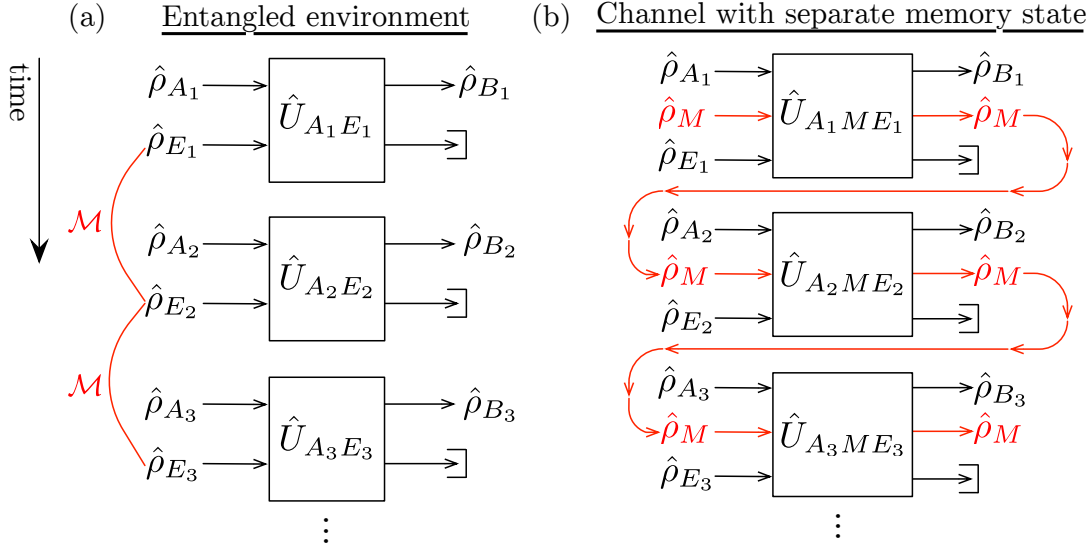


Figure 3.3.: Different models for a quantum memory channel: (a) The environment is entangled and therefore generates a memory \mathcal{M} between the channel uses. (b) The memory is modeled by a memory state $\hat{\rho}_M$ which is passed from each channel use to the next one.

We depict the latter in Fig. 3.3 (b). The memory channels that we consider in this work follow the model depicted in Fig. 3.3 (a), i.e. a channel that acts identically on each individual state but exhibits correlations over subsequent uses due to global noise correlations (which can be classical or quantum).

Now we explain how to use quantum channels for the transmission of information. Unlike in classical information theory, for quantum channels one has to differentiate between *classical information* and *quantum information* (which may be measured in qubits, as introduced before). Therefore, there exists the *classical capacity* and the *quantum capacity* of quantum channels, which both are upper bounds on the classical and quantum information transmission rate of the channel. In this work we focus only on the classical capacity, but also give the formal definition to the quantum capacity (see Sec. (3.5) below).

3.3. Holevo bound

The structure of a communication system containing a quantum channel (see Fig. 3.1) is equivalent to the one containing a classical channel (see Fig. 2.2). Before stating the classical capacity of a quantum channel we first derive a bound on the mutual information between Alice and Bob.

Suppose Alice encodes a given message with index $X = 0, 1, \dots, n$ in a quantum state $\hat{\rho}_X$ with probabilities p_0, \dots, p_n . Then Bob performs a *positive operator-valued measure-*

3. Quantum Information Theory

ment (POVM), i.e. he applies an operator \hat{E}_y belonging to the set $\{\hat{E}_0, \dots, \hat{E}_m\}$ with

$$\hat{E}_y = \hat{E}_y^\dagger \geq 0, \quad \sum_y \hat{E}_y = \mathbb{I}, \quad (3.30)$$

on Alice's state and obtains the measurement outcome Y . The conditional probability then reads

$$p(Y|X) = \text{Tr}[\hat{E}_Y \hat{\rho}_X]. \quad (3.31)$$

The upper bound for the mutual information between Alice and Bob is called *Holevo bound* [Hol73]

$$I(X; Y) \leq \chi(p_X, \hat{\rho}_X) \equiv S(\hat{\rho}) - \sum_x p_x S(\hat{\rho}_x), \quad (3.32)$$

where $\chi(p_X, \hat{\rho}_X)$ is called the *Holevo χ -quantity* and $S(\hat{\rho})$ is the von Neumann entropy and $\hat{\rho} = \sum_x p_x \hat{\rho}_x$ the averaged state of Alice. Here $S(\hat{\rho})$ is the entropy of the averaged state and $\sum_x p_x S(\hat{\rho}_x)$ corresponds to the averaged entropy.

3.4. Classical capacity

In the following section we formalize the classical capacity of quantum channels. We shall see that the quantum nature of the input signals (which allows for entanglement over subsequent uses of the channel) leads to a more complicated expression for the capacity than in the case of Shannon information theory.

Let us suppose that Alice sends a quantum state $\hat{\rho}_X$ that lives in a finite dimensional Hilbert space and is drawn with probability p_X through a noisy quantum channel. Bob receives the output state $\Psi[\hat{\rho}_X] = \hat{\rho}_Y$ and due to the noise in the channel *a priori* $X \neq Y$. The Holevo bound for the mutual information between Alice and Bob then is given by

$$\chi(p_X, \Psi[\hat{\rho}_X]) = S(\Psi[\hat{\rho}_{\text{in}}]) - \sum_x p_x S(\Psi[\hat{\rho}_x]), \quad (3.33)$$

where we underline here that $\hat{\rho}_{\text{in}}$ is Alice's averaged input state. In order for the encoding ensemble of Alice to be physical we need to impose an input energy constraint (just like in the case of classical Gaussian channels, see Sec. 2.3). The input ensemble $\{p_X, \hat{\rho}_X\}$ has to fulfill the energy constraint

$$\sum_x p_x \text{Tr} [\hat{\rho}_x \hat{a}^\dagger \hat{a}] = \text{Tr} [\hat{\rho}_{\text{in}} \hat{a}^\dagger \hat{a}] \leq \bar{N}, \quad (3.34)$$

where $\hat{a}^\dagger \hat{a}$ is the number operator and thus, \bar{N} corresponds to the maximal mean photon number. Then, the *one-shot capacity* or *Holevo χ -capacity* of a quantum channel Ψ is

given by³ [HJS⁺96, SW97, Hol98c]

$$\begin{aligned} C_\chi(\Psi, \bar{N}) &= \max_{\{p_X, \hat{\rho}_X\}} \chi(p_X, \Psi[\hat{\rho}_X]) \\ &= \max_{\{p_X, \hat{\rho}_X\}} \left\{ S(\Psi[\hat{\rho}_{\text{in}}]) - \sum_x p_x S(\Psi[\hat{\rho}_x]) \right\}. \end{aligned} \quad (3.35)$$

Alice can transmit classical information reliably to Bob at any rate below the one-shot capacity C_χ but is required to use multiple available copies of the channel Ψ *one at a time* (hence, “one-shot” capacity), coding her message into product states. Therefore, C_χ is sometimes referred to as the *product state* capacity. However, in full generality the notion has to be extended to the case when Alice is allowed to use entangled input states. For this reason, the *classical capacity* is given by

$$C(\Psi, \bar{N}) = \lim_{n \rightarrow \infty} \frac{1}{n} C_\chi(\Psi^{\otimes n}, \bar{N}), \quad (3.36)$$

where the maximization in C_χ is taken over all (possibly entangled) ensembles satisfying Eq. (3.34). In Eq. (3.36) $\Psi^{\otimes n}$ can be regarded either as n copies of the same channel (equivalent to a channel system $\Psi^{\otimes n}$) or n uses of the channel Ψ . Note, that we use Eq. (3.36) in the following as the definition of the classical capacity of channels $\Psi^{(n)}$ which can be expressed as a tensor product of n different channels.

An important inequality for the classical capacity is the *pipelining property*

$$C(\Psi_1 \circ \Psi_2) \leq \min(C(\Psi_1), C(\Psi_2)), \quad (3.37)$$

where \bar{N} photons are given to both Ψ_1 and Ψ_2 . This inequality essentially states that the capacity of the concatenation of two channels can never be larger than the capacity of one of the individual channels, as inevitably additional noise will be introduced.

Until recently the *additivity* of the one-shot capacity C_χ was conjectured, i.e.

$$C_\chi(\Psi_1 \otimes \Psi_2, \bar{N}) \stackrel{?}{=} C_\chi(\Psi_1, \bar{N}) + C_\chi(\Psi_2, \bar{N}), \quad \forall \Psi_1, \Psi_2. \quad (3.38)$$

In [Has09] an example of two channels Ψ_1 and Ψ_2 was found for which

$$C_\chi(\Psi_1 \otimes \Psi_2) > C_\chi(\Psi_1) + C_\chi(\Psi_2), \quad (3.39)$$

where due to the discrete system size the energy constraint was not needed to be considered⁴. In [FKM09] an expanded version of the proof stated in [Has09] is presented and in [BaH10, ASW10] alternative, simpler proofs are derived. Equation (3.39) states

³We remark here that in some works the one-shot capacity is given by the supremum instead of the maximum of the χ -quantity. We use throughout this thesis “max” in all subsequent definitions such as the Gaussian classical capacity (defined in the following).

⁴The energy constraint stated in Eq. (3.34) is only required when the input states live in an infinite dimensional Hilbert space. It guarantees that Alice cannot use symbol states that are infinitely distant from each other. In the case of qubit channels in contrary the input energy per symbol is fixed, given by e.g. one quanta per symbol if photons are used as information carriers.

3. Quantum Information Theory

the possible super additivity of the one-shot capacity and implies that in general, one has to carry out the limit in Eq. (3.36) in order to obtain the classical capacity.

Note that often one is concerned with a more restricted problem of additivity. Namely, whether the one-shot capacity of several copies of the same channel is additive, i.e.

$$C_\chi(\Psi^{\otimes n}, n\bar{N}) \stackrel{?}{=} nC_\chi(\Psi, \bar{N}). \quad (3.40)$$

Clearly, if the latter is fulfilled then $C_\chi(\Psi, \bar{N}) = C(\Psi, \bar{N})$ follows. Whenever we use in the following the term “the one-shot capacity of a quantum channel is additive” we state that Eq. (3.40) holds.

We remark that there exists also a more general problem concerning the additivity of the classical capacity, i.e.

$$C(\Psi_1 \otimes \Psi_2) \stackrel{?}{>} C(\Psi_1) + C(\Psi_2). \quad (3.41)$$

Due to the limit that needs to be taken in Eq. (3.36) the possible superadditivity of the one-shot capacity C_χ does not necessarily imply the superadditivity of the classical capacity C (see Refs. [Smi10, HG12] for details).

There are channels for which the additivity of the one-shot capacity was proven, i.e. $C_\chi = C$ (see, e.g. [Kin02, Sho02, GGL⁺04a, DM09]). One important example are *unital qubit channels*, i.e. channels for which $\mathcal{H}_A = \mathcal{H}_B = \mathbb{C}^2$ and $\Psi[\mathbb{I}] = \mathbb{I}$ [Kin02]. The *completely depolarizing channel* is for instance in the class of unital qubit channels. It acts as

$$\Psi_\lambda[\hat{\rho}] = \lambda\hat{\rho} + \frac{(1-\lambda)}{2}\mathbb{I}_{2 \times 2}, \quad (3.42)$$

where $-\frac{1}{3} \leq \lambda \leq 1$ and $\hat{\rho} \in \mathbb{C}^2$.

A second example is the *lossy bosonic Gaussian channel* with vacuum noise [GGL⁺04a] (bosonic Gaussian channels will be introduced in Sec. 5.3). Then, there exists also the class of *entanglement breaking channels* for which $C_\chi = C$ [Sho02]. Entanglement breaking channels destroy any entanglement that is present between the input state and another reference quantum system: for the total input state $\hat{\rho} \in \mathcal{B}(\mathcal{H}_A \otimes \mathcal{H}_R)$ (where \mathcal{H}_R is the Hilbert space of a reference system), the output state

$$(\Psi \otimes \mathbb{I}_R)[\hat{\rho}] \in \mathcal{B}(\mathcal{H}_A \otimes \mathcal{H}_R), \quad (3.43)$$

is separable, where $\mathbb{I}_R \in \mathcal{B}(\mathcal{H}_R)$ is the identity operator living in the reference system. Note that the one-shot capacity is also additive for entanglement breaking channels living in infinite dimensional systems as shown in [HS04].

A lot of studies have been devoted to the study of the classical capacity of quantum channels with memory [MP02, MPV04, BM04, KW05, BDM05, CCMR05, CCRM06, GM05, KDC06, KM06, Dae07, DD07, PZM08, DM09, DD09, DM09, LPM09, LMM09, LGM10, PLM12]. An important question is whether entanglement between subsequent input states of a quantum channel is required to achieve the capacity.

In the case of a quantum memory channel with discrete alphabet, the first study that showed that entanglement can enhance the classical capacity of memory channels was

presented in [BFS97], where two transmissions of a qubit through a Two-Pauli-channel were considered. Studies on the classical capacity of a (more general) depolarizing channel [MP02] and a quasiclassical depolarizing channel [MPV04] showed the existence of a threshold on the degree of memory above which entangled signals improve the transmission rate with respect to product states. Further studies [BM04, BDM05] on a qubit channel with finite memory derived bounds on the classical and quantum capacities. In Ref. [KW05], the classical and quantum capacities were discussed in a general framework, where furthermore, *forgetful* quantum channels, i.e. channels where the memory decreases with increasing number of channel uses, were considered. The classical capacity of a quantum channel with long-term memory Markovian correlated noise [DD07] and arbitrary Markovian correlated noise [DD09] was evaluated. The case of general Pauli channels with memory was studied explicitly [Dae07], where it was shown that the optimal states are either product states or Bell states separated by a memory threshold. For higher dimensions, it has been shown that the capacity of qudit channels exhibits the same threshold phenomenon as Pauli qubit channels [KM06].

For a quantum channel with continuous alphabet, it was first shown for an additive bosonic channel and a lossy bosonic channel⁵, respectively, [CCMR05, CCRM06, GM05] that in the presence of a memory, some degree of entanglement between the input states is necessary to achieve the capacity, which is in contrast to the behavior reported for discrete quantum channels. Indeed, the optimal input states correspond to Einstein-Podolski-Rosen (EPR) states⁶ [EPR35] with finite squeezing which increases with the degree of memory, in contrary to either maximally or non-entangled states in the discrete case. For a lossy bosonic channel with non-Markovian correlated noise it was shown as well that entanglement increases the transmission rate, when restricted to Gaussian encodings [PZM08, LPM09, PLM12] (this memory channel will be considered in detail in Sec. 8.2).

There are also cases of quantum channels with memory where entanglement does not enhance the transmission rate. In [DM09] a periodic channel with depolarizing channel branches and a convex combination of depolarizing channels were considered where it was shown that the classical capacity is achieved without the use of entangled input states. A bosonic channel with additive Markovian correlated noise was considered in [LMM09] where it was shown that the optimal input encoding is given by non-entangled coherent states⁷.

3.5. Quantum capacity

One may ask the question what is the maximal amount of quantum information that can be reliably transmitted via a noisy quantum channel? The answer is provided by the *quantum capacity*. First, we define the *coherent information* $I(\hat{\rho}, \Psi)$ that is the

⁵Bosonic channels will be introduced in detail in Chapter 5.3.

⁶The “EPR” states will be properly introduced in Sec. 5.1.

⁷We consider this channel and its solution in detail in Sec. 7.4.6.

3. Quantum Information Theory

analogous quantity to the mutual information in Shannon Information Theory. It reads

$$I(\hat{\rho}, \Psi) = S(\Psi[\hat{\rho}]) - S(\hat{\rho}, \Psi), \quad (3.44)$$

where $S(\hat{\rho}, \Psi)$ is the *entropy exchange* which is defined as

$$S(\hat{\rho}, \Psi) = S((\Psi_A \otimes \mathbb{I}_R)[\hat{\rho}_{AR}]), \quad (3.45)$$

where $\hat{\rho}_{AR}$ is the joint entangled input state shared by Alice A and a purifying reference system R and Ψ_A acts only on system A . Then, the *quantum capacity* is given by

$$C_Q = \lim_{n \rightarrow \infty} \frac{1}{n} \max_{\hat{\rho}^{(n)}} I(\hat{\rho}^{(n)}, \Psi^{\otimes n}), \quad (3.46)$$

where similar to the definition of the one-shot capacity C_χ here $\max_{\hat{\rho}} I(\hat{\rho}, \Psi)$ is the *one-shot quantum capacity*. There are known examples like e.g. depolarizing channels [SS, DSS98, SS07] for which it was shown that the one-shot quantum capacity is non-additive, and hence in general the limit in Eq. (3.46) has to be carried out.

4. Quantum Optics

In the following chapter we give a brief introduction to quantum optics. First, we quantize the electromagnetic field. Then we quickly review several examples of important quantum states. Finally, we treat all optical transformations that are of relevance for this thesis. Throughout the entire chapter we use definitions from [WM95], [Bra05b] and [KL10], unless stated explicitly otherwise.

4.1. Quantization of the electromagnetic field

The electromagnetic field in classical electrodynamics is characterized by the Maxwell equations, which, in the vacuum and without sources, read¹:

$$\nabla \cdot \mathbf{H} = 0, \quad (4.1)$$

$$\nabla \times \mathbf{E} = -\mu_0 \frac{\partial}{\partial t} \mathbf{H}, \quad (4.2)$$

$$\nabla \cdot \mathbf{E} = 0, \quad (4.3)$$

$$\nabla \times \mathbf{H} = \epsilon_0 \frac{\partial}{\partial t} \mathbf{E}, \quad (4.4)$$

where \mathbf{E} is the electric field, \mathbf{H} the magnetizing field, μ_0 and ϵ_0 are the magnetic constant and vacuum permeability, respectively. The electric and magnetizing field can be expressed in terms of a vector potential \mathbf{A} , i.e.

$$\mu_0 \mathbf{H} = \nabla \times \mathbf{A}, \quad (4.5)$$

$$\mathbf{E} = -\frac{\partial}{\partial t} \mathbf{A}. \quad (4.6)$$

Without loss of generality² we choose the Coulomb gauge for the vector potential, i.e. $\nabla \cdot \mathbf{A} = 0$. Inserting Eqs. (4.5) and (4.6) in the left and right hand sides of Eq. (4.4) leads to the wave equation

$$\nabla^2 \mathbf{A}(\mathbf{r}, t) = \frac{1}{c^2} \frac{\partial^2}{\partial t^2} \mathbf{A}(\mathbf{r}, t), \quad (4.7)$$

where we expressed the explicit dependency of \mathbf{A} on the space and time coordinates \mathbf{r} and t and where $c = 1/\sqrt{\mu_0 \epsilon_0}$ is the speed of light in vacuum. Decomposing $\mathbf{A}(\mathbf{r}, t)$ into

¹Source free means the charge density and the current density are equal to zero.

²The choice of the gauge leaves the Maxwell equations invariant.

4. Quantum Optics

its *orthonormal modes* and inserting it in Eq. (4.7) and Eq. (4.6) leads to the solution

$$\mathbf{E}(\mathbf{r}, t) = \sum_{j=1}^2 \sum_k E_k \mathbf{e}_k^{(j)} \left[\alpha_{k,j} e^{i(\mathbf{k} \cdot \mathbf{r} - \omega_k t)} + \alpha_{k,j}^* e^{-i(\mathbf{k} \cdot \mathbf{r} - \omega_k t)} \right], \quad (4.8)$$

$$E_k = \sqrt{\frac{\hbar \omega_k}{2\epsilon_0}},$$

where \mathbf{k} is the propagation vector, $\mathbf{e}_k^{(j)}$ is the polarization vector (with two possible polarizations $j = 1, 2$), ω_k is the angular frequency, α_k, α_k^* are the complex amplitudes of the mode k and \hbar is the reduced Planck constant.

We now quantize the electromagnetic field by replacing the complex amplitudes by the *annihilation* and *creation operators*³

$$\alpha_{k,j}, \alpha_{k,j}^* \rightarrow \hat{a}_{k,j}, \hat{a}_{k,j}^\dagger. \quad (4.9)$$

Photons are bosons which obey the commutation relations:

$$\begin{aligned} [\hat{a}_{k,j}, \hat{a}_{k',j'}^\dagger] &= \delta_{kk'} \delta_{jj'}, \\ [\hat{a}_{k,j}, \hat{a}_{k',j'}] &= [\hat{a}_{k,j}^\dagger, \hat{a}_{k',j'}^\dagger] = 0. \end{aligned} \quad (4.10)$$

The Hamiltonian of the free electromagnetic field reads⁴

$$\hat{H} = \sum_k \hbar \omega_k \left(\hat{N}_k + \frac{1}{2} \right), \quad (4.11)$$

where

$$\hat{N}_k = \hat{a}_k^\dagger \hat{a}_k. \quad (4.12)$$

Hence, the energy of the quantized electromagnetic field is given by the sum of the number of photons in each mode, where each term contains an additional $\hbar \omega_k / 2$ taking into account the zero-point energy.

4.2. Quadrature operators

The Hamiltonian (4.11) can be expressed in terms of two operators \hat{Q}_k, \hat{P}_k , that is

$$\hat{H}_k = \frac{1}{2} (\hat{P}_k^2 + \omega_k^2 \hat{Q}_k^2), \quad (4.13)$$

where

$$\begin{aligned} \hat{Q}_k &= \sqrt{\frac{\hbar}{2\omega_k}} (\hat{a}_k + \hat{a}_k^\dagger), \\ \hat{P}_k &= -i \sqrt{\frac{\hbar \omega_k}{2}} (\hat{a}_k - \hat{a}_k^\dagger). \end{aligned} \quad (4.14)$$

³We properly introduce the action of these operations in section 4.3.1.

⁴For simplicity we drop the sum over the possible polarizations.

The operators \hat{Q}_k and \hat{P}_k are called *quadrature operators* and are the observables corresponding to the electric and magnetic amplitude of the electromagnetic field. For a single-mode with angular frequency ω the quantized field [classically defined by Eq. (4.8)] can now be written as

$$\mathbf{E}(\mathbf{r}, t) = \frac{1}{2\epsilon_0} \mathbf{e} \left[\hat{Q} \cos(\mathbf{k} \cdot \mathbf{r} - \omega t) + \hat{P} \sin(\mathbf{k} \cdot \mathbf{r} - \omega t) \right]. \quad (4.15)$$

The operators \hat{Q}_k, \hat{P}_k fulfill the same commutation relations as the position and momentum operators of a particle, i.e.

$$\left[\hat{Q}_k, \hat{P}_{k'} \right] = i\hbar \delta_{kk'}. \quad (4.16)$$

The commutation relation (4.16) implies the famous Heisenberg uncertainty principle:

$$\Delta \hat{Q}_k \Delta \hat{P}_k \geq \frac{\hbar}{2}, \quad (4.17)$$

where $\Delta \hat{A}$ denotes the uncertainty of the measurement outcome of observable \hat{A} which corresponds here simply to the standard deviation of the quadrature operators. For simplicity we work in the following with rescaled operators, i.e.

$$\begin{aligned} \hat{q}_k &\equiv \sqrt{\omega_k} \hat{Q}_k = \sqrt{\frac{\hbar}{2}} \left(\hat{a}_k + \hat{a}_k^\dagger \right), \\ \hat{p}_k &\equiv \frac{1}{\sqrt{\omega_k}} \hat{P}_k = -i \sqrt{\frac{\hbar}{2}} \left(\hat{a}_k - \hat{a}_k^\dagger \right). \end{aligned} \quad (4.18)$$

The single-mode quadrature operators \hat{q}, \hat{p} (for simplicity we omit the mode index k) satisfy the eigenvalue equations

$$\hat{q} |q\rangle = q |q\rangle, \quad \hat{p} |p\rangle = p |p\rangle, \quad (4.19)$$

where $|q\rangle$ and $|p\rangle$ are the position and momentum eigenstates, respectively, and q and p are the corresponding (real) eigenvalues. The eigenvectors are orthogonal and form a complete basis, i.e.

$$\langle q|q'\rangle = \delta(q - q'), \quad \langle p|p'\rangle = \delta(p - p'), \quad (4.20)$$

and complete

$$\int_{-\infty}^{\infty} dq |q\rangle \langle q| = \mathbb{I}, \quad \int_{-\infty}^{\infty} dp |p\rangle \langle p| = \mathbb{I}. \quad (4.21)$$

The two eigenstates are mutually related to each other by the Fourier transformation:

$$|q\rangle = \frac{1}{\sqrt{\pi}} \int_{-\infty}^{\infty} dp e^{iqp} |p\rangle, \quad |p\rangle = \frac{1}{\sqrt{\pi}} \int_{-\infty}^{\infty} dq e^{-iqp} |q\rangle \quad (4.22)$$

Quadrature operators are useful for the calculation of the wave function ψ for a given quantum state.

$$\begin{aligned} \psi(q) &= \langle q|\psi\rangle, \\ \psi(p) &= \langle p|\psi\rangle. \end{aligned} \quad (4.23)$$

4.3. Quantum states of the electromagnetic field

In the following we present several important examples of quantum states of the electromagnetic field.

4.3.1. Fock states

Let us return to the Hamiltonian given in Eq. (4.11). Its eigenbasis is given by the so-called *Fock space*, spanned by eigenvectors $|n_k\rangle$, where $n_k = 0, 1, \dots, \infty$. This means the number operator $\hat{N}_k = \hat{a}_k^\dagger \hat{a}_k$ satisfies the eigenvalue equation

$$\hat{N}_k |n_k\rangle = n_k |n_k\rangle, \quad (4.24)$$

where one refers to $|n_k\rangle$ as a “Fock state” or “number state” with photon number n_k associated to the mode k . The operators \hat{a}_k and \hat{a}_k^\dagger act as “ladder-operators” when applied to number states, i.e.

$$\begin{aligned} \hat{a}_k |n_k\rangle &= \sqrt{n_k} |n_k - 1\rangle, \\ \hat{a}_k^\dagger |n_k\rangle &= \sqrt{n_k + 1} |n_k + 1\rangle. \end{aligned} \quad (4.25)$$

Note that the annihilation operator always decreases the photon number by one and after subsequent application eventually reaches the ground state or *vacuum state* $|0\rangle$, that is

$$\hat{a}_k |0\rangle = 0 |0\rangle = 0. \quad (4.26)$$

The Fock states form an orthonormal and complete basis, i.e.

$$\begin{aligned} \langle n_k | m_k \rangle &= \delta_{mn}, \\ \sum_{n=0}^{\infty} |n_k\rangle \langle n_k| &= 1. \end{aligned} \quad (4.27)$$

The expansion of a general pure quantum state $|\psi\rangle$ in terms of the Fock basis reads

$$|\psi\rangle = \sum_{n=0}^N c_n |n\rangle, \quad (4.28)$$

where c_n are complex coefficients that satisfy

$$\sum_{k=0}^N |c_k|^2 = 1. \quad (4.29)$$

Note, that N may be infinite. Therefore, depending on the given system a different representation may be more convenient.

4.3.2. Coherent states and displacement operator

The Fock state representation is particularly useful when describing quantum states which occupy number states with low photon numbers. For many applications in quantum optics a more suitable representation is given by the *coherent state*. These states belong to the class of *minimal uncertainty* states which saturate Heisenberg's uncertainty principle, i.e.

$$\Delta\hat{q}\Delta\hat{p} = \frac{1}{2}. \quad (4.30)$$

The quadrature operators of coherent states have in addition equal uncertainties,

$$\Delta\hat{q} = \Delta\hat{p}. \quad (4.31)$$

Due to these properties coherent states are often referred to as “quasi-classical” states. The coherent state $|\alpha\rangle$ is defined as the eigenvector of the annihilation operator,

$$\hat{a}|\alpha\rangle = \alpha|\alpha\rangle, \quad (4.32)$$

where α is a complex number. Furthermore, a coherent state can be generated by applying the unitary *displacement operator*

$$\hat{D}(\alpha) = e^{\alpha\hat{a}^\dagger - \alpha^*\hat{a}}, \quad (4.33)$$

where α is a complex number, on the vacuum state:

$$\hat{D}(\alpha)|0\rangle = e^{-|\alpha|^2/2}e^{\alpha\hat{a}^\dagger}|0\rangle = e^{-|\alpha|^2/2}\sum_{n=0}^{\infty}\frac{\alpha^n}{\sqrt{n!}}|n\rangle = |\alpha\rangle.$$

In addition, it has the properties

$$\hat{D}^\dagger(\alpha) = \hat{D}^{-1}(\alpha) = \hat{D}(-\alpha). \quad (4.34)$$

Applying $\hat{D}(\alpha)$ to \hat{a} will “displace” it by the complex number α , i.e.

$$\begin{aligned} \hat{D}^\dagger(\alpha)\hat{a}\hat{D}(\alpha) &= \hat{a} + \alpha, \\ \hat{D}^\dagger(\alpha)\hat{a}^\dagger\hat{D}(\alpha) &= \hat{a}^\dagger + \alpha^*. \end{aligned} \quad (4.35)$$

The action of the displacement operator on the quadrature operators reads

$$\begin{aligned} \hat{D}^\dagger(\alpha)\hat{q}\hat{D}(\alpha) &= \hat{q} + \sqrt{2\hbar}\Re\{\alpha\}, \\ \hat{D}^\dagger(\alpha)\hat{p}\hat{D}(\alpha) &= \hat{p} + \sqrt{2\hbar}\Im\{\alpha\}, \end{aligned} \quad (4.36)$$

and on the position eigenstate is given by

$$\hat{D}(\alpha)|q\rangle = e^{i\sqrt{2}q\Im\{\alpha\}/\sqrt{\hbar}}|q + \sqrt{2\hbar}\Re\{\alpha\}\rangle. \quad (4.37)$$

Note that the displacement operator only shifts the expectation values of the quadrature operators and leaves higher order moments such as the variance invariant. This is an

4. Quantum Optics

important property, because as we will show in Sec. 4.4 this implies that the entropy of the quantum state is not affected by displacements. The optical implementation of the displacement operator is discussed in Sec. 4.4.3.

The expansion of a coherent state in terms of Fock states reads

$$|\alpha\rangle = e^{-|\alpha|^2/2} \sum_n \frac{\alpha^n}{\sqrt{n!}} |n\rangle. \quad (4.38)$$

From expansion (4.38) it follows that the probability of measuring n photons in the state $|\alpha\rangle$ is given by the Poisson distribution, i.e.

$$P(n) = |\langle n|\alpha\rangle|^2 = e^{-\langle n\rangle} \frac{\langle n\rangle^n}{n!}, \quad (4.39)$$

where $\langle n\rangle = |\alpha|^2$ is the mean and variance of the photon number distribution. Finally, we remark that coherent states are non-orthogonal, that is

$$|\langle\beta|\alpha\rangle|^2 = e^{\frac{1}{2}(|\alpha|^2 + |\beta|^2 - 2\beta^*\alpha)}, \quad (4.40)$$

but become orthogonal in the limit $|\alpha - \beta| \gg 1$. Furthermore, coherent states form an over complete basis, i.e.

$$\int d^2\alpha |\alpha\rangle \langle\alpha| = \pi\mathbb{I}, \quad (4.41)$$

where $d^2\alpha = d\Re(\alpha) d\Im(\alpha)$.

4.3.3. Squeezed states

Coherent states can be generalized to a larger class of states that still satisfies the minimal uncertainty condition (4.30), but no longer have equal uncertainties in the quadratures. This class of states is called *squeezed states*. They can be generated using the *squeezing operator* defined as

$$S(\epsilon) = \exp\left[\frac{1}{2}(\epsilon^* \hat{a}^2 - \epsilon \hat{a}^{\dagger 2})\right], \quad (4.42)$$

where $\epsilon = se^{2i\phi}$, with the *squeezing parameter* s and the *squeezing angle* ϕ . Throughout this work we do not require a squeezing angle and therefore we fix $\epsilon = s$. Using definition (4.42) we can generate an arbitrary squeezed state from “squeezing the vacuum” and then displacing it, i.e.

$$|\alpha, s\rangle = D(\alpha)S(s)|0\rangle. \quad (4.43)$$

We discuss the optimal implementation of the squeezing operator in Sec. 4.4.4.

The expansion of the squeezed vacuum state in the Fock basis reads

$$S(s)|0\rangle = \frac{1}{\sqrt{\cosh s}} \sum_{n=0}^{\infty} \frac{\sqrt{(2n)!}}{2^n n!} \tanh^n s |2n\rangle. \quad (4.44)$$

We notice that the squeezed state contains only even Fock states. This becomes clear in Sec. 4.4 where the optical implementation of the squeezing operation is explained. The

mean number of photons of the squeezed vacuum state can be calculated using Eq. (4.44) and reads

$$\langle n \rangle = \sinh^2 r. \quad (4.45)$$

An alternative way to compute the latter is presented in Sec. 5.1 which treats Gaussian states.

4.4. Optical transformations

In this section we present the mode transformations that are of relevance for this thesis and can be implemented by optical elements. First, we shall discuss transformations that are passive (photon number preserving) and stem from linear optics, and then move to an example of an active (non-photon number preserving) operation that requires non-linear effects. We discuss the transformations on the level of the annihilation and creation operators, as well as the quadrature operators, respectively. Therefore, we work in the Heisenberg picture in which the time dependence is incorporated in the operators and the state-vectors are time-independent. The Heisenberg equation of motion of an operator A which has no explicit time dependence reads

$$\frac{dA}{dt} = \frac{i}{\hbar} [\hat{H}, A]. \quad (4.46)$$

For a given Hamiltonian \hat{H} this equation will lead to the transformation of the mode operators.

4.4.1. Phase shift

Let us start with the most simple single-mode passive transformation given by the Hamiltonian of the free field stated in Eq. (4.11) for a single-mode i.e.

$$\hat{H}_\phi = \hbar\omega\hat{a}^\dagger\hat{a}. \quad (4.47)$$

This Hamiltonian corresponds to the transmission of the field mode through free space without interaction with any medium. We shall see that the free oscillation of the field for a time duration Δt will lead to a phase shift. Equation (4.46) leads to the differential equation

$$\frac{d\hat{a}}{dt} = \frac{i}{\hbar} [\hat{H}_\phi, \hat{a}] = -i\omega\hat{a}. \quad (4.48)$$

With the initial condition that $\hat{a} = \hat{a}_{\text{in}}$ at $t = 0$ the solution to Eq. (4.48) reads

$$\hat{a}_{\text{out}} = \hat{a}_{\text{in}} e^{-i\phi}, \quad (4.49)$$

where $\phi = \omega\Delta t$ for an interaction time Δt . Equivalently, one obtains $\hat{a}_{\text{out}}^\dagger = \hat{a}_{\text{in}}^\dagger e^{i\phi}$. Solving the equation of motion for the quadrature operators \hat{q} and \hat{p} leads to the transformation

$$\begin{pmatrix} \hat{q}_{\text{out}} \\ \hat{p}_{\text{out}} \end{pmatrix} = \begin{pmatrix} \cos \phi & \sin \phi \\ -\sin \phi & \cos \phi \end{pmatrix} \begin{pmatrix} \hat{q}_{\text{in}} \\ \hat{p}_{\text{in}} \end{pmatrix}. \quad (4.50)$$

4. Quantum Optics

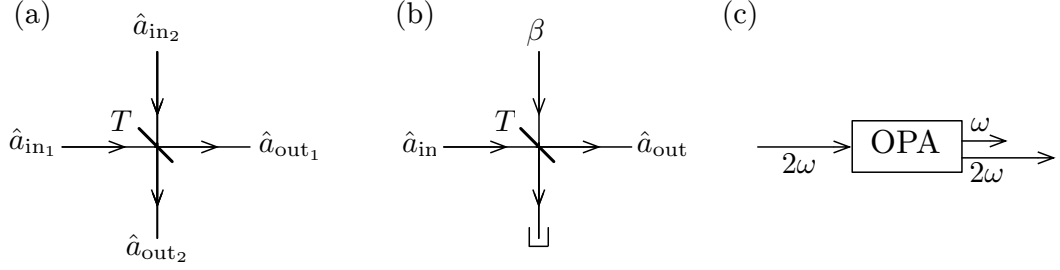


Figure 4.1.: Optical transformations: (a) Beamsplitter operation. (b) Implementation of the displacement operator by mixing an input field mode with operator \hat{a}_{in} with a classical coherent state $|\beta\rangle$ with $\beta = \alpha/\sqrt{1-T}$ and $|\beta| \gg 1$. (c) “Photon splitting” using optical parametric amplification.

We conclude that the phase shift corresponds to a rotation of the quadrature operators in phase space.

4.4.2. Beamsplitter

A fundamental passive two mode operation is the beamsplitter, which physically corresponds for instance to a plate of glass with a thin coating of aluminum. It mixes two incoming modes with mode operators \hat{a}_{in1} and \hat{a}_{in2} leading to output operators \hat{a}_{out1} and \hat{a}_{out2} [see Fig. 4.1 (a)]. The corresponding interaction Hamiltonian reads

$$\hat{H}_{BS} = \hbar\omega(e^{-i\beta}\hat{a}_2^\dagger\hat{a}_1 + e^{i\beta}\hat{a}_1^\dagger\hat{a}_2), \quad (4.51)$$

where β is the relative phase of the two modes. The Heisenberg equation of motion (4.46) leads to the system of differential equations

$$\begin{aligned} \frac{d\hat{a}_1}{dt} &= \frac{i}{\hbar}[\hat{H}_{BS}, \hat{a}_1] = -ie^{i\beta}\omega\hat{a}_2, \\ \frac{d\hat{a}_2}{dt} &= \frac{i}{\hbar}[\hat{H}_{BS}, \hat{a}_2] = -ie^{-i\beta}\omega\hat{a}_1. \end{aligned} \quad (4.52)$$

The solution to this system of equations reads

$$\begin{pmatrix} \hat{a}_{out1} \\ \hat{a}_{out2} \end{pmatrix} = \begin{pmatrix} \cos\phi & -ie^{i\beta}\sin\phi \\ -ie^{-i\beta}\sin\phi & \cos\phi \end{pmatrix} \begin{pmatrix} \hat{a}_{in1} \\ \hat{a}_{in2} \end{pmatrix}, \quad (4.53)$$

where $\phi = \omega\Delta t$, with interaction duration Δt . A physical beamsplitter is usually described with $\beta = 0$ or $\beta = \pi/2$, where we shall choose the latter. The beamsplitter transmissivity $T \in [0, 1]$ is simply given by $T = \cos^2(\phi)$. The four quadrature operators grouped in the vector $\hat{\mathbf{R}}_{in} = (\hat{q}_{in,1}, \hat{q}_{in,2}, \hat{p}_{in,1}, \hat{p}_{in,2})^\top$ are transformed by the beamsplitter as

$$\hat{\mathbf{R}}_{out} = \left[\begin{pmatrix} \sqrt{T} & \sqrt{1-T} \\ -\sqrt{1-T} & \sqrt{T} \end{pmatrix} \oplus \begin{pmatrix} \sqrt{T} & \sqrt{1-T} \\ -\sqrt{1-T} & \sqrt{T} \end{pmatrix} \right] \hat{\mathbf{R}}_{in}, \quad (4.54)$$

where $\hat{\mathbf{R}}_{out} = (\hat{q}_{out,1}, \hat{q}_{out,2}, \hat{p}_{out,1}, \hat{p}_{out,2})^\top$.

4.4.3. Displacement

An important application of the beamsplitter is the implementation of the displacement operator defined in Eq. (4.33). Mixing the input field mode with operator \hat{a}_{in} with a (classical) bright coherent state $|\beta\rangle$, $|\beta| \gg 1$, on a beamsplitter with transmissivity T yields according to Eq. (4.53) [see Fig. 4.1 (b)]

$$\hat{a}_{\text{out}} = \sqrt{T}\hat{a}_{\text{in}} + \sqrt{1-T}\beta. \quad (4.55)$$

If one now fixes $\beta = \frac{\alpha}{\sqrt{1-T}}$ for the given transmissivity then Eq. (4.55) simplifies to

$$\hat{a}_{\text{out}} = \sqrt{T}\hat{a}_{\text{in}} + \alpha. \quad (4.56)$$

We observe that the latter indeed realizes the displacement stated in Eq. (4.35) in the limit of perfect transmission $T \rightarrow 1$. However, in this limit the amplitude of the bright coherent state diverges to infinity. Therefore, in practical implementations there will be a tradeoff between the tuning of the transmissivity and the intensity of the classical state.

4.4.4. One-mode squeezing

The non-photon number preserving operation that is of great relevance in the following is the one-mode squeezing operation. Its implementation requires a non-linear dielectric medium, i.e. a medium where the relation between the polarization \mathbf{P} and the electric field \mathbf{E} is non-linear. In general, the polarization can be expanded as

$$\mathbf{P} \propto \chi^{(1)}\mathbf{E} + \chi^{(2)}\mathbf{E}^2 + \chi^{(3)}\mathbf{E}^3 + \dots, \quad (4.57)$$

where $\chi^{(n)}$ is the n th order susceptibility of the medium. A non-linear medium has terms that are proportional to $\chi^{(2)}$ and higher, where we restrict ourselves now to cases where quadratic terms are dominant and higher orders are negligible. Second order non-linearities can be used to generate a higher frequency $\omega_3 = \omega_2 + \omega_1$ when pumping a non-linear crystal with an intense beam of lower frequency ω_2 and idler ω_1 (“photon combining”). Another second order effect is “photon splitting”, i.e. the generation of two lower frequencies ω_1 and ω_2 out of one high frequency ω_3 . The latter is also referred to as “optical parametric amplification” (OPA) [see Fig. 4.1 (c)]. By choosing $\omega_3 = 2\omega$ one can generate two photons with frequencies ω out of one photon with frequency 2ω (by conservation of energy) [see Ref. [ST91] for details]. This realizes the Hamiltonian

$$\hat{H}_{\text{SQ}} = \hbar\omega(e^{-i\beta}\hat{a}^2 + e^{i\beta}\hat{a}^{\dagger 2}), \quad (4.58)$$

which leads after solving Eq. (4.46) to

$$\hat{a}_{\text{out}} = \cosh(r)\hat{a}_{\text{in}} - ie^{-i\beta} \sinh(r)\hat{a}_{\text{in}}^{\dagger}, \quad (4.59)$$

4. Quantum Optics

where $r = 2\omega\Delta t$ is the squeezing parameter. We fix here without loss of generality the phase to $\beta = 3\pi/2$ which yields the relations for the quadratures

$$\begin{pmatrix} \hat{q}_{\text{out}} \\ \hat{p}_{\text{out}} \end{pmatrix} = \begin{pmatrix} e^r & 0 \\ 0 & e^{-r} \end{pmatrix} \begin{pmatrix} \hat{q}_{\text{in}} \\ \hat{p}_{\text{in}} \end{pmatrix}. \quad (4.60)$$

Note that the squeezing parameter r here can be negative which is equivalent to a squeezing parameter $|r|$ and a phase $\beta = \pi/2$. For simplicity and without loss of generality we assume for the following that $r \in \mathbb{R}$ and we omit all phases β . Equation (4.60) shows the physical action of the one-mode squeezing operation. The variance of the p -quadrature is reduced and due to the Heisenberg uncertainty relation the variance of the q -variance is increased by the inverse factor. We refer to this reduction of variance as “squeezing of the quadrature (or quantum state)”.

4.5. Phase-space Representation

As we shall see in the following this work is focused on the information encoding in the field’s quadratures. For this reason we now introduce a useful formalism to describe those operators, namely the *phase-space* representation. This representation is comparable to the phase-space formalism known from classical mechanics. Whilst in classical mechanics a single point (q, p) describes the position q and momentum p of the system without uncertainty, an ensemble of particles with positions q_i and momenta p_i is described by a distribution function, as e.g. Liouville’s phase-space distribution. This corresponds to the properties of a quantum mechanical system, where due to Heisenberg’s uncertainty principle, a single measurement outcome (q, p) of the quadrature observables \hat{Q}, \hat{P} does not give any information of the system’s state. Quantum mechanics is a statistical theory and therefore requires many measurements of the same state in order to characterize it. Thus, it needs to be described by a distribution function just like an ensemble of particles in classical mechanics. In case of the phase-space this distribution is called *Wigner function* and can be regarded as a quasi-probability distribution. For a single mode of the field in the quantum state $\hat{\rho}$ the Wigner function reads (the definitions in this section are taken from [Bra05b, KL10])

$$W(q, p) = \frac{1}{2\pi\hbar} \int_{-\infty}^{\infty} dy e^{iyp/\hbar} \langle q - y/2 | \hat{\rho} | q + y/2 \rangle, \quad (4.61)$$

where q and p denote the coordinates in the phase space. The Wigner function completely characterizes the state $\hat{\rho}$ and vice versa. It can take negative values (e.g. for the Fock state $|1\rangle\langle 1|$), but is regarded as a quasi-probability distribution because it is properly normalized, i.e.

$$\int dq dp W(q, p) = 1, \quad (4.62)$$

and yields the proper marginal distributions

$$\int_{-\infty}^{\infty} W(q, p) dq = \langle p | \hat{\rho} | p \rangle, \quad \int_{-\infty}^{\infty} W(q, p) dp = \langle q | \hat{\rho} | q \rangle. \quad (4.63)$$

The Wigner function $W_d(q, p)$ of a displaced state $\hat{D}(\alpha)\hat{\rho}\hat{D}^\dagger(\alpha)$ is found using Eqs. (4.34) and (4.37):

$$\begin{aligned} W_d(q, p) &= \frac{1}{2\pi\hbar} \int_{-\infty}^{\infty} dy e^{iyp/\hbar} \langle q - y/2 | \hat{D}(\alpha)\hat{\rho}\hat{D}^\dagger(\alpha) | q + y/2 \rangle, \\ &= W(q - \sqrt{2\hbar}\Re(\alpha), p - \sqrt{2\hbar}\Im(\alpha)). \end{aligned} \quad (4.64)$$

This means that the displacement operator $\hat{D}(\alpha)$ leads to a translation (with opposite sign) of $-\sqrt{2\hbar}\alpha$ of the Wigner function in phase space.

We consider in the following a canonical quantum system that consists of n bosonic field modes. Each mode with quadrature operators \hat{q}_i and \hat{p}_i lives in an infinite dimensional Hilbert space \mathcal{H}_i spanned by Fock states $\{|n_i\rangle\}$. The total Hilbert space of the n -mode system is therefore given by

$$\mathcal{H} = \bigotimes_{i=1}^n \mathcal{H}_i. \quad (4.65)$$

We group the $2n$ quadrature operators together in one vector

$$\hat{\mathbf{R}}^{(\text{qq})} = (\hat{q}_1, \hat{q}_2, \dots, \hat{q}_n, \hat{p}_1, \hat{p}_2, \dots, \hat{p}_n)^\top. \quad (4.66)$$

Note that this ordering of operators is not unique and sometimes it may be more convenient to choose the alternative grouping

$$\hat{\mathbf{R}}^{(\text{qp})} = (\hat{q}_1, \hat{p}_1, \hat{q}_2, \hat{p}_2, \dots, \hat{q}_n, \hat{p}_n)^\top. \quad (4.67)$$

With the definition of the *symplectic* (or *commutation*) matrix

$$\mathbf{\Omega} = \begin{pmatrix} \mathbb{O}_{n \times n} & \mathbb{I}_{n \times n} \\ -\mathbb{I}_{n \times n} & \mathbb{O}_{n \times n} \end{pmatrix}, \quad (4.68)$$

the commutation relation given in Eq. (4.16) can for the dimensionless operators $\{\hat{q}_i, \hat{p}_j\}$ now be expressed as

$$[\hat{\mathbf{R}}_k^{(\text{qq})}, \hat{\mathbf{R}}_{k+n}^{(\text{qq})}] = i\mathbf{\Omega}_{k, k+n}. \quad (4.69)$$

For the alternative grouping $\hat{\mathbf{R}}^{(\text{qp})}$ the commutation matrix reads

$$\mathbf{\Omega}^{(\text{qp})} = \bigoplus_{i=1}^n \begin{pmatrix} 0 & 1 \\ -1 & 0 \end{pmatrix}, \quad (4.70)$$

4. Quantum Optics

and the commutation relations can be expressed as

$$[\hat{\mathbf{R}}_k^{(\text{qp})}, \hat{\mathbf{R}}_j^{(\text{qp})}] = i\Omega_{k,j}^{(\text{qp})}. \quad (4.71)$$

Throughout this thesis we use the convention $\hat{\mathbf{R}} = \hat{\mathbf{R}}^{(\text{qq})}$ unless stated otherwise. Furthermore, we fix from now on

$$\hbar = 1, \quad (4.72)$$

in order to simplify notations.

5. Gaussian states and operations

5.1. Gaussian states

The set of states that is of central interest in this work are the *Gaussian states*. They are highly relevant to experimentalists, since they model very well the state that exits a laser (= *coherent state*) and e.g. a the state of coherent light after having travelled through atmospheric fluctuations (= *thermal state*). Gaussian states, though having a density operator that lives in an infinite dimensional Hilbert space, have a very simple description in the phase space. Namely, the Wigner function of an n -mode Gaussian state $\hat{\rho}^G(\mathbf{d}, \mathbf{V})$ is given by the multi-variate Gaussian distribution (definitions and examples of this section can be found in [Bra05b, WPGP⁺12])

$$W(\mathbf{R}) = \frac{1}{(2\pi)^n \sqrt{\det \mathbf{V}}} \exp \left\{ -\frac{1}{2} (\mathbf{R} - \mathbf{d})^\top \mathbf{V}^{-1} (\mathbf{R} - \mathbf{d}) \right\}, \quad (5.1)$$

where $\mathbf{R} \in \mathbb{R}^{2n}$ are the real coordinates in the phase space, \mathbf{d} are the $2n$ first moments and \mathbf{V} is the $2n \times 2n$ covariance matrix (CM) defined as

$$\begin{aligned} \mathbf{d} &= \langle \hat{\mathbf{R}} \rangle = \text{Tr}[\hat{\rho} \hat{\mathbf{R}}], \\ V_{kj} &= \frac{1}{2} \langle \{ (\hat{\mathbf{R}}_k - \mathbf{d}_k), (\hat{\mathbf{R}}_j - \mathbf{d}_j) \} \rangle = \frac{1}{2} \text{Tr}[\hat{\rho} \{ (\hat{\mathbf{R}}_k - \mathbf{d}_k), (\hat{\mathbf{R}}_j - \mathbf{d}_j) \}]. \end{aligned} \quad (5.2)$$

In Eq. (5.2) the brackets $\{A, B\}$ denote the anti-commutator $\{A, B\} = AB + BA$. The Heisenberg uncertainty principle imposes a constraint on the CM of the Gaussian states, namely it has to fulfill

$$\mathbf{V} + \frac{i}{2} \boldsymbol{\Omega} \geq 0, \quad (5.3)$$

in order to correspond to a physical state. In the following we list a set of particular Gaussian states.

Vacuum state

The simplest quantum state is the vacuum state $|0\rangle$. It is (also) a Gaussian state and has in the case of an n -mode state the covariance matrix

$$\mathbf{V} = \frac{1}{2} \begin{pmatrix} \mathbb{I} & 0 \\ 0 & \mathbb{I} \end{pmatrix}. \quad (5.4)$$

The vacuum is the fundamental resource to generate any Gaussian state. We plot its Wigner function in Fig. 5.1 (a) and its variances schematically in Fig. 5.2 (a).

5. Gaussian states and operations

Wigner functions of Gaussian states

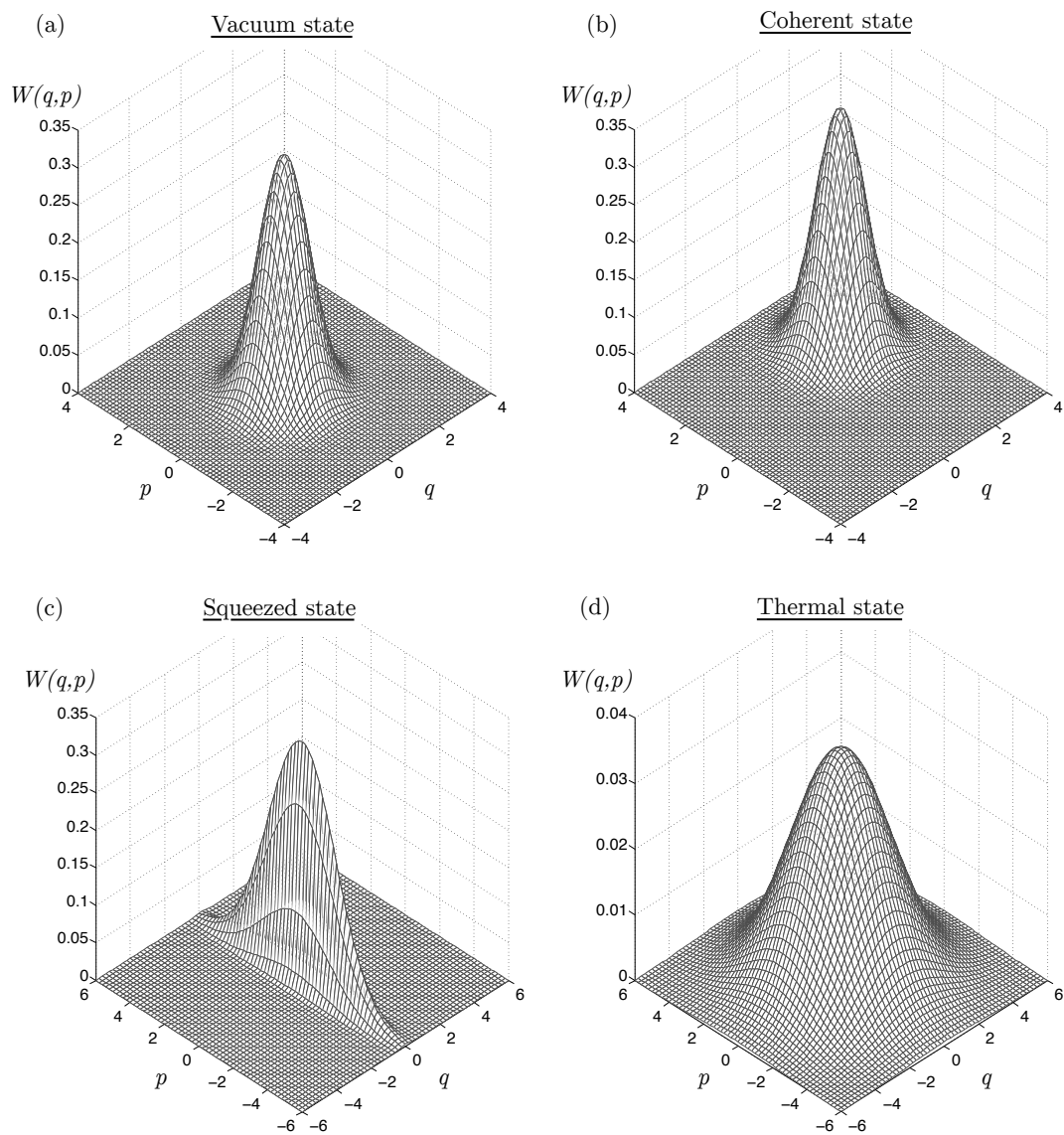


Figure 5.1.: Wigner functions of Gaussian states: (a) Vacuum state. (b) Coherent state (i.e. displaced vacuum state) with $\alpha = 1 + i1$, centered at $(\sqrt{2}, \sqrt{2})$. (c) Squeezed state with $s = 1$, centered at $(0, 0)$. (d) Thermal state with $M_{\text{env}} = 5$, centered at $(0, 0)$.

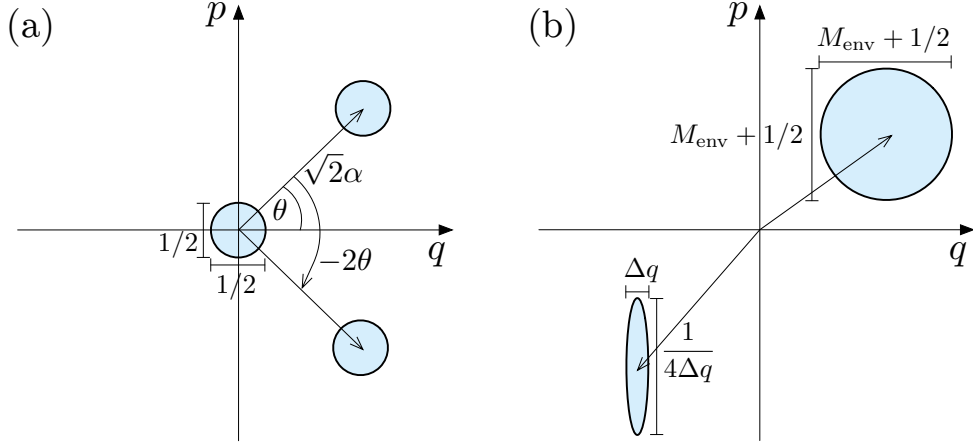


Figure 5.2.: Schematic plot of Wigner functions in phase space. The circles and ellipses represent the covariances of the corresponding Wigner functions: (a) one-mode vacuum state with equal variances $\Delta\hat{q} = \Delta\hat{p} = 1/2$ centered at $(0, 0)$, coherent state $|\alpha\rangle$ obtained by applying the displacement operator $\hat{D}(\alpha)$ to the vacuum and the same coherent state after phase rotation of -2θ . (b) Thermal state with equal variances $M_{\text{env}} + 1/2$ and squeezed state satisfying $\Delta\hat{p} = 1/(4\Delta\hat{q})$.

Coherent state

We introduced the coherent state already in Sec. 4.3.2. It is obtained by displacing the vacuum state. Since the displacement operator only changes the first moment of the state the covariance matrix remains invariant, so it is again given by Eq. (5.4). An example of the Wigner function of a coherent state is depicted in Fig. 5.1 (b) and we plot the variances schematically in Fig. 5.2 (a).

Squeezed state

The squeezed state introduced in Sec. 4.3.3 is also a Gaussian state. It is obtained by squeezing (and optionally displacing) the vacuum. In the case of one-mode its covariance matrix is given by

$$\mathbf{V} = \frac{1}{2} \begin{pmatrix} e^{2s} & 0 \\ 0 & e^{-2s} \end{pmatrix}, \quad (5.5)$$

where s is the squeezing parameter. We depict the Wigner function of a squeezed state in Fig. 5.1 (c) and its variances schematically in Fig. 5.2 (b).

Thermal state

A one-mode thermal state (sometimes referred to as “gauge-invariant” [HSH99, HW01]) $\hat{\rho}^{\text{th}}$ is the output of a one-mode *thermal Gaussian channel* when injecting vacuum (or a

5. Gaussian states and operations

coherent state). Those channels will be introduced and intensively discussed in Sec. 5.3. The expansion of a thermal state in the Fock basis reads [Hol98a]

$$\hat{\rho}_{M_{\text{env}}}^{\text{th}} = \frac{1}{M_{\text{env}} + 1} \sum_{n=0}^{\infty} \left(\frac{M_{\text{env}}}{M_{\text{env}} + 1} \right)^n |n\rangle \langle n|. \quad (5.6)$$

We state from [Hol98a] that the thermal state has the maximal von Neumann entropy among all density operators $\hat{\rho}$ satisfying

$$\text{Tr}[\hat{\rho} \hat{a}^\dagger \hat{a}] \leq M_{\text{env}}, \quad M_{\text{env}} \geq 0. \quad (5.7)$$

Since $\hat{a}^\dagger \hat{a}$ is the number operator M_{env} is the maximal mean number of photons of the state. The CM of $\hat{\rho}_{M_{\text{env}}}^{\text{th}}$ is simply given by

$$\mathbf{V}_{\text{th}} = \begin{pmatrix} M_{\text{env}} + \frac{1}{2} & 0 \\ 0 & M_{\text{env}} + \frac{1}{2} \end{pmatrix}. \quad (5.8)$$

An example of the Wigner function of a thermal state is shown in Fig. 5.1 (d) and its variances are depicted schematically in Fig. 5.2 (b).

Thermal photon number and mean photon number

For the following it will be useful to distinguish two different quantities of an n -mode Gaussian state with CM \mathbf{V} and mean $\mathbf{d} = 0$. The first quantity is the *mean photon number* \bar{N} which can be directly calculated by the trace of the CM, i.e.

$$\bar{N} = \frac{1}{2n} \text{Tr}[\mathbf{V}] - \frac{1}{2}, \quad (5.9)$$

where we do not count the number of photons of the vacuum. Interestingly, the determinant of the CM yields another useful quantity, namely the *number of thermal photons* given by

$$M_{\text{env}} = \sqrt[2n]{\det \mathbf{V}} - \frac{1}{2}. \quad (5.10)$$

The thermal photons of a Gaussian state may be regarded as a *measure of purity*, since for a pure state $M_{\text{env}} = 0$. In the case of the thermal state we have $\bar{N} = M_{\text{env}}$, i.e. all photons account for its temperature. Consider the example of a squeezed thermal state with CM

$$\mathbf{V} = \left(M_{\text{env}} + \frac{1}{2} \right) \begin{pmatrix} e^{2s} & 0 \\ 0 & e^{-2s} \end{pmatrix}, \quad s \in \mathbb{R}. \quad (5.11)$$

The number of thermal photons M_{env} remains invariant under the squeezing, however the mean photon number becomes now a function of the squeezing:

$$\bar{N} = \left(M_{\text{env}} + \frac{1}{2} \right) \cosh(2s) - \frac{1}{2}. \quad (5.12)$$

Two-mode squeezed vacuum

An important two-mode Gaussian state that is widely used in continuous variable quantum information (see Ref. [WPGP⁺12] for examples) due to its entanglement properties is the *two-mode squeezed vacuum* (TMSV). It can be generated by applying a two-mode squeezer (TMS) to the vacuum state, which will be introduced in Sec. 5.2.2. The covariance matrix of the two-mode squeezed vacuum state reads

$$\mathbf{V}_{\text{TMSV}} = \frac{1}{2} \begin{pmatrix} \cosh(2s) & \sinh(2s) & 0 & 0 \\ \sinh(2s) & \cosh(2s) & 0 & 0 \\ 0 & 0 & \cosh(2s) & -\sinh(2s) \\ 0 & 0 & -\sinh(2s) & \cosh(2s) \end{pmatrix}. \quad (5.13)$$

In the limit of infinite squeezing, i.e. $s \rightarrow \infty$ this state becomes an *EPR state*, which was first discussed in 1935 by Einstein, Podolski and Rosen [EPR35]. In this limit the q -quadratures become perfectly correlated and the p -quadratures perfectly anti-correlated, i.e.

$$\lim_{s \rightarrow \infty} \Delta(\hat{q}_1 - \hat{q}_2) = \lim_{s \rightarrow \infty} \Delta(\hat{p}_1 + \hat{p}_2) = 0. \quad (5.14)$$

This limit however, is unphysical, since the corresponding state would carry an infinite number of photons.

5.2. Gaussian operations

Gaussian operations are those quantum operations that map Gaussian states to Gaussian states. They are highly relevant to experimentalists since they are easily accessible in the laboratory. This is one of the main motivations for the use of Gaussian states in quantum information science. Gaussian states are fully characterized by their first and second moments and therefore, Gaussian operations are fully defined by their action on both moments.

5.2.1. Gaussian unitary operations

A particular set of Gaussian operations are those that are reversible, i.e. *Gaussian unitary operations* \hat{U}_G [Bra05b, WPGP⁺12]. The action $\hat{U}_G \hat{\rho}^G(\mathbf{d}_{\text{in}}, \mathbf{V}_{\text{in}}) \hat{U}_G^\dagger$ corresponds to a *symplectic transformation* $\mathbf{M} \in \text{Sp}(2n, \mathbb{R})$ acting on the first and second moment $\mathbf{d}_{\text{in}}, \mathbf{V}_{\text{in}}$ and reads

$$\begin{aligned} \mathbf{d}_{\text{out}} &= \mathbf{M} \mathbf{d}_{\text{in}}, \\ \mathbf{V}_{\text{out}} &= \mathbf{M} \mathbf{V}_{\text{in}} \mathbf{M}^\top, \end{aligned} \quad (5.15)$$

which furthermore satisfies the relation

$$\mathbf{M} \mathbf{\Omega} \mathbf{M}^\top = \mathbf{\Omega}, \quad (5.16)$$

5. Gaussian states and operations

in order to preserve the canonical commutation relations. All symplectic transformations satisfy $\det \mathbf{M} = 1$ but only *passive* ones (i.e. photon-number preserving) fulfill in addition $\mathbf{M}\mathbf{M}^\top = \mathbb{I}$.

An important property of symplectic transformations is Williamson's theorem [SCS99]. It states that for a Gaussian state with CM \mathbf{V} there exists a symplectic transformation \mathbf{M} which realizes a *symplectic diagonalization*, i.e.

$$\mathbf{M}\mathbf{V}\mathbf{M}^\top = \text{diag}(\nu_1, \nu_2, \dots, \nu_n; \nu_1, \nu_2, \dots, \nu_n), \quad (5.17)$$

such that the Gaussian state with CM $\mathbf{M}\mathbf{V}\mathbf{M}^\top$ is a tensor product of thermal states with CM $\mathbf{V}_{\text{th}_i} = \text{diag}(\nu_i, \nu_i)$. The values ν_i are called *symplectic eigenvalues* and are the doubly degenerate eigenvalues of the matrix $|i\Omega\mathbf{V}|$, where $|\mathbf{A}|$ stands for $\sqrt{\mathbf{A}^\dagger\mathbf{A}}$.

Heisenberg's uncertainty relation (5.3) implies

$$\nu_i \geq \frac{1}{2}, \quad \forall i = 1, \dots, n. \quad (5.18)$$

Note that since $\det \mathbf{M} = 1$, the symplectic eigenvalues are invariant under symplectic transformations \mathbf{M} , i.e.

$$\det \mathbf{V} = \det (\mathbf{M}\mathbf{V}\mathbf{M}^\top) = \prod_{i=1}^n \nu_i^2. \quad (5.19)$$

As we show in Appendix B the entropy of an n -mode Gaussian state is given by

$$S(\hat{\rho}^{\text{G}}(\mathbf{d}, \mathbf{V})) = S(\mathbf{V}) = \sum_{i=1}^n g\left(\nu_i - \frac{1}{2}\right), \quad (5.20)$$

where

$$g(x) = \begin{cases} (x+1) \log_2(x+1) - x \log_2(x), & x > 0, \\ 0, & x = 0. \end{cases} \quad (5.21)$$

We remark that for a thermal state $\hat{\rho}_{M_{\text{env}}}^{\text{th}}$ the entropy is given by $S(\hat{\rho}^{\text{th}}) = g(M_{\text{env}})$.

Now we present particular Gaussian unitary operations that are essential to many physical setups. Three important one-mode operations were in fact already presented in Sec. 4.4: the phase shift, displacement and one-mode squeezing operations all preserve the ‘‘Gaussianity’’ of a quantum state and we present them now in terms of their action on the mean and covariance matrix.

Rotation in phase space

The phase shift introduced in Sec. 4.4.1 corresponds to a rotation in the phase space. The symplectic transformation was already derived in Eq. (4.50), i.e. ¹

$$\mathbf{O}(\theta) = \begin{pmatrix} \cos \theta & -\sin \theta \\ \sin \theta & \cos \theta \end{pmatrix}. \quad (5.22)$$

Note that in the following we use often the notation $\Theta = \mathbf{O}(\theta)$. The action of the phase shift in the phase space is depicted in Fig. 5.2 (a).

¹We use here the usual convention for the rotation matrix, which corresponds to changing the rotation angle in Eq. (4.50) by $\theta \rightarrow -\theta$.

Beamsplitter

The beamsplitter transformation was introduced in Sec. 4.4.2 and its symplectic transformation stated in Eq. (4.54), i.e.

$$\mathbf{M}_{\text{BS}} = \begin{pmatrix} \sqrt{T} & \sqrt{1-T} & 0 & 0 \\ -\sqrt{1-T} & \sqrt{T} & 0 & 0 \\ 0 & 0 & \sqrt{T} & \sqrt{1-T} \\ 0 & 0 & -\sqrt{1-T} & \sqrt{T} \end{pmatrix}. \quad (5.23)$$

If one compares the latter with Eq. (5.22) and $T = \arccos(\theta)$ one confirms that it corresponds to a rotation matrix applied to two modes (leaving the $q-p$ correlations invariant). Since it preserves the photon number of the input state it is a passive transformation and therefore satisfies $\mathbf{M}_{\text{BS}}\mathbf{M}_{\text{BS}}^{\text{T}} = \mathbb{I}$.

Displacement

We already described in Sec. 4.3.2 the action of the displacement operator $\hat{D}(\alpha)$. Namely, it “displaces the vacuum” by the complex number α and generates a coherent state. As stated in Eq. (4.36) (here $\hbar = 1$) this shifts the quadratures by $\sqrt{2}\alpha$ as shown in Fig. 5.2 (a).

One-mode squeezer

The symplectic transformation of the one-mode squeezing operation was already stated in Eq. (4.60), i.e.

$$\mathbf{S}(s) = \begin{pmatrix} e^s & 0 \\ 0 & e^{-s} \end{pmatrix}. \quad (5.24)$$

Note that in the following, we sometimes omit the explicit dependence on s , namely, we use the notation $\mathbf{S} = \mathbf{S}(s)$ and consequently $\mathbf{S}^{-1} = \mathbf{S}(-s)$. The action of the one-mode squeezer is schematically shown in Fig. 5.2 (b). The one-mode squeezing operation is essential in many optical schemes because it can be used to generate the previously introduced two-mode squeezed state.

5.2.2. General symplectic transformation

In [Bra05a] it was shown, that for an arbitrary symplectic transformation \mathbf{M} acting on n -modes there exists a *Bloch-Messiah decomposition*. This decomposition consists of a general n -mode interferometer Θ_1 (a rotation acting on n modes, also called “multi-port”)², a set of n individual one-mode squeezers $\mathbf{S}_i = \text{diag}(e^{s_i}, e^{-s_i})$ followed by another n -mode interferometer Θ_2 [see Fig. 5.3]. The equation therefore reads

$$\begin{aligned} \mathbf{M} &= \Theta_1 \mathbf{S} \Theta_2, \\ \mathbf{S} &= \text{diag}(e^{s_1}, e^{s_2}, \dots, e^{s_n}; e^{-s_1}, \dots, e^{-s_n}). \end{aligned} \quad (5.25)$$

²Note that we use for the n -mode rotation for simplicity the same notation as for the one-mode phase rotation.

5. Gaussian states and operations

Bloch-Messiah Decomposition

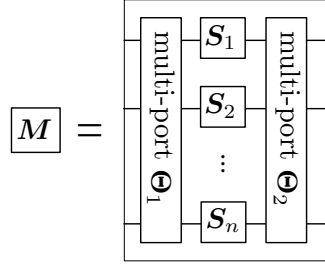


Figure 5.3.: Bloch-Messiah decomposition: Any symplectic transformation M can be decomposed into an n -mode interferometer Θ_1 , a set of n one-mode squeezers $\{S_i\}$ and another n -mode interferometer Θ_2 .

Two-Mode Squeezer

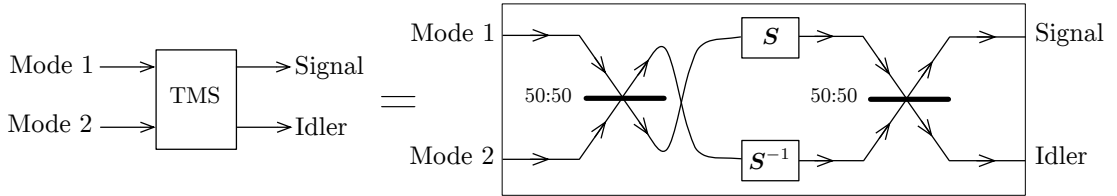


Figure 5.4.: Scheme of a two-mode squeezer (TMS) given by the Bloch-Messiah decomposition. The bold horizontal lines represent 50 : 50 beamsplitters and S and S^{-1} stand for a one-mode squeezer and a one-mode anti-squeezer with same squeezing parameter s . Note that the exits of the first beamsplitter are swapped.

Interferometers are passive transformations and therefore $M_{\Theta_1}^T M_{\Theta_1} = M_{\Theta_2}^T M_{\Theta_2} = \mathbb{I}$. We introduce in the following two important two-mode operations that are useful for many optical setups.

Two-mode squeezer

The two-mode squeezer (TMS) generates the two-mode squeezed vacuum state when fed with a two-mode vacuum state. It consists of a one-mode squeezer and a one-mode anti-squeezer (both with same squeezing value) and two 50 : 50 beamsplitters. The scheme is depicted in Fig 5.4, where we introduced the notion of the “signal” output for the first exit and the “idler” output for the second one. The TMS can be decomposed into three parts as follows: The first part corresponds to a transposed 50 : 50 beamsplitter, i.e. the exits are swapped. The second part consists of two individual single-mode squeezers, one with s and one with $-s$. Finally, the third part is a 50 : 50 beamsplitter. Using the transformation matrices for the beamsplitter (with $T = 1/2$) stated in Eq. (5.23) and

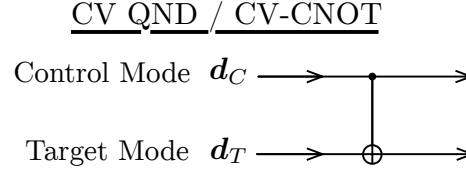


Figure 5.5.: Schematic scheme of the CV-QND gate. In a particular case of perfect interaction this becomes the CV-CNOT gate.

for the joint operation of the two one-mode squeezer stated in Eq. (5.25) (where $s_1 = s$ and $s_2 = -s$) we can compute the symplectic matrix of the TMS:

$$\begin{aligned}
 \mathbf{M}_{\text{TMS}} &= \mathbf{M}_{\text{BS}}^{\text{T}} (\mathbf{S} \oplus \mathbf{S}^{-1}) \mathbf{M}_{\text{BS}} \\
 &= \begin{pmatrix} \frac{1}{\sqrt{2}} & -\frac{1}{\sqrt{2}} & 0 & 0 \\ \frac{1}{\sqrt{2}} & \frac{1}{\sqrt{2}} & 0 & 0 \\ 0 & 0 & \frac{1}{\sqrt{2}} & -\frac{1}{\sqrt{2}} \\ 0 & 0 & \frac{1}{\sqrt{2}} & \frac{1}{\sqrt{2}} \end{pmatrix} \begin{pmatrix} e^s & 0 & 0 & 0 \\ 0 & e^{-s} & 0 & 0 \\ 0 & 0 & e^{-s} & 0 \\ 0 & 0 & 0 & e^s \end{pmatrix} \begin{pmatrix} \frac{1}{\sqrt{2}} & \frac{1}{\sqrt{2}} & 0 & 0 \\ -\frac{1}{\sqrt{2}} & \frac{1}{\sqrt{2}} & 0 & 0 \\ 0 & 0 & \frac{1}{\sqrt{2}} & \frac{1}{\sqrt{2}} \\ 0 & 0 & -\frac{1}{\sqrt{2}} & \frac{1}{\sqrt{2}} \end{pmatrix} \\
 &= \begin{pmatrix} \cosh(s) & \sinh(s) & 0 & 0 \\ \sinh(s) & \cosh(s) & 0 & 0 \\ 0 & 0 & \cosh(s) & -\sinh(s) \\ 0 & 0 & -\sinh(s) & \cosh(s) \end{pmatrix}.
 \end{aligned} \tag{5.26}$$

Using the latter one can easily confirm that $\mathbf{M}_{\text{TMS}} \frac{\mathbb{I}}{2} \mathbf{M}_{\text{TMS}}^{\text{T}}$ yields the covariance matrix of the two-mode squeezed state given by Eq. (5.13), hence the name “two-mode squeezer”. It will be useful for the following to use the parameter $G = \cosh^2(s)$. Then the transformation becomes

$$\mathbf{M}_{\text{TMS}} = \begin{pmatrix} \sqrt{G} & \sqrt{G-1} & 0 & 0 \\ \sqrt{G-1} & \sqrt{G} & 0 & 0 \\ 0 & 0 & \sqrt{G} & -\sqrt{G-1} \\ 0 & 0 & -\sqrt{G-1} & \sqrt{G} \end{pmatrix}. \tag{5.27}$$

The parameter G physically corresponds to a *gain*, since the TMS can be used to implement an amplification channel with gain G (see Sec. 5.3).

CV-CNOT gate

Another important two-mode operation is the continuous variable quantum non-demolition gate [Bra98] (CV-QND). It can be implemented via the interaction between polarized

5. Gaussian states and operations

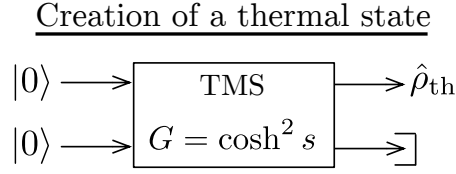


Figure 5.6.: Creation of a thermal state: Two vacuum modes are sent through a two-mode squeezer and one mode is “traced out”. The remaining state is a thermal state.

light and the total spin of an atomic cloud [FCP04]. In Fig. 5.5 the schematic representation of this gate is sketched. We group the first moments of the control mode $\mathbf{d}_C = (\mathbf{d}_{Cq}, \mathbf{d}_{Cp})^\top$ and of the target mode $\mathbf{d}_T = (\mathbf{d}_{Tq}, \mathbf{d}_{Tp})^\top$ in the vector

$$\mathbf{d}_{\text{in}} = (\mathbf{d}_{Cq}, \mathbf{d}_{Tq}, \mathbf{d}_{Cp}, \mathbf{d}_{Tp})^\top. \quad (5.28)$$

Then, the action of the symplectic matrix of the CV-QND M_{ND} reads

$$\mathbf{d}_{\text{out}} = M_{\text{ND}} \mathbf{d}_{\text{in}} = \begin{pmatrix} 1 & \kappa & 0 & 0 \\ 0 & 1 & 0 & 0 \\ 0 & 0 & 1 & 0 \\ 0 & 0 & -\kappa & 1 \end{pmatrix} \begin{pmatrix} \mathbf{d}_{Cq} \\ \mathbf{d}_{Tq} \\ \mathbf{d}_{Cp} \\ \mathbf{d}_{Tp} \end{pmatrix} = \begin{pmatrix} \mathbf{d}_{Cq} + \kappa \mathbf{d}_{Tq} \\ \mathbf{d}_{Tq} \\ \mathbf{d}_{Cp} \\ \mathbf{d}_{Tp} - \kappa \mathbf{d}_{Cp} \end{pmatrix}, \quad (5.29)$$

where $\kappa \geq 0$ is an interaction parameter. In the particular case $\kappa = 1$ the transformation M_{ND} becomes the continuous-variable analogue to the controlled-NOT gate³ (CV-CNOT) which will be very useful in this thesis.

5.2.3. Partial trace

Let us consider an arbitrary two-mode Gaussian state $\hat{\rho}_{AB}^G$ with CM

$$\mathbf{V}_{AB} = \begin{pmatrix} v^{QA} & v^{QAQB} & v^{QAPA} & v^{QAPB} \\ v^{QAQB} & v^{QB} & v^{QBPA} & v^{QBPB} \\ v^{QAPA} & v^{QBPA} & v^{PA} & v^{PAPB} \\ v^{QAPB} & v^{QBPB} & v^{PAPB} & v^{PB} \end{pmatrix}. \quad (5.30)$$

Applying the partial trace on the mode B (also called “tracing out” mode B) yields the reduced Gaussian state $\hat{\rho}_A^G$, i.e.

$$\hat{\rho}_A^G = \text{Tr}_B[\hat{\rho}_{AB}^G], \quad (5.31)$$

with 2×2 covariance matrix

$$\mathbf{V}_A = \begin{pmatrix} v^{QA} & v^{QAPA} \\ v^{QAPA} & v^{PA} \end{pmatrix}. \quad (5.32)$$

³The controlled-NOT gate, implemented by unitary U_{CNOT} , acts on a two qubit state as follows: $U_{\text{CNOT}} |c\rangle |t\rangle = |c\rangle |t \oplus c\rangle$, where $c, t \in \{0, 1\}$.

This rule can be straightforwardly generalized to Gaussian states of n -modes. However, for an n -mode state it is more convenient to choose the ordering $\hat{\mathbf{R}} = \hat{\mathbf{R}}^{(\text{qp})}$ defined in Eq. (4.67). Then, the CM of an n -mode bipartite state simply reads

$$\mathbf{V}_{AB}^{(\text{qp})} = \begin{pmatrix} \mathbf{V}_A^{(\text{qp})} & \mathbf{C} \\ \mathbf{C}^\top & \mathbf{V}_B^{(\text{qp})} \end{pmatrix}, \quad (5.33)$$

where $\mathbf{V}_A^{(\text{qp})}$ corresponds to the CM of system A , $\mathbf{V}_B^{(\text{qp})}$ to the CM of system B and the matrix \mathbf{C} contains the correlations between A and B . Tracing out system B corresponds simply to the reduction

$$\begin{pmatrix} \mathbf{V}_A^{(\text{qp})} & \mathbf{C} \\ \mathbf{C}^\top & \mathbf{V}_B^{(\text{qp})} \end{pmatrix} \xrightarrow[\text{over } B]{\text{partial trace}} \mathbf{V}_A^{(\text{qp})}, \quad (5.34)$$

such that the remaining state has the CM $\mathbf{V}_A^{(\text{qp})}$.

Note that the partial trace is not a unitary operation because one loses the information of the traced out system, and therefore it is not reversible. An example for the partial trace is depicted in Fig. 5.6. Two vacuum modes are sent through a TMS with gain G . Tracing out the second mode leads to a thermal state at the output. This is clear, since the output of the TMS is the two-mode squeezed state with CM stated in Eq. (5.13). Applying the above transformation leads to the reduced thermal state with CM

$$\mathbf{V}_{\text{th}} = \frac{1}{2} \begin{pmatrix} G & 0 \\ 0 & G \end{pmatrix}. \quad (5.35)$$

We observe that an infinitely entangled two-mode squeezed state would lead (after tracing out one mode) to a thermal state with an infinite number of thermal photons (or infinite temperature).

Partial measurement

Suppose we are given an $(n + 1)$ -mode state and we would like to measure the $n + 1$ st mode. With the ordering $\hat{\mathbf{R}} = \hat{\mathbf{R}}^{(\text{qp})}$ the CM can be written as

$$\mathbf{V}_{AB}^{(\text{qp})} = \begin{pmatrix} \mathbf{V}_A^{(\text{qp})} & \mathbf{C} \\ \mathbf{C}^\top & \mathbf{V}_B^{(\text{qp})} \end{pmatrix}, \quad (5.36)$$

where $\mathbf{V}_A^{(\text{qp})}$ is a $2n \times 2n$ CM, $\mathbf{V}_B^{(\text{qp})}$ a 2×2 CM and \mathbf{C} is of dimension $2n \times 2$. After the measurement of mode B the state will be reduced to an n -mode state whose covariance matrix depends on the type of measurement. We discuss in the following two standard measurement tools of quantum optics.

5. Gaussian states and operations

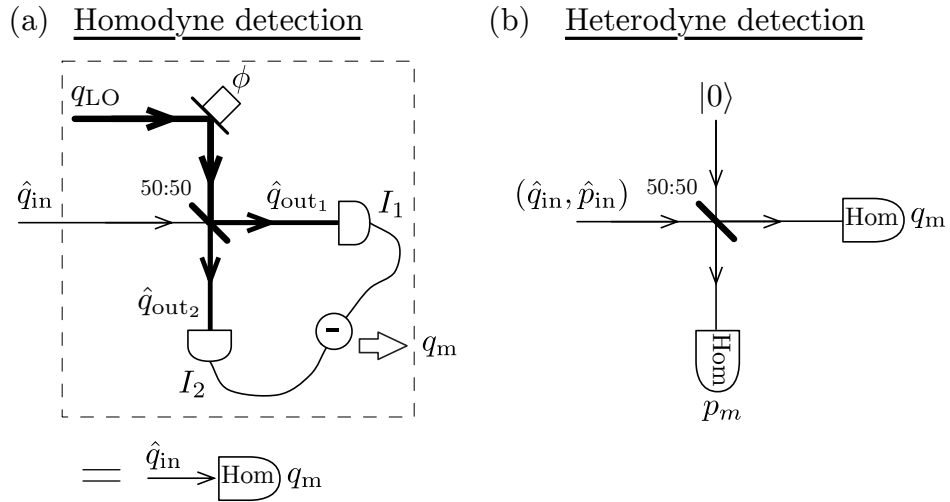


Figure 5.7.: (a) Homodyne detection: The input mode with quadrature \hat{q}_{in} is mixed on a 50 : 50 beamsplitter with a local oscillator with (classical) quadrature q_{LO} . The phase ϕ between the two incoming beams must be controlled (e.g. by using a piezoelectric crystal). The two outgoing beams enter two photodetectors that measure photocurrents I_1 and I_2 . Subtraction of the photocurrents enables the estimation of \hat{q}_{in} , i.e. leads to a measurement outcome q_m . In order to measure the conjugate quadrature \hat{p}_{in} the phase ϕ has to be shifted by $\pi/2$. (b) Heterodyne detection: The input mode is mixed on a 50 : 50 beamsplitter with a vacuum mode. The quadratures of the outgoing beam are then measured simultaneously by homodyne detections leading to outcomes q_m and p_m .

Homodyne detection

The quadratures of the electromagnetic field can be measured with the so-called *homodyne detection*⁴ [CLP07]. First, one mixes the Gaussian input state with quadratures $(\hat{q}_{\text{in}}, \hat{p}_{\text{in}})$ on a 50 : 50 beamsplitter with a classical coherent beam with quadrature q_{LO} (also called “local oscillator”). The fact that this beam is classical (with $\sim 10^9$ photons) allows us to choose without loss of generality $p_{\text{LO}} = 0$. The quadratures of two outgoing modes read (see Fig. 5.7)

$$\begin{aligned}\hat{q}_{\text{out}_1} &= (\hat{q}_{\text{in}} + q_{\text{LO}})/\sqrt{2}, \\ \hat{p}_{\text{out}_1} &= \hat{p}_{\text{in}}/\sqrt{2}, \\ \hat{q}_{\text{out}_2} &= (\hat{q}_{\text{in}} - q_{\text{LO}})/\sqrt{2}, \\ \hat{p}_{\text{out}_2} &= \hat{p}_{\text{in}}/\sqrt{2}.\end{aligned}\tag{5.37}$$

The photocurrents I_1 and I_2 of the two output beams are then measured by two identical high efficiency linear photodetectors. The difference of the photocurrents yields

$$I_1 - I_2 = c q_{\text{LO}} q_m,\tag{5.38}$$

where c is a constant. The intensity $c q_{\text{LO}}^2$ of the local oscillator can be measured without disturbing it, since it is classical. Then Eq. (5.38) leads to the measurement outcome of the quadrature \hat{q}_{in} denoted by q_m . The outcome of the conjugate quadrature \hat{p}_{in} is obtained in the same way but by introducing a phase shift $\phi = \pi/2$ to the local oscillator, such that it has classical quadratures $(0, p_{\text{LO}})$. The homodyne detection can be considered as a standard tool in continuous variable quantum information and has been implemented successfully with detection efficiencies of 90% [GVW⁺03, LDTBG05, ZVB04].

Now let us discuss how the covariance matrix of the general $(n+1)$ -mode Gaussian input state is transformed under a homodyne measurement. We choose again the ordering $\hat{\mathbf{R}} = \hat{\mathbf{R}}^{(\text{qp})}$ such that the CM reads as in Eq. (5.36), i.e.

$$\mathbf{V}_{AB}^{(\text{qp})} = \begin{pmatrix} \mathbf{V}_A^{(\text{qp})} & \mathbf{C} \\ \mathbf{C}^\top & \mathbf{V}_B^{(\text{qp})} \end{pmatrix}.\tag{5.39}$$

The homodyne measurement of mode B leads to the reduction [EP03]

$$\mathbf{V}_{AB}^{(\text{qp})} \rightarrow \mathbf{V}_A^{(\text{qp})} - \mathbf{C}(\tilde{\mathbf{X}}\mathbf{V}_B^{(\text{qp})}\tilde{\mathbf{X}})^{MP}\mathbf{C}^\top,\tag{5.40}$$

where $\tilde{\mathbf{X}} = \text{diag}(1, 0)$ and MP indicates the Moore-Penrose pseudo-inverse since the resulting matrix is no longer invertible⁵. Equation (5.40) is a limiting case of the general form stated in Eq. (C.3). Namely, it corresponds to the case when the CM \mathbf{V}_{in} in Eq. (C.3) becomes infinitely squeezed.

⁴We consider here only the ideal homodyne detection with perfect efficiency.

⁵For the case $M = \text{diag}(a, 0)$ the pseudo-inverse reads $M^{MP} = \text{diag}(1/a, 0)$.

5. Gaussian states and operations

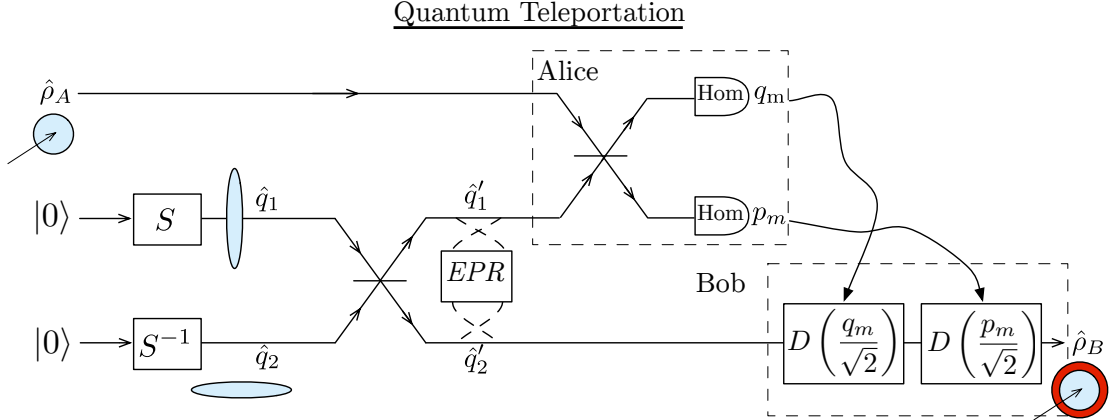


Figure 5.8.: Quantum teleportation: Alice receives an unknown state $\hat{\rho}_A$ and one half of an EPR pair (if $s \rightarrow \infty$). After two homodyne detections (corresponding to a Bell measurement) she sends the result to Bob. He applies two displacement operators (depending on the measurement outcome of Alice) on his half of the EPR pair, and thus teleporting Alice's state. In the case of perfect teleportation indeed $\hat{\rho}_A = \hat{\rho}_B$ holds. In general however, Bob's state will contain additional noise due to finite squeezing and imperfect homodyne detection.

Heterodyne detection

A heterodyne detection simply consists of two homodyne detections preceded by a balanced beamsplitter. The input mode is mixed with a vacuum mode and then both quadratures are measured simultaneously. Due to Heisenberg's uncertainty relation this leads to added noise to the quadratures outcomes. A heterodyne measurement of an $(n+1)$ -mode Gaussian state corresponds to the projection on the vacuum state. Namely, performing a homodyne measurement of mode B of the CM $\mathbf{V}_{AB}^{(\text{qp})}$ stated in Eq. (5.36) reads on the level of CM as

$$\mathbf{V}_{AB}^{(\text{qp})} \rightarrow \mathbf{V}_A^{(\text{qp})} - \mathbf{C} \left(\mathbf{V}_B^{(\text{qp})} + \frac{1}{2} \mathbb{I}_{2n \times 2n} \right)^{-1} \mathbf{C}^\top. \quad (5.41)$$

This follows directly from the general form of Gaussian operations (see Appendix C).

Quantum teleportation

The idea of *teleporting* the quantum state of a particle to the quantum state of another particle was theoretically proposed in [BBC⁺93] (see also the explanation in [NC00]). The scheme describes how the state of a spin- $\frac{1}{2}$ particle, described by a qubit $|\phi\rangle = \alpha|0\rangle + \beta|1\rangle$, is teleported from Alice to Bob, where here $\{|0\rangle, |1\rangle\}$ span a two dimensional Hilbert space. Each party shares one half of a maximally entangled *Bell state*, given by

e.g.

$$|\Psi^-\rangle = \frac{1}{\sqrt{2}}(|0\rangle|0\rangle - |1\rangle|1\rangle). \quad (5.42)$$

Then Alice performs a joint measurement on her half of the Bell state and on the state $|\phi\rangle$. She sends the (classical) outcome to Bob who then has to perform a unitary operation (depending on Alice's outcome) on his half of the Bell state. This completes the teleportation of the state $|\phi\rangle$ from Alice to Bob. The protocol was first realized experimentally in [BPM⁺97].

Shortly after, the equivalent continuous variable protocol [Vai94] was realized experimentally as well [FSB⁺98]. We depict the CV protocol in Fig. 5.8 (the following is taken from [KL10], we list here only the operations on the q -quadratures): First two vacuum modes are sent to two single-mode squeezers with squeezing parameters s and $-s$. This leads to quadratures

$$\begin{aligned} \hat{q}_1 &= e^s \hat{q}_1^{(v)}, \\ \hat{q}_2 &= e^{-s} \hat{q}_2^{(v)}, \end{aligned} \quad (5.43)$$

where $\hat{q}_{1,2}^{(v)}$ denote the q -quadratures of the vacuum modes. Then both modes are mixed on a balanced beamsplitter which leads to a two-mode squeezed vacuum state (TMSV) with quadratures

$$\begin{aligned} \hat{q}'_1 &= \frac{1}{\sqrt{2}}(e^{-s} \hat{q}_2^{(v)} - e^s \hat{q}_1^{(v)}), \\ \hat{q}'_2 &= \frac{1}{\sqrt{2}}(e^{-s} \hat{q}_2^{(v)} + e^s \hat{q}_1^{(v)}). \end{aligned} \quad (5.44)$$

Alice receives a quantum state $\hat{\rho}_A$ with quadrature \hat{q}_A and one half of the TMSV (see Sec. 5.1). She applies the CV equivalent of a Bell measurement, i.e. a balanced beamsplitter followed by two homodyne detections, leading to the quadrature outcome (p_m can be obtained similarly)

$$q_m = \frac{1}{\sqrt{2}} q_A + \frac{1}{2} (e^{-s} q_2^{(v)} - e^s q_1^{(v)}). \quad (5.45)$$

The outcomes q_m and p_m are sent to Bob who applies two displacement operators (depending on the outcomes) on his half of the TMSV, which then lead to state $\hat{\rho}_B$ with quadrature

$$\hat{q}_B = \hat{q}_A + \sqrt{2} e^{-s} \hat{q}_2^{(v)}. \quad (5.46)$$

In the case of an (unphysical) EPR pair as resource, i.e. $s \rightarrow \infty$ (and ideal homodyne detection) the resulting state at Bob's side becomes $\hat{\rho}_B = \hat{\rho}_A$.

5.3. Gaussian channels

The class of unitary Gaussian operations contains those operations that are reversible. However, there are also Gaussian operations that are irreversible. A subset of irreversible transformations, namely, the trace-preserving ones, are given by *Gaussian quantum channels*⁶. Gaussian channels model very well most optical communication links, such as optical fibers or free space information transmission [CD94, EW05, WHTH07, WPGP⁺12]. Therefore, they are of great relevance to experimentalists, in particular for the realization of quantum communication setups. Recall that in this work the quadratures are rescaled such that the electromagnetic field modes have unit frequency which implies that we do not have any operating bandwidth for the channel. Several channels with an operating bandwidth such as the wideband and narrowband channel have been studied in [CD94].

Note that throughout this thesis we focus on *bosonic* Gaussian channels, i.e. bosons such as photons are used for information transmission. There is also the notion of *fermionic* Gaussian channels where fermions (which obey the Pauli principle) are used as information carriers, see, e.g. [Bra05c]. We do not discuss fermionic Gaussian channels here, however, their mathematical description is strongly related to the one of bosonic channels.

A Gaussian channel Φ is a completely-positive trace-preserving map which is closed on the set of Gaussian states [HW01]. It transforms Gaussian input states $\hat{\rho}_{\text{in}}^{\text{G}} = \hat{\rho}^{\text{G}}(\mathbf{d}_{\text{in}}, \mathbf{V}_{\text{in}})$ with input moments $\{\mathbf{d}_{\text{in}}, \mathbf{V}_{\text{in}}\}$ to Gaussian output states

$$\Phi[\hat{\rho}^{\text{G}}(\mathbf{d}_{\text{in}}, \mathbf{V}_{\text{in}})] = \hat{\rho}^{\text{G}}(\mathbf{d}_{\text{out}}, \mathbf{V}_{\text{out}}), \quad (5.47)$$

with output moments $\{\mathbf{d}_{\text{out}}, \mathbf{V}_{\text{out}}\}$ according to

$$\mathbf{d}_{\text{out}} = \mathbf{X}\mathbf{d}_{\text{in}} + \mathbf{d}_{\text{env}}, \quad \mathbf{V}_{\text{out}} = \mathbf{X}\mathbf{V}_{\text{in}}\mathbf{X}^{\text{T}} + \mathbf{Y}, \quad (5.48)$$

where \mathbf{d}_{env} is the displacement introduced by the channel, \mathbf{X} is a $2n \times 2n$ real matrix, and \mathbf{Y} is a $2n \times 2n$ real, symmetric, and positive semidefinite matrix. For simplicity, we choose $\mathbf{d}_{\text{env}} = 0$ in the following discussion, because only first moments are affected by \mathbf{d}_{env} . As we shall see in sections 5.6 and 5.7 the first moments do not play a role in the calculation of transmission rates and capacities of Gaussian channels. Therefore, we focus on the action of the map Φ on second-order moments using the simplified notation $\Phi(\mathbf{V}_{\text{in}}) = \mathbf{V}_{\text{out}}$. Then, the map Φ is fully characterized by matrices \mathbf{X} and \mathbf{Y} , which must satisfy the relation [HW01]

$$\mathbf{Y} + \frac{i}{2} \left(\mathbf{\Omega} - \mathbf{X}\mathbf{\Omega}\mathbf{X}^{\text{T}} \right) \geq 0, \quad (5.49)$$

in order for the map to correspond to a quantum channel.

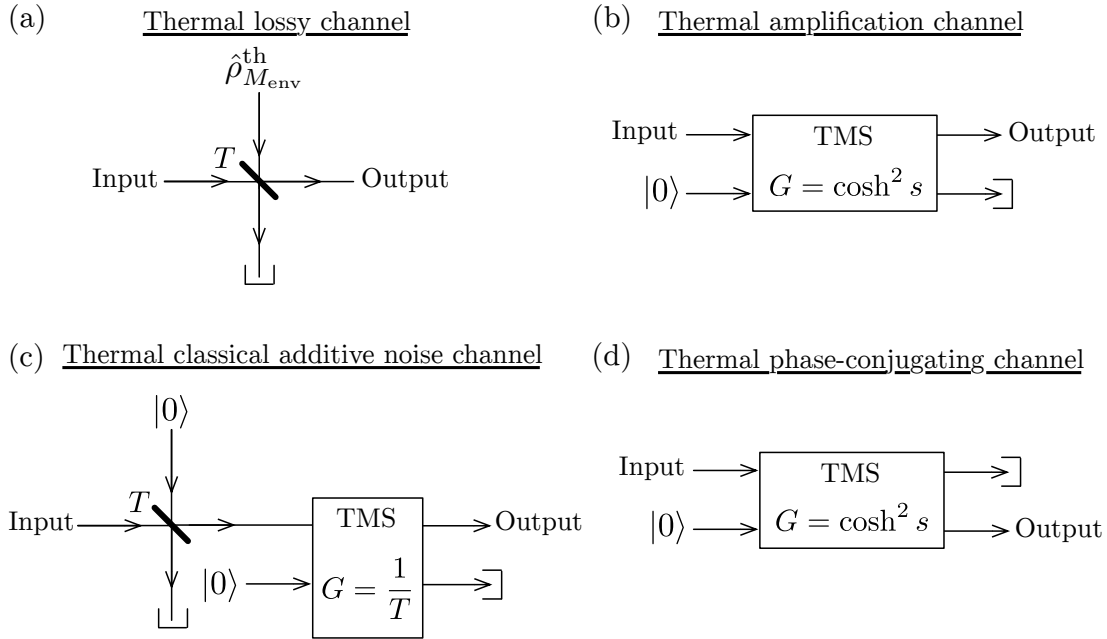


Figure 5.9.: Physical schemes of thermal Gaussian channels. (a) Thermal lossy channel: The input state is mixed with a thermal state $\hat{\rho}_{M_{env}}^{th}$ on a beamsplitter with transmissivity T . (b) Thermal amplification channel: the amplitude of the input state is amplified by a factor G and thermal noise is added. (c) Classical additive noise channel: The amplitude of the input state is not changed and classical noise is added. (d) The phase of the input state is conjugated, i.e. $p \rightarrow -p$.

5. Gaussian states and operations

5.3.1. One-mode Gaussian channels

In this subsection we focus on single-mode channels ($n = 1$). We first discuss the most common, i.e. most physical one-mode Gaussian channels which are the *thermal channels*. Those channels map thermal input states to thermal output states, which are sometimes referred to as “gauge-invariant” channels [HSH99, HW01]. Afterwards, we move on to the general one-mode case. The definitions throughout this subsection are taken from [Hol07, CGH06], and we partly use the nomenclature of [Hol07].

Thermal lossy channel

The *thermal lossy (or attenuation) channel* \mathcal{C}_T with transmissivity T is probably the most common Gaussian channel. It models very well transmission via an optical fibre and free space, because it incorporates the attenuation of the amplitude of the input signal as well as the addition of thermal noise. Its action is defined by

$$\mathbf{X}_{\mathcal{C}_T} = \begin{pmatrix} \sqrt{T} & 0 \\ 0 & \sqrt{T} \end{pmatrix}, \quad \mathbf{Y}_{\mathcal{C}_T} = (1 - T) \begin{pmatrix} M_{\text{env}} + \frac{1}{2} & 0 \\ 0 & M_{\text{env}} + \frac{1}{2} \end{pmatrix}, \quad (5.50)$$

where $0 \leq T \leq 1$ is the channel’s transmissivity and $M_{\text{env}} \geq 0$ is the number of thermal photons added by the channel. The channel can be implemented by mixing the input state with a thermal state $\hat{\rho}_{M_{\text{env}}}^{\text{th}}$ on a beamsplitter with transmissivity T , see Fig. 5.9 (a). Notice that by applying the thermal lossy channel on a thermal state $\hat{\rho}_{M_{\text{in}}}^{\text{th}}$ with a number of thermal photons M_{in} yields another thermal state with CM

$$\mathbf{V}_{\text{out}} = \mathbf{X}_{\mathcal{C}_T} \begin{pmatrix} M_{\text{in}} + \frac{1}{2} \\ \end{pmatrix} \mathbb{I} \mathbf{X}_{\mathcal{C}_T}^{\text{T}} + \mathbf{Y}_{\mathcal{C}_T} = \begin{pmatrix} M_{\text{out}} + \frac{1}{2} & 0 \\ 0 & M_{\text{out}} + \frac{1}{2} \end{pmatrix}, \quad (5.51)$$

where $M_{\text{out}} = TM_{\text{in}} + (1 - T)M_{\text{env}}$ is the number of thermal photons at the output.

Thermal amplification channel

The *thermal amplification channel* (also simply called “amplifier”) \mathcal{C}_G deterministically amplifies the amplitude of the input state by a factor $G \geq 1$. Due to Heisenberg’s uncertainty principle this amplification must induce noise. The action of the thermal amplifier reads

$$\mathbf{X}_{\mathcal{C}_G} = \begin{pmatrix} \sqrt{G} & 0 \\ 0 & \sqrt{G} \end{pmatrix}, \quad \mathbf{Y}_{\mathcal{C}_G} = \begin{pmatrix} \frac{G-1}{2} & 0 \\ 0 & \frac{G-1}{2} \end{pmatrix}. \quad (5.52)$$

The channel is realized by a TMS where the input mode is sent to the upper entry and an ancillary vacuum mode is sent to the lower entry. Then, the signal output corresponds to the output of the channel, see Fig. 5.9 (b).

⁶We refer to them in the following simply as “Gaussian channels”. Their classical counterparts will be referred to as “classical Gaussian channels”.

Thermal classical additive noise channel

Another important one-mode Gaussian channel is the *thermal classical additive noise channel* \mathcal{B}_2 . It can be used to describe the transmission through thermal fluctuations when losses are negligible. For conventional satellite communication the classical analogue, i.e. the classical Gaussian channel with white Gaussian noise (see Sec. 2.3.1) is often used as a model [CT05]. Since the added noise is classical it does not need to obey Heisenberg's uncertainty relation. Furthermore, the amplitude of the input signal is not changed, so the action of the channel reads

$$\mathbf{X}_{\mathcal{B}_2} = \mathbb{I}, \quad \mathbf{Y}_{\mathcal{B}_2} = \begin{pmatrix} M_{\text{env}} & 0 \\ 0 & M_{\text{env}} \end{pmatrix}, \quad (5.53)$$

where $M_{\text{env}} \geq 0$ here corresponds to the variance of the classical bivariate Gaussian distribution associated to the added noise. A physical scheme of this channel is depicted in Fig. 5.9 (c): By combining a lossy channel (with vacuum as second input) with transmissivity T and a thermal amplification channel with gain $G = 1/T$ one realizes the transformation stated in Eq. (5.53). The parameter M_{env} as a function of T and G reads simply $M_{\text{env}} = G - 1$.

Thermal phase-conjugating channel

The setup of the thermal amplification channel, depicted in Fig. 5.9 (b), can in fact realize another Gaussian channel. Namely, if one takes the idler output instead of the signal output one realizes the *thermal phase-conjugating channel* \mathcal{D} [see Fig. 5.9 (d)]. Its action is given by

$$\mathbf{X}_{\mathcal{D}} = \begin{pmatrix} \sqrt{G-1} & 0 \\ 0 & -\sqrt{G-1} \end{pmatrix} = \sqrt{G-1} \sigma_z, \quad \mathbf{Y}_{\mathcal{D}} = \begin{pmatrix} \frac{G}{2} & 0 \\ 0 & \frac{G}{2} \end{pmatrix}, \quad (5.54)$$

where $G \geq 1$ is the gain of the TMS in Fig. 5.9 (d) and $\sigma_z = \text{diag}(1, -1)$ is one of the Pauli matrices.

Canonical decomposition

In [Hol07] a *canonical decomposition* of the general one-mode Gaussian channel was presented. It states that any single-mode Gaussian channel Φ can be decomposed as

$$\Phi = U_2 \circ \Phi^{\text{C}} \circ U_1, \quad (5.55)$$

where U_1 and U_2 are Gaussian unitaries, and Φ^{C} is a *canonical channel* characterized by the matrices $(\mathbf{X}_{\text{C}}, \mathbf{Y}_{\text{C}})$ (further Refs. are [CGH06, ISS11]). Since the action of a Gaussian unitary \hat{U}_{G} on a Gaussian state can be completely specified by a symplectic transformation \mathbf{M} the canonical decomposition may be written as (we ignore the first moments here)

$$(U_2 \circ \Phi^{\text{C}} \circ U_1)(\mathbf{V}_{\text{in}}) = \mathbf{M}_2 \Phi^{\text{C}}(\mathbf{M}_1 \mathbf{V}_{\text{in}} \mathbf{M}_1^{\text{T}}) \mathbf{M}_2^{\text{T}}. \quad (5.56)$$

5. Gaussian states and operations

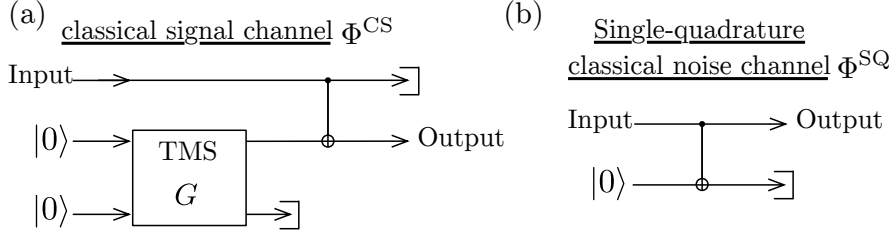


Figure 5.10.: Physical schemes of non-thermal canonical channels: (a) classical signal channel Φ^{CS} and (b) single-quadrature classical noise channel Φ^{SQ} .

There are seven classes of canonical channels Φ^{C} . Four of them we already discussed above: they are the thermal channels $\mathcal{B}_2, \mathcal{C}_T, \mathcal{C}_G$ and \mathcal{D} . There is in addition the (trivial) *zero-transmission channel* \mathcal{A}_1 which completely erases the input signal. Its action is given by a thermal lossy channel with $T = 0$. The other two of the seven canonical channels are non-thermal channels and will be presented in the following.

Non-thermal canonical channels

The sixth canonical channel is the *classical signal* (or quadrature erasing) channel, which we denote by Φ^{CS} . Its action is defined by

$$\mathbf{X}_{\text{CS}} = \begin{pmatrix} 1 & 0 \\ 0 & 0 \end{pmatrix}, \quad \mathbf{Y}_{\text{CS}} = \begin{pmatrix} y & 0 \\ 0 & y \end{pmatrix}, \quad y \geq \frac{1}{2}. \quad (5.57)$$

This channel can be physically implemented with the previously defined CV-CNOT gate stated in Eq. (5.29) with $\kappa = 1$. The corresponding scheme is depicted in Fig. 5.10 (a), where $y = \frac{G}{2}$. We show now that this scheme indeed leads to the desired output. As mentioned previously in Sec. 5.2.3 the output of the TMS in Fig. 5.10 after tracing out one of the output modes is a thermal state [see Fig. 5.6]. Therefore, one has to calculate the output of the CV-CNOT operation where the control mode is the input mode with CM

$$\mathbf{V}_{\text{in}} = \begin{pmatrix} v^{\text{q}} & v^{\text{qp}} \\ v^{\text{qp}} & v^{\text{p}} \end{pmatrix}, \quad (5.58)$$

and the target mode is the thermal state coming from the TMS with CM $\mathbf{V}_{\text{th}} = \text{diag}(G/2, G/2)$. The joint two-mode input state before the TMS therefore reads

$$\mathbf{V}_{\text{in,th}} = \begin{pmatrix} v^{\text{q}} & 0 & v^{\text{qp}} & 0 \\ 0 & \frac{G}{2} & 0 & 0 \\ v^{\text{qp}} & 0 & v^{\text{p}} & 0 \\ 0 & 0 & 0 & \frac{G}{2} \end{pmatrix}. \quad (5.59)$$

Using the expression for the symplectic transformation of the TMS, stated in Eq. (5.27), the two-mode output state of the CV-CNOT gate has the CM

$$\begin{aligned} \mathbf{V}_{\text{out,th}} &= \begin{pmatrix} 1 & 1 & 0 & 0 \\ 0 & 1 & 0 & 0 \\ 0 & 0 & 1 & 0 \\ 0 & 0 & -1 & 1 \end{pmatrix} \begin{pmatrix} v^q & 0 & v^{qp} & 0 \\ 0 & \frac{G}{2} & 0 & 0 \\ v^{qp} & 0 & v^p & 0 \\ 0 & 0 & 0 & \frac{G}{2} \end{pmatrix} \begin{pmatrix} 1 & 0 & 0 & 0 \\ 1 & 1 & 0 & 0 \\ 0 & 0 & 1 & -1 \\ 0 & 0 & 0 & 1 \end{pmatrix} \\ &= \begin{pmatrix} v^q + \frac{G}{2} & \frac{G}{2} & v^{qp} & -v^{qp} \\ \frac{G}{2} & \frac{G}{2} & 0 & 0 \\ v^{qp} & 0 & v^p & -v^p \\ -v^{qp} & 0 & -v^p & v^p + \frac{G}{2} \end{pmatrix}. \end{aligned} \quad (5.60)$$

Tracing out the control mode leads to the CM of the output state of Φ^{CS} :

$$\mathbf{V}_{\text{out}} = \begin{pmatrix} y & 0 \\ 0 & v^p + y \end{pmatrix} = \mathbf{X}_{\text{CS}} \mathbf{V}_{\text{in}} \mathbf{X}_{\text{CS}}^\top + \mathbf{Y}_{\text{CS}}, \quad (5.61)$$

where $y = \frac{G}{2}$. From Eq. (5.61) one confirms the name ‘‘classical signal’’: Φ^{CS} completely removes the q -quadrature of the input mode. Thus, one has only one degree of freedom that can be used for encoding, just like in the case of classical Gaussian channels [CT05]. However, unlike in the classical case the added noise is bounded from below (due to its ‘‘quantumness’’), i.e. $y \geq 1/2$.

The seventh and last canonical channel is the *single-quadrature classical noise channel*, which we name Φ^{SQ} . Its action is described by the matrices

$$\mathbf{X}_{\text{SQ}} = \mathbb{I}, \quad \mathbf{Y}_{\text{SQ}} = \begin{pmatrix} 0 & 0 \\ 0 & \frac{1}{2} \end{pmatrix}. \quad (5.62)$$

The physical realization is shown in Fig. 5.10 (b) and is in fact a particular case of the scheme depicted in Fig. 5.10 (a): Using Eq. (5.60) but for $G = 1$ (omitting the TMS) and tracing out the target mode one obtains precisely the desired output CM, namely

$$\mathbf{V}_{\text{out}} = \begin{pmatrix} v^q + \frac{1}{2} & v^{qp} \\ v^{qp} & v^p \end{pmatrix} = \mathbf{X}_{\text{SQ}} \mathbf{V}_{\text{in}} \mathbf{X}_{\text{SQ}}^\top + \mathbf{Y}_{\text{SQ}}, \quad (5.63)$$

where \mathbf{V}_{in} is defined as in Eq. (5.58). The name ‘‘single-quadrature classical noise’’ stems from the fact that it adds one unit of vacuum to one quadrature and no noise to the other one (the added noise is classical because $\det(\mathbf{Y}_{\text{SQ}}) \geq 0$).

An important question is: how does one obtain the canonical decomposition for a given arbitrary Gaussian channel, defined by \mathbf{X}, \mathbf{Y} ? The symplectic transformations that are stated in (5.55) can be further decomposed as $\mathbf{M} = \mathbf{\Theta}_2 \mathbf{S} \mathbf{\Theta}_1$ (using the Bloch-Messiah decomposition, see Eq. (5.25)), where $\mathbf{\Theta}_i$ are rotation matrices defined in Eq. (5.22) and \mathbf{S} is a one-mode squeezing operation given in Eq. (5.24). Since [Hol07] only states the existence of \mathbf{M}_1 and \mathbf{M}_2 , but does not explicitly show how to find them we will provide in Chapter 6 a method to derive explicitly matrices $\mathbf{M}_1, \mathbf{M}_2, \mathbf{X}_C$ and \mathbf{Y}_C for given matrices \mathbf{X} and \mathbf{Y} .

5. Gaussian states and operations

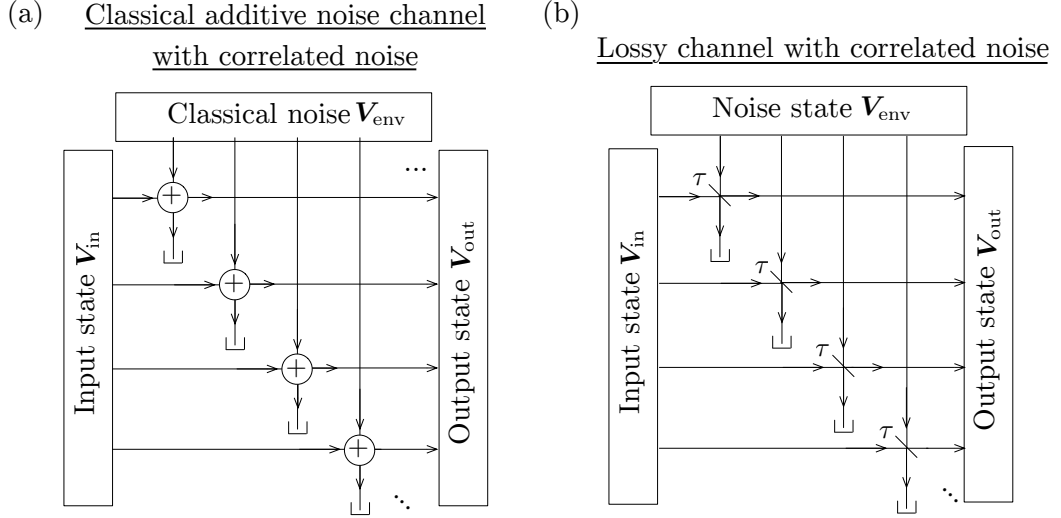


Figure 5.11.: Gaussian memory channels that are considered in this work: (a) Multi-mode classical additive noise channel. Classical noise is “added” to the input mode and may stem from classically correlated noise with CM \mathbf{V}_{env} . (b) Multi-mode lossy channel, where each beamsplitter has the same transmissivity τ . The action corresponds to mixing each input mode with a noise mode which stems from a possibly entangled n -mode state with CM \mathbf{V}_{env} .

5.3.2. Multi-mode Gaussian channels

Let us now move to the multi-mode case $n > 1$. In this work we are interested in Gaussian memory channels (recall the definition of quantum memory channels introduced in Sec. 3.2.2). We recall that a past use of a memory channel may affect future uses, unlike in the case of memoryless channels. For Gaussian channels one way to model a memory is to introduce non-diagonal matrices \mathbf{X} and/or \mathbf{Y} . In this work we consider only cases when

$$\mathbf{X}_{2n \times 2n} = \sqrt{|\tau|} \begin{pmatrix} \mathbb{I} & 0 \\ 0 & \text{sgn}(\tau)\mathbb{I} \end{pmatrix}. \quad (5.64)$$

The effective noise matrix \mathbf{Y} can then be parametrized as follows:

$$\mathbf{Y}_{2n \times 2n} = \begin{cases} |1 - \tau| \mathbf{V}_{\text{env}}, & \tau \neq 1, \\ \mathbf{V}_{\text{env}} & \tau = 1, \end{cases} \quad (5.65)$$

where \mathbf{V}_{env} is the covariance matrix of the n -mode Gaussian state of the environment that is mixed with the n -mode input state (if $\tau \neq 1$) or the covariance matrix of the classical added Gaussian distributed noise (i.e. its symplectic eigenvalues may be smaller than 1/2).

In particular, we are interested in the case $\tau = 1$, i.e. the n -mode classical additive noise channel. We depict the action of this channel schematically in Fig. 5.11 (a). In the

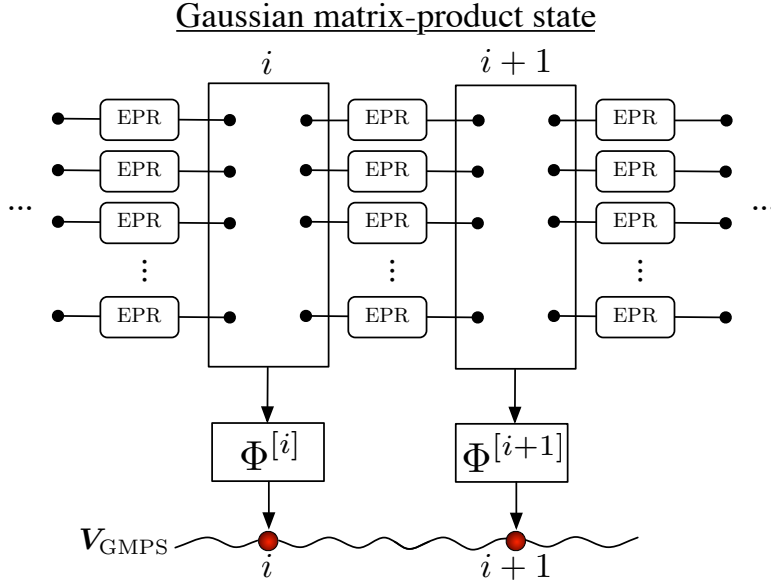


Figure 5.12.: Generation of a Gaussian matrix-product state: A Gaussian channel $\Phi^{[i]}$ is applied to one half of m EPR pairs on each site i , so that a $2m$ -mode state is mapped to a single output mode i .

case of $\tau \in [0, 1]$ the map corresponds to n beamsplitters with the same transmissivity τ , see Fig. 5.11 (b). The (effective) noise CM \mathbf{Y} of all channels that we study have to fulfill (at least asymptotically) a particular property: there exists a passive symplectic transformation $\Theta_{\mathbf{Y}}$ such that

$$\Theta_{\mathbf{Y}} \mathbf{Y} \Theta_{\mathbf{Y}}^{\top} = \text{diag}(y_{q_1}, y_{q_2}, \dots, y_{q_n}, y_{p_1}, \dots, y_{p_n}), \quad (5.66)$$

where we denote the first n eigenvalues (which belong to the q -quadratures) by y_{q_i} and the second n eigenvalues (which belong to the p -quadratures) by y_{p_i} .

5.4. Generation of Gaussian matrix product states

Recently, *matrix-product states* (MPS) [KSZ91, FNW92, KSZ93, PGVWC07] were shown to be a useful resource to sequentially generate (finite dimensional) multi-qubit entangled states in the realm of cavity QED [SSV⁺05, SHW⁺07]. We state here the definition of MPS taken from [PGVWC07]. One is given a pure quantum state $|\psi\rangle \in \mathbb{C}^{\otimes a^n}$ of a system containing n parties, e.g. spins. They are aligned on a ring and one assigns two ancillary systems of dimension D to each spin. The ancillas are in a maximally (unnormalized) entangled state $|I\rangle = \sum_{\alpha=1}^D |\alpha, \alpha\rangle$ (α should not be confused with a coherent

5. Gaussian states and operations

amplitude) and referred to as *bonds*. Then, one applies to each site i the map

$$\mathcal{A} = \sum_{i=1}^d \sum_{\alpha, \beta=1}^D A_{i, \alpha, \beta} |i\rangle \langle \alpha, \beta|, \quad (5.67)$$

where $A_{i, \alpha, \beta}$ are the elements of the $D \times D$ matrix \mathbf{A}_i . The dimension of $|I\rangle$ and \mathcal{A} may be different for each site, therefore one writes $\mathbf{A}_i^{[k]}$ for the $D_k \times D_{k+1}$ matrix corresponding to site $k \in \{1, \dots, n\}$. A state that is obtained by this procedure has the form

$$|\psi\rangle = \sum_{i_1, \dots, i_n=1}^d \text{Tr}[\mathbf{A}_{i_1}^{[1]} \mathbf{A}_{i_2}^{[2]} \dots \mathbf{A}_{i_n}^{[n]}] |i_1, i_2, \dots, i_n\rangle, \quad (5.68)$$

and is called matrix-product state. It was shown in [Vid03] that every state can be represented in this way if the bond dimensions D_k are sufficiently large. This brings us to the definition of the *Gaussian matrix-product state* (GMPS) introduced in [SWC08]. The GMPS is the extension of MPS to Gaussian states. The bonds are now Gaussian states and the operations applied on each site are Gaussian channels $\Phi^{[i]}$, such that Gaussian input states are mapped to Gaussian output states. The bonds for finite dimensional systems $|I\rangle$ were taken to be maximally entangled. The equivalent Gaussian state is the EPR state introduced in Sec. 5.1. These bonds are unphysical, so a general GMPS may not be implementable. However, for a subset of GMPS it is possible to replace them by finitely entangled ones⁷. The scheme of general GMPS is depicted in Fig. 5.12: At each site i a Gaussian channel $\Phi^{[i]}$ is applied to one-half of m EPR pairs, so that a $2m$ -mode state is mapped to a one-mode state. Note, that the output state of a Gaussian channel applied to an n -mode input state can equivalently be obtained (using the Choi-Jamiolkowski isomorphism) by projecting a Gaussian state of dimension $n + m$ onto a maximally entangled state (see Appendix C). In this work, we focus on a particular class of GMPS, i.e. GMPS with nearest-neighbor correlations. Those states are introduced and used in Chapter 8.

5.5. Encoding and decoding in phase space

Bosonic Gaussian quantum channels⁸ are highly relevant for information transmission, because as mentioned before, they model well natural environments as well as laboratory equipment such as optical fibers. However, they map input states to an infinite dimensional Hilbert space which makes the treatment of their classical capacity a challenging task. For this reason one may focus on a restricted set of encodings, such as Gaussian states and Gaussian modulations. The resulting quantity, the *Gaussian classical capacity* (or simply “Gaussian capacity”), can be treated analytically and at the same time provides a useful lower bound and (for a restricted range of parameters) a tight upper

⁷We shall see that for our purposes finitely entangled bonds perform well enough.

⁸In the following we will refer to “Bosonic Gaussian quantum channels” simply as “Gaussian channels”. Their classical counter parts will be referred to as “classical Gaussian channels”.

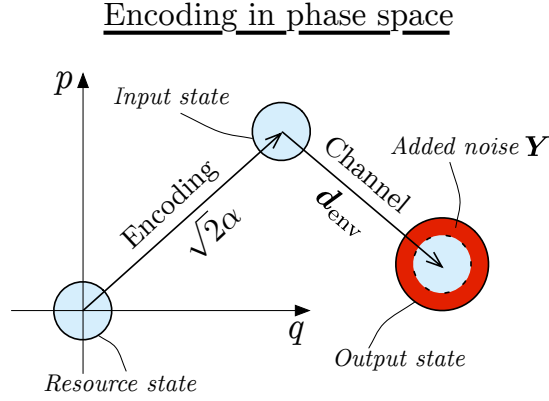


Figure 5.13.: Encoding and action of a thermal channel in phase space: The information may be encoded in a coherent state $|\alpha\rangle$ by displacing the vacuum. The channel adds a displacement \mathbf{d}_{env} to the first moment, changes the amplitude as well as adds a noise CM \mathbf{Y} to the input covariances.

bound. For particular Gaussian channels the Gaussian capacity was shown to coincide with the classical capacity. This is why it is conjectured to coincide with the classical capacity of all Gaussian channels (this will be discussed in more details in the following).

Let us now focus on the encoding of information in Gaussian states. A simple way for Alice to encode a message (or message index) α in a Gaussian state is provided by the displacement operator. For example, she can use the vacuum state $|0\rangle$ as a resource state and displace it by the complex number α , i.e. $D(\alpha)|0\rangle = |\alpha\rangle$. Thus, her symbol state is given by the coherent state $\hat{\rho}_\alpha = |\alpha\rangle\langle\alpha|$ and the complex amplitude of the state corresponds now to the classical information Alice tries to send to Bob via a Gaussian channel Φ . The state $\Phi[|\alpha\rangle\langle\alpha|]$ that Bob receives has a modified amplitude and *a priori* is no longer pure. We recall the action of a Gaussian channel Φ (see Sec. 5.3) on a Gaussian state $\hat{\rho}^G(\mathbf{d}_{\text{in}}, \mathbf{V}_{\text{in}})$:

$$\mathbf{d}_{\text{out}} = X\mathbf{d}_{\text{in}} + \mathbf{d}_{\text{env}}, \quad \mathbf{V}_{\text{out}} = X\mathbf{V}_{\text{in}}X^T + \mathbf{Y}, \quad (5.69)$$

where \mathbf{d}_{env} is an additional displacement of the channel. For the given example $\hat{\rho}^G = |\alpha\rangle\langle\alpha|$ we have $\mathbf{d}_{\text{in}} = (\sqrt{2}\Re\{\alpha\}, \sqrt{2}\Im\{\alpha\})^T$ and $\mathbf{V}_{\text{in}} = \frac{\mathbb{1}}{2}$. Therefore, the output state on Bob's side has a modified amplitude, is shifted by \mathbf{d}_{env} and has increased covariances. We depict the encoding and action of the noise in phase space for a thermal channel in Fig. 5.13.

Clearly, if Alice always sends the same displaced state $|\alpha\rangle\langle\alpha|$ then on average she does not send any information to Bob. Therefore, she needs to *modulate* her input state; in the case of a coherent state by varying its amplitude. One possibility is the encoding with same absolute amplitude $|\alpha|$ but varied, discretized angles. A corresponding example is a *two-state* protocol (=binary modulation) in which the input message is encoded in two

5. Gaussian states and operations

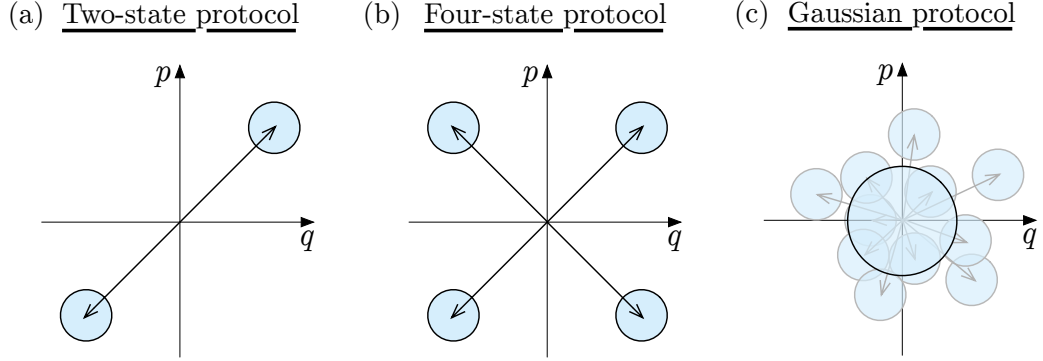


Figure 5.14.: Different protocols for encoding in phase-space: (a) two-state protocol/binary modulation: Alice encodes her information in either of two coherent states that have the same amplitude but are situated in opposite quadrants. (b) four-state protocol/quaternary modulation: Alice encodes her information in four coherent states with same amplitude, situated in all four quadrants. (c) Gaussian protocol: Alice encodes her information in Gaussian phase-space translates of coherent states; in the given example the Gaussian distribution is centered around zero.

quadrants of the phase-space [Rei00, HL06], see Fig. 5.14 (a). Alternatively, one may choose all quadrants of the phase-space [NH03, NH04], i.e. one performs a quaternary modulation, as shown in Fig. 5.14 (b). This may be generalized to protocols with higher-dimensions, see e.g. [SL10]. Alternatively, a continuous, *Gaussian modulation* can be used for information encoding: in [GVW⁺03, JKJL11, JKJL⁺13] coherent states and in [CLA01, CIV02] squeezed states are modulated according to a Gaussian distribution, which will also be the type of modulation considered in this thesis, see Fig. 5.14 (c). Alternatively, one can also encode information in the value of squeezing of an input squeezed state as proposed in [Ral99, Hil00]. All protocols mentioned in the previous paragraph are practically highly relevant, because they can be used for the distribution of keys using *quantum key distribution* (see Refs. stated above and references therein). Bob on his side (depending on the encoding protocol) may apply a homodyne detection to the state that he receives in order to discriminate the input states. Evidently, the more the input states are separated, the lower Bob's error rate will be and the higher the transmission rate becomes. Here, the separation is bounded by the energy that is available for the modulation of the states and the creation of the states. The total average input energy that is available to Alice is the input energy constraint that is imposed at the channel's input [see Eq. (3.34)]. If the Gaussian channel is non-thermal, i.e. acts in a non-symmetric way on the input quadratures, it may be favorable to spend some energy on the squeezing of the input states. In general this leads to a non-trivial trade-off between the energy spent for state preparation and energy that is left for the

modulation of the states.

5.6. Classical capacity of Gaussian channels

The main problem that this thesis is concerned with is the maximal transmission rate of Gaussian quantum channels, i.e. their classical capacity. Since Gaussian channels map arbitrary input states to an infinite dimensional Hilbert space the definition of the one-shot capacity stated in Eq. (3.35) must be generalized. Essentially, sums are replaced by integrals, and instead of a maximization over probability distribution p_i one maximizes over a probability measure $\mu(x)$. The input encoding is then defined by a set of states $\hat{\rho}_x$ associated to $\mu(x)$, where the average input state $\hat{\rho}_{\text{in}} \in \mathcal{E}_{\bar{N}}$ now reads

$$\hat{\rho}_{\text{in}} = \int \mu(dx) \hat{\rho}_x, \quad (5.70)$$

where $\mathcal{E}_{\bar{N}}$ is the set of quantum states which have a mean photon number equal to \bar{N} , i.e.

$$\text{Tr}[\hat{\rho}_{\text{in}} \hat{a}^\dagger \hat{a}] = \bar{N}. \quad (5.71)$$

Note that unlike in Eq. (3.34) we now saturate the input energy because we want to maximize the transmission rate (a lower input energy than allowed by the constraint would certainly not be optimal). The one-shot capacity of a Gaussian channel Φ then reads [HSH99]

$$\begin{aligned} C_\chi(\Phi, \bar{N}) &= \max_{\mu: \hat{\rho}_{\text{in}} \in \mathcal{E}_{\bar{N}}} \chi(\Phi, \mu), \\ \chi(\Phi, \mu) &= S(\Phi[\hat{\rho}_{\text{in}}]) - \int \mu(dx) S(\Phi[\hat{\rho}_x]). \end{aligned} \quad (5.72)$$

The classical capacity, previously stated in Eq. (3.36) now generalizes to [HSH99]

$$C(\Phi, \bar{N}) = \lim_{n \rightarrow \infty} \frac{1}{n} C_\chi(\Phi^{\otimes n}, n\bar{N}). \quad (5.73)$$

The problem of determining the classical capacity of Gaussian channels (as defined in Sec. 5.3) proved to be very challenging, since up to today only the solution of the lossy channel with vacuum noise is known for all input energies \bar{N} [GGL+04a]. This channel is a restricted case of the thermal lossy channel \mathcal{C}_T (see Sec. 6.1), i.e. the case when the noise becomes pure: $M_{\text{env}} = 0$. Its action is given by

$$\mathbf{X} = \tau \mathbb{I}, \quad \mathbf{Y} = \frac{(1-\tau)}{2} \mathbb{I}, \quad (5.74)$$

and for simplicity we denote the corresponding map by $\mathcal{C}_{T,0}$. Now we briefly review the solution to its classical capacity that was obtained in [GGL+04a]. The basic idea is to

5. Gaussian states and operations

upper bound the classical capacity by the difference of the maximum of the first term and the minimum of the second term, i.e.

$$C(\mathcal{C}_{T,0}, \bar{N}) \leq \lim_{n \rightarrow \infty} \frac{1}{n} \max_{\mu: \hat{\rho}_{\text{in}} \in \mathcal{E}_{\bar{N}}} S(\mathcal{C}_{T,0}^{\otimes n}[\hat{\rho}_{\text{in}}]) - \lim_{n \rightarrow \infty} \frac{1}{n} \min_{\mu} \int \mu(dx) S(\mathcal{C}_{T,0}^{\otimes n}[\hat{\rho}_x]). \quad (5.75)$$

Clearly this bound may be unphysical since one may violate the energy constraint by the independent optimizations. Let us first calculate the first term in Eq. (5.75). It is known that the von Neumann entropy of a state $\hat{\rho}$ with mean photon number \bar{N} is maximized by a thermal state $\hat{\rho}_{\bar{N}}^{\text{th}}$ (see Sec. 5.1). If we choose the averaged input state to be a thermal state, $\hat{\rho}_{\text{in}} = \hat{\rho}_{\bar{N}}^{\text{th}}$ its CM reads $\mathbf{V}_{\text{in}} = (\bar{N} + 1/2)\mathbb{I}$ and according to Eq. (5.74) the averaged output state is a thermal state as well, i.e. $\hat{\rho}_{\text{out}} = \hat{\rho}_{\bar{N}_{\text{out}}}^{\text{th}}$ with CM

$$\bar{\mathbf{V}}_{\text{out}} = \begin{pmatrix} \tau\bar{N} + \frac{1}{2} & 0 \\ 0 & \tau\bar{N} + \frac{1}{2} \end{pmatrix}, \quad (5.76)$$

with mean number of photons

$$\bar{N}_{\text{out}} = \frac{1}{2} \text{Tr}[\bar{\mathbf{V}}_{\text{out}}] - \frac{1}{2}. \quad (5.77)$$

This state can be generated by choosing as individual symbol states coherent states

$$\hat{\rho}_x = |x\rangle\langle x| \quad (5.78)$$

and as a measure a bivariate Gaussian density function, i.e.

$$\mu(x) = \frac{1}{\pi\bar{N}} e^{-\frac{|x|^2}{\bar{N}}}, \quad (5.79)$$

where here x is a complex number. Then, the averaged input state is obtained by a ‘‘Gaussian mixture’’ of displaced vacuum states, i.e.

$$\hat{\rho}_{\text{in}} = \frac{1}{\pi\bar{N}} \int dx e^{-\frac{|x|^2}{\bar{N}}} \hat{D}(x) |0\rangle\langle 0| \hat{D}^\dagger(x) = \frac{1}{\pi\bar{N}} \int dx e^{-\frac{|x|^2}{\bar{N}}} |x\rangle\langle x|. \quad (5.80)$$

Thus, we obtain for the first term

$$\lim_{n \rightarrow \infty} \frac{1}{n} \max_{\mu: \hat{\rho}_{\text{in}} \in \mathcal{E}_{\bar{N}}} S(\mathcal{C}_{T,0}^{\otimes n}[\hat{\rho}_{\text{in}}]) = S(\mathcal{C}_{T,0}[\hat{\rho}^{\text{th}}(\bar{N})]) = S(\hat{\rho}^{\text{th}}(\tau\bar{N})) = g(\tau\bar{N}), \quad (5.81)$$

where $g(x)$ is defined in Eq. (5.21). Let us now calculate the second term in Eq. (5.75) for the Gaussian measure that we defined in Eq. (5.79). Since we use always the same ‘‘seed’’ state, i.e. the vacuum $|0\rangle\langle 0|$ [which is then displaced according to $\mu(x)$] the output entropy of each symbol state is identical. The vacuum state is not changed when mixed on a beamsplitter with vacuum, as stated in Eq. (5.74), and thus, each output

5.6. Classical capacity of Gaussian channels

state has second moments $\mathbf{V}_{\text{out}} = \frac{\mathbb{I}}{2}$. By definition, the entropy of a pure state is equal to zero, so we find

$$\lim_{n \rightarrow \infty} \frac{1}{n} \min_{\mu} \int \mu(dx) S(\mathcal{C}_{T,0}^{\otimes n}[\hat{\rho}_x]) = 0. \quad (5.82)$$

Thus, the encoding defined in Eqs. (5.78) and (5.79) achieves at the same time the maximum of the first term and the minimum of the second term of Eq. (5.75). This means we saturate the upper bound by a physical encoding and thus found the classical capacity, i.e.

$$C(\mathcal{C}_{T,0}, \bar{N}) = g(\tau \bar{N}). \quad (5.83)$$

Equation (5.83) leads to the derivation of the classical capacity of the homogeneous broadband channel Φ_B [EW05]

$$C(\Phi_B, P) = t \frac{\sqrt{T}}{\ln 2} \sqrt{\frac{\pi P}{3}} + \mathcal{O}(1/t), \quad (5.84)$$

where P is the average input power, t is the transmission time related to the frequency spacing $\delta\omega = 2\pi/t$. In the lossless case $T = 1$ the capacity was previously derived in [YO93, CD94].

For n parallel lossy channels (with vacuum noise)

$$\mathcal{C}_{\{T_k\},0}^{(n)} = \mathcal{C}_{T_1,0} \otimes \mathcal{C}_{T_2,0} \otimes \cdots \otimes \mathcal{C}_{T_n,0}, \quad (5.85)$$

with different transmissivities T_k the additivity of C_χ follows straightforwardly: the one-shot capacity of each individual channel can be upper bounded as above and the total averaged output state is again optimal when chosen to be thermal. It follows that [GGL⁺04a]

$$C(\mathcal{C}_{\{T_k\},0}^{(n)}, \bar{N}) = \max_{\bar{N}_k} \sum_k g(T_k \bar{N}_k), \quad (5.86)$$

where the maximization over the optimal input energy distribution satisfying $\sum_k \bar{N}_k = \bar{N}$ must be carried out for the given transmissivities T_k .

The result stated in Eq. (5.83) was extended in [LPM09] to the case of a pure squeezed environment, where the capacity was calculated exactly above an input energy threshold. This will be discussed in detail in Sec. 6.4.1.

5.6.1. Minimum output entropy conjecture

In general, the upper bound (5.75) is not saturated by the encoding presented above for the lossy channel with vacuum noise. In the case of the thermal lossy channel \mathcal{C}_T thermal noise is added and then the second term in Eq. (5.75) no longer vanishes. However, due to the symmetry of the noise one may *conjecture* that vacuum (as input state) also minimizes the output entropy of \mathcal{C}_T . The so-called *minimum output entropy conjecture* [GGL⁺04b, LGM⁺09] states that

$$\min_{\hat{\rho}_x} S(\Phi^{\text{C}}[\hat{\rho}_x]) = S(\Phi^{\text{C}}[|0\rangle\langle 0|]), \quad \Phi^{\text{C}} \neq \{\Phi^{\text{CS}}, \Phi^{\text{SQ}}\}, \quad (5.87)$$

5. Gaussian states and operations

where here Φ^C is any of the four canonical thermal channels (we ignore the trivial zero-transmission channel \mathcal{A}_1 which is included as a limiting case of the thermal lossy channel). The right hand side of Eq. (5.87) is obtained as follows.

Note that originally the conjecture in [GGL⁺04b] was only stated for the thermal classical additive noise channel and thermal lossy channel, but we extended it here to all four thermal channels. In fact, if the conjecture is proven for any of the thermal channels it immediately implies that it holds for the remaining ones. This follows directly from the physical schemes of the thermal channels, shown in Fig. 5.9. An alternative Stinespring dilation for the thermal lossy channel is a beamsplitter followed by a TMS, both with vacua at the second entries (see details in Sec. 6.1). Then, if the state $|0\rangle\langle 0|$ minimizes the output entropy of the thermal lossy channel then it also minimizes the output entropy of the two-mode squeezer which is part of its Stinespring dilation because the initial beamsplitter leaves $|0\rangle\langle 0|$ invariant. In addition, the output entropy of both exits of the TMS is equal. As a conclusion, the vacuum minimizes the output entropy of the other three thermal channels (see Fig. 5.9).

If the minimum output entropy conjecture was proven to be true, then the encoding stated in Eqs. (5.78) and (5.79) would (trivially) be optimal and achieve the classical capacity of thermal channels.

We remark that the minimum output entropy conjecture was stated as well for one-mode fermionic Gaussian channels in [Bra05c], where the Gaussian capacity of one-mode fermionic attenuation channels was studied in detail.

5.7. Gaussian classical capacity

Since the classical capacity of Gaussian channels is in general difficult to treat one may restrict the input encoding, namely to Gaussian input states and Gaussian modulations. As already mentioned previously, Gaussian states are of great interest to experimentalists since they can be easily generated in the laboratory and furthermore easily manipulated and measured (using homodyne and heterodyne detection). Another motivation to restrict to Gaussian encodings is the minimum output entropy conjecture discussed above.

We call the capacity restricted to Gaussian encodings the *Gaussian classical capacity* (in the following simply “Gaussian capacity”) C^G and define it as

$$\begin{aligned} C^G(\Phi, \bar{N}) &= \lim_{n \rightarrow \infty} \frac{1}{n} C_\chi^G(\Phi^{\otimes n}, n\bar{N}), \\ C_\chi^G(\Phi, \bar{N}) &= \max_{\mu^G: \hat{\rho}^G \in \mathcal{E}_N^G} \chi(\Phi, \mu^G), \end{aligned} \quad (5.88)$$

where $C_\chi^G(\Phi, \bar{N})$ is the *one-shot Gaussian capacity*. The maximum is taken now over all measures μ^G for which

$$\hat{\rho}^G(\bar{\mathbf{d}}_{\text{in}}, \bar{\mathbf{V}}_{\text{in}}) = \int \mu^G(d\mathbf{d}, d\mathbf{V}) \hat{\rho}^G(\mathbf{d}, \mathbf{V}) \quad (5.89)$$

is in the set \mathcal{E}_N^G of Gaussian states with a mean photon number not greater than \bar{N} . Note that in Eq. (5.89) the mean \mathbf{d} and CM \mathbf{V} are the variables of integration, hence,

μ^G depends on the differentials $d\mathbf{d}$ and $d\mathbf{V}$, respectively. In a previous work [Hir06] the Gaussian capacity was defined as the classical capacity with the restriction that only the individual symbol states are Gaussian. Our definition requires both, the averaged and the individual state to be Gaussian. For the case of an n -mode Gaussian channel Φ the definition stated in Eq. (5.88) can be greatly simplified to the well known expression [EW05]:

$$C_{\chi}^G(\Phi, \bar{N}) = \max_{\mathbf{V}_{\text{in}}, \mathbf{V}_{\text{mod}}} \left\{ \chi^G(\{\nu_{\text{out}i}, \bar{\nu}_{\text{out}i}\}) \mid \text{Tr}[\mathbf{V}_{\text{in}} + \mathbf{V}_{\text{mod}}] \leq 2n\bar{N} + n \right\}. \quad (5.90)$$

$$\chi^G(\{\nu_{\text{out}i}, \bar{\nu}_{\text{out}i}\}) \equiv \sum_{i=1}^n \left[g\left(\bar{\nu}_{\text{out}i} - \frac{1}{2}\right) - g\left(\nu_{\text{out}i} - \frac{1}{2}\right) \right].$$

Here, \mathbf{V}_{in} is the CM of a pure Gaussian input state $\hat{\rho}^G(0, \mathbf{V}_{\text{in}})$ fulfilling $\det(2\mathbf{V}_{\text{in}}) = 1$, which may be regarded as a resource or seed state, and \mathbf{V}_{mod} is the CM of a classical Gaussian distribution used to displace this seed state. The displacement of the state \mathbf{V}_{in} generates the modulated input state $\hat{\rho}^G(0, \bar{\mathbf{V}}_{\text{in}})$ whose CM is $\bar{\mathbf{V}}_{\text{in}} = \mathbf{V}_{\text{in}} + \mathbf{V}_{\text{mod}}$ with $\text{Tr}[\bar{\mathbf{V}}_{\text{in}}] \leq 2n\bar{N} + n$. Furthermore, $\nu_{\text{out}i}$ and $\bar{\nu}_{\text{out}i}$ in Eq. (5.90) are the symplectic eigenvalues of the output and modulated output states with CM $\mathbf{V}_{\text{out}} = \Phi(\mathbf{V}_{\text{in}})$ and $\bar{\mathbf{V}}_{\text{out}} = \Phi(\bar{\mathbf{V}}_{\text{in}})$, respectively. Note that in [EW05] the Gaussian capacity was directly defined as in Eq. (5.90).

We prove in the following that Eq. (5.90) follows from our definition stated in Eq. (5.88).

Proof. Equation (5.90) states that among all possible Gaussian sources characterized by a measure $\mu^G(d\mathbf{d}, d\mathbf{V})$ over the set of Gaussian states $\hat{\rho}^G(\mathbf{d}, \mathbf{V})$ of mean \mathbf{d} and CM \mathbf{V} , the source optimizing the Gaussian capacity corresponds to a single pure Gaussian state $\hat{\rho}^G(0, \mathbf{V}_{\text{in}})$ with covariance \mathbf{V}_{in} fulfilling $\det(2\mathbf{V}_{\text{in}}) = 1$, modulated according to a Gaussian bivariate distribution with CM \mathbf{V}_{mod} . To achieve our goal we use the fact that the maximization inside the Gaussian capacity definition

$$C_{\chi}^G(\Phi, \bar{N}) = \max_{\mu^G: \hat{\rho}^G \in \mathcal{E}_{\bar{N}}^G} \left[S(\Phi[\hat{\rho}^G]) - \int \mu^G(d\mathbf{d}, d\mathbf{V}) S(\Phi[\hat{\rho}^G(\mathbf{d}, \mathbf{V})]) \right], \quad (5.91)$$

can be divided into two different steps. In the first step, among all the sources $\mu^G(d\mathbf{d}, d\mathbf{V})$ belonging to the set $\mathcal{F}_{\hat{\rho}^G}^G$ sharing the same average input state

$$\hat{\rho}^G \equiv \hat{\rho}^G(0, \bar{\mathbf{V}}_{\text{in}}) = \int \mu^G(d\mathbf{d}, d\mathbf{V}) \hat{\rho}^G(\mathbf{d}, \mathbf{V}), \quad (5.92)$$

we maximize the modified Holevo quantity

$$\tilde{\chi}(\Phi, \bar{N}, \hat{\rho}^G) = S(\Phi[\hat{\rho}^G]) - \min_{\mu^G \in \mathcal{F}_{\hat{\rho}^G}^G} \int \mu^G(d\mathbf{d}, d\mathbf{V}) S(\Phi[\hat{\rho}^G(\mathbf{d}, \mathbf{V})]). \quad (5.93)$$

Note that the choice of zero mean for the average input state $\hat{\rho}^G$ is natural because displacements do not change the entropy, however require energy. In the second and

5. Gaussian states and operations

final step we optimize $\tilde{\chi}(\Phi, \bar{N}, \hat{\rho}^G)$ over the average input state $\hat{\rho}^G$ satisfying the energy constraint \bar{N} , thus obtaining $C_\chi^G(\Phi, \bar{N})$. We use the fact that the minimum of the average output entropy appearing in equation (5.93) can be rewritten as the Gaussian entanglement of formation $E^G[\bar{\sigma}_{\text{BE}}]$ (see [W^GK⁺04]), i.e.

$$\min_{\mu^G \in \mathcal{F}_{\hat{\rho}^G}^G} \int \mu^G(d\mathbf{d}, d\mathbf{V}) S(\Phi[\hat{\rho}^G(\mathbf{d}, \mathbf{V})]) = E^G[\bar{\sigma}_{\text{BE}}] \quad (5.94)$$

of a given bipartite mixed state $\bar{\sigma}_{\text{BE}} = U_\Phi \hat{\rho}_B^G \otimes |0\rangle\langle 0|_E U_\Phi^\dagger$ with CM $\bar{\mathbf{V}}_{\text{BE}}$ obtained by the unitary (Stinespring) dilation U_Φ of channel Φ , such that $\Phi[\hat{\rho}^G] = \text{Tr}_E[\bar{\sigma}_{\text{BE}}]$. Indeed, the Gaussian entanglement of formation is defined as

$$E^G[\bar{\sigma}_{\text{BE}}] = E^G[U_\Phi \hat{\rho}^G \otimes |0\rangle\langle 0| U_\Phi^\dagger] = \min_{\mu^G \in \mathcal{F}_{\hat{\rho}^G}^G} \left[\int \mu^G(d\mathbf{d}, d\mathbf{V}) E[U_\Phi \hat{\rho}^G(\mathbf{d}, \mathbf{V}) \otimes |0\rangle\langle 0| U_\Phi^\dagger] \right]. \quad (5.95)$$

Here, $E[U_\Phi \hat{\rho}^G(\mathbf{d}, \mathbf{V}) \otimes |0\rangle\langle 0| U_\Phi^\dagger]$ is the entanglement of a bipartite Gaussian state $\sigma_{\text{BE}} = U_\Phi \hat{\rho}^G(\mathbf{d}, \mathbf{V}) \otimes |0\rangle\langle 0| U_\Phi^\dagger$ with CM \mathbf{V}_{BE} . The entanglement E of a bipartite state is quantified by the von Neumann entropy of any of its two reduced density operators. Equation (5.94) not only simplifies the capacity definition to

$$C_\chi^G(\Phi, \bar{N}) = \max_{\hat{\rho}^G \in \mathcal{E}_N^G} [S(\Phi[\hat{\rho}^G]) - E^G[\bar{\sigma}_{\text{BE}}]], \quad (5.96)$$

but also leads to the proof of Eq. (5.90). According to [W^GK⁺04]

$$E^G[\bar{\sigma}_{\text{BE}}] = \min_{\mathbf{V}_{\text{BE}}} \{E[\sigma_{\text{BE}}] \mid \mathbf{V}_{\text{BE}} \leq \bar{\mathbf{V}}_{\text{BE}}\}, \quad (5.97)$$

where the minimum is taken over a single pure bipartite Gaussian state with CM \mathbf{V}_{BE} . This implies the existence of a covariance matrix \mathbf{V}_{in} such that the output entropy of pure Gaussian states $\hat{\rho}^G(\mathbf{d}, \mathbf{V}_{\text{in}})$ achieves the minimum in Eq. (5.94) for any \mathbf{d} . Due to Eq. (5.97) and the fact that the symplectic transformation which corresponds to U_Φ does not change the positivity $\bar{\mathbf{V}}_{\text{BE}} - \mathbf{V}_{\text{BE}} \geq 0$ it follows that $\bar{\mathbf{V}}_{\text{in}} - \mathbf{V}_{\text{in}} \geq 0$. Then modulating $\hat{\rho}^G(\mathbf{d}, \mathbf{V}_{\text{in}})$ according to a Gaussian distribution with covariance matrix $\mathbf{V}_{\text{mod}} = \bar{\mathbf{V}}_{\text{in}} - \mathbf{V}_{\text{in}}$, generates a source with average input state $\hat{\rho}^G$ with CM $\bar{\mathbf{V}}_{\text{in}}$ saturating the bound of Eq. (5.93). We recall from Eq. (5.20) that the entropy of an n -mode Gaussian state $\hat{\rho}^G(\mathbf{d}, \mathbf{V})$ can be calculated in terms of the n symplectic eigenvalues ν_i of \mathbf{V} , namely

$$S(\hat{\rho}^G(\mathbf{d}, \mathbf{V})) = \sum_{i=1}^n g\left(\nu_i - \frac{1}{2}\right), \quad (5.98)$$

In conclusion, the one-shot Gaussian capacity of a general n -mode Gaussian channel simplifies to Eq. (5.90). \square

Let us clarify the physical meaning of Eq. (5.90) in the case of a one-mode channel. We discussed already in the beginning of this chapter the action of the Gaussian channel on

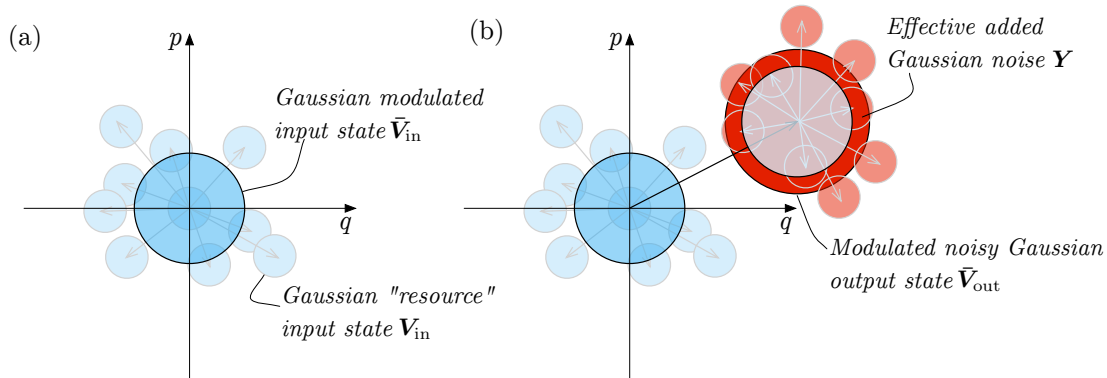
Action of Gaussian channels on Gaussian modulated input states

Figure 5.15.: Thermal Gaussian channel acting on a modulated Gaussian input state: (a) In this example the vacuum state is the resource Gaussian input state with CM \mathbf{V}_{in} . It is displaced by an uncorrelated Gaussian distribution, leading to the (thermal) Gaussian modulated input state with CM $\bar{\mathbf{V}}_{\text{in}}$. (b) The thermal channel displaces the input state and furthermore adds noise to both quadrature variances, leading to the Gaussian modulated output state with CM $\bar{\mathbf{V}}_{\text{out}}$. An example for a single Gaussian output state (with CM \mathbf{V}_{out}) was previously depicted in Fig. 5.13.

a coherent input state. Namely, its amplitude is changed, the state is displaced as well as noise is added to the variances. We proved above that the Gaussian capacity is achieved by a single Gaussian input state that is displaced by a Gaussian modulation. This shows that it is favorable to apply a continuous modulation opposed to a discrete modulation that we discussed previously in Sec. 5.5. We draw in Fig. 5.15. the “complete picture” of the action of Gaussian channels on Gaussian displaced input states in phase space: we depict the action of a thermal channel on the modulated Gaussian state that consists of the vacuum state displaced by an uncorrelated Gaussian distribution centered at $(0, 0)$. With all definitions at hand we can now begin to study in detail the classical capacity and the Gaussian capacity of bosonic Gaussian channels.

Part II.

Capacities of bosonic Gaussian channels

6. One-mode Gaussian channel

In this chapter we study in detail the classical capacity and Gaussian capacity of the most general one-mode Gaussian channel. Before treating capacities we first reduce the number of parameters by introducing a new equivalence relation between the general channel and a newly defined fiducial channel, which depends only on three parameters. Then, we study the fiducial channel in detail.

6.1. General thermal channel

We start by grouping the four thermal channels $\mathcal{C}_L, \mathcal{C}_A, \mathcal{B}_2$ and \mathcal{D} that we discussed in Sec. 5.3.1 to a single one. From Fig. 5.9 (a)-(d) we conclude that we only require a beamsplitter and a TMS to generate any of the four thermal channels. We call this new Gaussian channel Φ^{TH} *general thermal channel* or simply “thermal channel”, extending [GPNBL⁺12]. The scheme of Φ^{TH} is depicted in Fig. 6.1 (a). Before defining the action of Φ^{TH} we introduce two new parameters that will be very useful when dealing with one-mode Gaussian channels. For a given Gaussian channel with matrices \mathbf{X} and \mathbf{Y} we define

$$\tau = \det \mathbf{X}, \quad y = \sqrt{\det \mathbf{Y}}. \quad (6.1)$$

The condition (5.49) for the Gaussian channel to be a quantum channel now simplifies to

$$y \geq \frac{|\tau - 1|}{2}. \quad (6.2)$$

Then, the action of the thermal channel $\Phi^{\text{TH}} = \Phi_{(\tau, y)}^{\text{TH}}$ is defined by

$$\mathbf{X}_{\text{TH}} = \begin{pmatrix} \sqrt{|\tau|} & 0 \\ 0 & \text{sgn}(\tau)\sqrt{|\tau|} \end{pmatrix}, \quad \mathbf{Y}_{\text{TH}} = \begin{pmatrix} y & 0 \\ 0 & y \end{pmatrix}, \quad (6.3)$$

where $\tau \in \mathbb{R}$ and y are functions of the parameters T and G used in scheme depicted in Fig. 6.1. The exact relations between (τ, y) and (T, G) are listed in Table 6.1. If $\tau < 0$ then Φ^{TH} is phase-conjugating, if $0 \leq \tau \leq 1$ then Φ^{TH} corresponds to a thermal lossy channel, if $\tau \geq 1$ then Φ^{TH} is a thermal amplification channel and if $\tau = 1, y > 0$ then Φ^{TH} is a thermal classical additive noise channel [see Fig. 6.2 for a classification in terms of parameters (τ, y)]. There are two limiting cases that we also include in the map Φ^{TH} . Namely, the case $(\tau = 0, y \geq \frac{1}{2})$ which is a limiting case of the lossy channel and called *zero-transmission channel* \mathcal{A}_1 , and the case $(\tau = 1, y = 0)$, which is the perfect transmission channel and a limiting case of the lossy, the amplification channel and the classical additive noise channel (see Table 6.1).

6. One-mode Gaussian channel

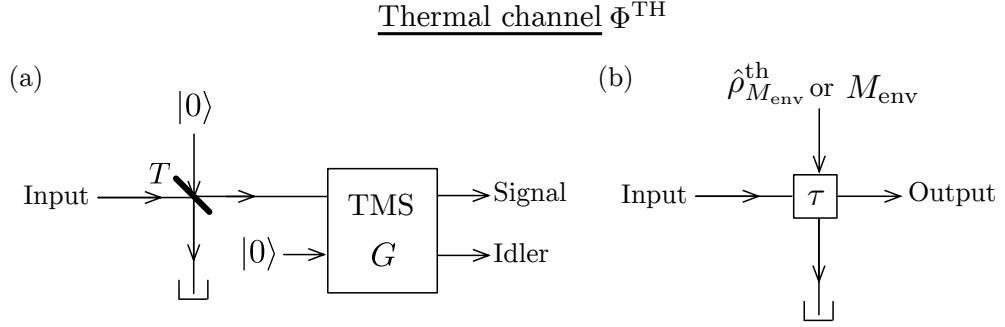


Figure 6.1.: Physical schemes of the thermal channel Φ^{TH} that contains the thermal lossy, thermal amplification, thermal classical additive noise, and the thermal phase-conjugating channel. (a) Realization in terms of a beamsplitter and a two-mode squeezer. (b) Alternative scheme where the input mode is mixed with a thermal state $\hat{\rho}_{M_{\text{env}}}^{\text{th}}$ (if $\tau \neq 1$) or with a classical Gaussian noise with variance M_{env} (if $\tau = 1, y > 0$). Depending on its value τ stands for e.g. a transmissivity or a gain.

We partially have discussed an alternative parametrization of the general thermal channel when we introduced the individual channels in Sec. 5.3.1. The parameter y can be expressed as a function of (T, G) (as shown before), depending on the domain of τ [see upper tabular in Table 6.1 and Fig. 6.1 (b)]. However, one can also express y as a function of τ and another parameter $M_{\text{env}} \geq 0$ (see lower tabular in Table 6.1). Here, M_{env} is the number of thermal photons of a thermal state $\hat{\rho}_{M_{\text{env}}}^{\text{th}}$ (if $\tau \neq 1$) or the variance of a classical Gaussian noise (if $\tau = 1, y > 0$) that is mixed with the input state. For the lossy channel τ is the transmissivity of the beamsplitter and for the amplification channel and phase-conjugating channel it is the amplification gain. Interestingly, we can express the parameter y of the thermal channel Φ^{TH} compactly as follows:

$$y = \begin{cases} |1 - \tau| (M_{\text{env}} + \frac{1}{2}), & \tau \neq 1, \\ M_{\text{env}}, & \tau = 1, \end{cases} \quad (6.4)$$

Note that $\tau = 1$ and $M_{\text{env}} = 0$ corresponds to the perfect transmission channel. We remark that in the parametrization (6.4) the case of the classical additive noise channel $\tau = 1, M_{\text{env}} > 0$ can be recovered as a limiting case from the other channels. For a given classical additive noise channel with parameter $y' = M'_{\text{env}}$ we observe that

$$M'_{\text{env}} = \lim_{\tau \rightarrow 1} |1 - \tau| \frac{M'_{\text{env}}}{|1 - \tau|} + \frac{|1 - \tau|}{2}. \quad (6.5)$$

Physically, this means that the classical additive noise channel can be recovered by an almost perfect transmission through a beamsplitter, where the input signal is mixed with a thermal state with mean number of photons diverging to infinity.

Since the class of thermal channels is just a subset of one-mode Gaussian channels we now move on to the most general one-mode case. The above parametrization is

6.1. General thermal channel

Channel	Symbol	Class	\mathbf{X}_C	\mathbf{Y}_C	τ	Domain of τ
Zero-Transmission	\mathcal{A}_1	Φ^{TH}	0	$(G - 1/2)\mathbb{I}$	0	0
Classical additive noise	\mathcal{B}_2		\mathbb{I}	$(G - 1)\mathbb{I}$	$TG = 1$	1
Lossy	\mathcal{C}_T		$\sqrt{\tau}\mathbb{I}$	$[G(1 - T/2) - 1/2]\mathbb{I}$	TG	$[0, 1]$
Amplification	\mathcal{C}_G		$\sqrt{\tau}\mathbb{I}$	$[G(1 - T/2) - 1/2]\mathbb{I}$	TG	$[1, \infty)$
Phase conjugating	\mathcal{D}		$\sqrt{ \tau }\sigma_z$	$[(1 - T)(G - 1) + G]/2\mathbb{I}$	$-T(G - 1)$	$(-\infty, 0]$
Classical-signal	\mathcal{A}_2	Φ^{CS}	$(\mathbb{I} + \sigma_z)/2$	$(G - 1/2)\mathbb{I}$	0	0
Single-quad. cl. noise	\mathcal{B}_1	Φ^{SQ}	\mathbb{I}	$(\mathbb{I} - \sigma_z)/4$	1	1

Channel	Symbol	Class	\mathbf{X}_C	y	Domain of τ	Domain of y
Zero-Transmission	\mathcal{A}_1	Φ^{TH}	0	$M_{\text{env}} + \frac{1}{2}$	0	$[1/2, \infty)$
Classical additive noise	\mathcal{B}_2		\mathbb{I}	M_{env}	1	$[0, \infty)$
Lossy	\mathcal{C}_T		$\sqrt{\tau}\mathbb{I}$	$(1 - \tau)(M_{\text{env}} + \frac{1}{2})$	$[0, 1]$	$[(1 - \tau)/2, \infty)$
Amplification	\mathcal{C}_G		$\sqrt{\tau}\mathbb{I}$	$(\tau - 1)(M_{\text{env}} + \frac{1}{2})$	$[1, \infty)$	$[(\tau - 1)/2, \infty)$
Phase conjugating	\mathcal{D}		$\sqrt{ \tau }\sigma_z$	$(1 + \tau)(M_{\text{env}} + \frac{1}{2})$	$(-\infty, 0]$	$[(1 - \tau)/2, \infty)$
Classical-signal	\mathcal{A}_2	Φ^{CS}	$(\mathbb{I} + \sigma_z)/2$	$M_{\text{env}} + \frac{1}{2}$	0	$[1/2, \infty)$
Single-quad. cl. noise	\mathcal{B}_1	Φ^{SQ}	\mathbb{I}	-	1	0

Table 6.1.: Canonical channels Φ^C with corresponding symbols as defined in [Hol07, CGH06, ISS11], new representation in terms of Φ^{TH} , Φ^{CS} , Φ^{SQ} and the corresponding matrices $(\mathbf{X}_C, \mathbf{Y}_C)$, where $\sigma_z = \text{diag}(1, -1)$. Upper tabular: Parametrization of y in terms of parameters (T, G) . The parameter $T \in [0, 1]$ is the transmissivity of the beamsplitter and the parameter $G \geq 1$ is the gain of the two-mode squeezer shown in the physical schemes in Fig. 6.1 and Fig. 5.10, respectively. Lower tabular: Parametrization of y in terms of (τ, M_{env}) , where $M_{\text{env}} \geq 0$ is the number of thermal photons of the “coupled” thermal state in Fig. 6.1 (if $\tau \neq 1$), or the variance of an added classical Gaussian noise (if $\tau = 1$).

6. One-mode Gaussian channel

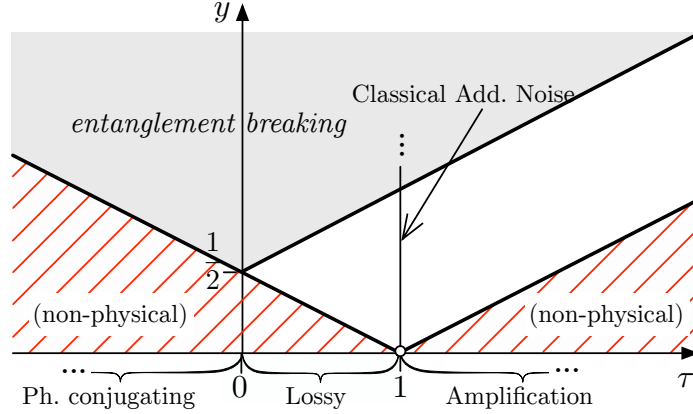


Figure 6.2.: Admissible regions in the parameter space (τ, y) for one-mode Gaussian quantum channels. Each thermal channel $\Phi_{(\tau, y)}^{\text{TH}}$ is associated with one point and vice-versa. The vertical line at $\tau = 0$ corresponds to the zero-transmission channel as well as the classical signal channel Φ^{CS} . The vertical line at $\tau = 1$ corresponds to the classical additive-noise channel. The limiting case $(\tau = 1, y = 0)$ is the perfect transmission channel as well as the single quadrature classical noise channel Φ^{SQ} .

very convenient for expressing the range of parameters when the canonical channels become entanglement breaking. In [Hol08] it was shown that a canonical channel Φ^{C} is entanglement-breaking if

$$y \geq \frac{|\tau| + 1}{2}. \quad (6.6)$$

This means that the thermal phase-conjugating channel $\mathcal{D} = \Phi_{(\tau < 0, y)}^{\text{TH}}$, as well as the classical signal channel Φ^{CS} ($\tau = 0, y \geq 1/2$) are always entanglement-breaking. For the classical signal channel Φ^{CS} this is obvious: since one input quadrature is completely removed by the channel any entanglement that was present at the input will have been destroyed at the output. It was shown in [Hol08] that the single-quadrature classical noise channel Φ^{SQ} is not entanglement-breaking. We plotted the condition (6.6) in Fig. 6.2. We exploit the entanglement-breaking property in the following when calculating the classical capacity.

6.2. Fiducial channel

The canonical decomposition stated in Eq. (5.55) is not always useful, especially when evaluation capacities of bosonic channels with input energy constraint. Indeed, the Gaussian unitary U_1 that precedes the canonical channel Φ^{C} changes, in general, the number of photons that are given at the input. Therefore, we introduce a new decomposition in terms of a *fiducial channel* Φ^{F} , where the preceding unitary is passive and does not

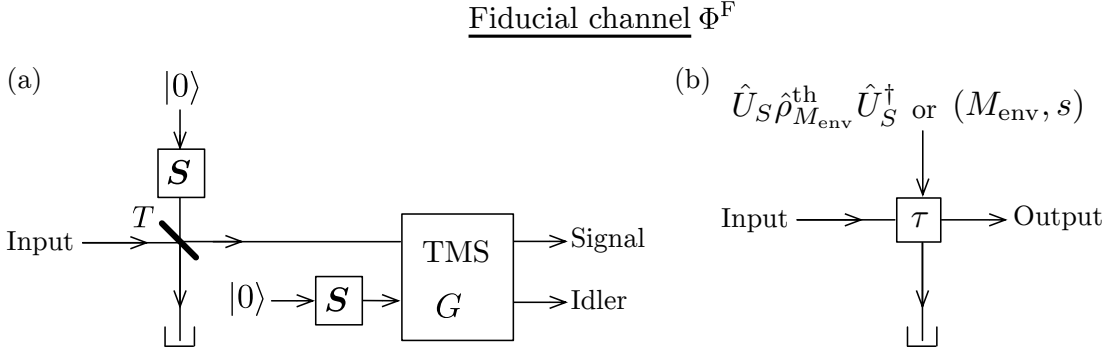


Figure 6.3.: Physical schemes of the fiducial channel Φ^F . (a) Scheme using a beamsplitter, a two-mode squeezer and two identical one-mode squeezers. (b) Alternative scheme (like in Fig. 6.1) where the input state is mixed with a squeezed thermal state or a classical Gaussian noise with “squeezed” variances.

affect the input energy restriction. In Sec 6.3 we show that this decomposition has the major advantage that the energy-restricted capacity of any Gaussian channel reduces to that of the fiducial channel Φ^F . The latter generalizes Φ^{TH} by adding a squeezing to the effective added noise, that is

$$\mathbf{X}_F = \mathbf{X}_{\text{TH}} = \begin{pmatrix} \sqrt{|\tau|} & 0 \\ 0 & \text{sgn}(\tau)\sqrt{|\tau|} \end{pmatrix}, \quad \mathbf{Y}_F = y \begin{pmatrix} e^{2s} & 0 \\ 0 & e^{-2s} \end{pmatrix}. \quad (6.7)$$

Thus, it depends on three parameters (τ, y, s) , and will be denoted by $\Phi_{(\tau, y, s)}^F$. This channel can be physically realized by the setup depicted in Fig. 6.3, where the “idler” corresponds again to the output of the phase-conjugating channel and the “signal” to the output of the other channels.

Equivalently to the general thermal channel Φ^{TH} we can parametrize y also in terms of τ and an additional parameter M_{env} as stated in Eq. (6.4). If $\tau \neq 1$ then the input state is mixed with a squeezed thermal state $\hat{U}_S \hat{\rho}_{M_{\text{env}}}^{\text{th}} \hat{U}_S^\dagger = \hat{\rho}^G(0, \mathbf{V}_{\text{env}})$, i.e. a Gaussian state with CM

$$\mathbf{V}_{\text{env}} = \left(M_{\text{env}} + \frac{1}{2} \right) \begin{pmatrix} e^{2s} & 0 \\ 0 & e^{-2s} \end{pmatrix}, \quad \tau \neq 1. \quad (6.8)$$

If $\tau = 1$ then the input state is mixed with a classical Gaussian noise with CM

$$\mathbf{V}_{\text{env}} = M_{\text{env}} \begin{pmatrix} e^{2s} & 0 \\ 0 & e^{-2s} \end{pmatrix}, \quad \tau = 1. \quad (6.9)$$

Then we can write the effective noise matrix as

$$\begin{aligned} \mathbf{Y}_F &= |1 - \tau| \mathbf{V}_{\text{env}}, & \tau \neq 1, \\ \mathbf{Y}_F &= \mathbf{V}_{\text{env}}, & \tau = 1. \end{aligned} \quad (6.10)$$

One of our central results is that the fiducial channel Φ^F can be used to decompose any Gaussian channel Φ (at least in a proper limit):

6. One-mode Gaussian channel

Theorem 1. For a single-mode Gaussian channel Φ defined by matrices \mathbf{X} and \mathbf{Y} , there exists a fiducial channel Φ^F defined by matrices $\mathbf{X}_F = \mathbf{X}_F(\tau)$, $\mathbf{Y}_F = \mathbf{Y}_F(y, s)$ with τ and y obtained from Eq. (6.1), a symplectic transformation \mathbf{M} , and a rotation in phase space Θ such that

$$\text{if } (\text{rank}(\mathbf{X}), \text{rank}(\mathbf{Y})) \in \{(2, 2), (0, 2), (2, 0)\} \quad (6.11)$$

$$\text{then } \mathbf{X} = \mathbf{M}\mathbf{X}_F\Theta, \mathbf{Y} = \mathbf{M}\mathbf{Y}_F\mathbf{M}^\top,$$

$$\text{if } \text{rank}(\mathbf{X}) = 1, \text{rank}(\mathbf{Y}) = 2 \quad (6.12)$$

$$\text{then } \mathbf{X} = \lim_{\tilde{s} \rightarrow \infty} \mathbf{M}(\tilde{s})\mathbf{X}_F(\tilde{s})\Theta(\tilde{s}), \mathbf{Y} = \lim_{\tilde{s} \rightarrow \infty} \mathbf{M}(\tilde{s})\mathbf{Y}_F\mathbf{M}^\top(\tilde{s}),$$

$$\text{if } \text{rank}(\mathbf{X}) = 2, \text{rank}(\mathbf{Y}) = 1 \quad (6.13)$$

$$\text{then } \mathbf{X} = \lim_{\tilde{s} \rightarrow \infty} \mathbf{M}(\tilde{s})\mathbf{X}_F\Theta(\tilde{s}), \mathbf{Y} = \lim_{\tilde{s} \rightarrow \infty} \mathbf{M}(\tilde{s})\mathbf{Y}_F(\tilde{s})\mathbf{M}^\top(\tilde{s}),$$

where the explicit dependencies of \mathbf{M} , Θ , s and \tilde{s} on the parameters of the channel Φ are presented in Eqs. (6.26), (6.36) and (6.41) (see following proof).

Proof. The action of the channel Φ on an input CM \mathbf{V} reads as in Eq. (5.48)

$$\Phi(\mathbf{V}) = \mathbf{X}\mathbf{V}\mathbf{X}^\top + \mathbf{Y}, \quad (6.14)$$

where \mathbf{X} is a real 2×2 matrix and \mathbf{Y} a real, symmetric and positive-semidefinite 2×2 matrix. Recall the definitions $\tau = \det \mathbf{X}$, $y = \sqrt{\det \mathbf{Y}}$, which have to satisfy Eq. (6.2) in order for the map to correspond to a quantum channel. In Eq. (5.56) we stated that for any Gaussian channel Φ there exists a canonical decomposition $U_2 \circ \Phi^C \circ U_1$, where Φ^C is a map belonging to one of the seven canonical types that are stated in Table 6.1. The corresponding action on the CM reads

$$\Phi(\mathbf{V}) = \mathbf{M}_2(\mathbf{X}_C\mathbf{M}_1\mathbf{V}\mathbf{M}_1^\top\mathbf{X}_C + \mathbf{Y}_C)\mathbf{M}_2^\top, \quad (6.15)$$

where $\mathbf{X}_C, \mathbf{Y}_C$ are the matrices defining the canonical channels (see Table 6.1). In the following we obtain the new decomposition in terms of the fiducial channel as stated in the Theorem and furthermore, confirm Eq. (6.15). The proof is structured as follows. For given matrices \mathbf{X}, \mathbf{Y} we have to distinguish three cases which depend on the ranks of \mathbf{X} and \mathbf{Y} and correspond to canonical decompositions for which Φ^C is either Φ^{TH} , Φ^{SQ} or Φ^{CS} . In the first case our new decomposition will contain finite squeezing operations, while for the other two cases the new decomposition is shown to be valid in a proper limit of infinite squeezing.

Recall the symplectic matrices of the phase-space rotation $\mathbf{O}(\theta)$ stated in Eq. (5.22) and squeezing operation $\mathbf{S}(s)$ stated in Eq. (5.24). Then, for the given CM \mathbf{Y} one can find a rotation $\Theta_Y = \mathbf{O}(\theta_Y)$, such that $\Theta_Y^\top \mathbf{Y} \Theta_Y = \text{diag}(y_1, y_2)$, where $y_1, y_2 \geq 0$ are the eigenvalues of \mathbf{Y} . Since matrix \mathbf{X} is always real it has a singular value decomposition (SVD)

$$\mathbf{X} = \Theta_{1X} \Lambda_X \mathbf{J} \Theta_{2X}, \quad (6.16)$$

where $\Theta_{1X} = \mathbf{O}(\theta_{1X})$ and $\Theta_{2X} = \mathbf{O}(\theta_{2X})$ are rotation matrices. Here

$$\Lambda_X = \text{diag}(x_1, x_2), \quad \mathbf{J} = \begin{cases} \mathbb{I} & \text{if } \tau \geq 0, \\ \sigma_z & \text{if } \tau < 0, \end{cases} \quad (6.17)$$

where $x_1, x_2 \geq 0$ are the singular values and $\sigma_z = \text{diag}(1, -1)$. Using equality $\det \mathbf{X} = \det(\Lambda_X \mathbf{J})$ and Eq. (6.1) we get $\tau = \pm x_1 x_2$ and $y = \sqrt{y_1 y_2}$. The condition on the determinants of \mathbf{X} and \mathbf{Y} stated in Eq. (6.2) allows us to exclude the following combinations of ranks because they are non-physical:

$$(\text{rank}(\mathbf{X}), \text{rank}(\mathbf{Y})) \notin \{(0, 0), (0, 1), (1, 0), (1, 1)\}. \quad (6.18)$$

The physically allowed combinations of ranks therefore read

$$(\text{rank}(\mathbf{X}), \text{rank}(\mathbf{Y})) \in \{(2, 2), (0, 2), (2, 0), (1, 2), (2, 1)\}. \quad (6.19)$$

Below we treat the first three ‘‘physical’’ couples together and the other two individually.

$\text{rank}(\mathbf{X}) = \text{rank}(\mathbf{Y}) = 2$: First, we derive the relations for the case of full ranks. The latter implies that $x_1, x_2, y_1, y_2 \neq 0$. Then we can construct the squeezing operation $\mathbf{S}_Y = \mathbf{S}(s_Y)$, with $s_Y = \frac{1}{4} \ln(y_1/y_2)$ such that $\mathbf{S}_Y^{-1} \text{diag}(y_1, y_2) \mathbf{S}_Y^{-1} = \text{diag}(y, y)$. This implies that

$$\mathbf{Y} = \Theta_Y \mathbf{S}_Y \mathbf{Y}_{\text{TH}} \mathbf{S}_Y \Theta_Y^\top = y \Theta_Y \mathbf{S}_Y^2 \Theta_Y^\top, \quad \mathbf{Y}_{\text{TH}} = \text{diag}(y, y). \quad (6.20)$$

Here the symplectic transformation $\Theta_Y \mathbf{S}_Y$ realizes the symplectic diagonalization of \mathbf{Y} , where y is the symplectic eigenvalue. Furthermore, we can define a squeezing operation $\mathbf{S}_X = \mathbf{S}(s_X)$, with $s_X = \frac{1}{2} \ln(x_1/x_2)$, such that Eq. (6.16) can be written as

$$\mathbf{X} = \Theta_{1X} \mathbf{S}_X \mathbf{X}_{\text{TH}} \Theta_{2X}, \quad \mathbf{X}_{\text{TH}} = \begin{pmatrix} \sqrt{|\tau|} & 0 \\ 0 & \text{sgn}(\tau) \sqrt{|\tau|} \end{pmatrix}. \quad (6.21)$$

Notice that the matrix \mathbf{X}_{TH} has the property that

$$\mathbf{X}_{\text{TH}} \mathbf{O}(\theta) = \mathbf{O}(\text{sgn}(\tau)\theta) \mathbf{X}_{\text{TH}}. \quad (6.22)$$

Now we obtain the decomposition $\mathbf{Y} = \mathbf{M} \mathbf{Y}_F \mathbf{M}^\top$ in the following way. We define

$$\mathbf{M} = \Theta_{1X} \mathbf{S}_X \Theta_F^\top. \quad (6.23)$$

Then, we multiply \mathbf{Y} in Eq. (6.20) from both sides with the identity matrix $\mathbb{I} = \mathbf{M} \Theta_F \mathbf{S}_X^{-1} \Theta_{1X}^\top$,

$$\mathbb{I} \mathbf{Y} \mathbb{I} = y \mathbf{M} \Theta_F \mathbf{S}_X^{-1} \Theta_{1X}^\top \Theta_Y \mathbf{S}_Y^2 \Theta_Y^\top \Theta_{1X} \mathbf{S}_X^{-1} \Theta_F^\top \mathbf{M}^\top. \quad (6.24)$$

Then we define

$$\mathbf{Y}_F = y \Theta_F \mathbf{S}_X^{-1} \Theta_{1X}^\top \Theta_Y \mathbf{S}_Y^2 \Theta_Y^\top \Theta_{1X} \mathbf{S}_X^{-1} \Theta_F^\top, \quad (6.25)$$

6. One-mode Gaussian channel

and thus, obtain the desired decomposition $\mathbf{Y} = \mathbf{M}\mathbf{Y}_F\mathbf{M}^\top$. Moreover, we choose the rotation Θ_F in a way such that matrix \mathbf{Y}_F is diagonal, i.e. $\mathbf{Y}_F = y \text{diag}(e^{2s}, e^{-2s})$. This implies the following expression for the squeezing parameter s

$$s = \frac{1}{2} \ln \left[\frac{1}{4} e^{-2(s_X+s_Y)} (\xi - \sqrt{-16e^{4(s_X+s_Y)} + \xi^2}) \right], \quad (6.26)$$

$$\xi = (1 + e^{4s_Y})(1 + e^{4s_X}) - (-1 + e^{4s_Y})(-1 + e^{4s_X}) \cos(2(\theta_Y - \theta_{1X})).$$

The angle θ_F of rotation $\Theta_F = \mathbf{O}(\theta_F)$ reads

$$\theta_F = -\arcsin \left(\frac{\text{sgn}(\lambda)}{\sqrt{1 + \lambda^2}} \right), \quad (6.27)$$

where

$$\lambda = -\frac{e^{-2s_X} (\tilde{\xi} + \sqrt{-16e^{4(s_X+s_Y)} + \xi^2})}{2 \sin(2(\theta_Y - \theta_{1X}))(-1 + e^{4s_Y})}, \quad (6.28)$$

$$\tilde{\xi} = (1 + e^{4s_Y})(-1 + e^{4s_X}) - (-1 + e^{4s_Y})(1 + e^{4s_X}) \cos(2(\theta_Y - \theta_{1X})).$$

Using definition $\mathbf{X}_F = \mathbf{X}_{\text{TH}}$ [see Eq. (6.7)] and Eq. (6.22) one can rewrite Eq. (6.21) as

$$\mathbf{X} = \Theta_{1X} \mathbf{S}_X \Theta_F^\top \Theta_F \mathbf{X}_F \Theta_{2X} = \Theta_{1X} \mathbf{S}_X \Theta_F^\top \mathbf{X}_F \mathbf{O}(\text{sgn}(\tau)\theta_F) \Theta_{2X} = \mathbf{M}\mathbf{X}_F\Theta, \quad (6.29)$$

where

$$\Theta = \mathbf{O}(\text{sgn}(\tau)\theta_F + \theta_{2X}). \quad (6.30)$$

In summary, we found that

$$\mathbf{X} = \mathbf{M}\mathbf{X}_F\Theta, \quad \mathbf{Y} = \mathbf{M}\mathbf{Y}_F\mathbf{M}^\top. \quad (6.31)$$

Thus, we have proven the theorem for the case $\text{rank}(\mathbf{X}) = \text{rank}(\mathbf{Y}) = 2$. Let us now extend it to different combinations of ranks.

$\text{rank}(\mathbf{X}) = 2, \text{rank}(\mathbf{Y}) = 0$: Since $\mathbf{Y} = 0$ it follows that $y = 0$, which together with Eq. (6.2) implies that $\tau = 1$. Therefore, the channel is unitarily equivalent to the perfect transmission channel. All relations derived above are found in the same way where one has to fix $s_Y = \theta_Y = 0$, which leads to $\mathbf{S}_Y = \Theta_Y = \mathbb{I}$.

$\text{rank}(\mathbf{X}) = 0, \text{rank}(\mathbf{Y}) = 2$: This case can also be treated using the above relations. In this case $\mathbf{X} = 0$, $\tau = 0$ which together with Eq. (6.2) implies that $y \geq 1/2$. This channel is unitarily equivalent to the zero-transmission channel and has trivially a capacity equal to zero. The decomposition containing the fiducial channel is found above where one has to fix $s_X = \theta_{1X} = \theta_{2X} = 0$.

We remark that for $(\text{rank}(\mathbf{X}), \text{rank}(\mathbf{Y})) \in \{(2, 2), (0, 2), (2, 0)\}$ the physical action of Φ corresponds (up to unitaries) to the action of Φ^{TH} . Indeed, by inserting Eqs. (6.20) and (6.21) in Eq. (6.14) one obtains the canonical decomposition $\Phi = U_2 \circ \Phi^{\text{TH}} \circ U_1$, which in terms of the symplectic transformations reads as in Eq. (6.15), with

$$\mathbf{X}_C = \mathbf{X}_{\text{TH}}, \quad \mathbf{Y}_C = \mathbf{Y}_{\text{TH}}, \quad \mathbf{M}_1 = \mathbf{S}_Y^{-1} \Theta_Y'^\top \Theta_{1X}' \mathbf{S}_X \Theta_{2X}, \quad \mathbf{M}_2 = \Theta_Y \mathbf{S}_Y, \quad (6.32)$$

where $\Theta'_Y = O(\text{sgn}(\tau)\theta_Y)$ and $\Theta'_{1X} = O(\text{sgn}(\tau)\theta_{1X})$. In Fig. 6.4 we sketched the equivalences found above.

rank(\mathbf{X}) = 2, rank(\mathbf{Y}) = 1: This implies $y = 0$ and together with Eq. (6.2) that $\tau = 1$. The eigenvalues of \mathbf{Y} now read $y_1 = 0, y_2 > 0$ (the case $y_1 > 0, y_2 = 0$ follows the same treatment). Similarly to the case rank(\mathbf{Y}) = 2 one can find a rotation Θ_Y such that $\Theta_Y^\top \mathbf{Y} \Theta_Y = \text{diag}(0, y_2)$. Then, one can construct a squeezing operation \mathbf{S}_Y with $s_Y = -\frac{1}{2} \ln(2y_2)$ which yields

$$\mathbf{Y} = \Theta_Y \mathbf{S}_Y \mathbf{Y}_{\text{SQ}} \mathbf{S}_Y \Theta_Y^\top, \quad \mathbf{Y}_{\text{SQ}} = \text{diag}\left(0, \frac{1}{2}\right), \quad (6.33)$$

The matrix \mathbf{Y}_{SQ} can be recovered with an additional squeezer $\tilde{\mathbf{S}} = \mathbf{S}(\tilde{s})$ in the limit of infinite squeezing, i.e. $\mathbf{Y}_{\text{SQ}} = \lim_{\tilde{s} \rightarrow \infty} \frac{1}{2} e^{-2\tilde{s}} \tilde{\mathbf{S}}^{-2}$ from which follows

$$\mathbf{Y} = \lim_{\tilde{s} \rightarrow \infty} \frac{1}{2} e^{-2\tilde{s}} \Theta_Y \mathbf{S}_Y \tilde{\mathbf{S}}^{-2} \mathbf{S}_Y \Theta_Y^\top = \lim_{\tilde{s} \rightarrow \infty} \frac{1}{2} e^{-2\tilde{s}} \Theta_Y \tilde{\mathbf{S}}_Y^2 \Theta_Y^\top, \quad (6.34)$$

where $\tilde{\mathbf{S}}_Y = \mathbf{S}(s_Y - \tilde{s})$. Since rank(\mathbf{X}) = 2 we can decompose \mathbf{X} as in Eq. (6.21) but with the simplification $\tau = 1$, i.e.

$$\mathbf{X} = \Theta_{1X} \mathbf{S}_X \mathbf{X}_{\text{SQ}} \Theta_{2X}, \quad \mathbf{X}_{\text{SQ}} = \mathbb{I}, \quad (6.35)$$

We observe that we can replace $\mathbf{X}_{\text{SQ}} = \mathbf{X}_F$, where \mathbf{X}_F is defined as above with $\tau = 1$. Thus, we get the same decomposition as stated in Eq. (6.21). Now one can recover both matrices \mathbf{X}, \mathbf{Y} as a limiting case of Eq. (6.31), namely,

$$\mathbf{X} = \lim_{\tilde{s} \rightarrow \infty} \mathbf{M} \mathbf{X}_F \Theta, \quad \mathbf{Y} = \lim_{\tilde{s} \rightarrow \infty} \mathbf{M} \mathbf{Y}_F \mathbf{M}^\top, \quad (6.36)$$

where in the definitions of \mathbf{M} (6.23), Θ (6.30) and \mathbf{Y}_F (6.25) one has to make replacements $\tau \rightarrow 1$, $s_Y \rightarrow s_Y - \tilde{s}$ and $y \rightarrow \frac{1}{2} e^{-2\tilde{s}}$. We remark that these replacements only affects matrix \mathbf{Y}_F and rotations Θ_F and Θ . Thus, we recovered both matrices \mathbf{X} and \mathbf{Y} as a limiting case of the decomposition stated in the theorem.

Note that the physical action of Φ in this case corresponds (up to unitaries) to the action of Φ^{SQ} : by inserting Eqs. (6.35) and (6.33) into Eq. (6.14) we find the canonical decomposition $\Phi = U_2 \circ \Phi^{\text{SQ}} \circ U_1$, which in terms of the symplectic transformations is given by Eq. (6.15), with

$$\mathbf{X}_C = \mathbf{X}_{\text{SQ}}, \quad \mathbf{Y}_C = \mathbf{Y}_{\text{SQ}}, \quad \mathbf{M}_1 = \mathbf{S}_Y^{-1} \Theta_Y^\top \Theta_{1X} \mathbf{S}_X \Theta_{2X}, \quad \mathbf{M}_2 = \Theta_Y \mathbf{S}_Y. \quad (6.37)$$

rank(\mathbf{X}) = 1, rank(\mathbf{Y}) = 2: Since in this case $\tau = 0$ it follows from Eq. (6.2) that $y \geq \frac{1}{2}$. The SVD of \mathbf{X} now reads $\mathbf{X} = \Theta_{1X} \text{diag}(x_1, 0)$ (the case $x_1 = 0, x_2 > 0$ follows the same treatment). One can define $\mathbf{S}_X = \mathbf{S}(s_X)$ with $s_X = \ln(x_1)$ such that

$$\mathbf{X} = \Theta_{1X} \mathbf{S}_X \mathbf{X}_{\text{CS}}, \quad \mathbf{X}_{\text{CS}} = \text{diag}(1, 0). \quad (6.38)$$

Since \mathbf{X}_{CS} can be expressed as $\mathbf{X}_{\text{CS}} = \lim_{\tilde{s} \rightarrow \infty} e^{-\tilde{s}} \tilde{\mathbf{S}}$, where $\tilde{\mathbf{S}} = \mathbf{S}(\tilde{s})$, Eq. (6.38) becomes

$$\mathbf{X} = \lim_{\tilde{s} \rightarrow \infty} e^{-\tilde{s}} \Theta_{1X} \mathbf{S}_X \tilde{\mathbf{S}} = \lim_{\tilde{s} \rightarrow \infty} e^{-\tilde{s}} \Theta_{1X} \tilde{\mathbf{S}}_X, \quad (6.39)$$

6. One-mode Gaussian channel

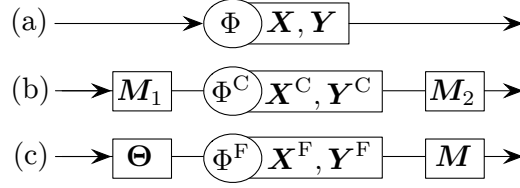


Figure 6.4.: Equivalence of (a) an arbitrary Gaussian channel Φ , (b) the canonical decomposition containing a canonical channel Φ^C and (c) the decomposition in terms of the fiducial channel Φ^F as stated in Theorem 1.

where $\tilde{S}_X = S(s_X + \tilde{s})$. Since $y \geq \frac{1}{2}$ we find as in the case $y > 0$ treated above [see derivation of Eq. (6.20)], a rotation Θ_Y and squeezing S_Y such that

$$\mathbf{Y} = \Theta_Y S_Y Y_{CS} S_Y^\top, \quad Y_{CS} = \text{diag}(y, y), \quad y \geq \frac{1}{2}. \quad (6.40)$$

Thus, we recover matrices \mathbf{X}, \mathbf{Y} as a limiting case of Eq. (6.31), i.e.

$$\mathbf{X} = \lim_{\tilde{s} \rightarrow \infty} \mathbf{M} \mathbf{X}_F \Theta, \quad \mathbf{Y} = \lim_{\tilde{s} \rightarrow \infty} \mathbf{M} \mathbf{Y}_F \mathbf{M}^\top, \quad (6.41)$$

where in the definitions of \mathbf{M} (6.23) and Θ (6.30) one has to make replacements $\theta_{2X} \rightarrow 0$, $s_X \rightarrow s_X + \tilde{s}$ and $\tau \rightarrow e^{-2\tilde{s}}$. Note that these replacements affects \mathbf{M} but does not affect matrix \mathbf{Y} stated in Eq. (6.40). Therefore, we found also for the last case both matrices \mathbf{X}, \mathbf{Y} as limiting cases of the decomposition stated in the theorem.

Now we demonstrate that (up to unitaries) the physical action of Φ in this case corresponds to the action of Φ^{CS} . By inserting Eqs. (6.40) and (6.38) in Eq. (6.14), we obtain

$$\Phi(\mathbf{V}) = \tilde{M}(\tilde{X} \mathbf{V} \tilde{X}^\top + Y_{CS}) \tilde{M}^\top, \quad \tilde{X} = S_Y^{-1} \Theta_Y^\top \Theta_{1X} S_X X_{CS}, \quad \tilde{M} = \Theta_Y S_Y. \quad (6.42)$$

For the real 2×2 matrix \tilde{X} one can again obtain the SVD which leads to $\tilde{X} = \tilde{\Theta}_X \tilde{S}_X X_{CS}$. Since $\tilde{S}_X X_{CS} = X_{CS} \tilde{S}_X$ we obtain the canonical decomposition $\Phi = U_2 \circ \Phi^{CS} \circ U_1$ in terms of the symplectic transformations as stated in Eq. (6.15), with

$$\mathbf{X}_C = X_{CS}, \quad \mathbf{Y}_C = Y_{CS}, \quad \mathbf{M}_1 = \tilde{S}_X, \quad \mathbf{M}_2 = \Theta_Y S_Y \tilde{\Theta}_X, \quad (6.43)$$

Thus, we extended the theorem to lower rank cases of \mathbf{X} and \mathbf{Y} . \square

Let us summarize the above presented equivalences. For an arbitrary Gaussian map, defined by matrices (\mathbf{X}, \mathbf{Y}) , there exists a canonical decomposition $\mathbf{X} = \mathbf{M}_2 \mathbf{X}_C \mathbf{M}_1$, $\mathbf{Y} = \mathbf{M}_2 \mathbf{Y}_C \mathbf{M}_1^\top$, where \mathbf{M}_1 and \mathbf{M}_2 are general (*a priori* non photon number preserving) symplectic transformations and $(\mathbf{X}_C, \mathbf{Y}_C)$ define one out of seven canonical channels. According to Theorem 1, there exists a *fiducial decomposition* in terms of the newly defined fiducial channel, defined by matrices $(\mathbf{X}_F, \mathbf{Y}_F)$ such that $\mathbf{X} = \mathbf{M} \mathbf{X}_F \Theta$,

$\mathbf{Y} = \mathbf{M}\mathbf{Y}_F\mathbf{M}^\top$, where now the preceding unitary Θ is passive (i.e. photon number preserving). This means that

$$\mathbf{V}_{\text{out}} = \mathbf{X}\mathbf{V}_{\text{in}}\mathbf{X}^\top + \mathbf{Y} = \mathbf{M}(\mathbf{X}_F\Theta\mathbf{V}_{\text{in}}\Theta^\top\mathbf{X}_F + \mathbf{Y}_F)\mathbf{M}^\top. \quad (6.44)$$

Therefore, the equivalence (up to displacements) in terms of Gaussian channels and unitaries can be written as

$$\Phi = U_2 \circ \Phi^C \circ U_1 = U \circ \Phi^F \circ U_\Theta, \quad (6.45)$$

where U and U_Θ are unitary transformations corresponding to the symplectic transformations \mathbf{M} and Θ , respectively (U_Θ is energy preserving). Note that in case of a canonical decomposition containing non-thermal channels, Eq. (6.45) is valid in a proper limit (as explained above in terms of symplectic transformations). The equivalences are also stated in Fig. 6.4. The usefulness of these equivalences will become clear in the following section.

6.3. Equivalence relations for capacities

We present now a way to greatly simplify the calculation of the classical capacity as well as the Gaussian capacity. We showed above that any Gaussian channel Φ is (up to displacements) equal to a fiducial channel Φ^F preceded by a passive Gaussian unitary transformation and followed by a general Gaussian unitary transformation. This implies the following corollary:

Corollary 1. *For a single-mode Gaussian channel Φ with parameters (τ, y) there exists a fiducial channel Φ^F as defined in Theorem 1 such that*

$$\begin{aligned} C(\Phi, \bar{N}) &= C(\Phi^F, \bar{N}), \quad (\text{rank}(\mathbf{X}), \text{rank}(\mathbf{Y})) \in \{(2, 2), (0, 2), (2, 0)\}, \\ C(\Phi, \bar{N}) &= \lim_{\tilde{s} \rightarrow \infty} C(\Phi^F(\tilde{s}), \bar{N}), \quad (\text{rank}(\mathbf{X}), \text{rank}(\mathbf{Y})) \in \{(1, 2), (2, 1)\}. \end{aligned} \quad (6.46)$$

Proof. First, any displacement $\mathbf{d}_{\text{env}} \neq 0$ that is introduced by Φ as well as the symplectic transformation \mathbf{M} that follows Φ^F in Theorem 1 does not change the entropies in the definition of χ . Second, there is no energy constraint at the output of the channel. Hence, \mathbf{M} can be dropped (even in the limit of infinite squeezing for the cases when $\text{rank}(\mathbf{X}) = 1$ or $\text{rank}(\mathbf{Y}) = 1$). Then, the rotation Θ preceding Φ^F in Theorem 1 may be regarded as change of a reference phase that can be chosen arbitrarily; therefore, Θ can be dropped as well. Thus,

$$\begin{aligned} C_\chi(\Phi, \bar{N}) &= C_\chi(\Phi^F, \bar{N}), \quad (\text{rank}(\mathbf{X}), \text{rank}(\mathbf{Y})) \in \{(2, 2), (0, 2), (2, 0)\}, \\ C_\chi(\Phi, \bar{N}) &= \lim_{\tilde{s} \rightarrow \infty} C_\chi(\Phi^F(\tilde{s}), \bar{N}), \quad (\text{rank}(\mathbf{X}), \text{rank}(\mathbf{Y})) \in \{(1, 2), (2, 1)\}. \end{aligned} \quad (6.47)$$

To evaluate the one-shot capacity of n copies of Φ the same reasoning can be applied, where now the preceding and following transformations are given by

$$\bigoplus_{i=1}^n \mathbf{M}, \quad \bigoplus_{i=1}^n \Theta, \quad (6.48)$$

6. One-mode Gaussian channel

respectively. Hence, it follows that

$$C_\chi(\Phi^{\otimes n}, n\bar{N}) = C_\chi((\Phi^F)^{\otimes n}, n\bar{N}), \quad (6.49)$$

which together with Eq. (5.73) implies Eq. (6.46) (as well as in the case of corresponding limiting expressions). \square

Corollary 1 has also other implications. If the corresponding fiducial channel $\Phi_{(\tau,y,s)}^F$ is entanglement breaking (see Sec. 6.1), then the one-shot capacities of both $\Phi_{(\tau,y,s)}^F$ and Φ are additive, implying

$$C(\Phi, \bar{N}) = C_\chi(\Phi^F, \bar{N}), \quad y \geq \frac{1+|\tau|}{2}. \quad (6.50)$$

For the case $\text{rank}(\mathbf{Y}) = 1$ it follows that $y = 0$ and so in this case the channel is not entanglement breaking. The other pathological case $\text{rank}(\mathbf{X}) = 1$ and $y \geq 1/2$ in contrary is always entanglement breaking and thus,

$$C(\Phi, \bar{N}) = \lim_{\tilde{s} \rightarrow \infty} C_\chi(\Phi^F(\tilde{s}), \bar{N}), \quad \text{rank}(\mathbf{X}) = 1, \text{rank}(\mathbf{Y}) = 2. \quad (6.51)$$

We can directly extend Corollary 1 to the Gaussian capacity since the proof works on the level of the χ -quantity. The Gaussian capacity is a restricted maximization over the χ -quantity which is left invariant under unitaries, as well as the energy constraint. Thus,

$$\begin{aligned} C^G(\Phi, \bar{N}) &= C^G(\Phi^F, \bar{N}), \quad (\text{rank}(\mathbf{X}), \text{rank}(\mathbf{Y})) \in \{(2, 2), (0, 2), (2, 0)\}, \\ C^G(\Phi, \bar{N}) &= \lim_{\tilde{s} \rightarrow \infty} C^G(\Phi^F(\tilde{s}), \bar{N}), \quad (\text{rank}(\mathbf{X}), \text{rank}(\mathbf{Y})) \in \{(1, 2), (2, 1)\}, \end{aligned} \quad (6.52)$$

as well as

$$\begin{aligned} C_\chi^G(\Phi, \bar{N}) &= C_\chi^G(\Phi^F, \bar{N}), \quad (\text{rank}(\mathbf{X}), \text{rank}(\mathbf{Y})) \in \{(2, 2), (0, 2), (2, 0)\}, \\ C_\chi^G(\Phi, \bar{N}) &= \lim_{\tilde{s} \rightarrow \infty} C_\chi^G(\Phi^F(\tilde{s}), \bar{N}), \quad (\text{rank}(\mathbf{X}), \text{rank}(\mathbf{Y})) \in \{(1, 2), (2, 1)\}. \end{aligned} \quad (6.53)$$

6.4. Gaussian capacity

Now we analyze C_χ^G and C^G of the one-mode Gaussian channel. For the particular case $0 \leq \tau < 1$ (and $\tau = 1, y = 0$) (i.e. the lossy channel), some of the following results were obtained independently and in parallel in [PLM12].

According to equations (6.52) and (6.53) it suffices to compute the Gaussian capacity C^G (as well as the one-shot Gaussian capacity C_χ^G) of the fiducial channel Φ^F in order to obtain it for an arbitrary one-mode Gaussian channel.

The quantity of interest is therefore $C_\chi^G(\Phi, \bar{N}) = C_\chi^G(\Phi^F, \bar{N})$, which reads (using Eq. (5.90) with $n = 1$)

$$\begin{aligned} C_\chi^G(\Phi, \bar{N}) &= \max_{\mathbf{V}_{\text{in}}, \mathbf{V}_{\text{mod}}} \left\{ \chi^G(\nu_{\text{out}}, \bar{\nu}_{\text{out}}) \mid \text{Tr}[\mathbf{V}_{\text{in}} + \mathbf{V}_{\text{mod}}] \leq 2\bar{N} + 1 \right\}, \\ \chi^G(\nu_{\text{out}}, \bar{\nu}_{\text{out}}) &= g\left(\bar{\nu}_{\text{out}} - \frac{1}{2}\right) - g\left(\nu_{\text{out}} - \frac{1}{2}\right), \\ \nu_{\text{out}} &= \sqrt{\det \mathbf{V}_{\text{out}}}, \quad \bar{\nu}_{\text{out}} = \sqrt{\det \bar{\mathbf{V}}_{\text{out}}}. \end{aligned} \quad (6.54)$$

Using the definition of the thermal photon number (5.10) we alternatively can express the Gaussian capacity as

$$C_{\chi}^G(\Phi, \bar{N}) = \max_{\mathbf{V}_{\text{in}}, \mathbf{V}_{\text{mod}}} \left[g(\bar{M}_{\text{out}}) - g(M_{\text{out}}) \mid \text{Tr}[\mathbf{V}_{\text{in}} + \mathbf{V}_{\text{mod}}] \leq 2\bar{N} + 1 \right], \quad (6.55)$$

where $M_{\text{out}} = \nu_{\text{out}} - 1/2$ and $\bar{M}_{\text{out}} = \bar{\nu}_{\text{out}} - 1/2$ are the number of thermal photons of the output state and modulated output state, respectively. From now on we choose the following notations for covariance matrices of the input state and modulation:

$$\mathbf{V}_{\text{in}} = \begin{pmatrix} i_{\text{q}} & i_{\text{qp}} \\ i_{\text{qp}} & i_{\text{p}} \end{pmatrix}, \quad \mathbf{V}_{\text{mod}} = \begin{pmatrix} m_{\text{q}} & m_{\text{qp}} \\ m_{\text{qp}} & m_{\text{p}} \end{pmatrix}. \quad (6.56)$$

The fact that the optimal input state is pure reads in terms of the CM

$$\det \mathbf{V}_{\text{in}} = i_{\text{q}} i_{\text{p}} - i_{\text{qp}}^2 = \frac{1}{4}. \quad (6.57)$$

The energy constraint is given by

$$\frac{1}{2} \text{Tr}[\mathbf{V}_{\text{in}} + \mathbf{V}_{\text{mod}}] - \frac{1}{2} = \bar{N} \quad (6.58)$$

which equivalently can be written as

$$i_{\text{q}} + i_{\text{p}} + m_{\text{q}} + m_{\text{p}} = 2\bar{N} + 1. \quad (6.59)$$

Recall the definition of the fiducial channel:

$$\mathbf{X}_{\text{F}} = \sqrt{|\tau|} \text{diag}(1, \text{sgn}(\tau)), \quad \mathbf{Y}_{\text{F}} = y \text{diag}(e^{2s}, e^{-2s}). \quad (6.60)$$

Then, the output CM \mathbf{V}_{out} and the modulated output CM $\bar{\mathbf{V}}_{\text{out}}$ are given by

$$\begin{aligned} \mathbf{V}_{\text{out}} &= \begin{pmatrix} |\tau| i_{\text{q}} + y e^{2s} & \text{sgn}(\tau) |\tau| i_{\text{qp}} \\ \text{sgn}(\tau) |\tau| i_{\text{qp}} & |\tau| i_{\text{p}} + y e^{-2s} \end{pmatrix}, \\ \bar{\mathbf{V}}_{\text{out}} &= \begin{pmatrix} |\tau| (i_{\text{q}} + m_{\text{q}}) + y e^{2s} & \text{sgn}(\tau) |\tau| (i_{\text{qp}} + m_{\text{qp}}) \\ \text{sgn}(\tau) |\tau| (i_{\text{qp}} + m_{\text{qp}}) & |\tau| (i_{\text{p}} + m_{\text{p}}) + y e^{-2s} \end{pmatrix}. \end{aligned} \quad (6.61)$$

The corresponding symplectic eigenvalues $\nu_{\text{out}} = \sqrt{\det \mathbf{V}_{\text{out}}}$, $\bar{\nu}_{\text{out}} = \sqrt{\det \bar{\mathbf{V}}_{\text{out}}}$, respectively, read

$$\begin{aligned} \nu_{\text{out}}^2 &= (|\tau| i_{\text{q}} + y e^{2s})(|\tau| i_{\text{p}} + y e^{-2s}) - \tau^2 i_{\text{qp}}^2, \\ \bar{\nu}_{\text{out}}^2 &= (|\tau| (i_{\text{q}} + m_{\text{q}}) + y e^{2s})(|\tau| (i_{\text{p}} + m_{\text{p}}) + y e^{-2s}) - \tau^2 (i_{\text{qp}} + m_{\text{qp}})^2, \end{aligned} \quad (6.62)$$

where furthermore

$$\nu_{\text{out}}^2 = \tau^2 \det \mathbf{V}_{\text{in}} + y^2 + |\tau| (i_{\text{q}} y e^{-2s} + i_{\text{p}} y e^{2s}). \quad (6.63)$$

In [PLM12] it was shown that for $0 \leq \tau < 1$ it is optimal to choose $i_{\text{qp}} = m_{\text{qp}} = 0$. We present now this proof and show that is also applicable to the fiducial channel.

6. One-mode Gaussian channel

Lemma 1. For the fiducial channel Φ^F it is optimal to choose

$$i_{\text{qp}} = m_{\text{qp}} = 0. \quad (6.64)$$

Proof. First, it cannot be optimal to choose $i_{\text{qp}}m_{\text{qp}} > 0$. If i_{qp} and m_{qp} have the same signs then we can replace $m_{\text{qp}} \rightarrow -m_{\text{qp}}$ (without violating the positivity of \mathbf{V}_{mod}) which leads to an increase of $\bar{\nu}_{\text{out}}$ and does not change ν_{out} . Thus, we obtain that

$$\text{sgn}(i_{\text{qp}}) = -\text{sgn}(m_{\text{qp}}). \quad (6.65)$$

The latter implies that

$$(i_{\text{qp}} + m_{\text{qp}})^2 = (|i_{\text{qp}}| - |m_{\text{qp}}|)^2. \quad (6.66)$$

Now we show that indeed $i_{\text{qp}} = m_{\text{qp}} = 0$ is optimal. If the latter does not hold then there are three possible scenarios:

1. $|m_{\text{qp}}| > |i_{\text{qp}}| \geq 0$
2. $|i_{\text{qp}}| > |m_{\text{qp}}| \geq 0$
3. $|m_{\text{qp}}| = |i_{\text{qp}}| > 0$

In the first case one can decrease $|m_{\text{qp}}|$ by choosing $m'_{\text{qp}} = -i_{\text{qp}}$ which preserves the positivity of \mathbf{V}_{mod} . This increases $\bar{\nu}_{\text{out}}$ and leaves ν_{out} unchanged. Thus, the first term in χ^G is increased and the second term is unchanged, which increases χ^G . Therefore, the first scenario can be excluded.

In the second case one can decrease $|i_{\text{qp}}|$ by choosing $i'_{\text{qp}} = -m_{\text{qp}}$ and choose $i'_q < i_q$ in order to preserve the purity constraint

$$i_q i_{\text{qp}} - i_{\text{qp}}^2 = i'_q i'_p - i_{\text{qp}}'^2 = \frac{1}{4}. \quad (6.67)$$

The decrease of i_q changes the total energy [according to Eq. (6.59)]. This can be compensated by adding the difference $i_q - i'_q$ to the modulation parameter m'_q such that $i'_q + m'_q = i_q + m_q$. Since $\det \mathbf{V}_{\text{in}}$ is not changed and $i'_q < i_q$ the value of ν_{out} is decreased according to Eq. (6.63). Then, the value of $\bar{\nu}_{\text{out}}$ is increased because $(i'_{\text{qp}} - m_{\text{qp}})^2 = 0$ and the first term in $\bar{\nu}_{\text{out}}$ is left unchanged. Thus, χ^G is increased and the second scenario can be excluded as well.

The last case is $|m_{\text{qp}}| = |i_{\text{qp}}| > 0$. One can always commonly decrease them to $|m'_{\text{qp}}| = |i'_{\text{qp}}| = 0$ leaving $\bar{\nu}_{\text{out}}$ unchanged. Then in order to guarantee purity one decreases i_q as in the second scenario. It follows that $\bar{\nu}_{\text{out}}$ is not changed but ν_{out} is decreased implying that the third case is non-optimal.

We excluded all three cases and proved therefore the Lemma. Note that if $\mathbf{V}_{\text{mod}} = \text{diag}(m_q, 0)$ or $\mathbf{V}_{\text{mod}} = \text{diag}(0, m_p)$, i.e. $m_{\text{qp}} = 0$, then only the second case can exist and is proven straightforwardly. \square

Therefore, the optimal input and modulation CM are of the form

$$\mathbf{V}_{\text{in}} = \text{diag}(i_q, i_p), \quad \mathbf{V}_{\text{mod}} = \text{diag}(m_q, m_p), \quad (6.68)$$

and are diagonal in the same basis as the effective noise CM $\mathbf{Y} = \text{diag}(y e^{2s}, y e^{-2s})$. This implies that the optimal matrices \mathbf{V}_{out} and $\bar{\mathbf{V}}_{\text{out}}$ are diagonal as well.

6.4.1. Quantum water-filling solution

Let us now calculate C_χ^G of the fiducial channel. Using Eq. (6.55) for C_χ^G we can state the upper bound

$$C_\chi^G(\Phi^F, \bar{N}) \leq \max_{\mathbf{V}_{\text{in}}, \mathbf{V}_{\text{mod}}} g(\bar{M}_{\text{out}}) - \min_{\mathbf{V}_{\text{in}}} g(M_{\text{out}}), \quad (6.69)$$

where \mathbf{V}_{in} and \mathbf{V}_{mod} are given by Eq. (6.68). First, we minimize the second term independently of the joint energy constraint stated in Eq. (6.55) (which may lead to an unphysical encoding). Again, since $g(x)$ is a concave function it is sufficient to minimize (maximize) its argument in order to minimize (maximize) its value. According to Eq. (6.62) and Lemma 1 we have

$$\begin{aligned} M_{\text{out}} &= \sqrt{(|\tau| i_{\text{q}} + y e^{2s})(|\tau| i_{\text{p}} + y e^{-2s})} - \frac{1}{2} \\ &= \sqrt{\frac{\tau^2}{2} + |\tau| y \left(i_{\text{q}} e^{-2s} + \frac{e^{2s}}{4i_{\text{q}}} \right) + y^2} - \frac{1}{2}, \end{aligned} \quad (6.70)$$

where we used the relation $i_{\text{q}} i_{\text{p}} = \frac{1}{4}$. The inner bracket is then straightforwardly minimized for

$$i_{\text{q}} = \frac{1}{2} e^{2s}, \quad (6.71)$$

which implies

$$i_{\text{p}} = \frac{1}{2} e^{-2s}. \quad (6.72)$$

and results to

$$M_{\text{out}} = y + \frac{|\tau| - 1}{2}. \quad (6.73)$$

We observe that the minimizing input state exactly matches the squeezing of the added noise. Second, we try to maximize the first term in Eq. (6.69). We know from Sec. 5.1 that a thermal state maximizes the entropy, so the first term is maximized if

$$\bar{\mathbf{V}}_{\text{out}} = \left(\bar{M}_{\text{out}} + \frac{1}{2} \right) \mathbb{I}. \quad (6.74)$$

Using Eq. (6.61) and Lemma 1 we have

$$\bar{\mathbf{V}}_{\text{out}} = \begin{pmatrix} |\tau|(i_{\text{q}} + m_{\text{q}}) + y e^{2s} & 0 \\ 0 & |\tau|(i_{\text{p}} + m_{\text{p}}) + y e^{-2s} \end{pmatrix}. \quad (6.75)$$

In order to satisfy Eq. (6.74) we need to satisfy the equation

$$|\tau|(i_{\text{q}} + m_{\text{q}}) + y e^{2s} = |\tau|(i_{\text{p}} + m_{\text{p}}) + y e^{-2s}. \quad (6.76)$$

This equation can be regarded as the quantum equivalent of the water-filling solution that we stated for classical information theory in Eq. (2.19). Therefore, we refer to

6. One-mode Gaussian channel

Eq. (6.76) as *quantum water-filling* (QWF) solution¹. Here, the variances of the two modulated output quadratures need to be equalized, which corresponds in the classical case to two different channels. However, the fact that the energy needs to be divided between the input state and its modulation adds additional difficulty to the problem. Let us take the minimizing solution for the input state derived in Eqs. (6.71) and (6.72) and inject it in Eq. (6.76):

$$e^{2s} \left(\frac{|\tau|}{2} + y \right) + |\tau| m_q = e^{-2s} \left(\frac{|\tau|}{2} + y \right) + |\tau| m_p. \quad (6.77)$$

Using furthermore the input energy constraint given in Eq. (6.59) we obtain the solutions

$$\begin{aligned} m_q &= \bar{N} + \frac{1}{2} - \frac{1}{2} e^{2s} + \frac{y}{|\tau|} \sinh(-2s), \\ m_p &= \bar{N} + \frac{1}{2} - \frac{1}{2} e^{-2s} + \frac{y}{|\tau|} \sinh(2s). \end{aligned} \quad (6.78)$$

Then, the number of thermal photons of the modulated output state reads

$$\bar{M}_{\text{out}} = |\tau| \bar{N} + y \cosh(2s) + \frac{|\tau| - 1}{2}, \quad (6.79)$$

and Eq. (6.74) is satisfied.

In order for the solutions stated in Eqs. (6.71), (6.72) and (6.78) to be physical we have the conditions $m_q \geq 0$ and $m_p \geq 0$ for the given input energy \bar{N} . For $s > 0$ we have $m_q < m_p$ (equivalently for $s < 0$ we have $m_p < m_q$), i.e. the less noisy quadrature is more modulated. This means that for given squeezing $s > 0$ the condition $m_q \geq 0$ suffices to guarantee that the solution is physical. The solution to the equation $m_q = 0$ (and equivalently to $m_p = 0$ for $s < 0$) is given by

$$\bar{N} = \bar{N}_{\text{thr}} \equiv \frac{1}{2} \left(e^{2|s|} - 1 \right) + \frac{y}{|\tau|} \sinh(2|s|). \quad (6.80)$$

where \bar{N}_{thr} is the *input energy threshold*. This means that for $\bar{N} \geq \bar{N}_{\text{thr}}$ the solutions given in Eqs. (6.71), (6.72) and (6.78) hold but for $\bar{N} < \bar{N}_{\text{thr}}$ become unphysical. We observe that \bar{N}_{thr} diverges for $\tau \rightarrow 0$ (and finite s) or $s \rightarrow \infty$. Therefore, we already see that this solution does not include the limiting cases of the fiducial decomposition stated in Eqs. (6.12) and (6.13).

Using Eq. (6.53) we obtain the following theorem:

Theorem 2. *The one-shot Gaussian capacity of a Gaussian channel Φ with parameters $(\tau \neq 0, y > 0)$ and input energy $\bar{N} \geq \bar{N}_{\text{thr}}$ is given by*

$$\begin{aligned} C_\chi^{\text{G}}(\Phi, \bar{N}) &= C_\chi^{\text{G}}(\Phi^{\text{F}}, \bar{N}) \\ &= g \left(|\tau| \bar{N} + y \cosh(2s) + \frac{|\tau| - 1}{2} \right) - g \left(y + \frac{|\tau| - 1}{2} \right), \quad \bar{N} \geq \bar{N}_{\text{thr}}. \end{aligned} \quad (6.81)$$

¹The notion of quantum water-filling appeared for the first time in the discussion of the capacity of a memoryless phase-dependent Gaussian channel [HSH99]. However, in [HSH99] the quantum information carriers were considered as part of the channel and only the energy cost of classical modulation was considered, thus making this solution a straightforward analog to the classical one.

Proof. We showed above that the input encoding presented in Eqs. (6.71), (6.72) and (6.78) is achievable for $\bar{N} \geq \bar{N}_{\text{thr}}$ and therefore achieves the upper bound in Eq. (6.69). For the given Gaussian channel Φ the squeezing parameter s of the corresponding fiducial channel can be obtained by the method presented in Sec. 6.2. \square

Note that for the alternative parametrization $\mathbf{Y} = \text{diag}(y_q, y_p)$ the one-shot Gaussian capacity reads

$$C_{\chi}^G(\Phi, \bar{N}) = g\left(|\tau|\bar{N} + \frac{y_q + y_p}{2} + \frac{|\tau| - 1}{2}\right) - g\left(y + \frac{|\tau| - 1}{2}\right), \quad \bar{N} \geq \bar{N}_{\text{thr}}, \quad (6.82)$$

where the input energy threshold for $y_q \geq y_p$ is given by²

$$\bar{N}_{\text{thr}} = \frac{1}{2} \left(\sqrt{\frac{y_q}{y_p}} + \frac{y_q - y_p}{|\tau|} - 1 \right). \quad (6.83)$$

The optimal input state and modulation (see Eqs. (6.71), (6.72) and (6.78)) is then given by

$$i_q = \frac{1}{2} \sqrt{\frac{y_q}{y_p}}, \quad i_p = \frac{1}{2} \sqrt{\frac{y_p}{y_q}}, \quad (6.84)$$

$$m_q = \bar{N} + \frac{1}{2} - \frac{1}{2} \sqrt{\frac{y_q}{y_p}} + \frac{y_p - y_q}{2|\tau|}, \quad m_p = \bar{N} + \frac{1}{2} - \frac{1}{2} \sqrt{\frac{y_p}{y_q}} + \frac{y_q - y_p}{2|\tau|}. \quad (6.85)$$

We depict the QWF solution (for $\tau = 1$) together with the optimal squeezed input state in Fig. 6.5 (a) in a stack plot and in Fig. 6.5 (b) and (c) in phase space. The *quantum water-filling level* is simply given by

$$\bar{v}_{\text{wf}} \equiv \bar{v}_q = \bar{v}_p = |\tau| \left(\bar{N} + \frac{1}{2} \right) + \frac{y_q + y_p}{2}. \quad (6.86)$$

A particular case is given by the lossy channel with (pure) squeezed noise, i.e. when $y = (1 - \tau)/2$. Then, we obtain $M_{\text{out}} = 0$, i.e. as in the case of the lossy channel with vacuum noise (see Sec. 5.6) the entropy of the output state vanishes. This is clear because the case $y = (1 - \tau)/2$ corresponds to mixing two identical (pure) squeezed states [i.e. the input and the noise state, see Fig. 6.3 (b)] on a beamsplitter which then outputs the same two pure squeezed states. Then, Eq. (6.81) becomes an upper bound on the actual one-shot capacity C_{χ} . Since only the first term in Eq. (6.81) needs to be maximized the additivity of the one-shot capacity follows from the subadditivity property of the von Neumann entropy such that the full classical capacity of the channel $\Phi_{(\tau, \frac{1-\tau}{2}, s)}^F$ is given by

$$C\left(\Phi_{(\tau, \frac{1-\tau}{2}, s)}^F\right) = g(\tau + (1 - \tau) \sinh^2 s), \quad \tau \in [0, 1], \quad \bar{N} \geq \bar{N}_{\text{thr}}. \quad (6.87)$$

²The choice $y_q \geq y_p$ is without loss of generality. For $y_p \geq y_q$ the Gaussian capacity remains unchanged and one simply needs to replace $q \rightarrow p$ and $p \rightarrow q$ in the energy threshold.

6. One-mode Gaussian channel

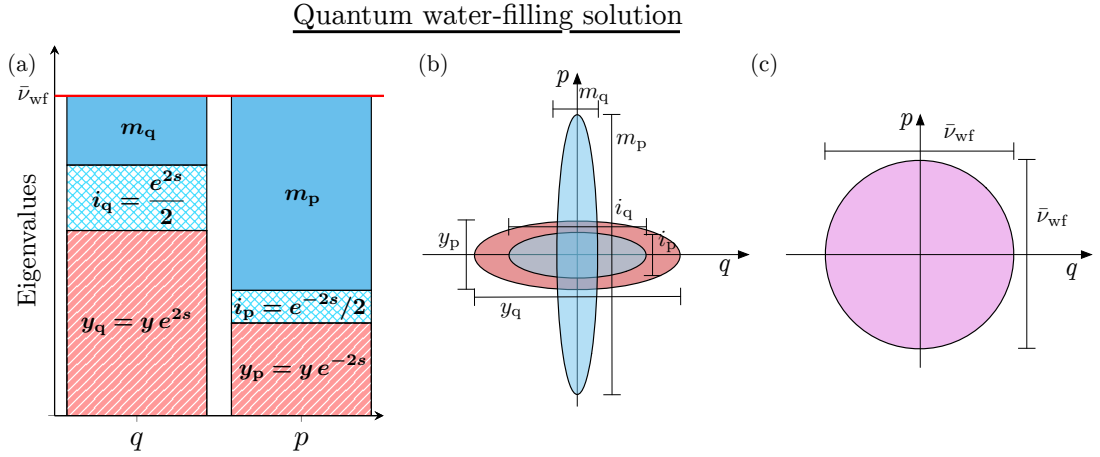


Figure 6.5.: Quantum water-filling solution (schematically for the case $\tau = 1$): (a) relations between optimal eigenvalues; the quantum water-filling level $\bar{\nu}_{\text{wff}}$ is given by the symplectic eigenvalue of the modulated output state [see Eq. (6.86)]. (b) schematic plot of the Wigner functions of the input state, the modulation and the noise state; the input state matches the squeezing of the noise and the less noisy quadrature is more modulated. (c) schematic plot of the modulated output state which is a thermal state.

This result was previously derived in [LPM09], where it was furthermore generalized to a collection of independent lossy channels with squeezed noise.

A second important case is the one-shot Gaussian capacity of the general thermal channel Φ^{TH} . It corresponds to the limiting case $s = 0$ for which $\bar{N}_{\text{thr}} = 0$. Thus, we have

$$C_{\chi}^G(\Phi^{\text{TH}}, \bar{N}) = g\left(|\tau|\bar{N} + y + \frac{|\tau| - 1}{2}\right) - g\left(y + \frac{|\tau| - 1}{2}\right). \quad (6.88)$$

This result was obtained for the different thermal channels previously in [Hol98a, HSH99, HW01, HG12] and summarized in [GLMS13].

In conclusion we have obtained an analytical expression for the Gaussian capacity, stated in Eq. (6.81), which generalizes previous results of particular cases.

The so-called *Holevo-Werner* conjecture states that Eq. (6.88) is the classical capacity of the general thermal channel [HW01]. For the thermal channel Φ^{TH} this would be already implied if the minimum output entropy conjecture (introduced in Sec. 5.6.1) was proven to be true: one can always present an encoding that realizes a thermal state for the modulated output state if the optimal input state is the (displaced) vacuum. In this case, additivity of the one-shot classical capacity follows straightforwardly [GPC13]. The minimum output entropy conjecture would even imply that the Gaussian capacity of an arbitrary one-mode Gaussian channel stated in Eq. (6.81) becomes the classical capacity for $\bar{N} \geq \bar{N}_{\text{thr}}$, as shown in [GPC13].

A particular channel of interest is the classical additive noise channel with thermal

noise, i.e. the case when $\tau = 1$ and $y = M_{\text{env}}$ (using the parametrization presented in Eq. (6.4)). The Gaussian capacity then becomes

$$C_{\chi}^{\text{G}} \left(\Phi_{(1, M_{\text{env}})}^{\text{TH}}, \bar{N} \right) = g(\bar{N} + M_{\text{env}}) - g(M_{\text{env}}). \quad (6.89)$$

This may be regarded as the *coherent rate* (properly defined below in Sec. 7.4.4) because it is a valid lower bound on the classical capacity, obtained by sending coherent states as input states. Furthermore, it was found to be the capacity of a bosonic *classical-quantum channel* (c-q channel) [Hol98a]. This channel is defined by a mapping of an input codeword α to a thermal state

$$\hat{D}(\alpha) \hat{\rho}_{M_{\text{env}}}^{\text{th}} \hat{D}(\alpha)^{\dagger}. \quad (6.90)$$

It does not fall into the class of one-mode Gaussian channels because there is no freedom to change the input state. The modulated “output” state of the channel is given by

$$\hat{\rho}_{\text{out}} = \int d^2\alpha p(\alpha) \hat{D}(\alpha) \hat{\rho}_{M_{\text{env}}}^{\text{th}} \hat{D}(\alpha)^{\dagger}. \quad (6.91)$$

Then, the one-shot capacity of the c-q channel reads

$$C_{\chi}^{\text{G}(c-q)} = \max_{p(\alpha)} \left\{ S(\hat{\rho}_{\text{out}}) - \int d^2\alpha p(\alpha) S \left(\hat{D}(\alpha) \hat{\rho}_{M_{\text{env}}}^{\text{th}} \hat{D}(\alpha)^{\dagger} \right) \right\}. \quad (6.92)$$

Since the displacement operator does not change the entropy the second term is equal to $S(\hat{\rho}_{M_{\text{env}}}^{\text{th}}) = g(M_{\text{env}})$, $\forall \alpha$. The first term is maximized for a symmetric bivariate Gaussian distribution such that the modulated “output” state becomes a thermal state as well. With the “input” energy constraint³

$$\int d^2\alpha |\alpha|^2 p(\alpha) \leq \bar{N}, \quad (6.93)$$

this yields $S(\hat{\rho}_{\text{out}}) = g(\bar{N} + M_{\text{env}})$ and thus, the classical capacity is given by Eq. (6.89). Note that Eq. (6.89) recovers the Shannon capacity C_{Sh} of a classical channel with additive white Gaussian noise in the classical limit, i.e. when the input energy \bar{N} as well as the noise variance M_{env} is increased up to infinity while the signal-to-noise $SNR = \bar{N}/M_{\text{env}}$ is kept constant. In this limit the arguments in the first and second term in Eq. (6.89) diverge and since

$$\lim_{x \rightarrow \infty} [g(x) - \log_2(x)] = \frac{1}{\ln 2}, \quad (6.94)$$

we replace $g(x)$ by the asymptotic function $\log_2(x)$ which yields

$$\lim_{\substack{\bar{N} \rightarrow \infty \\ M_{\text{env}} \rightarrow \infty \\ \frac{\bar{N}}{M_{\text{env}}} = SNR}} C_{\chi}^{\text{G}} \left(\Phi_{(1, M_{\text{env}})}^{\text{TH}}, \bar{N} \right) = \log_2(\bar{N} + M_{\text{env}}) - \log_2(M_{\text{env}}) = \log_2 \left(1 + \frac{\bar{N}}{M_{\text{env}}} \right) = 2C_{\text{Sh}}, \quad (6.95)$$

³Here the energy constraint is only imposed on the modulation.

6. One-mode Gaussian channel

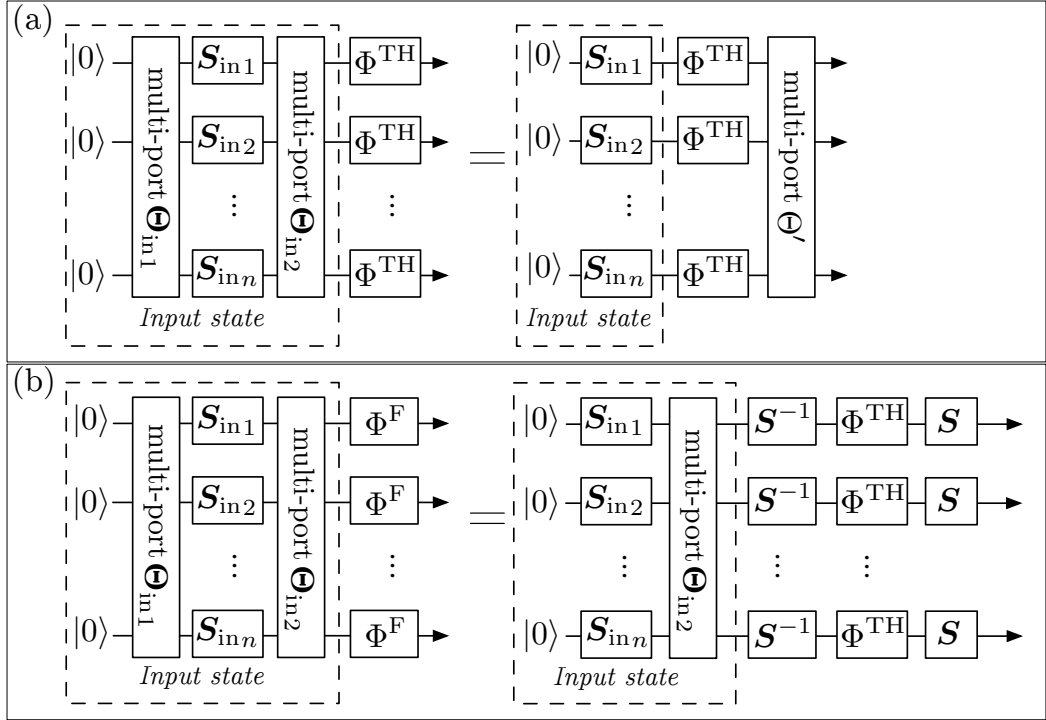


Figure 6.6.: Using the Bloch-Messiah decomposition any multimode pure Gaussian state can be generated from the vacuum and a set of single mode squeezers $\mathbf{S}_{in i}$ preceded and followed by linear multi-port interferometers $\Theta_{in1}, \Theta_{in2}$. (a) Reduction of the scheme for a collection of channels $(\Phi^{TH})^{\otimes n}$ and (b) decomposition for the fiducial channel $(\Phi^F)^{\otimes n}$.

where we stated C_{Sh} previously in Eq. (2.16). The factor 2 stems from the fact that the quantum channel has two degrees of freedom (i.e. two quadratures) and therefore in total twice the input energy of the classical counterpart.

6.4.2. Additivity of the Gaussian capacity

In the previous section we found the one-shot Gaussian capacity C_χ^G for $\bar{N} \geq \bar{N}_{thr}$. In this energy regime we can prove furthermore that it is additive and thus, equal to the Gaussian capacity C^G :

Theorem 3. *The Gaussian capacity of a Gaussian channel Φ with parameters $(\tau \neq 0, y > 0)$ and input energy $\bar{N} \geq \bar{N}_{thr}$ is given by*

$$C^G(\Phi, \bar{N}) = C_\chi^G(\Phi^F, \bar{N}), \quad (6.96)$$

where $C_\chi^G(\Phi^F, \bar{N})$ is stated in Eq. (6.81).

Proof. The proof is structured as follows. First, we prove that the Gaussian minimum output entropy of thermal channels Φ^{TH} is additive (corresponding to Φ^{F} with $s = 0$). Then we extend this proof to the fiducial channel for input energies above the input energy threshold \bar{N}_{thr} (we present a simple and physically motivated proof, which is an alternative to the one in [Hir06], where the energy constraint was not respected). Now we show that this also implies the additivity of the one-shot Gaussian capacity in this energy domain.

We introduced in Sec. 5.2.2 the Bloch-Messiah decomposition, which states that any pure n -mode Gaussian (input) state can be generated from a set of n vacuum modes, using n single-mode squeezers $\mathbf{S}_{\text{in}i}$ preceded and followed by a linear multi-port interferometer, corresponding to passive symplectic transformations $\Theta_{\text{in}1}$ and $\Theta_{\text{in}2}$ (see Fig. 5.3). The multi-mode vacuum state with CM $\mathbb{I}/2$ (where \mathbb{I} is the $2n \times 2n$ identity matrix) remains unchanged under the action of the first interferometer $\Theta_{\text{in}1}$ and therefore, we can omit it. The action of the channel $(\Phi_{(\tau,y)}^{\text{TH}})^{\otimes n}$ in terms of symplectic transformation then reads

$$\mathbf{V}_{\text{out}} = \frac{1}{2} \mathbf{X}_{\text{TH}} \Theta_{\text{in}2} \mathbf{S}_{\text{in}} \mathbb{I} \mathbf{S}_{\text{in}} \Theta_{\text{in}2}^{\text{T}} \mathbf{X}_{\text{TH}} + \mathbf{Y}_{\text{TH}}, \quad (6.97)$$

where

$$\mathbf{S}_{\text{in}} = \text{diag}(e^{s_{\text{in}1}}, e^{s_{\text{in}2}}, \dots, e^{s_{\text{in}n}}; e^{-s_{\text{in}1}}, \dots, e^{-s_{\text{in}n}}), \quad (6.98)$$

corresponds to the joint operation of single mode squeezers, $\Theta_{\text{in}2}$ is the symplectic transformation of the second linear multi-port interferometer and

$$\mathbf{X}_{\text{TH}} = \sqrt{|\tau|} \begin{pmatrix} \mathbb{I} & 0 \\ 0 & \text{sgn}(\tau) \mathbb{I} \end{pmatrix}, \quad \mathbf{Y}_{\text{TH}} = y \mathbb{I}. \quad (6.99)$$

Now we insert $\frac{1}{|\tau|} \mathbf{X}_{\text{TH}} \mathbf{X}_{\text{TH}} = \mathbb{I}$ between $\Theta_{\text{in}2}$ and \mathbf{S}_{in} and between \mathbf{S}_{in} and $\Theta_{\text{in}2}^{\text{T}}$ in Eq. (6.97) which leads to the equation

$$\begin{aligned} \mathbf{V}_{\text{out}} &= \frac{1}{2} \underbrace{\frac{1}{|\tau|} \mathbf{X}_{\text{TH}} \Theta_{\text{in}2} \mathbf{X}_{\text{TH}}}_{\equiv \Theta'_{\text{in}}} \mathbf{X}_{\text{TH}} \mathbf{S}_{\text{in}} \mathbb{I} \mathbf{S}_{\text{in}} \mathbf{X}_{\text{TH}} \underbrace{\frac{1}{|\tau|} \mathbf{X}_{\text{TH}} \Theta_{\text{in}2}^{\text{T}} \mathbf{X}_{\text{TH}}}_{\equiv \Theta'^{\text{T}}_{\text{in}}} + \mathbf{Y}_{\text{TH}} \\ &= \Theta'_{\text{in}} \left(\frac{1}{2} \mathbf{X}_{\text{TH}} \mathbf{S}_{\text{in}} \mathbb{I} \mathbf{S}_{\text{in}} \mathbf{X}_{\text{TH}} + \Theta'^{\text{T}}_{\text{in}} \mathbf{Y}_{\text{TH}} \Theta'_{\text{in}} \right) \Theta'^{\text{T}}_{\text{in}}. \end{aligned} \quad (6.100)$$

It is easy to prove that Θ'_{in} is a symplectic (rotation) matrix corresponding to another interferometer. In fact, for any matrix Θ' defined as $\Theta' = \frac{1}{|\tau|} \mathbf{X}_{\text{TH}} \Theta \mathbf{X}_{\text{TH}}$ (where Θ is a passive symplectic transformation) we confirm orthogonality:

$$\begin{aligned} \Theta' \Theta'^{\text{T}} &= \frac{1}{\tau^2} \mathbf{X}_{\text{TH}} \Theta \mathbf{X}_{\text{TH}} \mathbf{X}_{\text{TH}} \Theta^{\text{T}} \mathbf{X}_{\text{TH}} \\ &= \frac{|\tau|}{\tau^2} \mathbf{X}_{\text{TH}} \Theta \Theta^{\text{T}} \mathbf{X}_{\text{TH}} = \mathbb{I}, \end{aligned} \quad (6.101)$$

6. One-mode Gaussian channel

and the condition for the transformation to be a symplectic transformation:

$$\begin{aligned}
\Theta' \Omega \Theta'^T &= \frac{1}{\tau^2} \mathbf{X}_{\text{TH}} \Theta \underbrace{\mathbf{X}_{\text{TH}} \Omega \mathbf{X}_{\text{TH}}}_{=-\Omega} \Theta^T \mathbf{X}_{\text{TH}} \\
&= -\frac{1}{\tau^2} \mathbf{X}_{\text{TH}} \Theta \Omega \Theta^T \mathbf{X}_{\text{TH}} \\
&= -\frac{1}{\tau^2} \mathbf{X}_{\text{TH}} \Omega \mathbf{X}_{\text{TH}} = \mathbb{I}.
\end{aligned} \tag{6.102}$$

We remark that Eqs. (6.101) and (6.102) imply the commutation relation

$$[\Theta, \mathbf{X}_{\text{TH}}] = [\mathbf{X}_{\text{TH}}, \Theta']. \tag{6.103}$$

Furthermore, Θ'^T_{in} leaves the noise matrix \mathbf{Y}_{TH} invariant, i.e. $\Theta'_{\text{in}} \mathbf{Y}_{\text{TH}} \Theta'^T_{\text{in}} = \mathbf{Y}_{\text{TH}}$ and we obtain

$$\mathbf{V}_{\text{out}} = \Theta'_{\text{in}} \left(\frac{1}{2} \mathbf{X}_{\text{TH}} \mathbf{S}_{\text{in}} \mathbb{I} \mathbf{S}_{\text{in}} \mathbf{X}_{\text{TH}} + \mathbf{Y}_{\text{TH}} \right) \Theta'^T_{\text{in}}. \tag{6.104}$$

Thus, the general Gaussian input state entering the channel $(\Phi^{\text{TH}})^{\otimes n}$ is reduced to a product state [see right hand side of Fig. 6.6 (a)]. Now we upper bound the one-shot Gaussian capacity of $(\Phi^{\text{TH}})^{\otimes n}$ [in the same way as in Eq. (6.69)], i.e.

$$C_{\chi}^{\text{G}}((\Phi^{\text{TH}})^{\otimes n}, n\bar{N}) \leq \max_{\mathbf{V}_{\text{in}}, \mathbf{V}_{\text{mod}}} S(\bar{\mathbf{V}}_{\text{out}}) - \min_{\mathbf{V}_{\text{in}}} S(\mathbf{V}_{\text{out}}), \tag{6.105}$$

where $\bar{\mathbf{V}}_{\text{out}}$ is the CM of the n -mode modulated output state, \mathbf{V}_{out} the CM of the n -mode output state and

$$\mathbf{V}_{\text{in}} = \frac{1}{2} \mathbf{S}_{\text{in}} \mathbb{I} \mathbf{S}_{\text{in}} = \frac{1}{2} \text{diag}(e^{2s_{\text{in}1}}, e^{2s_{\text{in}2}}, \dots, e^{2s_{\text{in}n}}; e^{-2s_{\text{in}1}}, \dots, e^{-2s_{\text{in}n}}). \tag{6.106}$$

The second term in Eq. (6.105) is then given by

$$\min_{\mathbf{V}_{\text{in}}} S(\mathbf{V}_{\text{out}}) = \sum_i \min_{s_{\text{in}i}} g\left(\nu_{\text{out}i} - \frac{1}{2}\right), \tag{6.107}$$

where $s_{\text{in}i}$ are the input squeezing parameters and

$$\nu_{\text{out}i} = \sqrt{\left(\frac{|\tau|}{2} e^{2s_{\text{in}i}} + y\right) \left(\frac{|\tau|}{2} e^{-2s_{\text{in}i}} + y\right)}. \tag{6.108}$$

Clearly, the latter is minimized if $s_{\text{in}i} = 0$, i.e. the optimal Gaussian input state is the vacuum as before, which then leads to the minimum Gaussian output entropy

$$\min_{\mathbf{V}_{\text{in}}} S(\mathbf{V}_{\text{out}}) = n g\left(y + \frac{|\tau| - 1}{2}\right), \tag{6.109}$$

i.e. the minimum Gaussian output entropy of the one-mode thermal channel stated in Eq. (6.88). As mentioned before, due to the subadditivity property of the entropy we

know that the first term in Eq. (6.105) is upper bounded by the entropy of n thermal states with identical mean number of thermal photons, which is achieved by displacing the input vacuum states with a non-correlated Gaussian modulation [in the same way as in Eq. (6.76)]. Thus,

$$\max_{\mathbf{V}_{\text{in}}, \mathbf{V}_{\text{mod}}} S(\bar{\mathbf{V}}_{\text{out}}) = n g \left(|\tau| \bar{N} + y + \frac{|\tau| - 1}{2} \right), \quad (6.110)$$

from which follows that

$$\frac{1}{n} C_{\chi}^{\text{G}} ((\Phi^{\text{TH}})^{\otimes n}, n\bar{N}) = C_{\chi}^{\text{G}}(\Phi^{\text{TH}}, \bar{N}), \quad (6.111)$$

which then implies the theorem for $s = 0$. Let us extend this proof to the fiducial channel Φ^{F} , i.e. to the general case when $s \neq 0$ as depicted in Fig. 6.6 (b). We use again the Bloch-Messiah decomposition to decompose the general multi-mode Gaussian input state. The first interferometer $\Theta_{\text{in}1}$ can again be omitted because it does not affect the n -mode vacuum state. From the definition of the fiducial channel we have the equivalence

$$\mathbf{X}_{\text{F}} = \mathbf{X}_{\text{TH}}, \quad \mathbf{Y}_{\text{F}} = \mathbf{S} \mathbf{Y}_{\text{TH}} \mathbf{S}, \quad (6.112)$$

with $\mathbf{S} = \text{diag}(e^s, e^{-s})$. This leads to the equality

$$\Phi^{\text{F}}(\mathbf{V}) = \mathbf{S}(\mathbf{X}_{\text{TH}} \mathbf{S}^{-1} \mathbf{V} \mathbf{S}^{-1} \mathbf{X}_{\text{TH}} + \mathbf{Y}_{\text{TH}}) \mathbf{S}. \quad (6.113)$$

As a consequence we can replace each fiducial channel by a thermal channel preceded by an anti-squeezer and followed by a squeezer [see right hand side of Fig. 6.6 (b)].

Now we focus again on the minimization of the output entropy. Then, the set of squeezers \mathbf{S} (at the individual outputs of the thermal channels) can be omitted since they do not change the entropy and we have no energy constraint on the output. We showed above that the entropy for the joint map $(\Phi^{\text{TH}})^{\otimes n}$ is minimized by the n -mode vacuum state. Thus, the multi-mode input state that minimizes the output entropy of the fiducial channel has to be in the n -mode vacuum state after passing the n anti-squeezers \mathbf{S}^{-1} [see right hand side of Fig. 6.6 (b)].

Therefore, one fixes the interferometer $\Theta_{\text{in}2} = \mathbb{I}$ and chooses each individual input squeezer $\mathbf{S}_{\text{in}i}$ to undo the individual anti-squeezers \mathbf{S}^{-1} , which fixes the overall input state to

$$\mathbf{V}_{\text{in}} = \frac{1}{2} \begin{pmatrix} e^{2s} \mathbb{I}_{n \times n} & 0 \\ 0 & e^{-2s} \mathbb{I}_{n \times n} \end{pmatrix}. \quad (6.114)$$

It follows that

$$\min_{\mathbf{V}_{\text{in}}} S((\Phi^{\text{F}})^{\otimes n}(\mathbf{V}_{\text{in}})) = n g \left(y + \frac{|\tau| - 1}{2} \right), \quad (6.115)$$

as before in Eq. (6.109). Then, one again maximizes the first term in Eq. (6.105) by the entropy of n (identical) thermal states, which is obtained by the QWF solution for each mode. It follows that

$$\max_{\mathbf{V}_{\text{in}}, \mathbf{V}_{\text{mod}}} S(\bar{\mathbf{V}}_{\text{out}}) = n g \left(|\tau| \bar{N} + y \cosh(2s) + \frac{|\tau| - 1}{2} \right), \quad \bar{N} \geq \bar{N}_{\text{thr}}. \quad (6.116)$$

6. One-mode Gaussian channel

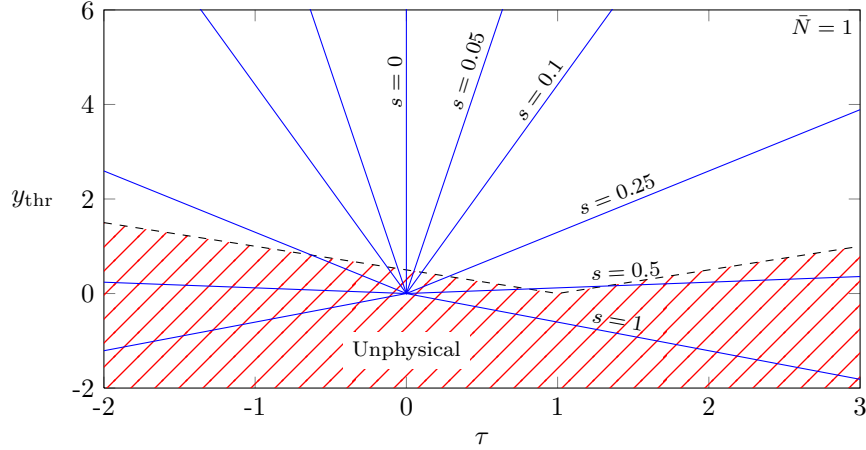


Figure 6.7.: Threshold function y_{thr} vs. τ for different values of s and fixed input energy $\bar{N} = 1$. All solid lines are mirror-symmetric around $\tau = 0$.

Thus, for $\bar{N} \geq \bar{N}_{\text{thr}}$ we maximize at the same time the first term and minimize the second term in Eq. (6.105) by the same encoding (per channel) as in the single-mode case and we find that

$$\frac{1}{n} C_{\chi}^{\text{G}}((\Phi^{\text{F}})^{\otimes n}, n\bar{N}) = C_{\chi}^{\text{G}}(\Phi^{\text{F}}, \bar{N}), \quad \bar{N} \geq \bar{N}_{\text{thr}}, \quad (6.117)$$

which proves the theorem. \square

In order to visualize the validity of Theorem 3 we express \bar{N}_{thr} in terms of a threshold on y . Namely, for given input energy \bar{N} we solve Eq. (6.80) for the parameter $y = y_{\text{thr}}$, which gives the threshold value

$$y_{\text{thr}} \equiv \frac{|\tau|(e^{-2|s|}(2\bar{N} + 1) - 1)}{1 - e^{-4|s|}}. \quad (6.118)$$

Now, the QWF solution is applicable (implying $C^{\text{G}} = C_{\chi}^{\text{G}}$) if $y \leq y_{\text{thr}}$ for given \bar{N} , s and τ . We plot examples of y_{thr} in the (y, τ) plane in Fig. 6.7 (recall Fig. 6.2). Since $y_{\text{thr}} \rightarrow \infty$ for $s \rightarrow 0$ we confirm that the one-shot Gaussian capacity of thermal channels is always additive.

We recall from Sec. 6.3 that the one-shot capacity C_{χ} is known to be additive for entanglement breaking channels. The proof that was presented in [HS04] can however not be straightforwardly extended to the definition of the one-shot Gaussian capacity C_{χ}^{G} and therefore it is not known if C_{χ}^{G} is additive in this domain as well.

6.4.3. Solution in the full input energy domain

Now we extend the solution to the one-shot Gaussian capacity to the input energy domain $\bar{N} < \bar{N}_{\text{thr}}$. Lemma 1 states that all CM are diagonal in the same basis so we

can choose the following notations:

$$\mathbf{V}_{\text{out}} = \text{diag}(v_q, v_p), \quad \bar{\mathbf{V}}_{\text{out}} = \text{diag}(\bar{v}_q, \bar{v}_p), \quad (6.119)$$

where

$$\begin{aligned} v_q &= |\tau| i_q + y e^{2s}, & v_p &= |\tau| \frac{1}{4i_q} + y e^{-2s}, \\ \bar{v}_q &= |\tau| (i_q + m_q) + y e^{2s}, & \bar{v}_p &= |\tau| \left(\frac{1}{4i_q} + m_p \right) + y e^{-2s}. \end{aligned} \quad (6.120)$$

Note that here we already introduced the purity constraint by replacing $i_p = 1/(4i_q)$.

The optimization problem can in general be solved with the method of Lagrange multipliers. We first obtain again the quantum water-filling solution with this method and then analyze when the resulting equations no longer hold. Then, we show how the optimization problem has to be modified in order to be valid for $\bar{N} < \bar{N}_{\text{thr}}$.

We define the Lagrangian

$$\mathcal{L} = g(\bar{M}_{\text{out}}) - g(M_{\text{out}}) - \frac{\bar{\beta}}{\ln 2} \left(\frac{1}{2} \left(i_q + \frac{1}{4i_q} + m_q + m_p \right) - \bar{N} - \frac{1}{2} \right), \quad (6.121)$$

where $\bar{\beta}$ is a Lagrange multiplier in order to satisfy the energy constraint⁴ stated in Eq. (6.59) and

$$M_{\text{out}} = \sqrt{v_q v_p} - \frac{1}{2}, \quad \bar{M}_{\text{out}} = \sqrt{\bar{v}_q \bar{v}_p} - \frac{1}{2}. \quad (6.122)$$

The extremum is obtained by solving

$$\nabla \mathcal{L} = 0, \quad \nabla = \left(\frac{\partial}{\partial i_q}, \frac{\partial}{\partial m_q}, \frac{\partial}{\partial m_p} \right)^{\text{T}}. \quad (6.123)$$

We show in Appendix D.1 that the solution to this system of equations is precisely given by the QWF solution

$$\bar{v}_q = \bar{v}_p, \quad (6.124)$$

together with the optimal input squeezing $i_q = e^{2s}/2$, as obtained previously in Sec. 6.4.1. For the more general parametrization

$$\mathbf{Y} = \begin{pmatrix} y_q & 0 \\ 0 & y_p \end{pmatrix}, \quad (6.125)$$

where $y_q = y e^{2s}$ and $y_p = y e^{-2s}$ this solution furthermore implies the relations

$$\frac{v_q}{v_p} = \frac{y_q}{y_p} = \frac{i_q}{i_p}, \quad (6.126)$$

⁴We divided here the multiplier by $\ln 2$ because both g -functions are expressed by $\log_2(x)$ (i.e. expressed in bits).

6. One-mode Gaussian channel

i.e. the squeezing of the output matches the squeezing of the noise and of the input state. However, we showed that in order for both modulations to be positive, i.e. $m_q \geq 0$ and $m_p \geq 0$ the input energy has to satisfy $\bar{N} \geq \bar{N}_{\text{thr}}$. Thus, if $\bar{N} < \bar{N}_{\text{thr}}$ we know that the resulting solution is unphysical. Therefore, the method of Lagrange multipliers has to be modified and the solution must lay at the boarder of the (m_q, m_p) plane (where trivially $m_q = m_p = 0$ cannot be optimal for $\bar{N} > 0$). Thus, we have

$$m_q = 0 \quad \vee \quad m_p = 0, \quad \bar{N} < \bar{N}_{\text{thr}}. \quad (6.127)$$

Therefore, the optimization problem depends only on two variables (with one constraint), while one of the two modulation eigenvalues is kept equal to zero. If $m_q = 0$ is optimal, then the solution to the optimization problem is found by solving $\nabla \mathcal{L} = 0$ with

$$\nabla = \left(\frac{\partial}{\partial i_q}, \frac{\partial}{\partial m_p} \right)^\top, \quad (6.128)$$

which leads to the same equation that was obtained for the QWF solution (see Appendix D.1)

$$\frac{g'(\bar{M}_{\text{out}})}{(\bar{M}_{\text{out}} + \frac{1}{2})} (\bar{v}_p - \bar{v}_q) = \frac{g'(M_{\text{out}})}{(M_{\text{out}} + \frac{1}{2})} y \left(e^{-2s} - \frac{e^{2s}}{4i_q^2} \right), \quad m_q = 0, \quad (6.129)$$

where, as mentioned above, for $\bar{N} < \bar{N}_{\text{thr}}$ the solution $\bar{v}_q = \bar{v}_p$ together with the solution $i_q = e^{2s}/2$ is no longer physical. If $m_p = 0$ is optimal then one equivalently obtains the equation

$$\frac{g'(\bar{M}_{\text{out}})}{(\bar{M}_{\text{out}} + \frac{1}{2})} (\bar{v}_q - \bar{v}_p) = \frac{g'(M_{\text{out}})}{(M_{\text{out}} + \frac{1}{2})} y (e^{2s} - 4i_q^2 e^{-2s}), \quad m_p = 0. \quad (6.130)$$

Both equations lead to the following Lemma:

Lemma 2. *For an input energy $\bar{N} < \bar{N}_{\text{thr}}$ the maximum of χ^G is achieved for*

$$\bar{v}_q \neq \bar{v}_p. \quad (6.131)$$

Proof. First, we state the following inequality:

$$\frac{g'(\bar{M}_{\text{out}})}{(\bar{M}_{\text{out}} + \frac{1}{2})} \leq \frac{g'(M_{\text{out}})}{(M_{\text{out}} + \frac{1}{2})}, \quad (6.132)$$

because by definition $\bar{M}_{\text{out}} \geq M_{\text{out}}$ and $\frac{1}{x}g'(x)$ is a monotonically decreasing function. Then, if $m_q = 0$ then Eq. (6.129) holds and implies that

$$|\bar{v}_p - \bar{v}_q| \geq y \left| e^{-2s} - \frac{e^{2s}}{4i_q^2} \right|, \quad m_q = 0. \quad (6.133)$$

Equivalently, if $m_p = 0$ then Eq. (6.130) holds and implies that

$$|\bar{v}_q - \bar{v}_p| \geq y |e^{2s} - 4i_q^2 e^{-2s}|, \quad m_p = 0. \quad (6.134)$$

Equality in Eqs. (6.133) and (6.134) can only be fulfilled (by a physical solution) if $\bar{N} \geq \bar{N}_{\text{thr}}$. This proves the Lemma. \square

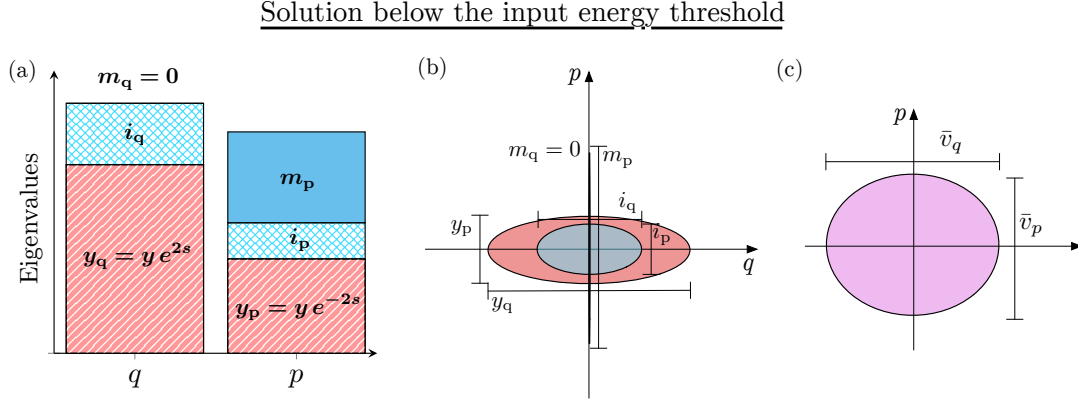


Figure 6.8.: Solution for $\bar{N} < \bar{N}_{\text{thr}}$ (shown schematically for $\tau = 1$): (a) the noisier quadrature is no longer modulated, i.e. $m_q = 0$. (b) and (c) resulting states in the phase-space.

Lemma 2 implies that it is no longer optimal to match the squeezing of the environment, i.e. $i_q \neq e^{2s}/2$ (if $m_q = 0$). Since at the same time $\bar{v}_q \neq \bar{v}_p$ we conclude that for $\bar{N} < \bar{N}_{\text{thr}}$ in χ^G neither the first is maximized nor the second term is minimized.

Now, we prove which modulation eigenvalue has to be fixed to zero:

Lemma 3. For an input energy $\bar{N} < \bar{N}_{\text{thr}}$ the χ^G is maximal if

$$\begin{aligned} m_q &= 0, & s > 0, \\ m_p &= 0, & s < 0, \end{aligned} \tag{6.135}$$

i.e. the noisier quadrature is no longer modulated.

Proof. We prove in the following the statement $m_q = 0, s > 0$. The second statement in Eq. (6.135) can be proven equivalently.

Let us assume that in contrary to the statement of the lemma we have $m_p = 0, s > 0$. We know that according to Lemma 2 we have two possible cases: $\bar{v}_q > \bar{v}_p$ or $\bar{v}_q < \bar{v}_p$.

Let us assume first that $\bar{v}_q > \bar{v}_p$ and that we have found an optimal solution. Suppose we remove a fraction of m_q which is smaller than half of the difference $\bar{v}_q - \bar{v}_p$ and set m_p equal to this fraction. This will not change the input energy as well as the output entropy (second term in χ^G). However, the overall modulated output entropy (first term in χ^G) will increase. The reason is that for a constant arithmetic mean $(a + b)/2$ the geometric mean \sqrt{ab} increases if the difference between a and b decreases. Therefore, by doing this we increased χ^G which shows that our original assumption is in fact not optimal. Thus, for $\bar{v}_q > \bar{v}_p$ it follows that $m_q = 0, s > 0$ is indeed optimal.

Now we consider $\bar{v}_q < \bar{v}_p$ and assume that we have found an optimal solution. Then from Eq. (6.133) it follows that

$$i_q > \frac{1}{2}e^{2s} \tag{6.136}$$

6. One-mode Gaussian channel

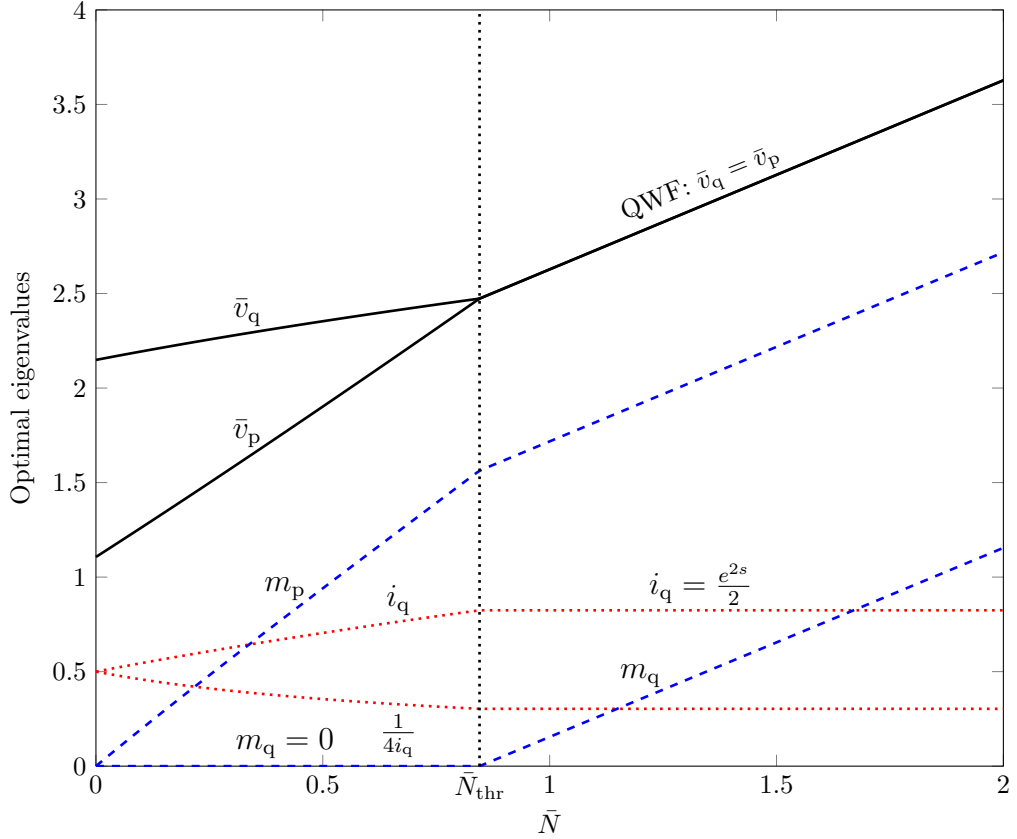


Figure 6.9.: Optimal eigenvalue vs. input energy \bar{N} for $\tau = 1$ (classical additive noise channel), $s = 0.25$, and $y = 1$. The upper and lower solid lines are \bar{v}_q and \bar{v}_p , the upper and lower dashed lines are m_p and m_q and the upper and lower dotted lines are i_q and $1/(4i_q)$. The input energy threshold is here given by $\bar{N}_{\text{thr}} = 0.846$.

and from the condition $s > 0$ we deduce easily that $i_q > 1/2 > 1/(4i_q)$. Taking into account that $m_q > m_p = 0$ we conclude that in fact $\bar{v}_q > \bar{v}_p$ which contradicts to our assumption. Thus, the lemma is proven. \square

Note that as a direct consequence of Lemma 3 it follows that

$$\frac{1}{2} \leq i_q < \frac{1}{2}e^{2s}, \quad \bar{N} < \bar{N}_{\text{thr}}. \quad (6.137)$$

Let us focus from now on (without loss of generality) to the case $s > 0$. We show that it is optimal to fix $m_q = 0$ for $\bar{N} < \bar{N}_{\text{thr}}$, which implies

$$\bar{v}_q = v_q, \quad s > 0, \quad \bar{N} < \bar{N}_{\text{thr}}, \quad (6.138)$$

i.e. the noisier output quadrature is equal to the noisier modulated output quadrature. In addition, we can replace the modulation eigenvalue m_p with the energy constraint:

$$m_p = 2\bar{N} + 1 - i_q - \frac{1}{4i_q}. \quad (6.139)$$

We showed above that the solution to the optimization problem is found by solving the transcendental equation (6.129). Now we can express this equation alternatively as an implicit function that (for given fixed channel parameters) depends only on i_q , i.e.

$$F(i_q) \equiv \frac{g'(\bar{M}_{\text{out}})}{(\bar{M}_{\text{out}} + \frac{1}{2})}(\bar{v}_p - v_q) - \frac{g'(M_{\text{out}})}{(M_{\text{out}} + \frac{1}{2})}y \left(e^{-2s} - \frac{e^{2s}}{4i_q^2} \right), \quad (6.140)$$

where we used the fact that $m_q = 0$ implies $\bar{v}_q = v_q$. The solution is now found by solving

$$F(i_q) = 0. \quad (6.141)$$

One way to prove that there exists only one solution to Eq. (6.141) is to prove that $\frac{\partial F(i_q)}{\partial i_q}$ has a definite sign. We prove in Appendix D.3.2 (see Eq. (D.66) and discussion before) that indeed

$$\frac{\partial F(i_q)}{\partial i_q} < 0, \quad \tau = 1. \quad (6.142)$$

For other values of τ one can find an example (e.g. $\bar{N} = 10, \tau = 0.15, M_{\text{env}} = 10^{-3}, s = 0.1$) for which the sign of the derivative changes (i.e. it has local extrema), and thus, Eq. (6.142) is not valid for arbitrary τ . Therefore, we do not exclude that in general $F(i_q) = 0$ may have more than one solution. Intensive numerical calculations did not lead to any case of more than one root and therefore, we take the uniqueness of the solution of $F(i_q) = 0$ in the following for granted.

Then, the one-shot Gaussian capacity can be expressed as

$$C_\chi^G(\Phi, \bar{N}) = C_\chi^G(\Phi^F, \bar{N}) = \left\{ g(\bar{M}_{\text{out}}(i_q)) - g(M_{\text{out}}(i_q)) \mid F(i_q) = 0 \right\}, \quad \bar{N} < \bar{N}_{\text{thr}}, \quad (6.143)$$

where we stated the explicit dependence on the input squeezing i_q .

We remark that up to now, we have not investigated the solution to the limiting cases $\text{rank}(\mathbf{X}) = 1$ or $\text{rank}(\mathbf{Y}) = 1$. We show in Sec. 6.4.7 that their solutions correspond in fact to limiting cases of Eq. (6.143).

The optimal eigenvalues for an example (with $\tau = 1$) are depicted in a stack plot in Fig. 6.8 (a) and as variances in phase space in (b) and (c). The transition from the QWF solution to the solution below the input energy solution is plotted in Fig. 6.9 (for particular chosen values): One clearly observes the ‘‘splitting’’ $\bar{v}_q \neq \bar{v}_p$ when \bar{N} is decreased below \bar{N}_{thr} . The noisier quadrature is then no longer modulated and we observe that the squeezing decreases monotonically with decreasing input energy (this is proven for $\tau = 1$ in Appendix D.3.2, see Eq. (D.67) and discussion before). At $\bar{N} = 0$ both modulation eigenvalues are equal to zero and the input state corresponds to the (unsqueezed) coherent state, i.e. $i_q = i_p = 1/2$.

6. One-mode Gaussian channel

6.4.4. Limiting cases

We begin by analyzing the behavior of C_χ^G when the channel parameters tend to infinity. We first investigate the Gaussian capacity in the limit $s \rightarrow \infty$. Since $\chi^G = g(\bar{M}_{\text{out}}) - g(M_{\text{out}})$ depends on \bar{M}_{out} and M_{out} we first study the behavior of these two parameters in this limit. Clearly, the input energy threshold \bar{N}_{thr} (in the form stated in Eq. (6.171)) diverges in this limit and thus the solution below the energy threshold applies. We observe that [using Eq. (D.7)]

$$\begin{aligned} \lim_{s \rightarrow \infty} M_{\text{out}} &\rightarrow \infty, \\ \lim_{s \rightarrow \infty} \bar{M}_{\text{out}} &\rightarrow \infty. \end{aligned} \tag{6.144}$$

In this limit we can replace the function $g(x)$ in χ^G by $\log_2(x)$ [using Eq. (6.94)] and thus,

$$\begin{aligned} \lim_{s \rightarrow \infty} \chi^G &= \lim_{s \rightarrow \infty} \log_2 \left(\frac{\bar{M}_{\text{out}}}{M_{\text{out}}} \right) \\ &= \frac{1}{2} \log_2(4i_{\text{q}}[2\bar{N} + 1 - i_{\text{q}}]). \end{aligned} \tag{6.145}$$

Since $\log_2(x)$ is a monotonous function it is sufficient to maximize its argument to find the capacity in this limit. The argument is maximized for the encoding

$$i_{\text{q}} = \bar{N} + \frac{1}{2}, \tag{6.146}$$

which leads to

$$\lim_{s \rightarrow \infty} C_\chi^G(\Phi^F, \bar{N}) = \log_2(2\bar{N} + 1). \tag{6.147}$$

The derivation can be repeated for the limiting case $s \rightarrow -\infty$ and leads to the same outcome. This result can be interpreted as follows: In the limit $s \rightarrow \infty$ one of the noise quadratures vanishes (here: the p -quadrature) and the other becomes infinite. Then, only one degree of freedom is available for information transmission but at the same time no longer suffers noise, except for the “noise” induced by the input state itself. We observe, that the one-shot Gaussian capacity then coincides with the Shannon capacity C_{Sh} stated in Eq. (2.50) with signal to noise ratio $\bar{N}/(1/2) = 2\bar{N}$. The limiting value stated in Eq. (6.147) is confirmed in Figs. 6.10, 6.11 and 6.12 (c).

Let us now consider the limit when τ tends to $\pm\infty$. In order to treat this limit we need to take into account the dependency of y on τ and therefore use the parametrization previously introduced in Eq. (6.10) (both limiting cases concern only the amplification channel and phase-conjugating channel)

$$\mathbf{Y}_F = |1 - \tau| \mathbf{V}_{\text{env}}, \tag{6.148}$$

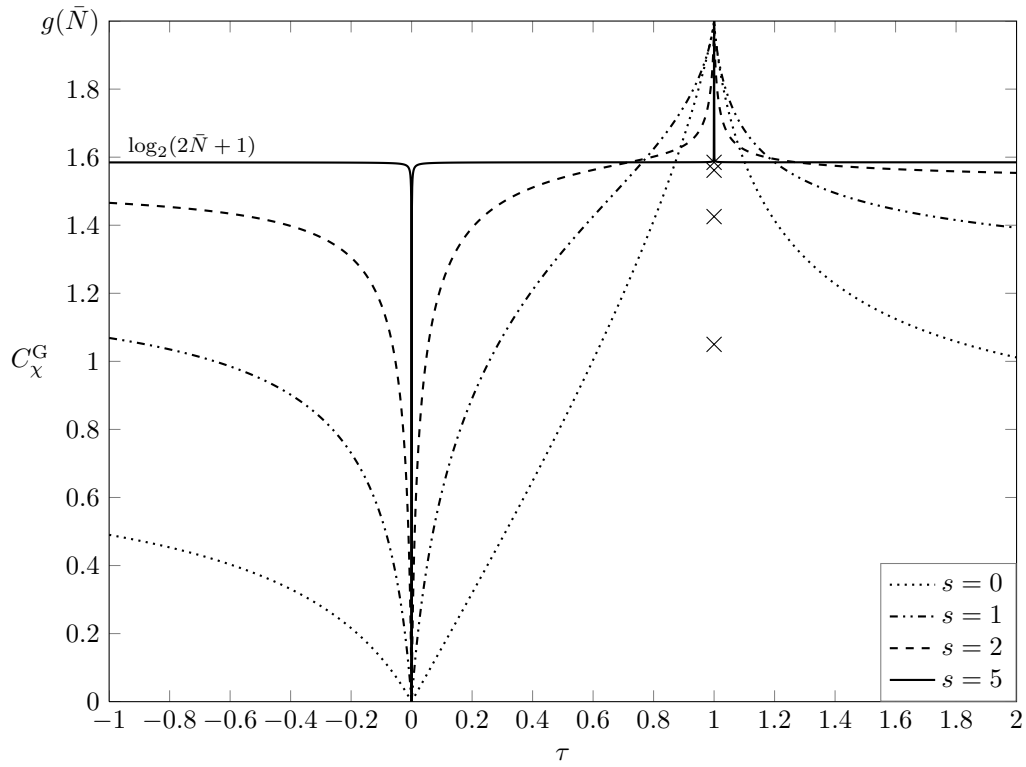


Figure 6.10.: Gaussian capacity C_χ^G vs. τ . The \times -markers are C_χ^G for the classical additive noise channel ($\tau = 1$), where from bottom to top $s = \{0, 1, 2, 5\}$. The lines are C_χ^G for the other channels (where $\tau = 1$ is the perfect transmission channel), where the dotted line corresponds to $s = 0$, the dashed-dotted line to $s = 1$, the dashed line to $s = 2$ and the solid line to $s = 5$. The other parameters are $\bar{N} = 1$ and $M_{\text{env}} = 0.1$.

6. One-mode Gaussian channel

where in addition we choose the parametrization:

$$\begin{aligned} \mathbf{V}_{\text{env}} &= \text{diag}(e_q, e_p), \\ e_q &= \left(M_{\text{env}} + \frac{1}{2}\right) e^{2s}, \\ e_p &= \left(M_{\text{env}} + \frac{1}{2}\right) e^{-2s}. \end{aligned} \quad (6.149)$$

According to Eqs. (6.120) and (6.122) the quantity χ^G only depends on the absolute values $|\tau|$ and $|1 - \tau|$. Therefore, χ^G tends in both limits $\tau \rightarrow \pm\infty$ to the value the limit $|\tau| \rightarrow \infty$. Thus, we only need to consider the latter. Again, both arguments M_{out} and \bar{M}_{out} , respectively, diverge [according to Eq. (6.122)] which implies that the difference of g -functions again can be replaced by a difference of logarithms, i.e.

$$\begin{aligned} \lim_{|\tau| \rightarrow \infty} \chi^G &= \lim_{|\tau| \rightarrow \infty} \log_2 \left(\frac{\bar{\nu}_{\text{out}} - \frac{1}{2}}{\nu_{\text{out}} - \frac{1}{2}} \right) \\ &= \lim_{|\tau| \rightarrow \infty} \log_2 \left(\frac{|\tau| \left[\sqrt{\left(i_q + m_p + \frac{|1-\tau|}{|\tau|} e_q\right) \left(i_p + m_q + \frac{|1-\tau|}{|\tau|} e_p\right)} - \frac{1}{2|\tau|} \right]}{|\tau| \left[\sqrt{\left(i_q + \frac{|1-\tau|}{|\tau|} e_q\right) \left(i_p + \frac{|1-\tau|}{|\tau|} e_p\right)} - \frac{1}{2|\tau|} \right]} \right) \\ &= \frac{1}{2} \log_2 \left(\frac{(i_q + m_q + e_q)(i_p + m_p + e_p)}{(i_q + e_q)(i_p + e_p)} \right) \equiv \chi_{(|\tau| \rightarrow \infty)}^G. \end{aligned} \quad (6.150)$$

The input energy threshold stated in Eq. (6.83) in this limit behaves as follows:

$$\begin{aligned} \lim_{|\tau| \rightarrow \infty} \bar{N}_{\text{thr}} &= \lim_{|\tau| \rightarrow \infty} \frac{1}{2} \left(\sqrt{\frac{e_q}{e_p}} + \frac{|1-\tau|}{|\tau|} (e_q - e_p) - 1 \right) \\ &= \frac{1}{2} \left(\sqrt{\frac{e_q}{e_p}} + e_q - e_p - 1 \right). \end{aligned} \quad (6.151)$$

Clearly, for input energies $\bar{N} \geq \bar{N}_{\text{thr}}$ the limiting function $\chi_{(|\tau| \rightarrow \infty)}^G$ is maximized by the quantum water-filling solution and optimal squeezing:

$$\begin{aligned} i_q + m_q + e_q &= i_p + m_p + e_p, \\ i_q &= \frac{1}{2} \sqrt{\frac{e_q}{e_p}}. \end{aligned} \quad (6.152)$$

For input energies $\bar{N} < \bar{N}_{\text{thr}}$ we have (as before) $m_q = 0$ and the limiting expression simplifies to

$$\chi_{(|\tau| \rightarrow \infty)}^G = \frac{1}{2} \log_2 \left(\frac{2\bar{N} + 1 - i_q + e_p}{\frac{1}{4i_q} + e_p} \right), \quad \bar{N} < \bar{N}_{\text{thr}}. \quad (6.153)$$

As in the case $s \rightarrow \infty$ it is sufficient to maximize the argument in order to maximize the logarithm. Deriving the argument with respect to i_q and equalizing it to 0 leads to the

equation

$$\frac{2\bar{N} + 1 - i_q + e_p}{\frac{1}{4i_q} + e_p} = 4i_q^2, \quad (6.154)$$

which yields

$$i_q = \frac{1}{2} \sqrt{1 + \frac{2\bar{N} + 1}{e_p} + \frac{1}{4e_p^2}} - \frac{1}{4e_p}. \quad (6.155)$$

The optimal input encodings for $\chi_{(|\tau| \rightarrow \infty)}^G$ lead to the solution of the one-shot Gaussian capacity in this limit:

$$\lim_{\tau \rightarrow \pm\infty} C_\chi^G(\Phi^F, \bar{N}) = \begin{cases} \log_2(2\bar{N} + 1 + e_q + e_p) - \log_2(1 + 2\sqrt{e_q e_p}), & \bar{N} \geq \bar{N}_{\text{thr}}, \\ \log_2\left(\sqrt{1 + (2\bar{N} + 1)e_p^{-1} + e_p^{-2}/4} - e_p^{-1}/2\right), & \bar{N} < \bar{N}_{\text{thr}}, \end{cases} \quad (6.156)$$

If we replace $e_p = (M_{\text{env}} + 1/2)e^{-2s}$ then it is straightforward to show that

$$\lim_{s \rightarrow \pm\infty} \lim_{\tau \rightarrow \pm\infty} C_\chi^G(\Phi^F, \bar{N}) = \log_2(2\bar{N} + 1), \quad (6.157)$$

i.e. we recover the limit stated in Eq. (6.147). In order to study the monotonicity of the classical capacity and Gaussian capacity on the parameter τ the following Lemma will be useful.

Lemma 4. *For given parameters τ_1, τ_2 where either $\tau_1, \tau_2 \geq 1$ or $\tau_1, \tau_2 \in [0, 1]$, the following equality holds:*

$$\Phi_{(\tau_2, |1-\tau_2|(M_{\text{env}}+1/2), s)}^F \circ \Phi_{(\tau_1, |1-\tau_1|(M_{\text{env}}+1/2), s)}^F = \Phi_{(\tau_1\tau_2, |1-\tau_1\tau_2|(M_{\text{env}}+1/2), s)}^F. \quad (6.158)$$

Proof. In the following proof we use the parametrization

$$\mathbf{Y} = |1 - \tau| \mathbf{V}_{\text{env}}, \quad \mathbf{V}_{\text{env}} = \left(M_{\text{env}} + \frac{1}{2} \right) \begin{pmatrix} e^{2s} & 0 \\ 0 & e^{-2s} \end{pmatrix}. \quad (6.159)$$

Let us first prove the Lemma for $\tau_1, \tau_2 \geq 1$, which implies that $y_i = (\tau_i - 1)(M_{\text{env}} + 1/2)$. In this case the total output covariance matrix of the concatenated channel stated on the left hand side of Eq. (6.158) reads

$$\begin{aligned} \mathbf{V}_{\text{out}} &= \tau_2(\tau_1 \mathbf{V}_{\text{in}} + (\tau_1 - 1) \mathbf{V}_{\text{env}}) + (\tau_2 - 1) \mathbf{V}_{\text{env}} \\ &= \tau_1 \tau_2 \mathbf{V}_{\text{in}} + (\tau_1 \tau_2 - 1) \mathbf{V}_{\text{env}}, \end{aligned} \quad (6.160)$$

which confirms the Lemma for $\tau_1, \tau_2 \geq 1$. Equivalently, in the case $\tau_1, \tau_2 \in [0, 1]$ we have $y_i = (1 - \tau_i)(M_{\text{env}} + 1/2)$ the total output CM reads

$$\begin{aligned} \mathbf{V}_{\text{out}} &= \tau_2(\tau_1 \mathbf{V}_{\text{in}} + (1 - \tau_1) \mathbf{V}_{\text{env}}) + (1 - \tau_2) \mathbf{V}_{\text{env}} \\ &= \tau_1 \tau_2 \mathbf{V}_{\text{in}} + (1 - \tau_1 \tau_2) \mathbf{V}_{\text{env}}, \end{aligned} \quad (6.161)$$

which completes the proof. \square

6. One-mode Gaussian channel

Using Lemma 4 we can straightforwardly prove the monotonicity of the capacities for the lossy channel ($\tau \in [0, 1]$) and amplification channel ($\tau \geq 1$). The classical capacity (as well as the Gaussian capacity) fulfills the pipelining property [stated in Eq. (3.37)]. Then, using Eq. (6.158) we have (where $\tau_1, \tau_2 \geq 1$ or $\tau_1, \tau_2 \in [0, 1]$)

$$\begin{aligned} & C \left(\Phi_{(\tau_2, |1-\tau_2|(M_{\text{env}}+1/2), s)}^{\text{F}} \circ \Phi_{(\tau_1, |1-\tau_1|(M_{\text{env}}+1/2), s)}^{\text{F}}, \bar{N} \right) \\ &= C \left(\Phi_{(\tau_1 \tau_2, |1-\tau_1 \tau_2|(M_{\text{env}}+1/2), s)}^{\text{F}}, \bar{N} \right) \leq C \left(\Phi_{(\tau_1, |1-\tau_1|(M_{\text{env}}+1/2), s)}^{\text{F}}, \bar{N} \right). \end{aligned} \quad (6.162)$$

In the case $\tau_1, \tau_2 \geq 1$ the effective gain parameter $\tau_{\text{eff}} \equiv \tau_1 \tau_2$ satisfies $\tau_{\text{eff}} \geq \tau_1, \tau_2$, $\forall \tau_1, \tau_2$. Thus, a channel with increased gain $\tau' > \tau$ can always be decomposed into an amplification channel with gain τ followed by another amplification channel. Due to the pipelining property the classical capacity (and the Gaussian capacity) of the channel with gain τ' cannot have increased. In the case of $\tau_1, \tau_2 \in [0, 1]$ the effective transmissivity $\tau_{\text{eff}} \equiv \tau_1 \tau_2$ satisfies $\tau_{\text{eff}} \leq \tau_1, \tau_2$, $\forall \tau_1, \tau_2$. Consequently, increasing the losses in the channel cannot increase the classical capacity (and Gaussian capacity).

For the amplification channel $\tau \geq 1$ the highest Gaussian capacity is given by the lossless case $\tau = 1$ for which $C^{\text{G}} = C = g(\bar{N})$. Since increasing τ cannot increase the Gaussian capacity and C_{χ}^{G} , we proved that C_{χ}^{G} monotonically tends from above to its limiting value stated in Eq. (6.156). Thus,

$$g(\bar{N}) \geq C_{\chi}^{\text{G}} \left(\Phi_{(\tau, y, s)}^{\text{F}}, \bar{N} \right) \geq \lim_{\tau' \rightarrow \infty} C_{\chi}^{\text{G}} \left(\Phi_{(\tau', y, s)}^{\text{F}}, \bar{N} \right), \quad \tau \geq 1. \quad (6.163)$$

We plot C_{χ}^{G} vs. τ for different values of squeezing in Fig. 6.10. We confirm the limiting behavior stated in Eq. (6.156) in Fig. 6.11, where we choose the same parameters as in Fig. 6.10 but plot for a larger range of τ . The limit $\lim_{\tau \rightarrow +\infty} C_{\chi}^{\text{G}}$ is reached from above (as proven above), whereas the limit $\lim_{\tau \rightarrow -\infty} C_{\chi}^{\text{G}}$ is reached from below (with decreasing τ). Unfortunately, the composition of two phase-conjugating channels with same noise parameters M_{env}, s does not lead to another phase-conjugating channel. Therefore, the above reasoning does not hold for the phase-conjugating channel and we have to rely on numerics to argue on the monotonicity of C_{χ}^{G} .

The last limiting case to consider is the case $M_{\text{env}} \rightarrow \infty$. In this limit again both values M_{out} and \bar{M}_{out} diverge, and thus, one can apply the same method as for the limit $|\tau| \rightarrow \infty$ in order to find C_{χ}^{G} in this limit. One straightforwardly confirms the expected result:

$$\lim_{M_{\text{env}} \rightarrow \infty} C_{\chi}^{\text{G}}(\Phi^{\text{F}}, \bar{N}) = 0. \quad (6.164)$$

Since Bob at the output of the channel receives a signal which is maximally noisy (in both quadratures) its decoded value becomes completely random and thus, the capacity inevitably tends to zero.

We plot in Fig. 6.12 the one-shot Gaussian capacity C_{χ}^{G} with respect to the input energy \bar{N} and the thermal photons M_{env} , where we choose the parametrization stated in Eq. (6.4). We plot in Fig. 6.12 (a)-(c) C_{χ}^{G} with respect to $\bar{N}, M_{\text{env}}, \tau$ and s . We observe in Fig. 6.12 (a) that C_{χ}^{G} increases monotonically with \bar{N} . Any other behavior

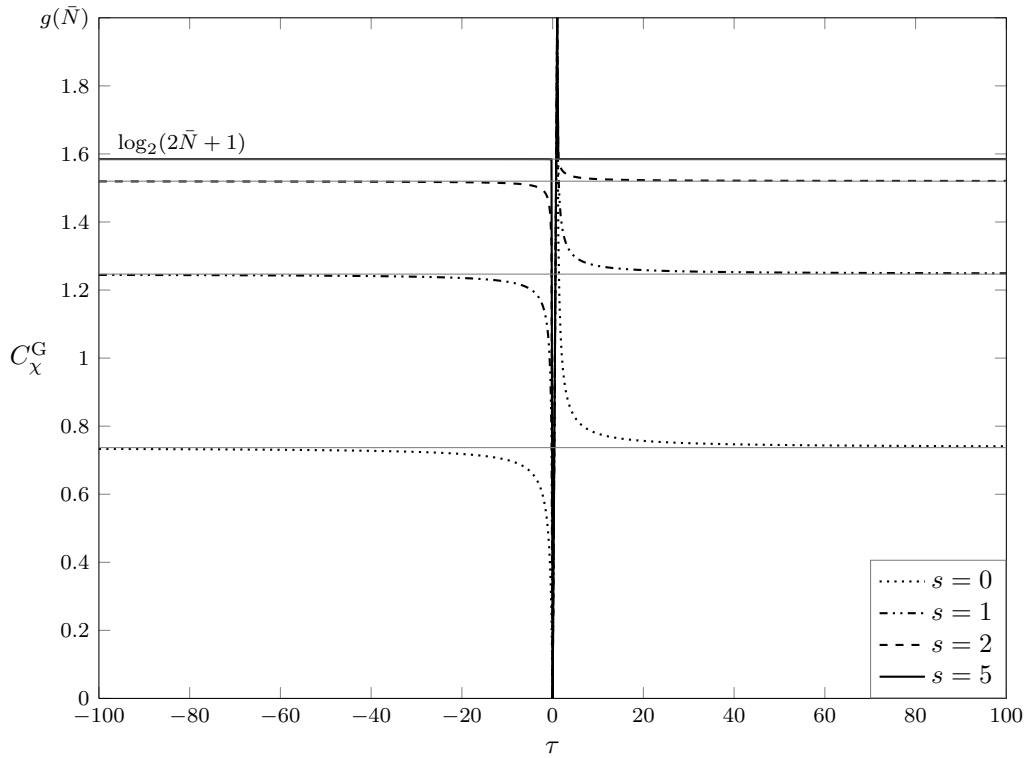


Figure 6.11.: Gaussian capacity C_χ^G vs. τ , where we do not plot the values for $\tau \in (0, 1)$ and choose the same parameters as in Fig. 6.10, i.e. $\bar{N} = 1$ and $M_{\text{env}} = 0.1$: the dotted line corresponds to $s = 0$, the dashed-dotted line to $s = 1$, the dashed line to $s = 2$ and the solid line to $s = 5$. The gray horizontal lines correspond to the analytical limiting values stated for $\lim_{\tau \rightarrow \pm\infty} C_\chi^G$ stated in Eq. (6.156).

6. One-mode Gaussian channel

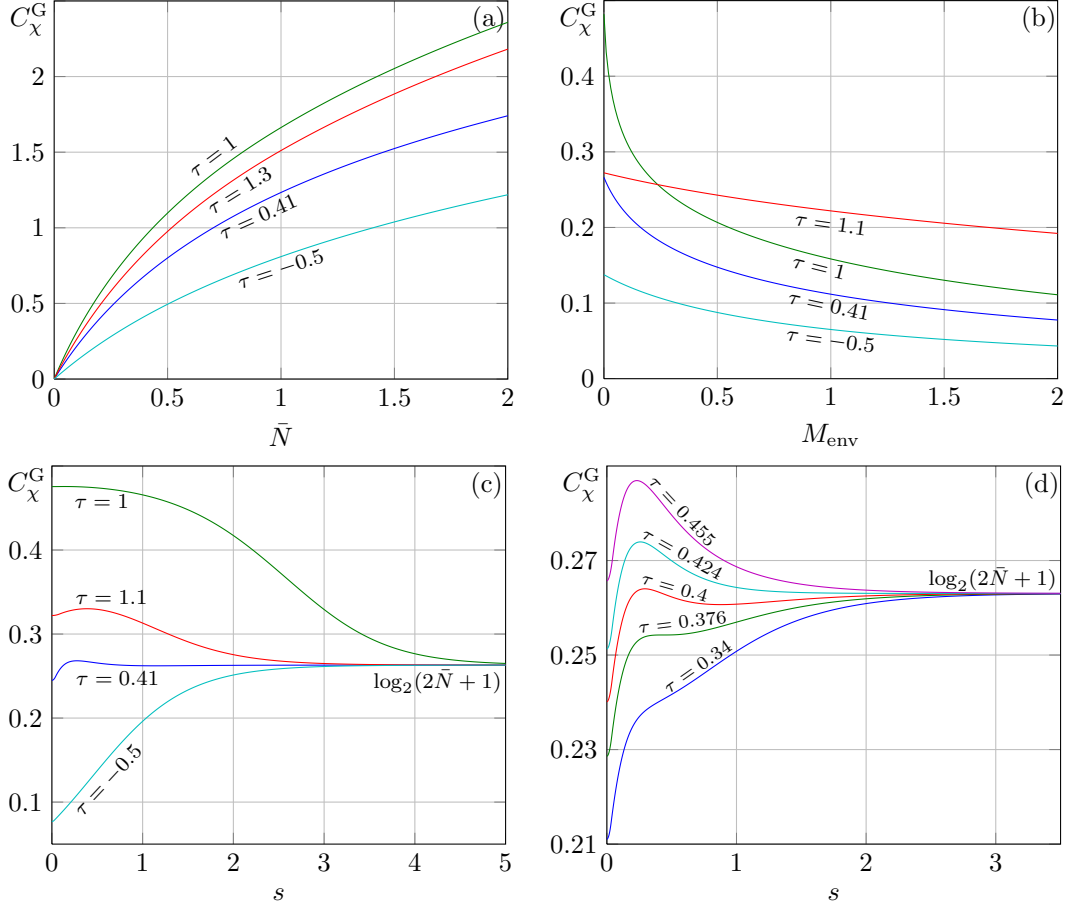


Figure 6.12.: One-shot Gaussian capacity C_χ^G vs. channel parameters. (a) C_χ^G vs \bar{N} , from top to bottom $\tau = \{1, 1.3, 0.41, -0.5\}$; the other parameters are $s = 0.5$ and $M_{\text{env}} = 0.1$. (b) C_χ^G vs M_{env} , from top to bottom $\tau = \{1, 1.3, 0.41, -0.5\}$; the other parameters are $s = 0.5$ and $\bar{N} = 0.1$. (c) C_χ^G vs s , from top to bottom $\tau = \{1, 1.1, 0.41, -0.5\}$; (d) C_χ^G vs s , from top to bottom $\tau = \{0.34, 0.3759, 0.4, 0.4238, 0.455\}$; the other parameters for (c) and (d) are $\bar{N} = 0.1$ and $M_{\text{env}} = 10^{-3}$.

would be non-physical: an optimal transmission rate $C_\chi^G(\Phi, \bar{N}')$ achieved for $\bar{N}' > \bar{N}$ must be higher than $C_\chi^G(\Phi, \bar{N})$ since any increase in input energy can be used to use the same input states with an increased modulation (note that in this comparison all other channel parameters are fixed).

We confirm in Fig. 6.12 (b) that C_χ^G decreases with M_{env} , which is the expected behavior as well (though we do not provide an analytical proof here).

Finally, we observe in Figs. 6.12 (c) and (d) that the behavior with respect to the environment squeezing s is *not monotonous* (in the case of the lossy channel we depict an example where a maximum followed by a minimum appears). For this reason we investigate the dependence of the Gaussian capacity on the environment squeezing in detail in the following section where we introduce as well a new parametrization.

6.4.5. Frequency parametrization

In the following section we investigate the role of the channel parameters, in particular the dependency of the one-shot Gaussian capacity on the environment squeezing. We choose a new parametrization where we represent the squeezing in terms of “frequencies”⁵: all optimal CM were shown to be diagonal which permits us to choose the general form

$$\mathbf{V} = \left(M + \frac{1}{2} \right) \begin{pmatrix} \omega^{-1} & 0 \\ 0 & \omega \end{pmatrix}, \quad (6.165)$$

for all covariance matrices that represent quantum states. A thermal state is then simply given by $\omega = 1$. For the effective added noise of the fiducial channel we choose the form

$$\mathbf{Y}_F = y \begin{pmatrix} \omega_{\text{env}}^{-1} & 0 \\ 0 & \omega_{\text{env}} \end{pmatrix}, \quad (6.166)$$

keeping the parameter y invariant. Without loss of generality we assume in the following that $\omega_{\text{env}} < 1$ (which is equivalent to $s > 0$ in the other parametrization). The CM of the pure input state and modulated input state $\bar{\mathbf{V}}_{\text{in}} = \mathbf{V}_{\text{in}} + \mathbf{V}_{\text{mod}}$ read, respectively,

$$\mathbf{V}_{\text{in}} = \frac{1}{2} \begin{pmatrix} \omega_{\text{in}}^{-1} & 0 \\ 0 & \omega_{\text{in}} \end{pmatrix}, \quad \bar{\mathbf{V}}_{\text{in}} = \left(\bar{M}_{\text{in}} + \frac{1}{2} \right) \begin{pmatrix} \bar{\omega}_{\text{in}}^{-1} & 0 \\ 0 & \bar{\omega}_{\text{in}} \end{pmatrix}, \quad (6.167)$$

and the CM of the output and modulated output CM are given by

$$\mathbf{V}_{\text{out}} = \left(M_{\text{out}} + \frac{1}{2} \right) \begin{pmatrix} \omega_{\text{out}}^{-1} & 0 \\ 0 & \omega_{\text{out}} \end{pmatrix}, \quad \bar{\mathbf{V}}_{\text{out}} = \left(\bar{M}_{\text{out}} + \frac{1}{2} \right) \begin{pmatrix} \bar{\omega}_{\text{out}}^{-1} & 0 \\ 0 & \bar{\omega}_{\text{out}} \end{pmatrix}. \quad (6.168)$$

We remark that since \mathbf{V}_{mod} corresponds to a classical Gaussian distribution it physically makes no sense to associate a frequency to it. Therefore, in the following we work instead with the states with covariance matrices \mathbf{V}_{in} and $\bar{\mathbf{V}}_{\text{in}}$.

⁵We underline that ω is not a frequency as it does not have the same physical dimension. However, in the solution the modulated output “frequency” enters in the same way as an actual frequency as shown in what follows. We omit the quotation marks from now on for simplicity.

6. One-mode Gaussian channel

This new parametrization offers a very elegant form for the solution to the optimization problem. The quantum water-filling solution $\bar{v}_q = \bar{v}_p$ is now simply expressed as

$$\bar{\omega}_{\text{out}} = 1, \quad \bar{N} \geq \bar{N}_{\text{thr}}. \quad (6.169)$$

The optimal squeezing $i_q = e^{2s}/2$ is now expressed as a ‘‘resonance’’ of the input, environment as well as the output state [see Eq. (6.126)], i.e.

$$\omega_{\text{in}} = \omega_{\text{env}} = \omega_{\text{out}}, \quad \bar{N} \geq \bar{N}_{\text{thr}}. \quad (6.170)$$

The input energy threshold [see Eq. (6.80)] in this new parametrization reads

$$\bar{N}_{\text{thr}} = \frac{1}{2\omega_{\text{env}}} \left[1 + \frac{y}{|\tau|} (1 - \omega_{\text{env}}^2) \right] - \frac{1}{2}, \quad (6.171)$$

where again for a thermal noise $\omega_{\text{env}} = 1$ the threshold vanishes. Then, one can find an alternative expression for the energy threshold by solving $\bar{N} = \bar{N}_{\text{thr}}$ with respect to the noise frequency $\omega_{\text{env}} \equiv \omega_{\text{thr}}$, i.e. one obtains the ‘‘threshold frequency’’

$$\omega_{\text{thr}} = \frac{\sqrt{4y(y + |\tau|) + \tau^2(1 + 2\bar{N})^2 - |\tau|(1 + 2\bar{N})}}{2y}. \quad (6.172)$$

For given parameters $y, |\tau|$ and \bar{N} we know that for $\omega_{\text{env}} < \omega_{\text{thr}}$ we have $\bar{N} < \bar{N}_{\text{thr}}$. With the solution stated in Eqs. (6.169) and (6.170) the one-shot Gaussian capacity reads

$$C_{\chi}^G(\Phi, \bar{N}) = g \left(|\tau| \bar{N} + \frac{y}{2} (\omega_{\text{env}}^{-1} + \omega_{\text{env}}) + \frac{|\tau| - 1}{2} \right) - g \left(y + \frac{|\tau| - 1}{2} \right), \quad \bar{N} \geq \bar{N}_{\text{thr}}. \quad (6.173)$$

We treat the solution for $\bar{N} < \bar{N}_{\text{thr}}$ again with the method of Lagrange multipliers but choose different degrees of freedom. Namely, we choose

$$\nabla = \left(\frac{\partial}{\partial \omega_{\text{in}}}, \frac{\partial}{\partial \bar{\omega}_{\text{out}}} \right)^{\top}. \quad (6.174)$$

The Lagrangian is given by

$$\mathcal{L} = g(\bar{M}_{\text{out}}) - g(M_{\text{out}}) - \frac{\bar{\beta}_{\text{out}}}{\ln 2} \left(\frac{1}{2} \left(\bar{M}_{\text{out}} + \frac{1}{2} \right) (\bar{\omega}_{\text{out}}^{-1} + \bar{\omega}_{\text{out}}) - \bar{N}_{\text{out}} - \frac{1}{2} \right), \quad (6.175)$$

where the input energy constraint \bar{N} is now translated to an output energy constraint using the relation

$$\bar{N}_{\text{out}} = \frac{1}{2} \text{Tr}[\bar{\mathbf{V}}_{\text{out}}] - \frac{1}{2} = \frac{|\tau|}{2} (2\bar{N} + 1) + \frac{y}{2} (\omega_{\text{env}} + \omega_{\text{env}}^{-1}) - \frac{1}{2}, \quad (6.176)$$

because the noise parameters (y, ω_{env}) are fixed. The absence of modulation in the noisier quadrature ($m_q = 0$) is now expressed as

$$\left(\bar{M}_{\text{in}} + \frac{1}{2} \right) \frac{1}{\bar{\omega}_{\text{in}}} - \frac{1}{2\omega_{\text{in}}} = 0, \quad \bar{N} < \bar{N}_{\text{thr}}. \quad (6.177)$$

We obtain in Appendix D.2 the solution to the optimization problem in the new parametrization. First, we find that the optimal number of thermal photons of the modulated output state is given by a *Bose-Einstein statistics*:

$$\bar{M}_{\text{out}} = \frac{1}{e^{\bar{\omega}_{\text{out}} \bar{\beta}_{\text{out}}} - 1}, \quad (6.178)$$

which means that the multiplier $\bar{\beta}_{\text{out}}$ can be regarded as an *inverse temperature* of the modulated output state. We can justify the definition of the inverse temperature further: In thermodynamics the inverse temperature is defined as

$$\frac{\partial S}{\partial E} \equiv \beta. \quad (6.179)$$

where E is the (fixed) energy of the system. Here, this quantity corresponds to the mean number of photons \bar{N}_{out} (at the output). If we choose \bar{N}_{out} as a variable and define the Lagrangian accordingly, i.e.

$$\mathcal{L}' = g(\bar{M}_{\text{out}}) - g(M_{\text{out}}) - \frac{\bar{\beta}_{\text{out}}}{\ln 2} \left(\bar{N}_{\text{out}} - \frac{1}{2} \text{Tr}[\bar{\mathbf{V}}_{\text{out}}] - \frac{1}{2} \right), \quad (6.180)$$

then

$$\frac{\partial \mathcal{L}'}{\partial \bar{N}_{\text{out}}} = \frac{\partial g(\bar{M}_{\text{out}})}{\partial \bar{N}_{\text{out}}} - \frac{\bar{\beta}_{\text{out}}}{\ln 2} = 0, \quad (6.181)$$

and we obtain

$$\frac{\partial S(\hat{\rho}_{M_{\text{out}}}^{\text{G}})}{\partial \bar{N}_{\text{out}}} = \frac{\bar{\beta}_{\text{out}}}{\ln 2}, \quad (6.182)$$

which coincides with the definition of thermodynamics⁶. The use of $\bar{\beta}_{\text{out}}$ will become clear when discussing the solution to a collection of one-mode Gaussian channels in Chapter 7, where we show that the joint solution can indeed be interpreted as a “thermal equilibrium” of all individual channels with common temperature $\bar{\beta}_{\text{out}}^{-1}$. Note, that Eq. (6.178) was already derived previously for the lossy channel ($\tau \in [0, 1]$) in [PLM12].

We define now in general the inverse temperature as the function

$$\beta(M, \omega) = \frac{g'(M) \ln 2}{\omega}. \quad (6.183)$$

Then, we use the additional short notation

$$\beta_{\text{out}} = \beta(M_{\text{out}}, \omega_{\text{out}}). \quad (6.184)$$

This leads (see Appendix D.2) to the following solution to the optimization problem (in the full input energy domain):

$$\bar{\omega}_{\text{out}} = \begin{cases} \sqrt{1 - \frac{\beta_{\text{out}}}{\beta_{\text{in}}} (\omega_{\text{in}}^2 - \omega_{\text{out}}^2)}, & \omega_{\text{env}} < \omega_{\text{thr}}, \\ 1, & \omega_{\text{env}} \geq \omega_{\text{thr}}. \end{cases} \quad (6.185)$$

⁶The factor $\ln 2$ accounts for the fact that we use in the definition of the von Neumann entropy logarithms to the base 2.

6. One-mode Gaussian channel

“Resonance” occurs when $\omega_{\text{in}} = \omega_{\text{out}}$, i.e. we confirm that Eq. (6.185) recovers Eq. (6.169) in the limit $\omega_{\text{in}} \rightarrow \omega_{\text{out}}$ for $\bar{N} \rightarrow \bar{N}_{\text{thr}}$. Thus, we have an “off-resonance” solution if $\omega_{\text{env}} < \omega_{\text{thr}}$ (i.e. $\bar{N} < \bar{N}_{\text{thr}}$) and a “resonance solution” if $\omega_{\text{env}} \geq \omega_{\text{thr}}$ (i.e. $\bar{N} \geq \bar{N}_{\text{thr}}$). Note that in order to evaluate Eq. (6.185) one needs to express $\beta_{\text{out}}, \bar{\beta}_{\text{out}}, \omega_{\text{out}}$ and ω_{in} as functions of $\bar{\omega}_{\text{out}}$, the given noise parameters $(\tau, y, \omega_{\text{env}})$ and the input energy constraint \bar{N} , or alternatively the output energy constraint \bar{N}_{out} . We express all parameters as functions of ω_{in} in Eq. (D.25) in the Appendix.

Finally, the one-shot Gaussian capacity for input energies below the threshold can be expressed as

$$C_{\chi}^{\text{G}}(\Phi, \bar{N}) = \left\{ g(\bar{M}_{\text{out}}(\omega_{\text{in}})) - g(M_{\text{out}}(\omega_{\text{in}})) \mid \bar{\omega}_{\text{out}} = \sqrt{1 - \frac{\beta_{\text{out}}}{\bar{\beta}_{\text{out}}} (\omega_{\text{in}}^2 - \omega_{\text{out}}^2)} \right\}, \omega_{\text{env}} < \omega_{\text{thr}}. \quad (6.186)$$

In Fig. 6.13 we plot one-shot Gaussian capacities and different frequencies vs. the environment frequency ω_{env} . We clearly observe the transition to the resonance solution when ω_{in} and ω_{out} coincide for $\omega_{\text{env}} \geq \omega_{\text{thr}}$. In addition, we see that $\bar{\omega}_{\text{out}} = 1$ in this regime. Interestingly, the modulated input frequency fulfills $\bar{\omega}_{\text{in}} = 1$ whenever C_{χ}^{G} has an extremum. This will be further elaborated in the following.

6.4.6. Dependency on channel parameters

Now we analyze the behavior of the capacity with respect to its channel parameters, primarily with respect to the environment frequency ω_{env} .

First, recall the solution in the limit $s \rightarrow \infty$, which corresponds now to $\omega_{\text{env}} \rightarrow 0$. Interestingly, Eq. (6.146) implies together with Eq. (6.177) that in this limit the optimal modulated input state is a thermal state, *i.e.*

$$\bar{\omega}_{\text{in}} = 1, \quad \bar{M}_{\text{in}} = \bar{N}. \quad (6.187)$$

The latter leads furthermore to the equation

$$\left(\bar{M}_{\text{out}} + \frac{1}{2} \right) \left(\bar{\omega}_{\text{out}} - \frac{1}{\bar{\omega}_{\text{out}}} \right) = y \left(\omega_{\text{env}} - \frac{1}{\omega_{\text{env}}} \right), \quad (6.188)$$

which states that the difference in the variances of the modulated output state are exactly matched by the difference in the noise variances.

Next, we investigate the behavior of the capacity with respect to ω_{env} , where $0 \leq \omega_{\text{env}} \leq 1$. Namely, we try to find extrema of the capacity with respect to ω_{env} .

First, we investigate the behavior for $\bar{N} \geq \bar{N}_{\text{thr}}$, or, equivalently $\omega_{\text{env}} \geq \omega_{\text{thr}}$, where ω_{thr} is stated in Eq. (6.172). From Eq. (6.173) it is straightforward to deduce that

$$\frac{\partial C_{\chi}^{\text{G}}}{\partial \omega_{\text{env}}} < 0, \quad \frac{\partial^2 C_{\chi}^{\text{G}}}{\partial \omega_{\text{env}}^2} > 0, \quad \omega_{\text{env}} \geq \omega_{\text{thr}}, \quad (6.189)$$

i.e. the capacity is decreasing with ω_{env} and a convex function with respect to ω_{env} . Therefore, the extremum (or extrema) lays in the region $[0, \omega_{\text{thr}}]$.

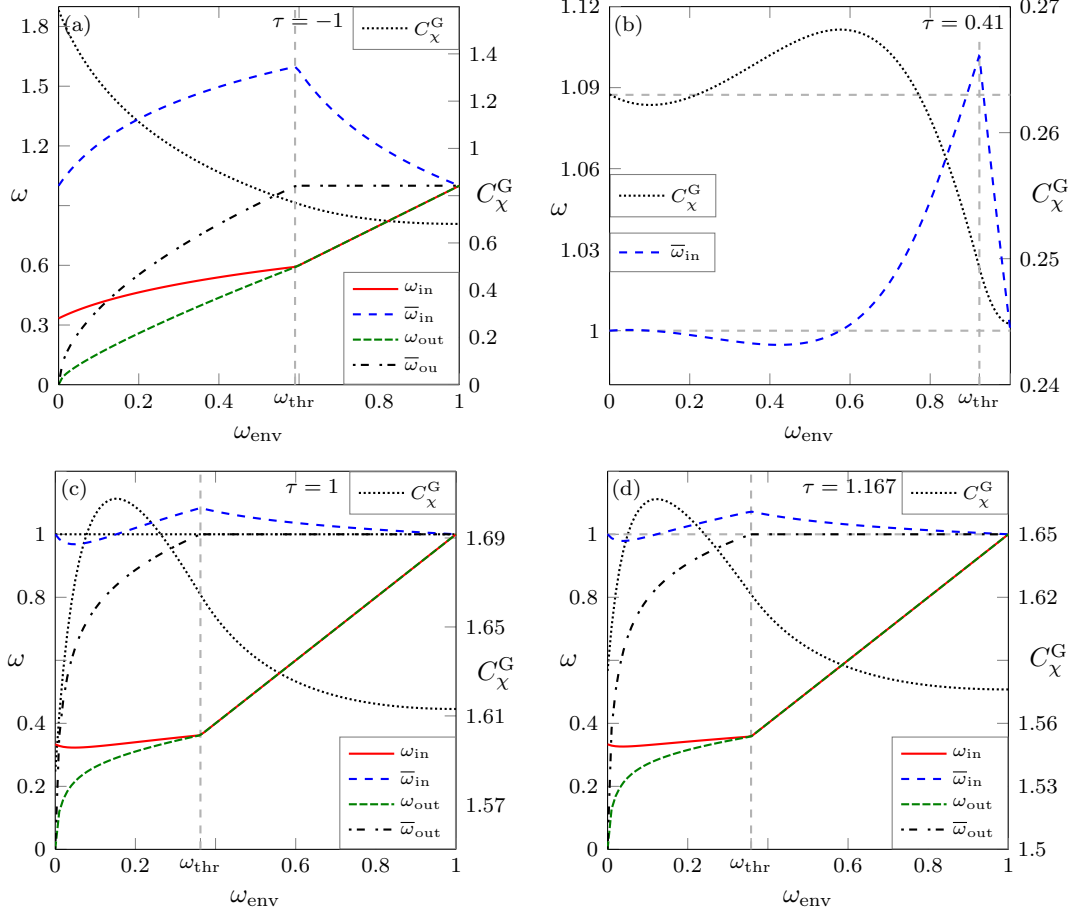


Figure 6.13.: Frequencies (left axis) and one-shot Gaussian capacity C_χ^G (right axis) vs. ω_{env} . The dashed vertical line is ω_{thr} . For $\tau = 0.41$ only $\bar{\omega}_{\text{in}}$ and C_χ^G are plotted and the horizontal dashed line indicates the value 1. Values are: (a) ($\tau = -1, \bar{N} = 1, M_{\text{env}} = 0.1, \omega_{\text{thr}} = 0.59$), (b) ($\tau = 0.41, \bar{N} = 0.1, M_{\text{env}} = 10^{-3}, \omega_{\text{thr}} = 0.92$), (c) ($\tau = 1, \bar{N} = 1, M_{\text{env}} = 0.1, \omega_{\text{thr}} = 0.362$), and (d) ($\tau = 1.167, \bar{N} = 1, M_{\text{env}} = 0.1, \omega_{\text{thr}} = 0.358$). One confirms in Fig. (b)-(d) that if C_χ^G is extremal then $\bar{\omega}_{\text{in}} = 1$.

6. One-mode Gaussian channel

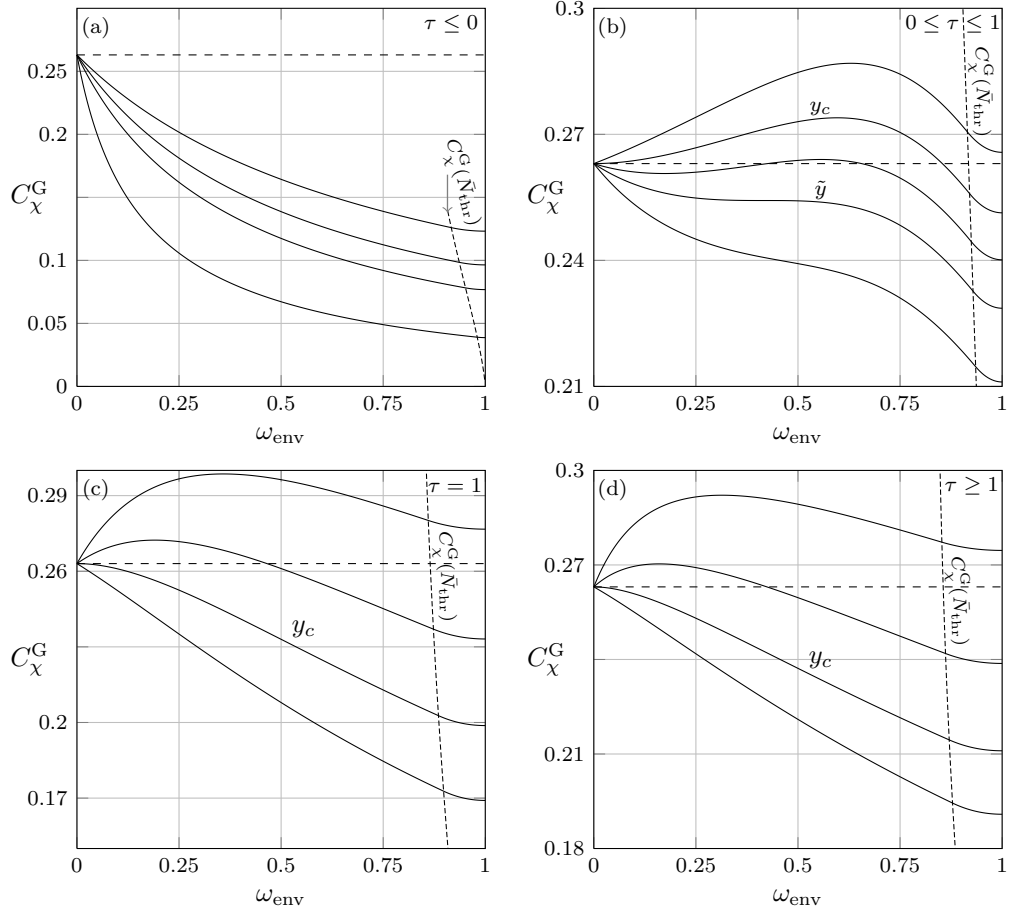


Figure 6.14.: Capacities C_χ^G vs. environment frequency ω_{env} (where for each plot from bottom to top) (a): $\tau = \{-0.125, -0.5, -1, -4\}$, (b): $\tau = \{0.34, 0.3759, 0.4, 0.4238, 0.455\}$, (c): $y = \{0.125, 0.2, 1/\sqrt{12}, 0.4\}$ and (d): $\tau = \{1.2, 1.35, 1 + 1/\sqrt{3}, 1.9\}$. For all plots $\bar{N} = 0.1$, and furthermore $M_{\text{env}} = 10^{-3}$ except for the case $\tau = 1$ (classical additive noise channel), where $y = M_{\text{env}}$. For $\tau \in [0, 1]$ the curve corresponding to $y = \tilde{y}$ has exactly a saddle point at finite squeezing, two extrema can be found for $\tilde{y} < y < y_c$ and one maximum is found for $y < y_c$. For the classical additive noise channel ($\tau = 1$) and the amplifier ($\tau \geq 1$) the curves corresponding to $y \geq y_c = 1/\sqrt{12}$ are monotonically increasing with decreasing ω_{env} where for $y < y_c$ a maximum appears. The densely dashed curve indicates $C_\chi^G(\bar{N} = \bar{N}_{\text{thr}})$ at $\omega_{\text{env}} = \omega_{\text{thr}}$ for given y : for $\omega_{\text{env}} \geq \omega_{\text{thr}}$ the quantum water-filling solution holds, for $\omega_{\text{env}} < \omega_{\text{thr}}$ it is no longer satisfied.

Again, in order to find an extremum we use the method of Lagrange multipliers. Since we extremize now with respect to ω_{env} as well, the gradient reads

$$\nabla = \left(\frac{\partial}{\partial \omega_{\text{in}}}, \frac{\partial}{\partial \bar{\omega}_{\text{out}}}, \frac{\partial}{\partial \omega_{\text{env}}} \right)^\top. \quad (6.190)$$

and the Lagrangian reads still as in Eq. (6.175). Note however, that the output energy constraint \bar{N}_{out} depends on ω_{env} and thus, we need to derive with respect to \bar{N}_{out} as well. Now $\nabla \mathcal{L} = 0$ is a system of three equations which leads to the additional solution (see Appendix D.2 for details):

$$\bar{\omega}_{\text{out}} = \sqrt{\omega_{\text{env}}^2 - \frac{\beta_{\text{out}}}{\bar{\beta}_{\text{out}}}(\omega_{\text{env}}^2 - \omega_{\text{out}}^2)}. \quad (6.191)$$

We can use Eq. (6.185) to express $\beta_{\text{out}}/\bar{\beta}_{\text{out}}$ and insert it in the latter leading to

$$\frac{\bar{\omega}_{\text{out}}^2 - 1}{\bar{\omega}_{\text{out}}^2 - \omega_{\text{env}}^2} = \frac{\omega_{\text{out}}^2 - \omega_{\text{in}}^2}{\omega_{\text{out}}^2 - \omega_{\text{env}}^2}. \quad (6.192)$$

By injecting the definition for ω_{out} , stated in Eq. (D.25), in Eq. (6.192) its right hand side is simplified to

$$\frac{\omega_{\text{out}}^2 - \omega_{\text{in}}^2}{\omega_{\text{out}}^2 - \omega_{\text{env}}^2} = -\frac{2y\omega_{\text{in}}}{|\tau|\omega_{\text{env}}}. \quad (6.193)$$

Inserting the expression for $\bar{\omega}_{\text{out}}$, given in Eq. (D.25), in the left hand side of (6.192) and equalizing it with Eq. (6.193) leads to the joint solution

$$\frac{\partial C_\chi^{\text{G}}}{\partial \omega_{\text{env}}} = 0, \quad \omega_{\text{in}} = \frac{1}{(1 + 2\bar{N})}, \quad \bar{\omega}_{\text{in}} = 1, \quad \bar{M}_{\text{in}} = \bar{N}, \quad (6.194)$$

identical to the case $\lim_{\omega_{\text{env}} \rightarrow 0} C_\chi^{\text{G}}$ [see Eqs. (6.146) and (6.187)]. This joint solution is shown for several examples in Fig. 6.13. Solving the transcendental equation (6.191) with the solution for ω_{in} stated in Eq. (6.194) leads to the value of ω_{env} (if there is a solution) for which C_χ^{G} is extremal. For the following, we shall use the notations to denote a maximum, minimum and saddle point:

$$\begin{aligned} \left. \frac{\partial C_\chi^{\text{G}}}{\partial \omega_{\text{env}}} \right|_{\omega_{\text{env}}=\omega_{\text{env,max}}} &= 0, & \left. \frac{\partial^2 C_\chi^{\text{G}}}{\partial \omega_{\text{env}}^2} \right|_{\omega_{\text{env}}=\omega_{\text{env,max}}} &< 0, \\ \left. \frac{\partial C_\chi^{\text{G}}}{\partial \omega_{\text{env}}} \right|_{\omega_{\text{env}}=\omega_{\text{env,min}}} &= 0, & \left. \frac{\partial^2 C_\chi^{\text{G}}}{\partial \omega_{\text{env}}^2} \right|_{\omega_{\text{env}}=\omega_{\text{env,min}}} &> 0, \\ \left. \frac{\partial C_\chi^{\text{G}}}{\partial \omega_{\text{env}}} \right|_{\omega_{\text{env}}=\tilde{\omega}_{\text{env}}} &= \left. \frac{\partial^2 C_\chi^{\text{G}}}{\partial \omega_{\text{env}}^2} \right|_{\omega_{\text{env}}=\tilde{\omega}_{\text{env}}} &= 0. \end{aligned} \quad (6.195)$$

Interestingly, according to Eq. (6.194) the optimal encoding at the squeezing value where the capacity is extremal coincides with the optimal encoding at $\omega_{\text{env}} \rightarrow 0$. Injecting

6. One-mode Gaussian channel

$\omega_{\text{in}} = (1 + 2\bar{N})^{-1}$ into the transcendental Eq. (6.191) leads to the solutions for the points $\omega_{\text{env,max}}$ and $\omega_{\text{env,min}}$ (when they exist), where numerical evidence shows that there are only the following types of solutions to Eq. (6.192):

1. No solution, i.e. no extremum
2. One solution corresponding to a maximum at squeezing $\omega_{\text{env}} = \omega_{\text{env,max}} \in (0, \omega_{\text{thr}})$
3. Two solutions corresponding to a maximum at squeezing $\omega_{\text{env}} = \omega_{\text{env,max}} \in (0, \omega_{\text{thr}})$ and a minimum at squeezing $\omega_{\text{env}} = \omega_{\text{env,min}} \in (0, \omega_{\text{thr}})$
4. One solution corresponding to a saddle point at squeezing $\omega_{\text{env}} = \tilde{\omega}_{\text{env}} \in (0, \omega_{\text{thr}})$

Only for the lossy channel ($\tau \in [0, 1]$) we observe that all four scenarios occur (confirming [PLM12]), whereas for the other channels either no solution (i.e. no extremum) or one maximum can be found. We justify this in detail in what follows. The dependency on ω_{env} can be classified using this numerical observation, i.e. that there are at most two extrema, and the behavior of the capacity in the limit $\omega_{\text{env}} \rightarrow 0$. Since in this limit the encoding $\omega_{\text{in}} = (1 + 2\bar{N})^{-1}$ was shown above to be optimal, we evaluate the Taylor expansion around $\omega_{\text{env}} = 0$ of χ^{G} with this encoding. This is equivalent to expanding C_{χ}^{G} in this limit, *i.e.*

$$C_{\chi}^{\text{G}} \approx \log_2(1 + 2\bar{N}) + a\omega_{\text{env}} + b\omega_{\text{env}}^2 + c\omega_{\text{env}}^3 + \mathcal{O}(\omega_{\text{env}}^4), \quad (6.196)$$

where

$$\begin{aligned} a &= K_1(12y^2 - 1), \\ b &= K_2 \\ &\times \left(\frac{3}{20} + \frac{(3 - 10\tau^2)\bar{\lambda}^2}{20} - 2y^2(\bar{\lambda}^2 + 1) + 12y^4(\bar{\lambda}^2 + 1) \right), \\ K_j &= \frac{\bar{\lambda}^2 - 1}{12(y|\tau|\bar{\lambda})^j \ln 2}, \end{aligned} \quad (6.197)$$

$\bar{\lambda} \equiv 1 + 2\bar{N}$ and c is not explicitly stated as its exact form is of no further use. We observe that the dominant linear term is canceled if

$$y_c \equiv \frac{1}{\sqrt{12}}, \quad (6.198)$$

which implies that $\partial C_{\chi}^{\text{G}}/\partial\omega_{\text{env}} = 0$ in the vicinity of $\omega_{\text{env}} = 0$. Using the fact that for $\omega_{\text{env}} \in [\omega_{\text{thr}}, 1]$ the capacity is a monotonically increasing and convex function of ω_{env} and the previous claim that the capacity has never more than two extrema we conclude: if $y < y_c$ then there is one maximum at a value $\omega_{\text{env,max}} \in [0, \omega_{\text{thr}}]$. Furthermore, for $y < y_c$ the limiting value $\lim_{\omega_{\text{env}} \rightarrow 0} C_{\chi}^{\text{G}} = \log_2(2\bar{N} + 1)$ is reached from above with decreasing ω_{env} .

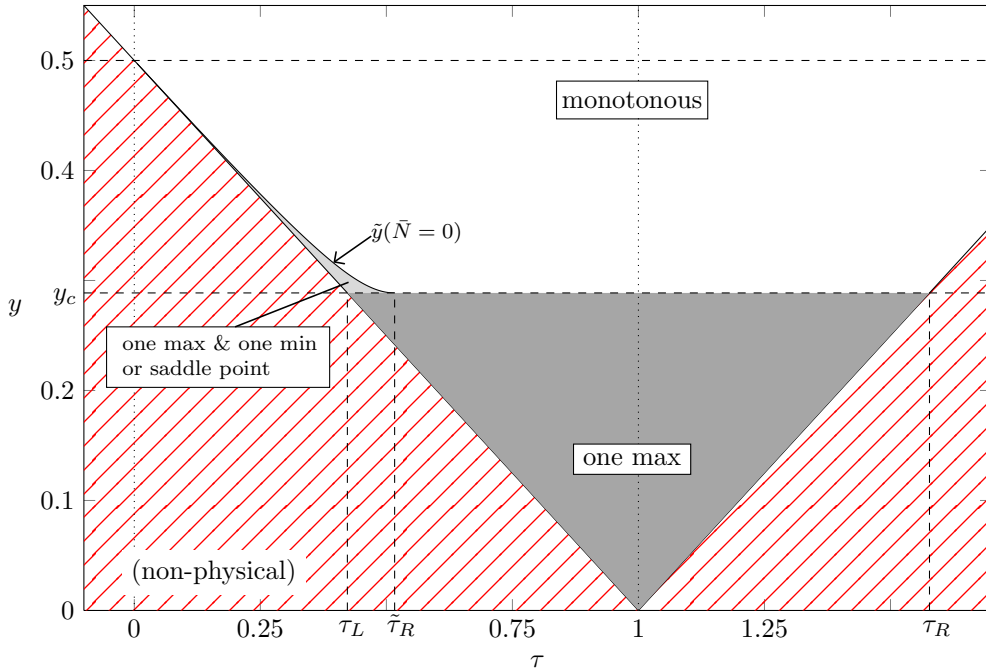


Figure 6.15.: Extremality properties of C_χ^G (one-mode) with respect to environment “frequency” ω_{env} , determined by y and τ , where $\tau = 1$ corresponds to the classical additive noise channel. North-East lines ($y \leq |1 - \tau|/2$): zone where y no longer corresponds to a quantum channel. Dark gray triangular region ($y < y_c$): the capacity exhibits one maximum. Light gray region [$y_c < y < \tilde{y}(\bar{N} = 0)$]: the capacity either exhibits one minimum and one maximum or one saddle point (see Fig. 6.16 for a full classification and Fig. 6.17 for concrete examples). White region ($y \geq \tilde{y}$, $y \geq y_c$): the capacity is a monotonously decreasing function of ω_{env} .

6. One-mode Gaussian channel

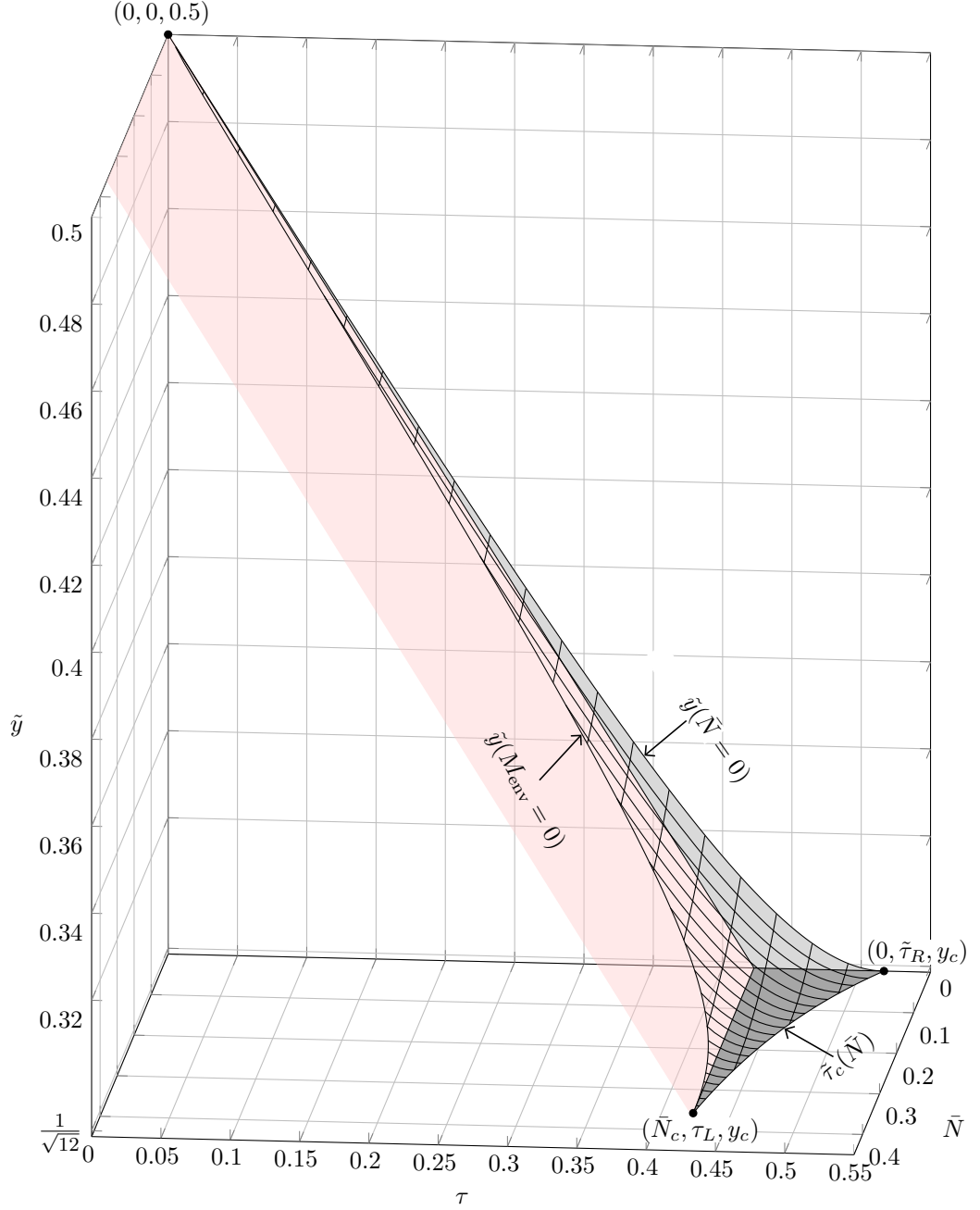


Figure 6.16.: Parameter \tilde{y} vs. \bar{N} and τ with respect to the noise squeezing ω_{env} (or equivalently s). The semi-opaque diagonal surface is the physicality constraint $y \geq \frac{|1-\tau|}{2}$. If the given parameter y lays on the “grid” surface (i.e. $y = \tilde{y}$) then there exists a saddle point at finite squeezing. Above the surface ($y > \tilde{y}$) no extrema exist. Underneath the surface ($y < \tilde{y}$) one maximum and one minimum can be found (at finite squeezing values). For $y = y_c = 1/\sqrt{12}$ (dark gray area) the maximum is at infinite noise squeezing $\omega_{\text{env}} = 0$ (or equivalently $s \rightarrow \infty$). For values below, i.e. $y < y_c$ there exists one maximum at finite squeezing [see Figs. 6.15 and 6.17].

Since y is a function of τ for the given range of τ , the condition $y = y_c$ can only be fulfilled when τ lays in a particular regime. We recall that for pure noise

$$y(M_{\text{env}} = 0) = \frac{|1 - \tau|}{2}, \quad (6.199)$$

is a lower bound on the physical region of y (see Fig. 6.15). Note, that at $\tau = 1$ the lower bound reads $y(M_{\text{env}} = 0) = 0$, which corresponds to the perfect transmission channel. The solutions of the equation $y = y_c$ with respect to τ are given by

$$\tau_c = 1 \pm \frac{1}{\sqrt{12}(M_{\text{env}} + 1/2)} \quad (6.200)$$

which leads to the domain

$$\tau_L \leq \tau_c \leq \tau_R, \quad (6.201)$$

where

$$\tau_L \equiv 1 - \frac{1}{\sqrt{3}}, \quad \tau_R \equiv 1 + \frac{1}{\sqrt{3}}. \quad (6.202)$$

This means that if $\tau \neq \tau_c$ (or $\tau_c \notin [\tau_L, \tau_R]$) then the parameter $y = y_c$ becomes unphysical. Note, that for the classical additive noise channel τ_c is not defined since $\tau = 1$ and thus, the condition $y = y_c$ can always be fulfilled.

We observe numerically that for $y \geq y_c$ there is either no extremum, a saddle point or a maximum followed by a minimum; all located in $0 < \omega_{\text{env}} \leq \omega_{\text{thr}}$, see Fig. 6.14. In order to discriminate the number of extrema further we need to study the term quadratic in ω_{env} of the expansion stated in Eq. (6.196). If we fix $y = y_c$ such that $a = 0$ then the quadratic term becomes dominant and its sign is determined by the sign of b . By jointly solving $a = b = 0$ we find

$$\tilde{\tau}_c \equiv \sqrt{\frac{2}{15}} \sqrt{1 + \frac{1}{(1 + 2\bar{N})^2}}, \quad (6.203)$$

where the range $\bar{N} \in [0, \infty)$ implies

$$\tilde{\tau}_L \leq \tilde{\tau}_c \leq \tilde{\tau}_R, \quad (6.204)$$

where

$$\tilde{\tau}_L \equiv \sqrt{\frac{2}{15}}, \quad \tilde{\tau}_R \equiv \frac{2}{\sqrt{15}}. \quad (6.205)$$

For $y = y_c$ and $\tau = \tilde{\tau}_c$ jointly $\partial C_\chi^G / \partial \omega_{\text{env}} = \partial^2 C_\chi^G / \partial \omega_{\text{env}}^2 = 0$, *i.e.* a saddle point lays in the vicinity of $\omega_{\text{env}} = 0$. We observe that for small input energies \bar{N} and in the neighborhood of the critical parameters τ_c, y_c the polynomial can develop two extrema, *i.e.* a minimum followed by a maximum (when increasing ω_{env} from 0 to 1). Since the expansion given in Eq. (6.196) can approximate arbitrary well C_χ^G in a certain regime $\omega_{\text{env}} \in [0, \delta]$ we deduce that these two extrema have to be present for C_χ^G for

6. One-mode Gaussian channel

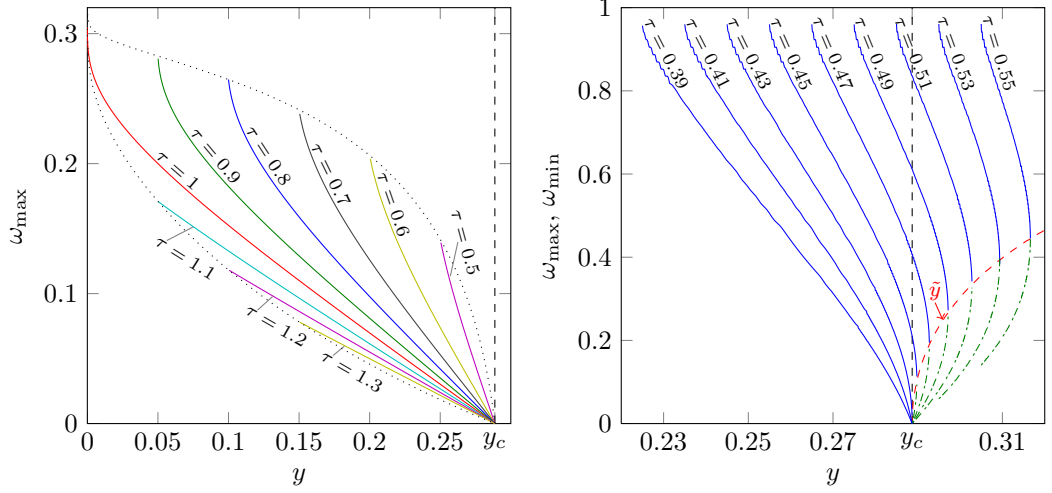


Figure 6.17.: Value of squeezing for which C_χ^G is extremal: (a) $\omega_{\text{env,max}}$ vs. y : from bottom to top (solid lines): $\tau = \{1.3, 1.2, 1.1, 1, 0.9, 0.8, 0.7, 0.6, 0.5\}$. The dotted, encircling curve corresponds to the value at the physical lower bound of y , i.e. $\omega_{\text{env,max}}(y = |1 - \tau|/2)$. We fixed the input energy $\bar{N} = 1 > \bar{N}_c$. All maxima tend to infinite squeezing $\omega_{\text{env,max}} \rightarrow 0$ when $y \rightarrow y_c = 1/\sqrt{12}$. (b) Squeezing at saddle point $\tilde{\omega}_{\text{env}}(\tilde{y})$ (dashed line), $\omega_{\text{env,max}}$ (solid lines above \tilde{y}) and $\omega_{\text{env,min}}$ (dashed-dotted lines below \tilde{y}), where from left to right $\tau = \{0.39, 0.41, 0.43, 0.45, 0.47, 0.49, 0.51, 0.53, 0.55\}$. We choose $\bar{N} = 0.01 < \bar{N}_c \approx 0.36$. One clearly observes the “splitting” of the saddle point into a maximum and a minimum when y is decreased from \tilde{y} up to $y_c = 1/\sqrt{12}$. Below y_c no minimum is observed but the maximum continues to exist.

$y \in$		$\tau \in$		
		$(-\infty, 0]$	$(0, \tilde{\tau}_R)$	$[\tilde{\tau}_R, \infty)$
$[0, y_c)$		Monotonous	One max.	One max.
$[y_c, \infty)$	$[y_c, \tilde{y})$	Monotonous	One max.+one min.	Monotonous
	$y = \tilde{y}$		Saddle point	
	(\tilde{y}, ∞)		Monotonous	

Table 6.2.: Extremality properties of C_χ^G with respect to ω_{env} .

$0 < \omega_{\text{env}} < \omega_{\text{thr}}$. This is confirmed numerically, see Fig. 6.17. In [PLM12] it was shown that the two extrema fall together to one saddle point for $0 < \omega_{\text{env}} < \omega_{\text{thr}}$ precisely when

$$\begin{aligned}
y = \tilde{y} &= (1 - \tilde{\tau}) \left(M_{\text{env}} + \frac{1}{2} \right), \\
M_{\text{env}} \leq M_c &= \frac{1}{2} \left[\left(\sqrt{3} - \frac{2}{\sqrt{5}} \right)^{-1} - 1 \right] \approx 0.0969, \\
\bar{N} \leq \bar{N}_c &= \frac{1}{2} \left[\sqrt{\frac{3}{2} + \frac{5}{\sqrt{12}}} - 1 \right] \approx 0.3578,
\end{aligned} \tag{6.206}$$

where

$$\tilde{\tau} \equiv \left\{ \tau \left| \frac{\partial C_\chi^G}{\partial \omega_{\text{env}}} = \frac{\partial^2 C_\chi^G}{\partial \omega_{\text{env}}^2} = 0, 0 < \omega_{\text{env}} < \omega_{\text{thr}} \right. \right\}, \tag{6.207}$$

can be found by a numerical algorithm. The ultimate bound on $\tilde{\tau}$ is given by the value of τ when both extrema fall together at $\omega_{\text{env}} = 0$, i.e. from Eq. (6.203) and Eq. (6.204) we have:

$$0 \leq \tilde{\tau} \leq \tilde{\tau}_c(\bar{N}) \leq \frac{2}{\sqrt{15}}. \tag{6.208}$$

The parameters M_c and \bar{N}_c are the solutions of the equations

$$\begin{aligned}
y_c &= (1 - \tilde{\tau}_R) \left(M_c + \frac{1}{2} \right), \\
\tau_L &= \tilde{\tau}(\bar{N} = \bar{N}_c).
\end{aligned} \tag{6.209}$$

In summary, we found the following behavior for the different channels, distinguished by the domain of τ (also depicted in Figs. 6.15, 6.16 and summarized in Table 6.2):

1. $\tau \leq 0$ (phase-conjugating channel): since $y \geq 1/2$, the linear term in the expansion in Eq. (6.196) always dominates which means the limiting value $\log_2(2\bar{N} + 1)$ for $\omega_{\text{env}} \rightarrow 0$ is always approached from below. Thus, there are no solutions for $y = y_c$ and $y = \tilde{y}$ and the capacity is always monotonically decreasing with ω_{env} .

6. One-mode Gaussian channel

2. $0 \leq \tau \leq \tilde{\tau}_R$ (lossy channel): The solutions $y = y_c$ and $y = \tilde{y}$ both exist and all four behaviors can be observed: i) for $y < y_c = 1/\sqrt{12}$ one maximum exists, ii) for $y_c \leq y < \tilde{y}$ one maximum and one minimum coexist, iii) for $y = \tilde{y}$ a saddle point exists and iv) for $y \geq \max(y_c, \tilde{y})$ the capacity is monotonically decreasing with ω_{env} .
3. $\tau \geq \tilde{\tau}_R$ (lossy channel, classical additive noise channel and amplification channel): The solution $y = y_c$ exists, which means one maximum appears for $y < y_c$. For $y \geq y_c$ the capacity is a monotonically decreasing function of ω_{env} (monotonically increasing with s).

This completes the characterization of the fiducial channel on the environment squeezing. We now move on to the channels with non-full rank matrices \mathbf{X} and \mathbf{Y} .

6.4.7. Non-thermal canonical channels

We studied above the Gaussian capacity of the fiducial channel for the cases when the corresponding ‘‘fiducial decomposition’’ is obtained for full rank matrices \mathbf{X} and \mathbf{Y} , i.e. $\text{rank}(\mathbf{X}) = \text{rank}(\mathbf{Y}) = 2$ as well as the perfect transmission and zero-transmission channel⁷. Now we extend this study to the cases $\text{rank}(\mathbf{X}) = 2, \text{rank}(\mathbf{Y}) = 1$ and $\text{rank}(\mathbf{X}) = 1, \text{rank}(\mathbf{Y}) = 2$. We showed in the proof of Theorem 1 that the physical action of the channel is unitarily equivalent to the two non-thermal canonical channels Φ^{SQ} (single quadrature additive noise channel) and Φ^{CS} (classical signal channel)⁸. Furthermore, we showed that both cases can effectively be recovered as a limiting case of the ‘‘fiducial decomposition’’. Therefore, we analyze now for both cases the Gaussian capacity in their respective limits.

We recall that the action of the Gaussian channel and the equivalent fiducial channel:

$$\mathbf{V}_{\text{out}} = \mathbf{X}\mathbf{V}_{\text{in}}\mathbf{X}^{\text{T}} + \mathbf{Y} = \mathbf{M}(\mathbf{X}_{\text{F}}\mathbf{\Theta}\mathbf{V}_{\text{in}}\mathbf{\Theta}^{\text{T}}\mathbf{X}_{\text{F}} + \mathbf{Y}_{\text{F}})\mathbf{M}^{\text{T}}. \quad (6.210)$$

Since \mathbf{M}^{T} is acting after the channel and not subject to an energy constraint it is irrelevant for the Gaussian capacity. The rotation $\mathbf{\Theta}$ at the input is just an initial reference phase and therefore irrelevant to the capacity, as well⁹. Therefore we need to study matrices \mathbf{X}_{F} and \mathbf{Y}_{F} in the particular limits, i.e.

$$C_{\chi}^{\text{G}}(\Phi, \bar{N}) = \lim_{\bar{s} \rightarrow \infty} C_{\chi}^{\text{G}}(\Phi^{\text{F}}, \bar{N}). \quad (6.211)$$

Let us first treat the case $\text{rank}(\mathbf{X}) = 2, \text{rank}(\mathbf{Y}) = 1$ (i.e. the channel unitarily equivalent to Φ^{SQ}). The matrix \mathbf{X}_{F} is in this case independent of the limit, namely [see

⁷We remark that our study also contained the perfect transmission channel $\text{rank}(\mathbf{X}) = 2, \text{rank}(\mathbf{Y} = 0)$ and zero-transmission channel $\text{rank}(\mathbf{X}) = 0, \text{rank}(\mathbf{Y} = 2)$ since they do not require a separate treatment as shown in the proof of Theorem 1.

⁸In the following we sometimes omit the notion ‘‘unitarily equivalent’’ and refer to both combinations of ranks simply as channels Φ^{SQ} and Φ^{CS} , respectively.

⁹For any given rotation $\mathbf{\Theta}$ one can always find the best input CM $\tilde{\mathbf{V}}_{\text{in}} = \mathbf{\Theta}\mathbf{V}_{\text{in}}\mathbf{\Theta}^{\text{T}}$ and then rotate it afterwards in order to express it in the original basis.

Eq. (6.35)] $\mathbf{X}_F = \mathbf{X}_{SQ} = \mathbb{I}$ which corresponds to a replacement $\tau \rightarrow 1$. For the effective noise matrix one has to make replacements $y \rightarrow \frac{1}{2}e^{-2\tilde{s}}$ and $s_Y \rightarrow s_Y - \tilde{s}$, which then in this limit is given by [see Eqs. (6.25) and (6.36)]

$$\begin{aligned} \lim_{\tilde{s} \rightarrow \infty} \mathbf{Y}_F &= \lim_{\tilde{s} \rightarrow \infty} \frac{1}{2} e^{-2\tilde{s}} \mathbf{\Theta}_F \mathbf{S}_X^{-1} \mathbf{\Theta}_{XY} \mathbf{S}_Y^2 \mathbf{\Theta}_{XY}^\top \mathbf{S}_X^{-1} \mathbf{\Theta}_F^\top, \\ &= \lim_{\tilde{s} \rightarrow \infty} \mathbf{\Theta}_F \mathbf{S}_X^{-1} \mathbf{\Theta}_{XY} \begin{pmatrix} \frac{1}{2} e^{2s_Y - 4\tilde{s}} & 0 \\ 0 & \frac{1}{2} e^{-2s_Y} \end{pmatrix} \mathbf{\Theta}_{XY}^\top \mathbf{S}_X^{-1} \mathbf{\Theta}_F^\top, \end{aligned} \quad (6.212)$$

where $\mathbf{\Theta}_{XY} = \mathbf{\Theta}_{1X}^\top \mathbf{\Theta}_Y = \mathbf{O}(\theta_Y - \theta_{1X}) = \mathbf{O}(\theta_{XY})$. Again, any outer rotation $\mathbf{\Theta}_F$ is irrelevant to the Gaussian capacity and thus we choose without loss of generality $\mathbf{\Theta}_F = \mathbb{I}$. Then, Eq. (6.212) can be further simplified:

$$\begin{aligned} \lim_{\tilde{s} \rightarrow \infty} \mathbf{Y}_F &= \frac{e^{-2s_Y}}{2} \mathbf{S}_X^{-1} \mathbf{\Theta}_{XY} \begin{pmatrix} 0 & 0 \\ 0 & 1 \end{pmatrix} \mathbf{\Theta}_{XY}^\top \mathbf{S}_X^{-1}, \\ &= \frac{e^{-2s_Y}}{2} \begin{pmatrix} e^{-2s_X} \sin^2(\theta_{XY}) & \cos(\theta_{XY}) \sin(\theta_{XY}) \\ \cos(\theta_{XY}) \sin(\theta_{XY}) & e^{2s_X} \cos^2(\theta_{XY}) \end{pmatrix} \equiv \tilde{\mathbf{Y}}_{SQ}. \end{aligned} \quad (6.213)$$

Then, we can find a rotation

$$\begin{aligned} \tilde{\mathbf{\Theta}}_{SQ} &= \mathbf{O}(\theta_{SQ}), \\ \theta_{SQ} &= \arcsin \left(\frac{\text{sgn}(\cot(\theta_{XY}))}{\sqrt{1 + e^{4s_X} \cot^2(\theta_{XY})}} \right), \end{aligned} \quad (6.214)$$

where $\mathbf{O}(\theta)$ is a rotation matrix (see Eq. (5.22)), which diagonalizes $\tilde{\mathbf{Y}}_{SQ}$, i.e.

$$\begin{aligned} \tilde{\mathbf{\Theta}}_{SQ} \tilde{\mathbf{Y}}_{SQ} \tilde{\mathbf{\Theta}}_{SQ}^\top &= \text{diag} \left(0, \frac{\zeta}{2} \right), \\ \zeta(s_X, s_Y, \theta_{XY}) &= \frac{e^{-2s_Y}}{2} [\cosh(2s_X) + \cos(2\theta_{XY}) \sinh(2s_X)]. \end{aligned} \quad (6.215)$$

Thus, we found that the action of the channel in this limit reads

$$\begin{aligned} \lim_{\tilde{s} \rightarrow \infty} \mathbf{X}_F \mathbf{V}_{in} \mathbf{X}_F + \mathbf{Y}_F &= \mathbf{V}_{in} + \tilde{\mathbf{\Theta}}_{SQ} \tilde{\mathbf{Y}}_{SQ} \tilde{\mathbf{\Theta}}_{SQ}^\top \\ &= \tilde{\mathbf{\Theta}}_{SQ}^\top (\tilde{\mathbf{\Theta}}_{SQ} \mathbf{V}_{in} \tilde{\mathbf{\Theta}}_{SQ}^\top + \tilde{\mathbf{Y}}_{SQ}) \tilde{\mathbf{\Theta}}_{SQ}. \end{aligned} \quad (6.216)$$

Therefore the rotation $\tilde{\mathbf{\Theta}}_{SQ}$ is again a reference phase which does not change the capacity and we choose it without loss of generality $\tilde{\mathbf{\Theta}}_{SQ} = \mathbb{I}$. In conclusion, we have reduced the problem of finding the Gaussian capacity to the map $\tilde{\Phi}^{SQ}$ with output CM

$$\mathbf{V}_{out} = \mathbf{V}_{in} + \text{diag}(0, \zeta). \quad (6.217)$$

The map $\tilde{\Phi}^{SQ}$ is equivalently a limiting case of (another) fiducial channel Φ^F with replacements $\tau = 1$, $y = \zeta e^{2s}$ where $s \rightarrow -\infty$, i.e.

$$\text{diag}(0, \zeta) = \lim_{s \rightarrow -\infty} \zeta e^{2s} \begin{pmatrix} e^{2s} & 0 \\ 0 & e^{-2s} \end{pmatrix}. \quad (6.218)$$

6. One-mode Gaussian channel

In conclusion, the Gaussian capacity is given by the fiducial with these replacements and in this particular limit, i.e. (we omit for simplicity in this equation the parameter \bar{N})

$$\begin{aligned} C_\chi^G(\Phi) &= C_\chi^G(\tilde{\Phi}^{\text{SQ}}) = \lim_{\bar{s} \rightarrow \infty} C_\chi^G \left(\Phi_{(1, \frac{e^{-2\bar{s}}}{2}, s(s_X, s_Y - \bar{s}, \theta_{XY}))}^{\text{F}} \right), \\ &= \lim_{s \rightarrow -\infty} C_\chi^G \left(\Phi_{(1, \zeta e^{2s}, s)}^{\text{F}} \right), \quad \text{rank}(\mathbf{X}) = 2, \text{rank}(\mathbf{Y}) = 1. \end{aligned} \quad (6.219)$$

In the following we consider the parameter $\zeta = \zeta(s_X, s_Y, \theta_{XY})$ as a single noise parameter without discussing the sub-dependencies on s_X, s_Y and θ_{XY} . Clearly, in the limit $s \rightarrow -\infty$ the input energy constraint \bar{N}_{thr} diverges to infinity and thus, we have to consider the solution $\bar{N} < \bar{N}_{\text{thr}}$. Then, we fix the modulation of the noisier quadrature to zero, i.e. $m_p = 0$ which implies $\bar{v}_p = v_p$. The eigenvalues of the CM of the output and modulated output state become with replacements $\tau = 1$ and $y = \zeta e^{2s}$ in this limit

$$\begin{aligned} \lim_{s \rightarrow -\infty} v_q &= \lim_{s \rightarrow -\infty} i_q + \zeta e^{4s} = i_q, \\ \lim_{s \rightarrow -\infty} \bar{v}_q &= \lim_{s \rightarrow -\infty} i_q + m_q + \zeta e^{4s} = i_q + m_q, \\ \lim_{s \rightarrow -\infty} \bar{v}_p &= v_p = \lim_{s \rightarrow -\infty} \frac{1}{4i_q} + \zeta = \frac{1}{4i_q} + \zeta. \end{aligned} \quad (6.220)$$

The solution, i.e. the optimal input eigenvalue i_q , is obtained by taking the limit of equation (6.129) (which resulted from the Lagrange multiplier method), with replacements $\tau = 1, y = \zeta e^{2s}$, i.e.

$$\lim_{s \rightarrow -\infty} \frac{g'(\bar{M}_{\text{out}})}{(\bar{M}_{\text{out}} + \frac{1}{2})} (\bar{v}_q - \bar{v}_p) = \frac{g'(M_{\text{out}})}{(M_{\text{out}} + \frac{1}{2})} \zeta e^{2s} (e^{2s} - 4i_q^2 e^{-2s}) \quad (6.221)$$

$$\Leftrightarrow \frac{g'(\bar{M}_{\text{out}})}{(\bar{M}_{\text{out}} + \frac{1}{2})} (\bar{v}_q - \bar{v}_p) = -4 \frac{g'(M_{\text{out}})}{(M_{\text{out}} + \frac{1}{2})} \zeta i_q^2, \quad (6.222)$$

where in Eq. (6.222) all parameters are replaced by their limiting expressions stated in Eq. (6.220). Note that Eq. (6.222) can also be obtained by applying the Lagrange multiplier method directly to the limiting channel stated in Eq. (6.217).

First, we observe that

$$\lim_{\zeta \rightarrow \infty} \text{diag}(0, \zeta) = \lim_{s \rightarrow -\infty} y \text{diag}(e^{2s}, e^{-2s}). \quad (6.223)$$

Thus, by Eq. (6.147) we conclude that

$$\lim_{\zeta \rightarrow \infty} C_\chi^G(\tilde{\Phi}^{\text{SQ}}, \bar{N}) = \lim_{s \rightarrow -\infty} C_\chi^G \left(\Phi_{(\tau, y, s)}^{\text{F}}, \bar{N} \right) = \log_2(2\bar{N} + 1), \quad \text{rank}(\mathbf{X}) = 2, \text{rank}(\mathbf{Y}) = 1. \quad (6.224)$$

Furthermore, we obtain (trivially) the solution when the channel becomes the perfect transmission channel, i.e.

$$\lim_{\zeta \rightarrow 0} C_\chi^G(\tilde{\Phi}^{\text{SQ}}) = g(\bar{N}), \quad \text{rank}(\mathbf{X}) = 2, \text{rank}(\mathbf{Y}) = 1. \quad (6.225)$$

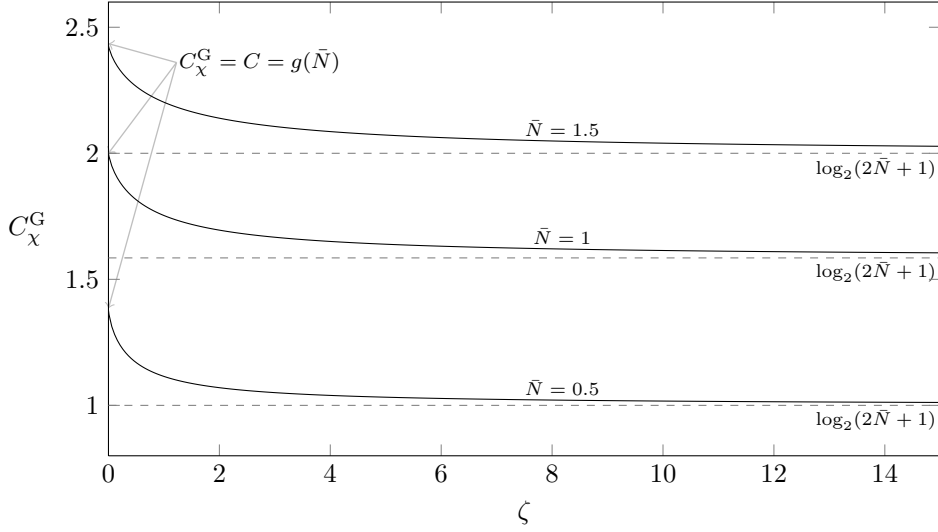


Figure 6.18.: C_χ^G vs. ζ (channel Φ^{SQ}). From bottom to top we fixed $\bar{N} = \{0.5, 1, 1.5\}$; the dashed horizontal lines indicate for each case the limiting values $\log_2(2\bar{N} + 1)$. At $\zeta = 0$ the one-shot Gaussian capacity achieves the classical capacity $C_\chi^G = C = g(\bar{N})$.

Unfortunately, Eq. (6.222) remains a transcendental equation and is therefore difficult to analyze with respect to the parameter ζ . However, it is easy to show that C_χ^G is (as expected) a monotonically decreasing function of ζ . Since $v_q = i_q$, $\bar{v}_q = i_q + m_q$, $v_p = \bar{v}_p = 1/(4i_q) + \zeta$ we have for any fixed (possibly non optimal) encoding (i_q, m_q) :

$$\chi^G(x) = f(x) = g\left(\sqrt{(i_q + m_q)x(\zeta)} - \frac{1}{2}\right) - g\left(\sqrt{i_q x(\zeta)} - \frac{1}{2}\right), \quad x = \frac{1}{4i_q} + \zeta. \quad (6.226)$$

It is straightforward to show that $f(x - \delta) > f(x)$, $\forall \delta > 0$, $\delta < x$. Since this holds for any given encoding it implies that

$$\frac{\partial C_\chi^G}{\partial \zeta} < 0, \quad \text{rank}(\mathbf{X}) = 2, \text{rank}(\mathbf{Y}) = 1. \quad (6.227)$$

As a consequence we find, using the exact limits (6.224) and (6.225), that

$$\log_2(2\bar{N} + 1) \leq C_\chi^G(\Phi, \bar{N}) \leq C(\Phi, \bar{N}) \leq g(\bar{N}), \quad \text{rank}(\mathbf{X}) = 2, \text{rank}(\mathbf{Y}) = 1. \quad (6.228)$$

Clearly, the upper bound $g(\bar{N})$ is an obvious one, since any Gaussian channel is upper bounded by the capacity of the perfect transmission channel. Interestingly though the lower bound on the one-shot Gaussian capacity provides an analytical lower bound on the actual classical capacity C . Since $g(x) - \log_2(2x - 1)$ is a monotonically increasing function and furthermore

$$\lim_{x \rightarrow \infty} [g(x) - \log_2(2x - 1)] = \frac{1}{\ln 2} - 1, \quad (6.229)$$

6. One-mode Gaussian channel

we proved that¹⁰

$$C_\chi^G(\Phi, \bar{N}) \leq C(\Phi, \bar{N}) \leq C_\chi^G(\Phi, \bar{N}) + \frac{1}{\ln 2} - 1, \quad \text{rank}(\mathbf{X}) = 2, \text{rank}(\mathbf{Y}) = 1, \quad (6.230)$$

i.e. for this combination of ranks the classical capacity does not exceed the Gaussian capacity by more than ~ 0.44 bits. We plotted C_χ^G vs. ζ for different input energies \bar{N} in Fig. 6.18. Finally, we prove that the channel Φ that is unitarily equivalent to Φ^{SQ} is optimal among all one-mode channels with $\tau = 1$ and noise constraint $\zeta = \text{Tr}[\mathbf{Y}]$:

Lemma 5. *Let Φ' be a one-mode Gaussian channel with $\tau = 1$ and $\mathbf{Y} = \text{diag}(0, \zeta)$ (or $\mathbf{Y} = \text{diag}(\zeta, 0)$) and let Φ be a one-mode Gaussian channel with $\tau = 1$ and $\zeta = \text{Tr}[\mathbf{Y}]$. Then*

$$C_\chi^G(\Phi', \bar{N}) \geq C_\chi^G(\Phi, \bar{N}), \quad (6.231)$$

where equality holds iff \mathbf{Y} is identical for both channels.

Proof. The proof follows directly from Lemma 9 stated in Appendix D.3.4. \square

Let us now treat the other case $\text{rank}(\mathbf{X}) = 1, \text{rank}(\mathbf{Y}) = 2$, i.e. the channel unitarily equivalent to Φ^{CS} . We have to treat the limit stated in (6.211) as a limit of the whole map, since \mathbf{X}_F and \mathbf{Y}_F depend on the parameter \tilde{s} . With replacements $\tau \rightarrow e^{-2\tilde{s}}, \theta_{2X} \rightarrow 0, s_X \rightarrow s_X + \tilde{s}$ [see Eqs. (6.38) to (6.41)] and definitions $\tilde{\mathbf{S}} = S(\tilde{s}), \Theta_{XY} = \Theta_{1X}^\top \Theta_Y$ we obtain

$$\begin{aligned} & \lim_{\tilde{s} \rightarrow \infty} \mathbf{X}_F \mathbf{V}_{\text{in}} \mathbf{X}_F + \mathbf{Y}_F \\ &= \lim_{\tilde{s} \rightarrow \infty} e^{-2\tilde{s}} \mathbf{V}_{\text{in}} + y \Theta_F \tilde{\mathbf{S}}^{-1} \mathbf{S}_X^{-1} \Theta_{XY} \mathbf{S}_Y^2 \Theta_{XY}^\top \mathbf{S}_X^{-1} \tilde{\mathbf{S}}^{-1} \Theta_F^\top, \\ &= \lim_{\tilde{s} \rightarrow \infty} \Theta_F \tilde{\mathbf{S}}^{-1} \mathbf{S}_X^{-1} (e^{-2\tilde{s}} \tilde{\mathbf{S}} \mathbf{S}_X \Theta_F^\top \mathbf{V}_{\text{in}} \Theta_F \mathbf{S}_X \tilde{\mathbf{S}} + y \Theta_{XY} \mathbf{S}_Y^2 \Theta_{XY}^\top) \mathbf{S}_X^{-1} \tilde{\mathbf{S}}^{-1} \Theta_F^\top, \end{aligned} \quad (6.232)$$

Now we can again omit the symplectic transformation $\Theta_F \tilde{\mathbf{S}}^{-1} \mathbf{S}_X^{-1}$ at the output, as well as the initial reference phase Θ_F^\top since they do not change the entropy and we have no energy constraint on the output. Thus, we found another map with the same capacity which has the output CM

$$\begin{aligned} \mathbf{V}_{\text{out}} &= \lim_{\tilde{s} \rightarrow \infty} e^{-2\tilde{s}} \tilde{\mathbf{S}} \mathbf{S}_X \mathbf{V}_{\text{in}} \mathbf{S}_X \tilde{\mathbf{S}} + y \Theta_{XY} \mathbf{S}_Y^2 \Theta_{XY}^\top \\ &= \mathbf{X}_{\text{CS}} \mathbf{S}_X \mathbf{V}_{\text{in}} \mathbf{S}_X \mathbf{X}_{\text{CS}} + y \Theta_{XY} \mathbf{S}_Y^2 \Theta_{XY}^\top \\ &= e^{2s_X} \text{diag}(i_q, 0) + y \Theta_{XY} \mathbf{S}_Y^2 \Theta_{XY}^\top \\ &= \Theta_{XY} \mathbf{S}_Y (e^{2s_X} i_q \mathbf{S}_Y^{-1} \Theta_{XY}^\top \text{diag}(1, 0) \Theta_{XY} \mathbf{S}_Y^{-1} + y \mathbb{I}) \mathbf{S}_Y \Theta_{XY}^\top. \end{aligned} \quad (6.233)$$

where we used the definitions

$$\mathbf{X}_{\text{CS}} = \begin{pmatrix} 1 & 0 \\ 0 & 0 \end{pmatrix}, \quad \mathbf{V}_{\text{in}} = \begin{pmatrix} i_q & i_{\text{qp}} \\ i_{\text{qp}} & i_p \end{pmatrix}, \quad (6.234)$$

¹⁰We discuss bounds on the classical capacity in more details in Sec. 6.5.

and again moved the symplectic transformation behind the channel. Then, equivalently to Eq. (6.213), we have

$$\begin{aligned} & e^{2s_X} i_q \mathbf{S}_Y^{-1} \mathbf{\Theta}_{XY}^T \text{diag}(1, 0) \mathbf{\Theta}_{XY} \mathbf{S}_Y^{-1} \\ &= e^{2s_X} i_q \begin{pmatrix} e^{-2s_Y} \cos^2(\theta_{XY}) & -\cos(\theta_{XY}) \sin(\theta_{XY}) \\ -\cos(\theta_{XY}) \sin(\theta_{XY}) & e^{s_Y} \sin^2(\theta_{XY}) \end{pmatrix} \equiv \tilde{\mathbf{X}}_{\text{CS}}. \end{aligned} \quad (6.235)$$

Now we find the rotation

$$\begin{aligned} \tilde{\mathbf{\Theta}}_{\text{CS}} &= \mathbf{O}(\theta_{\text{CS}}), \\ \theta_{\text{CS}} &= \arccos \left(\frac{\text{sgn}(\tan(\theta_{XY}))}{\sqrt{1 + e^{4s_Y} \tan^2(\theta_{XY})}} \right), \end{aligned} \quad (6.236)$$

such that

$$\tilde{\mathbf{\Theta}}_{\text{CS}} \tilde{\mathbf{X}}_{\text{CS}} \tilde{\mathbf{\Theta}}_{\text{CS}}^T = \text{diag}(2i_q \tilde{\zeta}, 0), \quad (6.237)$$

where $\tilde{\zeta}$ reads as in Eq. (6.215) but with replacements $s_X \rightarrow -s_Y$ and $s_Y \rightarrow -s_X$, i.e.

$$\tilde{\zeta} = \zeta(-s_Y, -s_X, \theta_{XY}) = \frac{e^{2s_X}}{2} [\cosh(2s_Y) - \cos(2\theta_{XY}) \sinh(2s_Y)]. \quad (6.238)$$

Then we can insert $\mathbb{I} = \tilde{\mathbf{\Theta}}_{\text{CS}}^T \tilde{\mathbf{\Theta}}_{\text{CS}}$ in the last line of Eq. (6.233):

$$\begin{aligned} & \lim_{\tilde{s} \rightarrow \infty} e^{-2\tilde{s}} \tilde{\mathbf{S}} \mathbf{S}_X \mathbf{V}_{\text{in}} \mathbf{S}_X \tilde{\mathbf{S}} + y \mathbf{\Theta}_{XY} \mathbf{S}_Y^2 \mathbf{\Theta}_{XY}^T \\ &= \mathbf{\Theta}_{XY} \mathbf{S}_Y \tilde{\mathbf{\Theta}}_{\text{CS}}^T (e^{2s_X} i_q \tilde{\mathbf{\Theta}}_{\text{CS}} \mathbf{S}_Y^{-1} \mathbf{\Theta}_{XY}^T \text{diag}(1, 0) \mathbf{\Theta}_{XY} \mathbf{S}_Y^{-1} \tilde{\mathbf{\Theta}}_{\text{CS}}^T + y \mathbb{I}) \mathbf{S}_Y \mathbf{\Theta}_{XY}^T \tilde{\mathbf{\Theta}}_{\text{CS}} \\ &= \mathbf{\Theta}_{XY} \mathbf{S}_Y \tilde{\mathbf{\Theta}}_{\text{CS}}^T (\text{diag}(2i_q \tilde{\zeta}, 0) + y \mathbb{I}) \mathbf{S}_Y \mathbf{\Theta}_{XY}^T \tilde{\mathbf{\Theta}}_{\text{CS}}. \end{aligned} \quad (6.239)$$

We omit again the symplectic transformation $\mathbf{\Theta}_{XY} \mathbf{S}_Y \tilde{\mathbf{\Theta}}_{\text{CS}}^T$ at the output and therefore have found a simpler map $\tilde{\Phi}^{\text{CS}}$ with the same capacity and energy constraint. The map $\tilde{\Phi}^{\text{CS}}$ can be expressed as the limiting case of another fiducial channel, i.e.

$$\text{diag}(2i_q \tilde{\zeta}, 0) + y \mathbb{I} = \lim_{s \rightarrow -\infty} 2\tilde{\zeta} e^{2s} \mathbf{S}^{-1} \mathbf{V}_{\text{in}} \mathbf{S}^{-1} + y \mathbb{I} \quad (6.240)$$

$$= \lim_{s \rightarrow -\infty} \mathbf{S}^{-1} (2\tilde{\zeta} e^{2s} \mathbf{V}_{\text{in}} + y \mathbf{S}^2) \mathbf{S}^{-1}. \quad (6.241)$$

where $\mathbf{S} = \text{diag}(e^s, e^{-s})$. Thus, we found the following equality for the Gaussian capacity (we omit for simplicity the dependency on the parameter \bar{N})

$$\begin{aligned} C_\chi^{\text{G}}(\Phi) &= C_\chi^{\text{G}}(\tilde{\Phi}^{\text{CS}}) = \lim_{\tilde{s} \rightarrow \infty} C_\chi^{\text{G}} \left(\Phi_{(e^{-2\tilde{s}}, y, s(s_X + \tilde{s}, s_Y, \theta_{XY}))}^{\text{F}} \right), \\ &= \lim_{s \rightarrow -\infty} C_\chi^{\text{G}} \left(\Phi_{(2\tilde{\zeta} e^{2s}, y, s)}^{\text{F}} \right), \quad \text{rank}(\mathbf{X}) = 1, \text{rank}(\mathbf{Y}) = 2. \end{aligned} \quad (6.242)$$

In the following we consider the parameter $\tilde{\zeta} = \tilde{\zeta}(s_X, s_Y, \theta_{XY})$ again as a fixed gain parameter. Unlike in the case of the channel Φ^{SQ} we have an additional degree of freedom, namely the parameter $y \geq 1/2$. Due to the limit of infinite squeezing the input

6. One-mode Gaussian channel

energy threshold diverges in this case as well and we have to consider the solution in the regime $\bar{N} < \bar{N}_{\text{thr}}$. We derive the optimal solution now using the method of Lagrange multipliers for the limiting map stated on the left hand side in Eq. (6.240). Here, the p -quadrature is completely erased and we have only one degree of freedom for information transmission (hence “classical signal”), implying that it is optimal to fix $m_p = 0$. Then, we have the following lists of eigenvalues and thermal photons:

$$\begin{aligned}
v_q &= 2\tilde{\zeta}i_q + y, \\
\bar{v}_q &= 2\tilde{\zeta}(i_q + m_q) + y, \\
\bar{v}_p &= v_p = y. \\
M_{\text{out}} &= \sqrt{(2\tilde{\zeta}i_q + y)y - \frac{1}{2}}, \\
\bar{M}_{\text{out}} &= \sqrt{(2\tilde{\zeta}(i_q + m_q) + y)y - \frac{1}{2}}.
\end{aligned} \tag{6.243}$$

Following the same steps as in the general case (see Appendix D.1) one obtains the solution

$$i_q = \frac{1}{2} \sqrt{\frac{(M_{\text{out}} + \frac{1}{2})g'(\bar{M}_{\text{out}})}{(\bar{M}_{\text{out}} + \frac{1}{2})g'(M_{\text{out}})}}, \tag{6.244}$$

which, despite its compact form, is a transcendental equation as well.

It is straightforward to show that, as in the case of the channel Φ^{SQ} , the limit $\tilde{\zeta} \rightarrow \infty$ is equivalent to the limit of infinite squeezing of the fiducial channel. The symplectic output eigenvalue ν_{out} of a fiducial channel $\Phi_{(\tau,y,s)}^{\text{F}}$ in the limit $s \rightarrow -\infty$ reads

$$\begin{aligned}
\lim_{s \rightarrow -\infty} \nu_{\text{out}}^2 &= \lim_{s \rightarrow -\infty} (|\tau|i_q + ye^{2s}) \left(\frac{|\tau|}{4i_q} + ye^{-2s} \right), \\
&= \lim_{s \rightarrow -\infty} \left(\frac{|\tau|}{e^{2s}} i_q + y \right) \left(\frac{|\tau|}{4i_q e^{-2s}} + y \right), \\
&= \lim_{\tilde{\zeta} \rightarrow \infty} (|\tau|\tilde{\zeta}i_q + y) \left(\frac{|\tau|}{4i_q \tilde{\zeta}} + y \right), \\
&= \lim_{\tilde{\zeta} \rightarrow \infty} (\tilde{\zeta}i_q + y)y.
\end{aligned} \tag{6.245}$$

The same relations hold for the symplectic eigenvalue $\bar{\nu}_{\text{out}}$ with replacement $i_q \rightarrow i_q + m_q$. Thus, in this limit the arguments of χ^{G} coincide and we showed that

$$\lim_{\tilde{\zeta} \rightarrow \infty} C_{\chi}^{\text{G}}(\tilde{\Phi}^{\text{CS}}, \bar{N}) = \lim_{s \rightarrow -\infty} C_{\chi}^{\text{G}}(\Phi_{(\tau,y,s)}^{\text{F}}, \bar{N}) = \log_2(2\bar{N} + 1), \quad \text{rank}(\mathbf{X}) = 1, \text{rank}(\mathbf{Y}) = 2. \tag{6.246}$$

Furthermore, we (trivially) can evaluate the other limiting case, i.e.

$$\lim_{\tilde{\zeta} \rightarrow 0} C_{\chi}^{\text{G}}(\tilde{\Phi}^{\text{CS}}, \bar{N}) = 0, \quad \text{rank}(\mathbf{X}) = 1, \text{rank}(\mathbf{Y}) = 2. \tag{6.247}$$

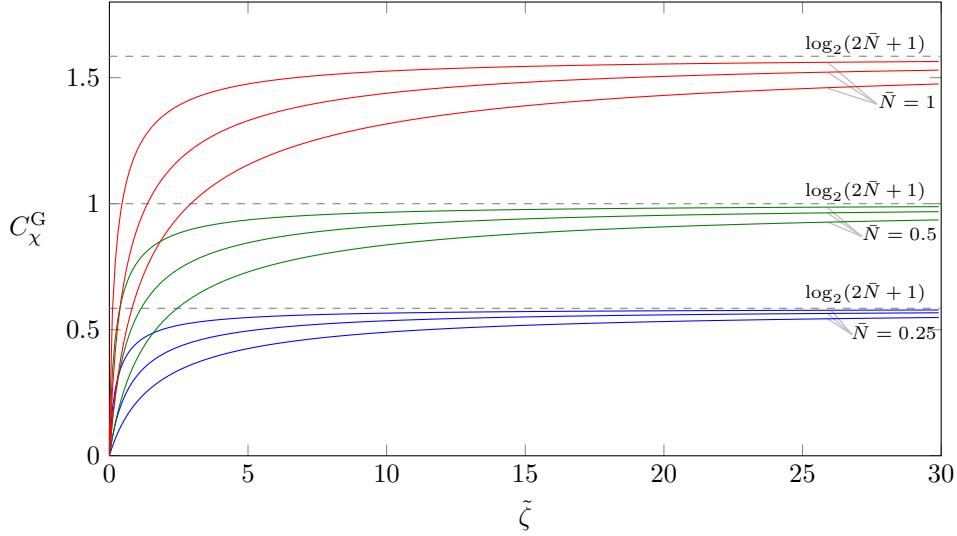


Figure 6.19.: C_χ^G vs. $\tilde{\zeta}$ (channel Φ^{CS}). For the upper three lines we fixed $\bar{N} = 1$, for the three middle lines $\bar{N} = 0.5$ and for the three bottom lines $\bar{N} = 0.25$. For each group of lines with fixed input energy we choose (from top to bottom) $y = \{0.5, 1, 2\}$. For $\tilde{\zeta} \rightarrow \infty$ we observe that $C_\chi^G \rightarrow \log_2(2\bar{N} + 1)$. At $\tilde{\zeta} = 0$ the channel becomes the zero-transmission channel and thus $C = C_\chi^G = 0$.

This shows that in the limit $\tilde{\zeta} \rightarrow 0$ the channel becomes the zero transmission channel. In the same way as we showed the monotonicity of C_χ^G over ζ for $\text{rank}(\mathbf{X}) = 2, \text{rank}(\mathbf{Y}) = 1$ one can straightforwardly show that

$$\frac{\partial C_\chi^G}{\partial \tilde{\zeta}} > 0, \quad \text{rank}(\mathbf{X}) = 1, \text{rank}(\mathbf{Y}) = 2. \quad (6.248)$$

Together with limits (6.246) and (6.247) it follows that

$$C_\chi^G(\Phi, \bar{N}) \leq \log_2(2\bar{N} + 1), \quad \text{rank}(\mathbf{X}) = 1, \text{rank}(\mathbf{Y}) = 2. \quad (6.249)$$

We plot C_χ^G for different values of $\tilde{\zeta}$ and y in Fig. 6.19.

6.5. Bounds on the classical capacity

In this section we show that the one-shot Gaussian capacity serves as a useful bound on the classical capacity. For the general thermal channel $\Phi_{(\tau, y)}^{\text{TH}}$ with $\tau > 0$ it was recently proven that [KS13]

$$C^G(\Phi^{\text{TH}}, \bar{N}) \leq C(\Phi^{\text{TH}}, \bar{N}) \leq C^G(\Phi^{\text{TH}}, \bar{N}) + \frac{1}{\ln 2}. \quad (6.250)$$

We can straightforwardly extend this result to the general case, above the input energy threshold:

6. One-mode Gaussian channel

Corollary 2. For a single-mode Gaussian channel Φ with parameters $(\tau > 0, y > 0)$ and $\bar{N} \geq \bar{N}_{\text{thr}}$,

$$\begin{aligned} C^{\text{G}}(\Phi, \bar{N}) &\leq C(\Phi, \bar{N}) \leq \bar{C} \leq C^{\text{G}}(\Phi, \bar{N}) + \frac{1}{\ln 2}, \\ \bar{C} &= g\left(\frac{2\tau\bar{N} + (2y + 1 - \tau)\sinh^2 s}{2y + 1 + \tau}\right), \end{aligned} \quad (6.251)$$

where $C^{\text{G}}(\Phi, \bar{N})$ is stated in Eq. (6.81).

Proof. The fiducial channel corresponding to Φ can according to its definition be decomposed as

$$\Phi_{(\tau, y, s)}^{\text{F}} = \Phi_{(G, \frac{G-1}{2}, s)}^{\text{F}} \circ \Phi_{(T, \frac{1-T}{2}, s)}^{\text{F}}, \quad (6.252)$$

with $T = 2\tau/(2y + \tau + 1)$ [see Fig. 6.3 and Table 6.1]. Since the capacity fulfills the pipelining property [stated in Eq. (3.37)] we can upper bound the capacity of $\Phi_{(\tau, y, s)}^{\text{F}}$ by the capacity of the first channel, i.e.

$$C(\Phi, \bar{N}) = C\left(\Phi_{(\tau, y, s)}^{\text{F}}, \bar{N}\right) \leq C\left(\Phi_{(T, \frac{1-T}{2}, s)}^{\text{F}}, \bar{N}\right) \leq \bar{C},$$

where

$$\bar{C} = g(T\bar{N} + (1 - T)\sinh^2 s), \quad (6.253)$$

is the classical capacity of the lossy channel with (pure) squeezed noise, stated in Eq. (6.87). We define the function

$$\begin{aligned} \Delta(s) &\equiv \bar{C} - C^{\text{G}} = g[A(B + 1)^{-1}] - g(A + B \cosh^2 s) + g(B), \\ A &= \tau\bar{N} + \left[y + \frac{1 - \tau}{2}\right] \sinh^2 s, \\ B &= y + \frac{\tau - 1}{2}. \end{aligned} \quad (6.254)$$

It was shown in [KS13] that $\Delta(0) < 1/\ln 2$. Since

$$\Delta(s) \leq \Delta(0), \quad \forall s, \quad (6.255)$$

the Corollary is proven. \square

Note that the upper bound $C(\Phi, \bar{N}) \leq \bar{C}$ holds independently of the input energy. However, for high values of squeezing it diverges and can even overcome the ultimate bound $g(\bar{N})$ (i.e. it becomes useless above a certain squeezing value). Nevertheless it is a valid bound even for the case $\tau < 0$, where now \bar{C} is given by Eq. (6.251) with the replacement $y \rightarrow -y$ (in this case the last inequality in Eq. (6.251) does not hold). We remark that for all \bar{N} the last inequality in Eq. (6.251) holds for all channels unitarily equivalent to Φ^{SQ} , i.e. for $\text{rank}(\mathbf{X}) = 2, \text{rank}(\mathbf{Y}) = 1$, since it is included in the even tighter bound presented in Eq. (6.230).

6.5. Bounds on the classical capacity

We can generalize several additional bounds that were found for the thermal channel Φ^{TH} in [GLMS13]. The bounds were obtained by maximizing the first term of the classical capacity and by obtaining a lower bound b on the second term, i.e.

$$C(\Phi, \bar{N}) \leq \max_{\mu: \hat{\rho}_{\text{in}} \in \mathcal{E}_{\bar{N}}} S(\Phi^{\text{TH}}[\hat{\rho}_{\text{in}}]) - \underbrace{\lim_{n \rightarrow \infty} \frac{1}{n} \min_{\mu} \int \mu(dx) S((\Phi^{\text{TH}})^{\otimes n}[\hat{\rho}_x])}_{\geq b} \quad (6.256)$$

where in total six bounds b are stated in [GLMS13]. We stated in the proof of Corollary 3 that the fiducial channel is equivalent to a thermal channel preceded by an anti-squeezer and followed by a squeezer [see Fig. 6.6 (b)]. The following squeezer does not change the output entropy. Furthermore, one can always undo the preceding squeezer because the bound b is not subject to an energy constraint. Therefore, any lower bound b on the minimal output entropy of the thermal channel is as well a lower bound on the minimal output entropy of the fiducial channel:

$$C(\Phi^{\text{F}}, \bar{N}) \leq \max_{\mu: \hat{\rho}_{\text{in}} \in \mathcal{E}_{\bar{N}}} S(\Phi^{\text{F}}[\hat{\rho}_{\text{in}}]) - b. \quad (6.257)$$

The first term of the bound stated in (6.257) is known to be maximized by a (Gaussian) thermal state carrying the total number of photons. It corresponds precisely to the first term of the one-shot Gaussian capacity (in case of the quantum water-filling solution) stated in Eq. (6.81), i.e.

$$\max_{\mu: \hat{\rho}_{\text{in}} \in \mathcal{E}_{\bar{N}}} S(\Phi^{\text{F}}[\hat{\rho}_{\text{in}}]) = g\left(|\tau|\bar{N} + y \cosh(2s) + \frac{|\tau| - 1}{2}\right) \equiv g(\bar{M}_{\text{out}}^{\text{qwf}}), \quad (6.258)$$

Corollary 1 states that $C(\Phi, \bar{N}) = C(\Phi^{\text{F}}, \bar{N})$. Therefore, any bound on the classical capacity of the fiducial channel Φ^{F} is also a bound on the classical capacity of an arbitrary channel Φ . By replacing b in Eq. (6.258) by bounds stated in [GLMS13] which are relevant¹¹ we obtain the following upper bounds on the capacity of Φ (we omit here for simplicity the explicit dependence on Φ and \bar{N}):

$$C \leq \bar{C}_{\text{EB}} = g(\bar{M}_{\text{out}}^{\text{qwf}}) - g\left(y - \frac{(1 + |\tau|)}{2}\right), \quad \tau > 0, y > \frac{1 + |\tau|}{2}, \quad (6.259)$$

$$C \leq \bar{C}_{\log 2} = g(\bar{M}_{\text{out}}^{\text{qwf}}) - \log_2(2y + \tau), \quad 0 \leq \tau \leq 1, \quad (6.260)$$

$$C \leq \bar{C}_{1/k} = g(\bar{M}_{\text{out}}^{\text{qwf}}) - \begin{cases} \frac{(k-1)}{k} g\left(\frac{k}{k-1} \left[y + \frac{\tau-1}{2}\right]\right), & \tau < 1/k, \\ \frac{(k-1)}{k} g\left(\frac{k}{k-1} \left[y - \frac{(1+\tau)}{2} + \frac{1}{k}\right]\right), & \tau \geq 1/k, \end{cases} \quad (6.261)$$

where inequality 6.261 holds for all integers $k > 1$. Equations (6.260) holds for the lossy channel $\tau \in [0, 1]$ as well as the classical additive noise channel $\tau = 1$ and inequality (6.259) only applies when the channel is entanglement breaking. Note that with increasing s those bounds become less and less tight because the second term does

¹¹We state only the dominant bounds here.

6. One-mode Gaussian channel

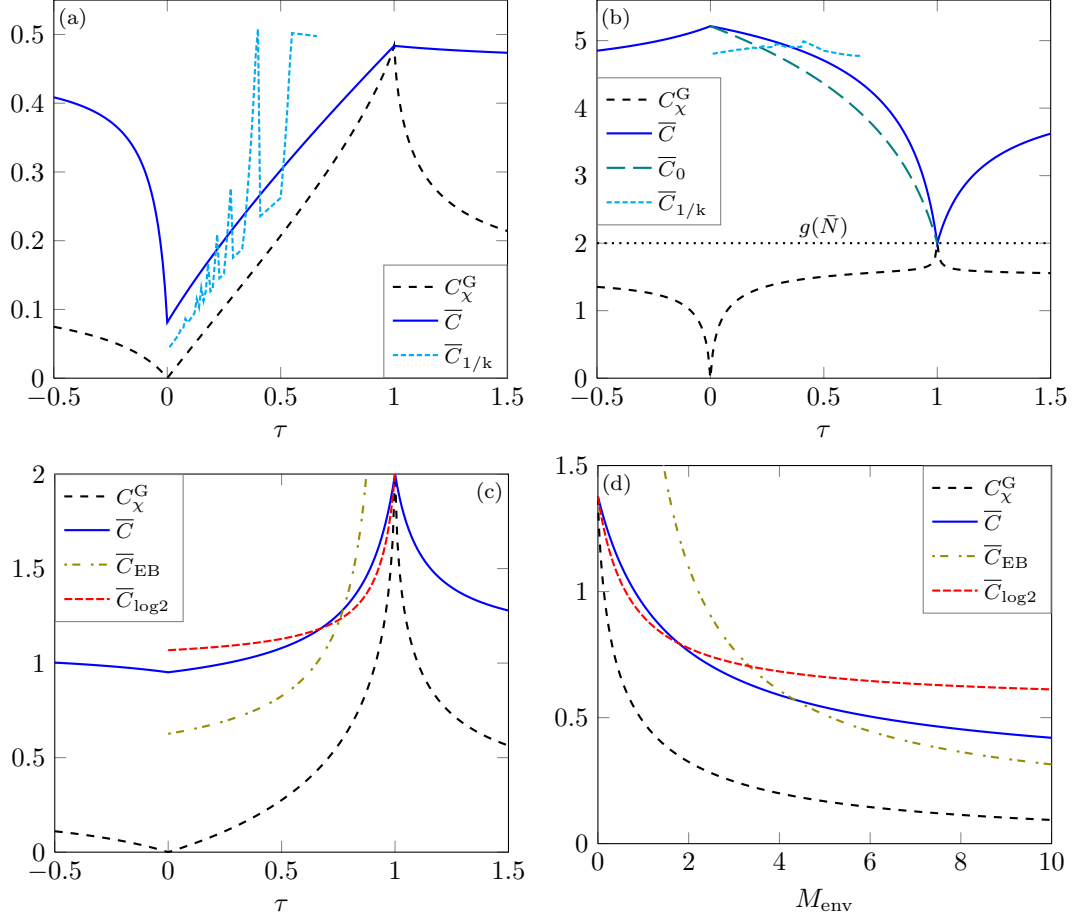


Figure 6.20.: Dominant upper bounds (to the classical capacity) and one-shot Gaussian capacity C_X^G : (a) vs. τ where $\bar{N} = 0.1, M_{\text{env}} = 0.1$ and $s = 0.1$; (b) vs. τ where $\bar{N} = 1, M_{\text{env}} = 1$ and $s = 2$; (c) vs. τ where $\bar{N} = 1, M_{\text{env}} = 10$ and $s = 0.5$; (d) vs. $M_{\text{env}} = y$, where $\bar{N} = 0.5, s = 0.5$ and $\tau = 1$ (classical additive noise channel). For (a)-(c) $\tau = 1$ corresponds to the perfect transmission channel.

6.5. Bounds on the classical capacity

not depend on s (and $g(\bar{M}_{\text{out}}^{\text{qwf}})$ increases with s). At last, we can state an additional (obvious) upper bound: for the case $\tau \in [0, 1]$ the classical capacity is always lower than the one of the lossy channel with pure vacuum noise stated in Eq. (6.87):

$$C(\Phi, \bar{N}) \leq \bar{C}_0 = g(\tau \bar{N} + (1 - \tau) \sinh^2 s). \quad (6.262)$$

We recall that the right hand side of the latter becomes the classical capacity if $\bar{N} \geq \bar{N}_{\text{thr}}$, where $y = (1 - \tau)/2$. Again, this quantity is a valid bound (for any \bar{N}) but becomes less and less tight with increasing s .

We compare the different bounds in Fig. 6.20, where we choose the parametrization $y = |1 - \tau|(M_{\text{env}} + 1/2)$ for $\tau \neq 1$ and $y = M_{\text{env}}$ for $\tau = 1$. For $\tau \leq 0$ and ($\tau > 1, y < (1 + \tau)/2$) even for the thermal channels our bound \bar{C} is the only one that exists to our knowledge. Interestingly, for $0 \leq \tau \leq 1$ in general all bounds are in competition as seen in Fig. 6.20. For high squeezing values the bounds diverge and are even outperformed by the trivial bound $C \leq g(\bar{N})$ as seen in Fig. 6.20 (b). This shows the need for bounds that do not diverge with increasing squeezing.

7. Multi-mode Gaussian channels

In this chapter we study the Gaussian capacity of multi-mode Gaussian channels with memory models previously discussed in Sec. 5.3.2. First, we obtain a solution that, equivalently to the single-mode case, is only valid above an input energy threshold. For input energies below the input energy threshold we discuss the solution in detail for the multi-mode classical additive noise channel.

7.1. Multi-mode Gaussian memory channel

The n -mode Gaussian memory channel $\Phi_M^{(n)}$ that we discuss in the following has zero displacement ($\mathbf{d}_{\text{env}} = 0$) and is defined by the following matrices (recall Sec. 5.3.2):

$$\mathbf{X}_M = \mathbf{X}_{\text{TH}} = \sqrt{|\tau|} \begin{pmatrix} \mathbb{I} & 0 \\ 0 & \text{sgn}(\tau)\mathbb{I} \end{pmatrix}, \quad \mathbf{Y}_M = \Theta_Y^\top \mathbf{Y}_\Lambda \Theta_Y, \quad (7.1)$$

where $\mathbf{Y}_\Lambda = \text{diag}(y_{q_1}, y_{q_2}, \dots, y_{q_n}, y_{p_1}, \dots, y_{p_n})$ and $\Theta_Y^\top \Theta_Y = \mathbb{I}$.¹ The output CM then reads

$$\mathbf{V}_{\text{out}} = \mathbf{X}_M \mathbf{V}_{\text{in}} \mathbf{X}_M + \Theta_Y^\top \mathbf{Y}_\Lambda \Theta_Y \quad (7.2)$$

$$= \Theta_Y^\top (\Theta_Y \mathbf{X}_M \mathbf{V}_{\text{in}} \mathbf{X}_M \Theta_Y^\top + \mathbf{Y}_\Lambda) \Theta_Y \quad (7.3)$$

$$= \Theta_Y^\top (\mathbf{X}_M \Theta_Y' \mathbf{V}_{\text{in}} \Theta_Y'^\top \mathbf{X}_M + \mathbf{Y}_\Lambda) \Theta_Y, \quad (7.4)$$

where we used in the last line the commutation relation $[\Theta_Y, \mathbf{X}_M] = [\mathbf{X}_M, \Theta_Y']$, where Θ_Y' is another rotation [see Eq. (6.103)]. Then Θ_Y' can be regarded as a reference phase and in addition the transformation Θ_Y at the output does not change the entropy. Thus, we conclude that

$$C_\chi^G(\Phi_M^{(n)}, n\bar{N}) = C_\chi^G(\Phi_\Lambda^{(n)}, n\bar{N}), \quad (7.5)$$

where $\Phi_\Lambda^{(n)}$ is defined by matrices $\mathbf{X} = \mathbf{X}_{\text{TH}}$ and $\mathbf{Y} = \mathbf{Y}_\Lambda$ (and zero displacement $\mathbf{d}_{\text{env}} = 0$). The map $\Phi_\Lambda^{(n)}$ can therefore be expressed as a tensor product of one-mode fiducial channels:

$$\Phi_\Lambda^{(n)} = \Phi_{(\tau, y_1, s_1)}^F \otimes \Phi_{(\tau, y_2, s_2)}^F \otimes \dots \otimes \Phi_{(\tau, y_n, s_n)}^F, \quad (7.6)$$

where

$$y_i = \sqrt{y_{q_i} y_{p_i}}, \quad s_i = \frac{1}{4} \ln \left(\frac{y_{q_i}}{y_{p_i}} \right). \quad (7.7)$$

¹In other words: we only consider those noise CM \mathbf{Y}_M which can be diagonalized by a passive symplectic operation given by matrix Θ_Y .

7. Multi-mode Gaussian channels

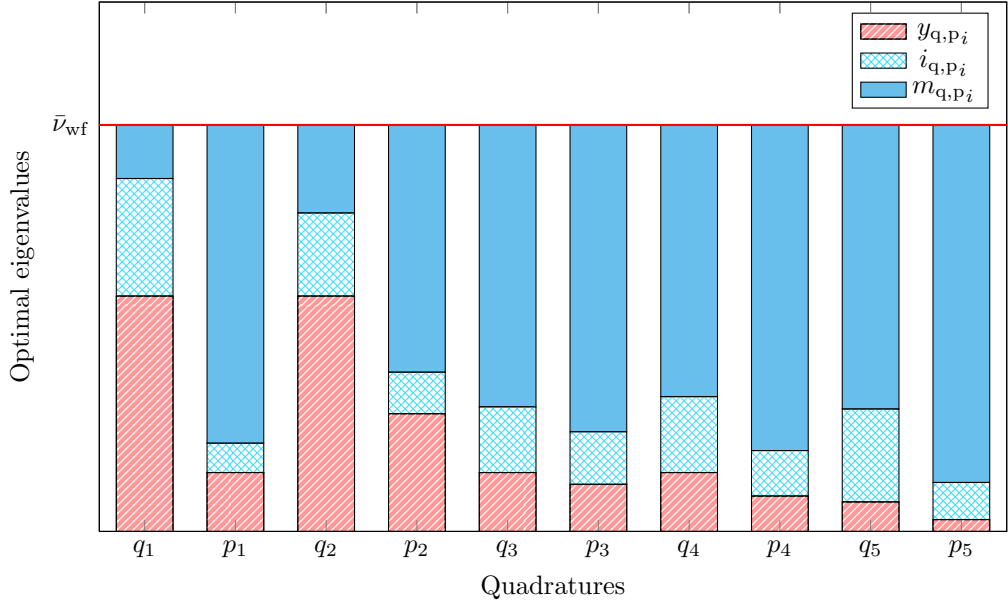


Figure 7.1.: Global quantum water-filling solution: the quantum water-filling solution is satisfied for all modes if $\bar{N} \geq \bar{N}_{\text{glthr}}$ (here depicted schematically for $\tau = 1$ and five modes). The common water-filling level is given by $\bar{\nu}_{\text{wf}}$.

In [LGM10] a multi-mode memory channel was studied, which was shown to be unitarily equivalent to a collection of lossy channels with different transmissivities, i.e. unitarily equivalent to the form stated Eq. (7.6) with

$$y_i = \frac{1 - \tau_i}{2}, \quad \tau_i \in [0, 1], \quad (7.8)$$

and $s_i = 0, \forall i$. For this channel an analytical expression for the classical capacity was found [using Eq. (5.86)] [LGM10]:

$$C = \frac{1}{2\pi} \int_0^{2\pi} dz g(\tau(z)\bar{N}(z)), \quad (7.9)$$

where $\bar{N}(z)$ is the optimal mean photon distribution found by solving a Lagrange multiplier problem.

7.2. Global quantum water-filling solution

Let us now study C_χ^G of the channel $\Phi_\Lambda^{(n)}$ where we first obtain a solution valid above an input energy constraint and then move on to the full input energy domain. Equivalently to the one-mode case we state the (possibly unphysical) upper bound:

$$C_\chi^G(\Phi_\Lambda^{(n)}, n\bar{N}) \leq \max_{\mathbf{V}_{\text{in}}, \mathbf{V}_{\text{mod}}} S(\bar{\mathbf{V}}_{\text{out}}) - \min_{\mathbf{V}_{\text{in}}} S(\mathbf{V}_{\text{out}}), \quad (7.10)$$

7.2. Global quantum water-filling solution

where $\bar{\mathbf{V}}_{\text{out}} = \mathbf{X}_{\text{TH}}\bar{\mathbf{V}}_{\text{in}}\mathbf{X}_{\text{TH}} + \mathbf{Y}_{\Lambda}$ is the CM of the modulated output state, with $\bar{\mathbf{V}}_{\text{in}} = \mathbf{V}_{\text{in}} + \mathbf{V}_{\text{mod}}$. In [Hir06] it was shown that the minimal output entropy of multi-mode Gaussian channels for multimode channels of the form stated in Eq. (7.6) is additive, i.e.

$$\min_{\mathbf{V}_{\text{in}}} S(\mathbf{V}_{\text{out}}) = \sum_{i=1}^n \min_{\mathbf{V}_{\text{in}i}} S(\mathbf{V}_{\text{out}i}), \quad (7.11)$$

where $\mathbf{V}_{\text{out}i}$ is the CM of the one-mode fiducial channel $\Phi_{(\tau, y_i, s_i)}^{\text{F}}$. Thus, instead of minimizing over all (possibly entangled) n -mode Gaussian input states it is sufficient to minimize over the individual input states, i.e. to minimize each individual term $S(\mathbf{V}_{\text{out}i})$. The minimum is achieved (for each fiducial channel) if one injects for each channel i a squeezed input state with CM $\mathbf{V}_{\text{in}i} = \text{diag}(i_{\text{q}i}, i_{\text{p}i})$, where (just like in the one-mode case, see Sec. 6.4.1)

$$\frac{i_{\text{q}i}}{i_{\text{p}i}} = \frac{y_{\text{q}i}}{y_{\text{p}i}}, \quad \forall i, \quad (7.12)$$

which together with the purity constraint $i_{\text{q}i}i_{\text{p}i} = 1/4$ yields

$$i_{\text{q}i} = \frac{1}{2}e^{2s_i} = \frac{1}{2}\sqrt{\frac{y_{\text{q}i}}{y_{\text{p}i}}}, \quad i_{\text{p}i} = \frac{1}{2}e^{-2s_i} = \frac{1}{2}\sqrt{\frac{y_{\text{p}i}}{y_{\text{q}i}}}, \quad \forall i. \quad (7.13)$$

Then, the output entropy reads

$$\min_{\mathbf{V}_{\text{in}}} S(\mathbf{V}_{\text{out}}) = \sum_{i=1}^n g\left(y_i + \frac{|\tau| - 1}{2}\right). \quad (7.14)$$

The first term in Eq. (7.10) is (again) maximized for a thermal state, i.e. if all modulated output states have the same number of thermal photons \bar{M}_{out} :

$$\bar{\mathbf{V}}_{\text{out}} = \left(\bar{M}_{\text{out}} + \frac{1}{2}\right) \mathbb{I}_{2n \times 2n}. \quad (7.15)$$

The latter is fulfilled if the quantum water-filling solution holds for all modes, i.e.

$$|\tau|(i_{\text{q}i} + m_{\text{q}i}) + y_{\text{q}i} = |\tau|(i_{\text{p}i} + m_{\text{p}i}) + y_{\text{p}i}, \quad \forall i. \quad (7.16)$$

This solutions is called *global quantum water-filling solution* (see Fig. 7.1) with water-filling level

$$\begin{aligned} \bar{\nu}_{\text{wf}} &= \bar{M}_{\text{out}} + \frac{1}{2} = \frac{1}{2n} \sum_{i=1}^n (y_{\text{q}i} + y_{\text{p}i}) + \underbrace{\frac{|\tau|}{2n} \sum_{i=1}^n (i_{\text{q}i} + i_{\text{p}i} + m_{\text{q}i} + m_{\text{p}i})}_{=|\tau|\text{Tr}[\bar{\mathbf{V}}_{\text{in}}]=|\tau|\bar{N}+\frac{|\tau|}{2}} \\ &= \frac{1}{2n} \sum_{i=1}^n (y_{\text{q}i} + y_{\text{p}i}) + |\tau|\bar{N} + \frac{|\tau|}{2}. \end{aligned} \quad (7.17)$$

7. Multi-mode Gaussian channels

In order to satisfy the solutions stated in Eqs. (7.14), (7.15) and (7.17) the (average) input energy \bar{N} needs to fulfill the inequality

$$\bar{N} \geq \bar{N}_{\text{glthr}} = \frac{1}{n} \sum_{i=1}^n \bar{N}_{\text{thri}} = \frac{1}{n} \sum_{i=1}^n \frac{1}{2} \left(\sqrt{\frac{y_{\text{qi}}}{y_{\text{pi}}}} + \frac{y_{\text{qi}} - y_{\text{pi}}}{|\tau|} - 1 \right), \quad (7.18)$$

where \bar{N}_{thri} is stated in Eq. (6.83) and we choose without loss of generality the convention $y_{\text{qi}} \geq y_{\text{pi}}, \forall i$.

Then we can express the Gaussian capacity of the channel $\Phi_{\Lambda}^{(n)}$ (and consequently of $\Phi_{\text{M}}^{(n)}$) for an input energy above the energy constraint:

Theorem 4. *The Gaussian capacity of the Gaussian memory channel Φ_{M} is given by*

$$\begin{aligned} C^{\text{G}}(\Phi_{\text{M}}, \bar{N}) &= C^{\text{G}}(\Phi_{\Lambda}, \bar{N}) \\ &= g \left(|\tau| \bar{N} + \frac{1}{2n} \sum_{i=1}^n (y_{\text{qi}} + y_{\text{pi}}) + \frac{|\tau| - 1}{2} \right) - \frac{1}{n} \sum_{i=1}^n g \left(y_i + \frac{|\tau| - 1}{2} \right), \quad \bar{N} \geq \bar{N}_{\text{glthr}}. \end{aligned} \quad (7.19)$$

Proof. For input energy $\bar{N} \geq \bar{N}_{\text{glthr}}$ we showed above that the upper bound in Eq. (7.10) is achievable. Since the minimum output entropy of the channel $\Phi_{\Lambda}^{(n)}$ was proven to be additive it follows that (for $\bar{N} \geq \bar{N}_{\text{glthr}}$) the one-shot Gaussian capacity is additive. Then, injecting the solution stated in Eqs. (7.14), (7.15) and (7.17) in Eq. (7.10) leads to the Gaussian capacity stated in Eq. (7.19). \square

Let us now derive the limiting expression in the case of an infinite number of uses. In this case the solutions for the optimal input spectra read

$$|\tau| [i_{\text{q}}(x) + m_{\text{q}}(x)] + y_{\text{q}}(x) = |\tau| [i_{\text{p}}(x) + m_{\text{p}}(x)] + y_{\text{p}}(x), \quad i_{\text{q}}(x) = \frac{1}{2} \sqrt{\frac{y_{\text{q}}(x)}{y_{\text{p}}(x)}}, \forall x \quad (7.20)$$

The limit of the expression stated in Eq. (7.19) then reads

$$\begin{aligned} C^{\text{G}}(\Phi_{\Lambda}, \bar{N}) &= g \left(|\tau| \bar{N} + \frac{1}{2|A|} \int_{x \in A} dx [y_{\text{q}}(x) + y_{\text{p}}(x)] + \frac{|\tau| - 1}{2} \right) \\ &\quad - \frac{1}{|A|} \int_{x \in A} dx g \left(\sqrt{y_{\text{q}}(x) y_{\text{p}}(x)} + \frac{|\tau| - 1}{2} \right), \quad \bar{N} \geq \bar{N}_{\text{glthr}}, \end{aligned} \quad (7.21)$$

where $y_{\text{q}}(x), y_{\text{p}}(x)$ are the noise eigenvalue spectra. For noise spectra $y_{\text{q}}(x) \geq y_{\text{p}}(x), \forall x$, the input energy threshold \bar{N}_{glthr} in this limit becomes

$$\bar{N}_{\text{glthr}} = \frac{1}{2|A|} \int_{x \in A} dx \left(\sqrt{\frac{y_{\text{q}}(x)}{y_{\text{p}}(x)}} + \frac{y_{\text{q}}(x) - y_{\text{p}}(x)}{|\tau|} - 1 \right). \quad (7.22)$$

In the following we will compare the optimal transmission rate C^G with suboptimal rates. One of them is the *coherent rate* R_{coh} , i.e. the optimal transmission rate when restricted to coherent states at the input. We define this quantity equivalently to Eq. (5.90), but unlike in the case of the one-shot Gaussian capacity it is already normalized by n :

$$R_{\text{coh}}(\Phi, \bar{N}) = \frac{1}{n} \max_{\mathbf{V}_{\text{mod}}} \left\{ \chi^G(\{\nu_{\text{out}i}, \bar{\nu}_{\text{out}i}\}) \mid \text{Tr}[\mathbf{V}_{\text{mod}}] \leq 2n\bar{N} \right\}, \quad (7.23)$$

$$= \frac{1}{n} \left(\max_{\mathbf{V}_{\text{mod}}} [S(\bar{\mathbf{V}}_{\text{out}})] - S(\mathbf{V}_{\text{out}}) \right), \quad (7.24)$$

where the input covariance matrix is fixed² to $\mathbf{V}_{\text{in}} = \mathbb{I}/2$ and thus, only the first term is maximized. R_{coh} is easily calculated: the restriction to coherent input states leads to the fixed output CM

$$\mathbf{V}_{\text{out}} = \frac{|\tau|}{2} \mathbb{I} + \mathbf{Y}, \quad (7.25)$$

i.e. it is simply given by the noise spectra shifted by the variance of the vacuum. Thus, we obtain

$$\frac{1}{n} S(\mathbf{V}_{\text{out}}) = \frac{1}{n} \sum_{i=1}^n g \left(\sqrt{\left(y_{\text{q}i} + \frac{|\tau|}{2} \right) \left(y_{\text{p}i} + \frac{|\tau|}{2} \right)} - \frac{1}{2} \right). \quad (7.26)$$

The entropy of the first term reads

$$\frac{1}{n} S(\bar{\mathbf{V}}_{\text{out}}) = \frac{1}{n} \sum_{i=1}^n g \left(\bar{\nu}_{\text{out}i} - \frac{1}{2} \right). \quad (7.27)$$

This term can be maximized under the common energy constraint by the method of Lagrange multipliers, which leads to the same solution as in the case of classical Gaussian channels (recall Sec. 2.3.2), i.e. the (classical) water-filling solution stated in Eq. (2.19) satisfied for all quadratures, i.e.

$$\begin{aligned} m_{\text{q}i} &= (\bar{\nu}_{\text{wf}} - \bar{\nu}_{\text{q}i})^+, \\ m_{\text{p}i} &= (\bar{\nu}_{\text{wf}} - \bar{\nu}_{\text{p}i})^+, \end{aligned} \quad (7.28)$$

where the water-filling level $\bar{\nu}_{\text{wf}}$ is given by Eq. (7.17). This means quadratures that are too noisy will be excluded from information transmission, just as in the case of the classical water-filling solution. The coherent rate is thus given by $R_{\text{coh}} = [S(\bar{\mathbf{V}}_{\text{out}}) - S(\mathbf{V}_{\text{out}})]/n$, where the solutions stated in Eqs. (7.26) and (7.28) have to be injected in both terms.

A particular solution is given by a global water-filling, i.e. if $\bar{\nu}_{\text{q}i} = \bar{\nu}_{\text{p}i}, \forall i$, which is simplified in this case to

$$|\tau| m_{\text{q}i} + y_{\text{q}i} = |\tau| m_{\text{p}i} + y_{\text{p}i}, \quad \forall i. \quad (7.29)$$

²For this reason the variance of the vacuum is removed from the energy constraint

7. Multi-mode Gaussian channels

Then all modulated output states are given by the same thermal state (just as in the case of the global quantum water-filling) such that the first term in R_{coh} becomes equal to the first term of C^{G} stated in Eq. (7.19), i.e.

$$R_{\text{coh}}(\Phi, \bar{N}) = g \left(|\tau| \bar{N} + \frac{1}{2n} \sum_{i=1}^n (y_{\text{q}_i} + y_{\text{p}_i}) + \frac{|\tau| - 1}{2} \right) - \frac{1}{n} \sum_{i=1}^n g \left(\sqrt{\left(y_{\text{q}_i} + \frac{|\tau|}{2} \right) \left(y_{\text{p}_i} + \frac{|\tau|}{2} \right)} - \frac{1}{2} \right), \quad \bar{N} \geq \bar{N}_{\text{cohthr}} \quad (7.30)$$

with

$$\bar{N}_{\text{cohthr}} = \frac{1}{n} \sum_{i=1}^n \frac{y_{\text{q}_i} - y_{\text{p}_i}}{2|\tau|}, \quad (7.31)$$

where we choose without loss of generality the convention $y_{\text{q}_i} \geq y_{\text{p}_i}, \forall i$. The threshold \bar{N}_{cohthr} is obtained using Eq. (7.18) and substituting $\frac{1}{2} \sqrt{\frac{y_{\text{q}_i}}{y_{\text{p}_i}}} = i_{\text{q}_i} = \frac{1}{2}$ (i.e. the input states are all fixed to coherent states).

7.3. Full solution for the classical additive noise channel ($\tau = 1$)

For input energies $\bar{N} < \bar{N}_{\text{glthr}}$ the global quantum water-filling solution can no longer be satisfied and we require again another treatment. The first problem we encounter is that Eq. (7.11) does not help us to calculate the one-shot Gaussian capacity. The reason is that we have not enough energy to realize the maximum of the first term and at the same time the minimum of the second term. In fact, it is optimal to neither maximize the first term nor to minimize the second one, and as a consequence to maximize the difference (as in the one-mode case). For this reason the one-shot Gaussian capacity of the multi-mode channel $\Phi_{\Lambda}^{(n)}$ is in general greater or equal than the sum of individual one-shot Gaussian capacities:

$$C_{\chi}^{\text{G}}(\Phi_{\Lambda}^{(n)}, n\bar{N}) \geq \max_{\bar{N}_i} \sum_{i=1}^n C_{\chi}^{\text{G}}(\Phi_{(\tau, y_i, s_i)}^{\text{F}}, \bar{N}_i), \quad n\bar{N} = \sum_{i=1}^n \bar{N}_i, \quad \bar{N} < \bar{N}_{\text{glthr}}. \quad (7.32)$$

However, for simplicity we denote in the following the right hand side of Eq. (7.32) by $C_{\chi}^{\text{G}}(\Phi_{\Lambda}^{(n)}, n\bar{N})$. For this reason the one-shot Gaussian capacity $C_{\chi}^{\text{G}}(\Phi_{\Lambda}^{(n)}, n\bar{N}), \bar{N} < \bar{N}_{\text{glthr}}$, obtained in the following must be regarded as a *lower bound on the one-shot Gaussian capacity*.

According to the right hand side of Eq. (7.32) the problem of finding $C_{\chi}^{\text{G}}(\Phi_{\Lambda}^{(n)}, n\bar{N})$ is reduced to finding the *optimal input energy distribution* \bar{N}_i . This problem can again be solved with the method of Lagrange multipliers where we now obtain a system of n equations with a common input energy constraint \bar{N} . The fact that the solution of the system of equations indeed maximizes χ^{G} follows from the results on convex separable minimization subject to bounded variables found in [Ste01].

7.3. Full solution for the classical additive noise channel ($\tau = 1$)

We treat now the solution in details for the case $\tau = 1$ (i.e. the classical additive noise channel) and use for compactness the following Lagrangian:

$$\mathcal{L} = \sum_{i=1}^n g(\bar{M}_{\text{out}i}) - g(M_{\text{out}i}) - \mu \left(\sum_{i=1}^n (i_{\text{q}i} + i_{\text{p}i} + m_{\text{q}i} + m_{\text{p}i}) - \bar{\lambda} \right), \quad (7.33)$$

where the total input energy is expressed by

$$\bar{\lambda} = \sum_{i=1}^n \bar{\lambda}_i, \quad \bar{\lambda}_i = 2\bar{N}_i + 1 = i_{\text{q}i} + i_{\text{p}i} + m_{\text{q}i} + m_{\text{p}i}, \quad (7.34)$$

and the input energy distribution is given by $\{\bar{\lambda}_i\}$. The total output energy equivalently is defined as

$$\bar{\lambda}_{\text{out}} = \bar{\lambda} + \sum_{i=1}^n y_{\text{q}i} + y_{\text{p}i}. \quad (7.35)$$

The system of equations we need to solve is then given by

$$\begin{aligned} \nabla_i \mathcal{L} &= 0, \quad \forall i, \\ \nabla_i &= \left(\frac{\partial}{\partial i_{\text{q}i}}, \frac{\partial}{\partial m_{\text{q}i}}, \frac{\partial}{\partial m_{\text{p}i}} \right)^\top. \end{aligned} \quad (7.36)$$

Note that we obtain a maximum by the solution of Lagrange multipliers provided that for the one-mode case χ^{G} is a concave function of $\bar{\lambda}$ on the solution. We present this proof in Appendix D.3.3.

For the following it will be useful to relate the multiplier μ explicitly to the input energy $\bar{\lambda}$. We derive the relations for the one-mode case ($n = 1$) and then apply them to the solution of the general, multi-mode case. The solution to the one-mode case (previously derived in Appendix D.1) for $\tau = 1$ and the noise parametrization $\mathbf{Y} = \text{diag}(y_{\text{q}}, y_{\text{p}})$ reads

$$\frac{g'(\bar{\nu}_{\text{out}} - \frac{1}{2})}{\bar{\nu}_{\text{out}}} (\bar{\nu}_{\text{p}} - \bar{\nu}_{\text{q}}) = \frac{g'(\nu_{\text{out}} - \frac{1}{2})}{\nu_{\text{out}}} \left(y_{\text{p}} - \frac{y_{\text{q}}}{4i_{\text{q}}^2} \right). \quad (7.37)$$

Given the Lagrangian stated in Eq. (7.33) we find the following solution for the Lagrange multiplier μ (equal to $\bar{\beta}$ in Eq. (D.10) up to a factor 2):

$$\mu = \frac{g'(\bar{M}_{\text{out}})}{2(\bar{M}_{\text{out}} + \frac{1}{2})} \bar{\nu}_{\text{q}} = \frac{g'(\bar{\nu}_{\text{out}} - \frac{1}{2})}{2\bar{\nu}_{\text{out}}} \bar{\nu}_{\text{q}}. \quad (7.38)$$

For $\bar{\lambda} \geq \bar{\lambda}_{\text{thr}}$, where

$$\bar{\lambda}_{\text{thr}} = \sqrt{\frac{y_{\text{q}}}{y_{\text{p}}}} + y_{\text{q}} - y_{\text{p}}, \quad (7.39)$$

the quantum water-filling solution holds which for $\tau = 1$ is now given by [see Eq. (6.76)]

$$i_{\text{q}} + m_{\text{q}} + y_{\text{q}} = i_{\text{p}} + m_{\text{p}} + y_{\text{p}}, \quad (7.40)$$

7. Multi-mode Gaussian channels

where the optimal input state is given by [see Eq. (7.13)]

$$i_q = \frac{1}{2} \sqrt{\frac{y_q}{y_p}}, \quad i_p = \frac{1}{2} \sqrt{\frac{y_p}{y_q}}. \quad (7.41)$$

In addition, the water-filling level simplifies according to Eq. (6.86) to

$$\bar{\nu}_{\text{wf}} = \bar{\nu}_q = \bar{\nu}_p = \frac{\bar{\lambda} + y_q + y_p}{2}. \quad (7.42)$$

Inserting $\bar{\nu}_{\text{out}} = \bar{\nu}_{\text{wf}}$ in Eq. (7.38) links the multiplier to the water-filling level, i.e.

$$\mu = \frac{g'(\bar{\nu}_{\text{wf}} - \frac{1}{2})}{2}, \quad \bar{\nu}_{\text{wf}} = \frac{1}{2} \coth(\mu \ln 2), \quad \bar{\lambda} \geq \bar{\lambda}_{\text{thr}}. \quad (7.43)$$

Since $g'(x)$ is a monotonically decreasing function it follows that for $\bar{\lambda} \geq \bar{\lambda}_{\text{thr}}$ the multiplier μ is a monotonously decreasing function of $\bar{\lambda}$. For $\bar{\lambda} < \bar{\lambda}_{\text{thr}}$ we prove it in Lemma 7 in Appendix D.3.2. This property allows us to relate $\bar{\lambda}_{\text{thr}}$ via Eq. (7.43) to

$$\mu_{\text{thr}} = \frac{1}{2} g' \left(\frac{1}{2} (\bar{\lambda}_{\text{thr}} + y_q + y_p) - \frac{1}{2} \right), \quad (7.44)$$

such that if $\bar{\lambda} \geq \bar{\lambda}_{\text{thr}}$, then the corresponding $\mu \leq \mu_{\text{thr}}$. Moreover, for the lowest input energy $\bar{\lambda} = 1$ (i.e. $\bar{N} = 0$) we can define [using Eq. (7.38)] an upper bound μ_0 for all possible values of μ that correspond to $\bar{\lambda} > 1$, that reads

$$\mu_0 = \frac{1}{2} g' \left(\sqrt{\left(y_q + \frac{1}{2} \right) \left(y_p + \frac{1}{2} \right)} - \frac{1}{2} \right) \sqrt{\frac{y_q + \frac{1}{2}}{y_p + \frac{1}{2}}}. \quad (7.45)$$

Note that even for $\bar{\lambda} < \bar{\lambda}_{\text{thr}}$ one can consider $\bar{\nu}_{\text{wf}}$ in Eq. (7.43) as a “virtual” water-filling level which links all modes together (see an example further below in Fig. 7.2).

In general, the maximum of the Lagrangian given in Eq. (7.33) corresponds to a partition of n modes into three different sets, corresponding to one of three types of input energy distributions within each mode: the case of a quantum water-filling solution, the case of one vanishing modulation eigenvalue, or the case when *both modulation eigenvalues vanish* and the mode does not participate in information transmission (i.e., unmodulated vacuum is sent). We denote the corresponding sets by: \mathcal{N}_3 , \mathcal{N}_2 and \mathcal{N}_1 . Furthermore, the number of modes in the sets is defined as $n^{(1)}$, $n^{(2)}$ and $n^{(3)}$, with $n = n^{(1)} + n^{(2)} + n^{(3)}$. In addition, we denote the input energies per set by $\bar{\lambda}^{(1)}$, $\bar{\lambda}^{(2)}$, $\bar{\lambda}^{(3)}$, where

$$\bar{\lambda}^{(1)} = \sum_{i \in \mathcal{N}_1} \bar{\lambda}_i, \quad \bar{\lambda}^{(2)} = \sum_{i \in \mathcal{N}_2} \bar{\lambda}_i, \quad \bar{\lambda}^{(3)} = \sum_{i \in \mathcal{N}_3} \bar{\lambda}_i, \quad (7.46)$$

which sum up to the total input energy $\bar{\lambda}$.

7.3. Full solution for the classical additive noise channel ($\tau = 1$)

Set \mathcal{N}_3 : Modes with water-filling solution

For all modes that belong to \mathcal{N}_3 the quantum water-filling solution stated in Eq. (7.40) is satisfied. This means that the input energy allocated to each mode cannot be lower than its corresponding energy threshold, i.e.

$$\bar{\lambda}_i \geq \bar{\lambda}_{\text{thri}}, \quad i \in \mathcal{N}_3, \quad (7.47)$$

where $\bar{\lambda}_{\text{thri}}$ reads as in Eq. (7.39) ($\forall i$). Then for all $i \in \mathcal{N}_3$ the energy equipartition (7.40) holds. Moreover, Eq. (7.43) guarantees that $\bar{\nu}_{\text{wf}}$ is the common water-filling level for all modes due to the common Lagrange multiplier μ , which is a monotonous function of $\bar{\nu}_{\text{wf}}$, which now reads

$$\bar{\nu}_{\text{wf}} = \bar{\nu}_{\text{qi}} = \bar{\nu}_{\text{pi}} = \frac{\bar{\lambda}_{\text{out}}^{(3)}}{2n^{(3)}}, \quad i \in \mathcal{N}_3, \quad (7.48)$$

where $\bar{\lambda}_{\text{out}}^{(3)}$ is the total energy at the output of the modes belonging to set \mathcal{N}_3 .

As the partition of the input energy between the modes is *a priori* not known the distribution of the modes between the sets is also not defined. However, we can determine whether a particular mode belongs to set \mathcal{N}_3 using the Lagrange multiplier μ . This is possible, because as mentioned before, μ is a monotonically decreasing function of the input energy $\bar{\lambda}$. For $\bar{\lambda}_i \geq \bar{\lambda}_{\text{thri}}$ we have $\mu \leq \mu_{\text{thri}}$ [see (7.44)], where μ_{thri} depends only on the noise eigenvalues of mode i . Then we can formalize the definition of \mathcal{N}_3 using μ_{thri} as

$$\mathcal{N}_3 = \{i \mid \mu_{\text{thri}} \geq \mu\}. \quad (7.49)$$

If $\mu_{\text{thri}} \geq \mu$ for all i then the set \mathcal{N}_3 contains all modes and we have

$$\bar{\lambda}^{(3)} = \bar{\lambda}. \quad (7.50)$$

In this case, Eqs. (7.40), (6.84), and (7.48) determine the global quantum water-filling solution (which we stated for the general case in Sec. 7.2) with

$$\bar{\nu}_{\text{wf}} = \frac{\bar{\lambda}_{\text{out}}}{2n}, \quad (7.51)$$

and

$$\nu_{\text{out}i} = \sqrt{y_{\text{qi}}y_{\text{pi}}} + \frac{1}{2}. \quad (7.52)$$

If the condition (7.47) is not satisfied for at least one mode, then this solution has no physical meaning because it will lead to negative values of some modulation eigenvalues.

Set \mathcal{N}_1 : Modes excluded from information transmission

Modes for which both modulation eigenvalues are 0 do not contribute to the Holevo quantity or, consequently to the information transmission. The zero modulation eigenvalues $m_{\text{qi}} = m_{\text{pi}} = 0$, $i \in \mathcal{N}_1$ imply

$$\bar{\nu}_{\text{qi}} = \nu_{\text{qi}}, \quad \bar{\nu}_{\text{pi}} = \nu_{\text{pi}}, \quad i \in \mathcal{N}_1. \quad (7.53)$$

7. Multi-mode Gaussian channels

Obviously if the mode is not modulated there is no reason to spend input energy on the squeezing of this mode, which results in the vacuum state being the optimal input state

$$i_{q_i} = i_{p_i} = \frac{1}{2}, \quad i \in \mathcal{N}_1. \quad (7.54)$$

This is consistent with (7.37) from which we obtain Eq. (7.54) for $\bar{\lambda}_i = 1$.

In order to deduce the set of modes that are excluded from information transmission we can use the threshold value μ_{0_i} defined in Eq. (7.45) which corresponds to $\bar{\lambda}_i = 1$ (vacuum energy)

$$\mathcal{N}_1 = \{i \mid \mu \geq \mu_{0_i}\}.$$

Set \mathcal{N}_2 : Single-quadrature modulated modes

For the modes for which $1 < \bar{\lambda} < \bar{\lambda}_{\text{thr}_i}$ the water-filling solution no longer holds. We have to set the modulation eigenvalue of the noisier quadrature to 0 in the same way as in the one-mode case. Again, as in the one mode case we assume that for each mode i the q -quadrature is noisier than the p -quadrature. We can do this without loss of generality because, first, for a one-mode channel a swap of the noise quadratures does not change C_χ^G , and second, C_χ^G of the discussed multimode channel is assumed to be additive. Then we have to set the modulation of the q -quadrature for all modes belonging to set \mathcal{N}_2 to 0, i.e.,

$$m_{q_i} = 0, \quad i \in \mathcal{N}_2. \quad (7.55)$$

This implies

$$\bar{v}_{q_i} = v_{q_i}, \quad i \in \mathcal{N}_2. \quad (7.56)$$

With the functions μ_{thr_i} and μ_{0_i} defined in (7.44), (7.45) we can simply define this set, i.e.,

$$\mathcal{N}_2 = \{i \mid \mu_{\text{thr}_i} < \mu < \mu_{0_i}\}. \quad (7.57)$$

The eigenvalues that solve the optimization problem for the modes of this set are found using Eq. (7.37), (7.38).

We note that both, μ_{0_i} and μ_{thr_i} depend only on the noise eigenvalues. Therefore, the partition into the three sets is completely determined by only one parameter μ . Furthermore, we recall that μ is the common parameter which enters the equations for sets $\mathcal{N}_2, \mathcal{N}_3$.

Algorithm for arbitrary number of modes

Finite number of modes

Recall that the solution of the problem for n modes is given by the optimal distribution of the input energy between the modes. The optimal energy distribution within one mode depends on its corresponding set, which is given by the noise spectrum and the global parameter μ .

7.3. Full solution for the classical additive noise channel ($\tau = 1$)

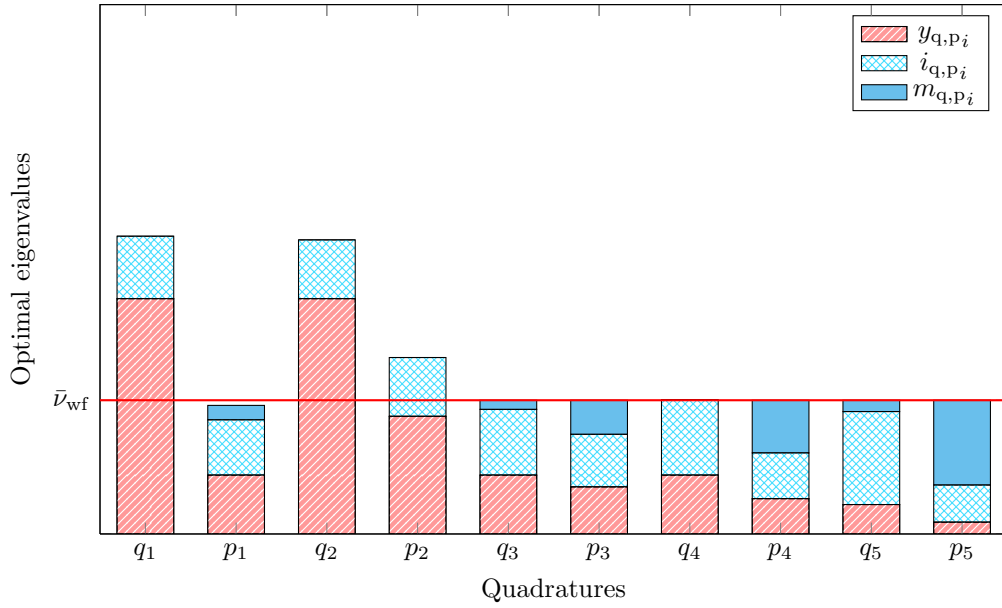


Figure 7.2.: Solution (with $\tau = 1$) for input energies $\bar{N} < \bar{N}_{\text{glthr}}$ and five noisy channels: channel 2 is in set \mathcal{N}_1 (completely excluded from information transmission), channels 1 and 4 are in set \mathcal{N}_2 (the noisier quadrature is not modulated) and channels 3 and 5 are in set \mathcal{N}_3 (quantum water-filling solution can be satisfied). Here, $\bar{\nu}_{\text{wf}}$ is the “virtual” water-filling level as defined in Eq. (7.43). We visualized the common Lagrange multiplier, i.e. the common inverse temperature in Fig. 7.3.

7. Multi-mode Gaussian channels

Now we present the algorithm that allows us to find the solution of our optimization problem. First, we further develop the equations that correspond to modes of set \mathcal{N}_2 . We call the right-hand side of Eq. (7.37)

$$f(i_{q_i}) \equiv \frac{g'(\nu_{\text{out}i} - \frac{1}{2})}{2\nu_{\text{out}i}} \left(v_{p_i} - \frac{i_{p_i}}{i_{q_i}} v_{q_i} \right). \quad (7.58)$$

We note that for given noise eigenvalues f is a function of only one independent variable i_{q_i} . Using the definition of $\bar{\lambda}_i$ (see (7.34)) and the fact that, for the modes belonging to the second set $m_{q_i} = 0$, we rewrite

$$\bar{v}_{p_i} - \bar{v}_{q_i} = \bar{\lambda}_i - 2i_{q_i} - y_{q_i} + y_{p_i}. \quad (7.59)$$

Furthermore, from (7.38) we express

$$\frac{g'(\bar{\nu}_{\text{out}i} - \frac{1}{2})}{2\bar{\nu}_{\text{out}i}} = \frac{\mu}{\bar{v}_{q_i}}. \quad (7.60)$$

Then we insert Eqs. (7.59) and (7.60) together into the left hand side of Eq. (7.37) and obtain with $\bar{v}_{q_i} = v_{q_i}$ and (7.58)

$$\bar{\lambda}_i(i_{q_i}, \mu) = \frac{v_{q_i}}{\mu} f(i_{q_i}) + 2i_{q_i} + y_{q_i} - y_{p_i}. \quad (7.61)$$

This means that we have established a relation between the optimal input eigenvalues i_{q_i} , $i \in \mathcal{N}_2$, the global parameter μ and the optimal input energy distribution $\bar{\lambda}_i$ between the modes in \mathcal{N}_2 . Using Eq. (7.61) and definition (7.34) we can now eliminate variable $\bar{\lambda}_i$ from Eq. (7.59). Thus, we obtain a transcendental equation that determines the optimal input eigenvalues i_{q_i} as an implicit function of μ :

$$g' \left(v_{q_i} \sqrt{1 + \frac{f(i_{q_i})}{\mu}} - \frac{1}{2} \right) = 2\mu \sqrt{1 + \frac{f(i_{q_i})}{\mu}}. \quad (7.62)$$

Now we are ready to calculate the input energies of all three sets for a given μ . First, we evaluate the total input energy of “water-filling” modes, i.e. modes in \mathcal{N}_3 . Using Eqs. (7.34), (7.46) and (7.48) we deduce the total input energy used for the modes in \mathcal{N}_3 as a function of μ

$$\bar{\lambda}^{(3)}(\mu) = \sum_{i \in \mathcal{N}_3} (2\bar{\nu}_{\text{wf}}(\mu) - y_{q_i} - y_{p_i}). \quad (7.63)$$

Second, the total (vacuum) energy of modes belonging to \mathcal{N}_1 , using (7.45), reads

$$\bar{\lambda}^{(1)}(\mu) = \sum_{i \in \mathcal{N}_1} 1 = n^{(1)}. \quad (7.64)$$

7.3. Full solution for the classical additive noise channel ($\tau = 1$)

Functions $\bar{\lambda}^{(1)}(\mu)$ and $\bar{\lambda}^{(3)}(\mu)$ depend on μ through $\mathcal{N}_1, \mathcal{N}_3$ and $\bar{\nu}_{\text{wf}}$, which are only functions of μ and the noise eigenvalues. The total input energy for modes in \mathcal{N}_2 is the sum

$$\bar{\lambda}^{(2)}(\mu) = \sum_{i \in \mathcal{N}_2} \bar{\lambda}_i(i_{\text{qi}}, \mu). \quad (7.65)$$

Now we apply the overall input energy constraint

$$\bar{\lambda}^{(1)}(\mu) + \bar{\lambda}^{(2)}(\mu) + \bar{\lambda}^{(3)}(\mu) = \bar{\lambda}. \quad (7.66)$$

Thus, Eq. (7.66) is a closed equation depending on μ which we can be solved by iterations. The solution of the system of equations stated in Eq. (7.62) together with Eq. (7.66) provides us the $n^{(2)}$ optimal eigenvalues i_{qi} and μ , which determine all other eigenvalues. Once the optimal spectra are obtained one can calculate the one-shot Gaussian capacity of the n -mode channel $\Phi_{\Lambda}^{(n)}$ (where $\tau = 1$), i.e. Eq. (7.32) simplifies to

$$C_{\chi}^{\text{G}}(\Phi_{\Lambda}^{(n)}, n\bar{N}) = \left\{ \sum_{i=1}^n \left[g\left(\bar{\nu}_{\text{out}i} - \frac{1}{2}\right) - g\left(\nu_{\text{out}i} - \frac{1}{2}\right) \right] \left| \bar{\lambda}^{(1)}(\mu) + \bar{\lambda}^{(2)}(\mu) + \bar{\lambda}^{(3)}(\mu) = \bar{\lambda} \right. \right\}, \quad (7.67)$$

where here $\bar{\nu}_{\text{out}i}, \nu_{\text{out}i}$ contain the obtained optimal input and modulation spectra. We plot the optimal eigenvalue distribution for an example in Fig. 7.2 where all three sets $\mathcal{N}_1, \mathcal{N}_2$ and \mathcal{N}_3 are occupied.

Let us take a look at the physical interpretation of the solution. In the same way as for the one-mode solution we choose the modified Lagrangian stated previously in Eq. (6.180)³

$$\mathcal{L}' = \sum_{i=1}^n g(\bar{M}_{\text{out}i}) - g(M_{\text{out}i}) - \frac{\bar{\beta}_{\text{out}}}{\ln 2} \left(\bar{N}_{\text{out}} - \frac{1}{2n} \text{Tr}[\bar{\mathbf{V}}_{\text{out}}] - \frac{1}{2} \right), \quad (7.68)$$

where $M_{\text{out}i}$ and $\bar{M}_{\text{out}i}$ can be expressed in terms of the $2n$ symplectic eigenvalues $\nu_{\text{out}i}, \bar{\nu}_{\text{out}i}$, respectively, as

$$M_{\text{out}i} = \nu_{\text{out}i} - \frac{1}{2}, \quad \bar{M}_{\text{out}i} = \bar{\nu}_{\text{out}i} - \frac{1}{2}. \quad (7.69)$$

We recall that the parameter $\bar{\beta}_{\text{out}}$ (and hence μ) can indeed be regarded as a common inverse temperature, since the solution satisfies

$$\frac{\partial \mathcal{L}'}{\partial \bar{N}_{\text{out}}} = \frac{\partial g(\bar{M}_{\text{out}i})}{\partial \bar{N}_{\text{out}}} - \frac{\bar{\beta}_{\text{out}}}{\ln 2} = 0, \quad \forall i, \quad (7.70)$$

from which it follows that

$$\ln 2 \frac{\partial g(\bar{M}_{\text{out}i})}{\partial \bar{N}_{\text{out}}} = \bar{\beta}_{\text{out}}, \quad \forall i. \quad (7.71)$$

³Since the noise distribution is fixed (it is a part of the given channel parameters) imposing an output energy constraint \bar{N}_{out} is equivalent to imposing an input energy constraint constraint \bar{N} .

7. Multi-mode Gaussian channels

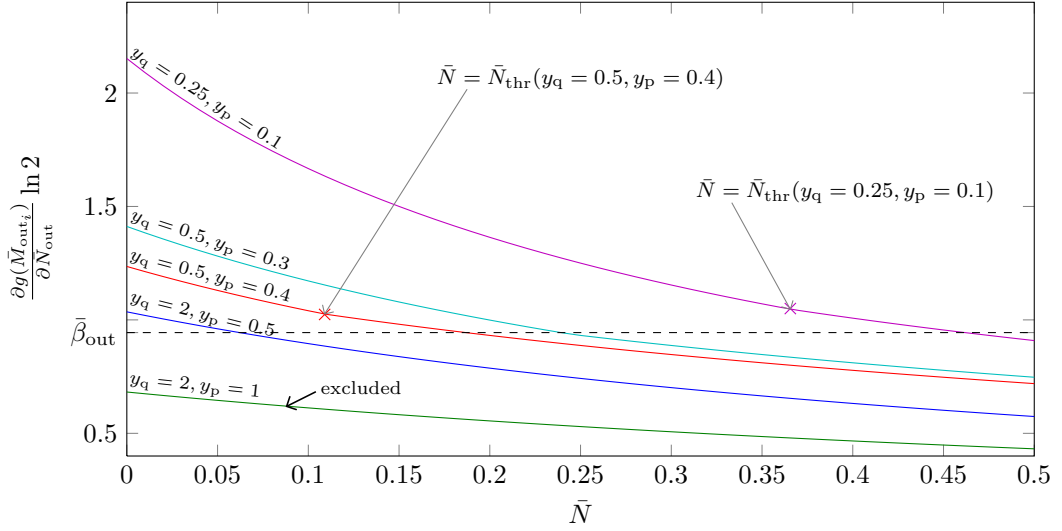


Figure 7.3.: Solution for $\bar{N} < \bar{N}_{\text{glthr}}$, visualization of “thermal equilibrium”: We plot $\ln 2 \frac{\partial g(\bar{M}_{\text{out}_i})}{\partial \bar{N}_{\text{out}}}$ [left hand side of Eq. (7.71)] vs. \bar{N} for individual channels, as well as the common inverse temperature $\bar{\beta}_{\text{out}}$ (noise values given in the plot; we choose the same noise distribution as in Fig. 7.2 and present here exact values). The noisiest channel with $y_q = 2, y_p = 1$ (channel 2 in Fig. 7.2) is excluded from information transmission, i.e. $\bar{N}_2 = 0$ (it belongs to \mathcal{N}_1). The channel $y_q = 2, y_p = 0.5$ receives $\bar{N}_1 = 0.062$ and channel $y_q = 0.5, y_p = 0.3$ receives $\bar{N}_4 = 0.239$ (channels 1 and 4 in Fig. 7.2). Since for both input energies $\bar{N} < \bar{N}_{\text{thr}}$ they belong to set \mathcal{N}_2 . The channel $y_q = 0.5, y_p = 0.4$ receives $\bar{N}_3 = 0.187 > \bar{N}_{\text{thr}}$ and channel $y_q = 0.25, y_p = 0.1$ receives $\bar{N}_5 = 0.462 > \bar{N}_{\text{thr}}$ (channels 3 and 5 in Fig. 7.2), i.e. they both receive enough energy to satisfy locally the quantum water-filling solution and therefore belong to set \mathcal{N}_3 . The total input energy constraint was fixed to $\bar{N} = 0.95$.

7.4. Classical additive channel with Gauss-Markov correlated noise

Thus, the energy constraint (associated to $\bar{\beta}_{\text{out}}$) implies that the capacity is achieved when the modes (that participate in information transmission) are in *thermal equilibrium* (too noisy modes are excluded as mentioned above). Note that Eq. (7.70), as mentioned already in Sec. (6.4.5), can be expressed as a *Bose-Einstein statistics*:

$$\bar{M}_{\text{out}i} = \frac{1}{e^{\bar{\omega}_{\text{out}i}\bar{\beta}_{\text{out}}} - 1}, \quad (7.72)$$

where $\bar{\omega}_{\text{out}i}$ is defined ($\forall i$) as in Eq. (6.168). We illustrate the “thermal equilibrium” stated in Eq. (7.68) in Fig. 7.3 for the same five noise distributions that were schematically depicted in Fig. 7.2.

Infinite number of modes

In order to make the transition to an infinite number of channel uses we have to consider a parallel channel system with an infinite number of one-mode channels, $n \rightarrow \infty$. In this limit all functions previously labeled with i depend now on a continuous parameter x defined on a proper domain which depends on the particular noise model. All sums that run from $i = 1, \dots, n$, now become integrals over the whole domain of x . The three sets become now sets of continuous variables and cover the whole domain of x ; they read

$$\begin{aligned} \mathcal{N}_1 &= \{x \mid \mu_0(x) \leq \mu\}, \\ \mathcal{N}_2 &= \{x \mid \mu_{\text{thr}}(x) < \mu < \mu_0(x)\}, \\ \mathcal{N}_3 &= \{x \mid \mu_{\text{thr}}(x) \geq \mu\}, \end{aligned} \quad (7.73)$$

where $\mu_{\text{thr}}(x), \mu_0(x)$ are defined as in (7.44), (7.45) where index i is replaced by x . Equations (7.62)-(7.65) remain the same, with the replacements $i_{\text{q}i}$ by $i_{\text{q}}(x)$ and the sums over i by integrals over x .

Once the μ is found which is the solution of (7.66) we can determine the optimal spectra $i_{\text{q}}(x), i_{\text{p}}(x)$ and $m_{\text{q}}(x), m_{\text{p}}(x)$, respectively. The found optimal spectra are used to evaluate the Gaussian capacity in the limit $n \rightarrow \infty$:

$$\begin{aligned} C^{\text{G}}(\Phi_{\Lambda}, \bar{N}) &= \lim_{n \rightarrow \infty} \frac{1}{n} C_{\chi}^{\text{G}}(\Phi_{\Lambda}^{(n)}, n\bar{N}) \\ &= \frac{1}{|A|} \int_{x \in A} dx \left[g\left(\bar{\nu}(x) - \frac{1}{2}\right) - g\left(\nu_{\text{out}}(x) - \frac{1}{2}\right) \right], \end{aligned} \quad (7.74)$$

where A is the spectral domain of x and $|A|$ is its size. In case of a global quantum water-filling, i.e. if $\mu_{\text{thr}}(x) \geq \mu, \forall x$ the solution reads as in Eq. (7.21).

7.4. Classical additive channel with Gauss-Markov correlated noise

We consider now a concrete example of a memory model, namely, a Markov correlated noise. We use the same noise model that we already studied for classical Gaussian

7. Multi-mode Gaussian channels

channels in Sec. 2.3.4. Since this noise is “classical” (i.e. its symplectic eigenvalues can be smaller than 1/2) we use it only for the multi-mode classical additive noise channel, i.e. when $\mathbf{X} = \mathbb{I}$. As mentioned in Sec. 5.3.2, in this case $\mathbf{Y} = \mathbf{V}_{\text{env}}$. This channel may be regarded as the quantum counterpart of the one defined in Eq. (2.35), with the difference that in the quantum case we have two degrees of freedom as we have two input quadratures.

Let us now construct the full noise covariance matrix \mathbf{V}_{env} of the memory channel. We choose the q -quadratures to be correlated and the p -quadratures to be anti-correlated. Namely, the full noise CM reads

$$\mathbf{Y} = \mathbf{V}_{\text{env}} = \begin{pmatrix} \mathbf{V}_{\text{MK}}(\phi) & 0 \\ 0 & \mathbf{V}_{\text{MK}}(-\phi) \end{pmatrix}, \quad (7.75)$$

where $\mathbf{V}_{\text{MK}}(-\phi)$ is the matrix given in Eq. (2.33) with replacement $\phi \rightarrow -\phi$. Let us confirm that \mathbf{V}_{env} can indeed be diagonalized by a passive symplectic transformation [as requested from our channel definition stated in Eq. (7.2)]

Due to the particular block structure of \mathbf{V}_{env} the rotation Θ that diagonalizes \mathbf{V}_{env} (or equivalently \mathbf{Y}) is of the form

$$\Theta = \begin{pmatrix} \Theta^q & 0 \\ 0 & \Theta^p \end{pmatrix}. \quad (7.76)$$

Therefore, in order for Θ to be a symplectic transformation we find the requirement that

$$\Theta^{qT} \Theta^p = \Theta^q \Theta^{pT} = \mathbb{I}, \quad (7.77)$$

where Θ^q, Θ^p are orthogonal transformations. In the limit $n \rightarrow \infty$ both quadrature blocks

$$\mathbf{V}_{\text{env}}^q = \mathbf{V}_{\text{MK}}(\phi), \quad \mathbf{V}_{\text{env}}^p = \mathbf{V}_{\text{MK}}(-\phi), \quad (7.78)$$

of the noise CM (7.75) are diagonalized by the same orthogonal transformation $\Theta^q, \Theta^p = \mathbf{Q}$, where \mathbf{Q} is stated in the Appendix in Eq. (A.10), implying

$$\lim_{n \rightarrow \infty} [\mathbf{V}_{\text{env}}^q, \mathbf{V}_{\text{env}}^p] = 0. \quad (7.79)$$

Thus Θ corresponds asymptotically to a passive symplectic transformation and requirement (5.66) is fulfilled. In addition we find that $[\mathbf{V}_{\text{env}}^q, \mathbf{V}_{\text{env}}^p] = 0$ for the case $n = 2$. The latter was intensively studied numerically in [CCMR05, CCRM06] where it was shown that entanglement at the input helps to increase the transmission rate. We shall confirm those results analytically in the following and then extend it to the general case of infinite modes.

7.4.1. Two modes

Let us first consider the case $n = 2$. The noise matrix reads in this case

$$\mathbf{Y}_M^{(2)} = N \begin{pmatrix} 1 & \phi & 0 & 0 \\ \phi & 1 & 0 & 0 \\ 0 & 0 & 1 & -\phi \\ 0 & 0 & -\phi & 1 \end{pmatrix}, \quad N \geq 0, \phi \in [0, 1], \quad (7.80)$$

7.4. Classical additive channel with Gauss-Markov correlated noise

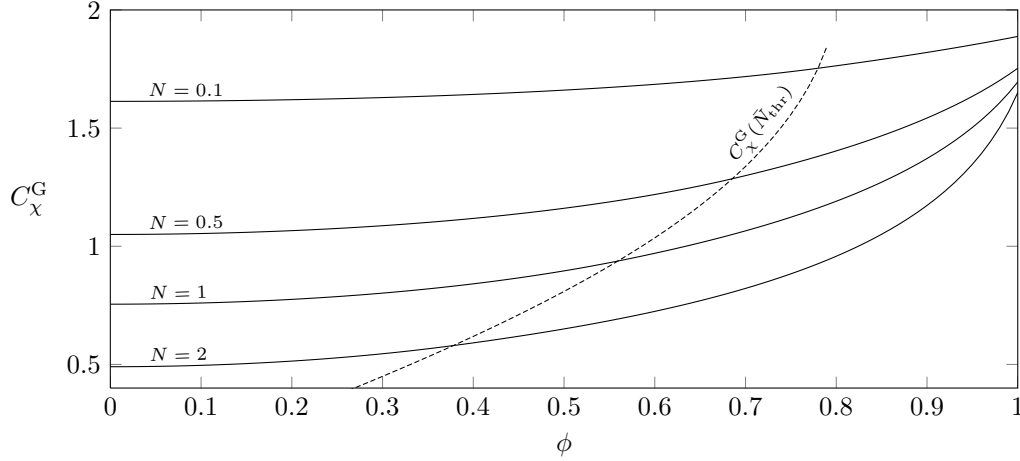


Figure 7.4.: $C_{\chi}^G(\Phi_{(1,y,s)}^F, \bar{N}) = C_{\chi}^G(\Phi_{\Lambda}^{(2)}, 2\bar{N})/2$ vs. ϕ , where $s(\phi)$ is given by Eq. (7.83). We confirm that the one-shot Gaussian capacity is monotonically increasing with ϕ , where here (from bottom to top) $N = \{2, 1, 0.5, 0.1\}$. In the limit $\phi = 1$ the capacity coincides with the one of the one-mode channel with $\text{rank}(\mathbf{X}) = 2, \text{rank}(\mathbf{Y}) = 1$, see Sec. 6.4.7. The dashed curve is the one-shot Capacity at $\bar{N} = \bar{N}_{\text{thr}}(\phi_{\text{thr}}, N_{\text{thr}})$: for fixed N and $\phi \leq \phi_{\text{thr}}$ the quantum water-filling solution is satisfied.

i.e. the two channels (or modes) are correlated with the parameter ϕ . This can alternatively be seen as two successive, correlated uses of the same channel. When brought to diagonal form we obtain the effective noise matrix $\mathbf{Y}_{\Lambda}^{(2)}$ of the channel $\Phi_{\Lambda}^{(2)}$ (which has the same capacity), i.e.

$$\mathbf{Y}_{\Lambda}^{(2)} = N \text{diag}(1 - \phi, 1 + \phi, 1 + \phi, 1 - \phi). \quad (7.81)$$

We conclude that the channel $\Phi_{\Lambda}^{(2)}$ is equivalent to two independent one-mode fiducial channels with identical but swapped noise variances, i.e.

$$\Phi_{\Lambda}^{(2)} = \Phi_{(1,y,s)}^F \otimes \Phi_{(1,y,-s)}^F, \quad (7.82)$$

where

$$s = \frac{1}{4} \ln \left(\frac{1 + \phi}{1 - \phi} \right) \Leftrightarrow \phi = \tanh(2s). \quad (7.83)$$

Since “noise inversion” does not change the capacity, i.e. $C_{\chi}^G(\Phi_{(\tau,y,s)}^F) = C_{\chi}^G(\Phi_{(\tau,y,-s)}^F)$, it follows that

$$C_{\chi}^G(\Phi_{\Lambda}^{(2)}, 2\bar{N}) = 2C_{\chi}^G(\Phi_{(1,y,s)}^F, \bar{N}). \quad (7.84)$$

For input energies $\bar{N} \geq \bar{N}_{\text{thr}}$ we find the full Gaussian capacity [using Eq. (6.96)]

$$C_{\chi}^G(\Phi_{\Lambda}^{(2)}, \bar{N}) = g(\bar{N} + N) - g\left(N\sqrt{1 - \phi^2}\right), \quad \bar{N} \geq \bar{N}_{\text{thr}} = \frac{1}{2} \sqrt{\frac{1 + \phi}{1 - \phi}} + N\phi - \frac{1}{2}. \quad (7.85)$$

7. Multi-mode Gaussian channels

Let us take a look at the dependency of C_χ^G on the parameters N and ϕ . With the substitution stated in Eq. (7.83) we can write the noise matrix of the one-mode fiducial channel $\Phi_{(1,y,s)}^F$ as

$$\mathbf{Y} = N \begin{pmatrix} 1 + \phi & 0 \\ 0 & 1 - \phi \end{pmatrix}, \quad \phi \in [0, 1]. \quad (7.86)$$

Note that since the noise in this case is classical the limiting case $\phi = 1$ is physically allowed. In fact, this case is even *the optimal noise distribution*, as proven in Lemma 9 (see Appendix Sec. D.3.4), i.e.

$$\frac{\partial C_\chi^G(\Phi_{(1,y,s)}^F)}{\partial \phi} > 0. \quad (7.87)$$

We plot C_χ^G vs. ϕ in Fig. 7.4 and confirm that indeed the capacity is monotonically increasing with the correlation parameter ϕ . Recall that this behavior is not observed when the parameter s is varied (recall Sec. 6.4.6), i.e. we observed that for $y < 1/\sqrt{12}$ a maximum appears at a finite squeezing s . For the two parameterizations we have

$$\begin{aligned} \frac{1}{2} \text{Tr}[\mathbf{Y}] &= y \cosh(2s), & \sqrt{\det \mathbf{Y}} &= y, \\ \frac{1}{2} \text{Tr}[\mathbf{Y}] &= N, & \sqrt{\det \mathbf{Y}} &= N \sqrt{1 - \phi^2}. \end{aligned} \quad (7.88)$$

Thus, increasing s leaves the determinant invariant and increases $\text{Tr}[\mathbf{Y}]$; increasing ϕ leaves the trace invariant and decreases the determinant of \mathbf{Y} . We summarize these findings (valid for $\tau = 1$):

- $C_\chi^G(\Phi_{(1,y,s)}^F)$ is monotonically decreasing with $\sqrt{\det \mathbf{Y}} = N \sqrt{1 - \phi^2} = y$.
- $C_\chi^G(\Phi_{(1,y,s)}^F)$ is (for $y < 1/\sqrt{12}$) a non-monotonous function of $\text{Tr}[\mathbf{Y}] = 2N$.

Let us now discuss the optimal input state for the two-mode case. Recall that the channel $\Phi_\Lambda^{(2)}$ is equivalent to two single-mode channels (with inverse squeezing) and thus, the optimal two-mode input state corresponds to a product state consisting of two one-mode squeezed states. If $\bar{N} \geq \bar{N}_{\text{glthr}}$ both input squeezed states exactly match the squeezing of the noise such that the optimal input CM of $\Phi_\Lambda^{(2)}$ becomes

$$\mathbf{V}_{\text{in},\Lambda}^{(2)} = \frac{1}{2} \text{diag}(e^{2s}, e^{-2s}, e^{-2s}, e^{2s}), \quad \bar{N} \geq \bar{N}_{\text{glthr}}. \quad (7.89)$$

Then, the optimal input state $\mathbf{V}_{\text{in},M}^{(2)}$ for the memory channel $\Phi_M^{(2)}$ is given by $\mathbf{V}_{\text{in},\Lambda}^{(2)}$, rotated back to the original basis, i.e.

$$\mathbf{V}_{\text{in},M}^{(2)} = \Theta_Y^\top \mathbf{V}_{\text{in},\Lambda}^{(2)} \Theta_Y. \quad (7.90)$$

7.4. Classical additive channel with Gauss-Markov correlated noise

where $\Theta_Y Y_\Lambda \Theta_Y^\top = Y_M$. The rotation Θ_Y in the two mode case reads

$$\Theta_Y = \frac{1}{\sqrt{2}} \begin{pmatrix} -1 & 1 & 0 & 0 \\ 1 & 1 & 0 & 0 \\ 0 & 0 & 1 & -1 \\ 0 & 0 & 1 & 1 \end{pmatrix}, \quad (7.91)$$

i.e. (up to a local and global phase) corresponds exactly to the symplectic transformation of a beamsplitter (see Sec. 5.2.1). As a result the optimal input state in the original, correlated basis is given by the two-mode squeezed vacuum state (where here $s \rightarrow -s$)

$$\mathbf{V}_{\text{in},M}^{(2)} = \mathbf{V}_{\text{TMSV}} = \frac{1}{2} \begin{pmatrix} \cosh(2s) & -\sinh(2s) & 0 & 0 \\ -\sinh(2s) & \cosh(2s) & 0 & 0 \\ 0 & 0 & \cosh(2s) & \sinh(2s) \\ 0 & 0 & \sinh(2s) & \cosh(2s) \end{pmatrix}, \quad \bar{N} \geq \bar{N}_{\text{glthr}}. \quad (7.92)$$

where \mathbf{V}_{TMSV} was introduced in Sec. 5.1. For input energies \bar{N} below the threshold \bar{N}_{glthr} the input state will still be of the form as in Eq. (7.92) but with a squeezing parameter $r < s$. We conclude that for the Markov correlated noise model and $n = 2$ the optimal input state is entangled (as previously suggested in [CCMR05, CCRM06]). This is indeed not very surprising because already in the case of classical Gaussian channels with correlated noise (see Sec. 2.3.3) we observed that the optimal modulation has to be diagonalized in the same basis as the (correlated) noise matrix. As a consequence it must be correlated in the original, correlated noise basis.

7.4.2. Infinite number of modes

We now move to the other case for which the matrix \mathbf{Y}_M can be diagonalized by a passive symplectic transformation, namely, the case $n \rightarrow \infty$. In this limit the spectra of the two blocks of the correlation matrix stated in Eq. (7.75) become continuous (as already discussed in Sec. 2.3.4) and read

$$\begin{aligned} y_q(x) &\equiv \lambda^{(\mathbf{V}_{\text{MK}}(\phi))}(x) = N \frac{1 - \phi^2}{1 + \phi^2 - 2\phi \cos(x)}, \\ y_p(x) &\equiv \lambda^{(\mathbf{V}_{\text{MK}}(-\phi))}(x) = N \frac{1 - \phi^2}{1 + \phi^2 + 2\phi \cos(x)}, \end{aligned} \quad (7.93)$$

where $y_q(x)$ is the noise spectrum of the q -quadrature given by the spectrum of $\lim_{n \rightarrow \infty} \mathbf{V}_{\text{MK}}(\phi)$ and $y_p(x)$ the noise spectrum of the p -quadrature given by the spectrum of $\lim_{n \rightarrow \infty} \mathbf{V}_{\text{MK}}(-\phi)$. Then, the spectra stated in Eq. (7.93) define the action of the channel

$$\Phi_\Lambda^{(\infty)} \equiv \lim_{n \rightarrow \infty} \Phi_\Lambda^{(n)}. \quad (7.94)$$

First, we compute the input energy threshold associated to the global quantum water-filling solution. We stated the general formula in the limit of an infinite number of uses

7. Multi-mode Gaussian channels

in Eq. (7.22). However, this equation requires $y_q(x) \geq y_p(x), \forall x$. For the given noise spectrum there is an easier way to compute the water-filling threshold. The noise spectra are symmetric, i.e.

$$\lambda^{(\mathbf{V}_{\text{MK}}(\phi))}(x) = \lambda^{(\mathbf{V}_{\text{MK}}(-\phi))}(\pi - x), \quad (7.95)$$

and $\lambda^{(\mathbf{V}_{\text{MK}}(\phi))}(x)$ is monotonically decreasing in x (for $x \in [0, \pi]$) which implies that the optimal input spectrum $i_q(x) = \frac{1}{2} \sqrt{y_q(x)/y_p(x)}$ is monotonically decreasing in x (for $x \in [0, \pi]$) and symmetric [$i_q(x) = i_p(\pi - x)$] as well. Thus, in order to satisfy the global quantum water-filling solution the following equation needs to be satisfied:

$$i_q(0) + y_q(0) = \bar{\nu}_{\text{wf}} = \underbrace{\frac{1}{2\pi} \int_0^\pi dx [y_q(x) + y_p(x)]}_{= \frac{1}{\pi} \int_0^\pi dx y_q(x) = N} + \bar{N}_{\text{glthr}} + \frac{1}{2}, \quad (7.96)$$

where the water-filling level $\bar{\nu}_{\text{wf}}$ was previously defined (for a finite number of uses) in Eq. (7.17). Equation (7.96) simplifies to

$$\bar{N}_{\text{glthr}} = \left(\frac{1 + \phi}{1 - \phi} - 1 \right) \left(N + \frac{1}{2} \right). \quad (7.97)$$

Then, the Gaussian capacity is obtained as in Eq. (7.21) inserting the given noise spectra:

$$\begin{aligned} C^{\text{G}} \left(\Phi_\Lambda^{(\infty)}, \bar{N} \right) &= \lim_{n \rightarrow \infty} \frac{1}{n} C_\chi^{\text{G}} \left(\Phi_\Lambda^{(n)}, n\bar{N} \right) \\ &= g(\bar{N} + N) - \frac{1}{\pi} \int_0^\pi dx g \left(\frac{N(1 - \phi^2)}{\sqrt{1 + \phi^4 - 2\phi^2 \cos(x)}} \right), \quad \bar{N} \geq \bar{N}_{\text{glthr}}. \end{aligned} \quad (7.98)$$

We note that for some noise parameters the threshold functions $\mu_0(x), \mu_{\text{thr}}(x)$ may have a complicated profile as depicted in Fig. 7.6. In Fig. 7.7 we illustrate for a particular choice of the noise parameters (N, ϕ) different partitions of the spectral domain between the sets for different input energies $\bar{\lambda}$ corresponding to different μ .

Our result confirms that the modes belonging to \mathcal{N}_2 are squeezed in the less noisy quadrature (which is the one that is modulated), as depicted in Fig. 7.8. An example plot of optimal input and modulation spectra for $\bar{N} < \bar{N}_{\text{glthr}}$ is shown in Fig. 7.5 (b). We see the naturally expected behavior of the capacity in Fig. 7.9. It decreases with increasing noise variance N and increases with increasing noise correlations ϕ . We note that the capacity increases with ϕ up to the noiseless capacity $C = g(\bar{N})$ at “full correlations” ($\phi \rightarrow 1$). This limit will be discussed in section 7.4.4.

7.4.3. Optimal quantum input state

We discuss now the covariance matrix of the optimal input state in the original “correlated” basis. We know that in the basis where the noise, modulation, and input matrices

7.4. Classical additive channel with Gauss-Markov correlated noise

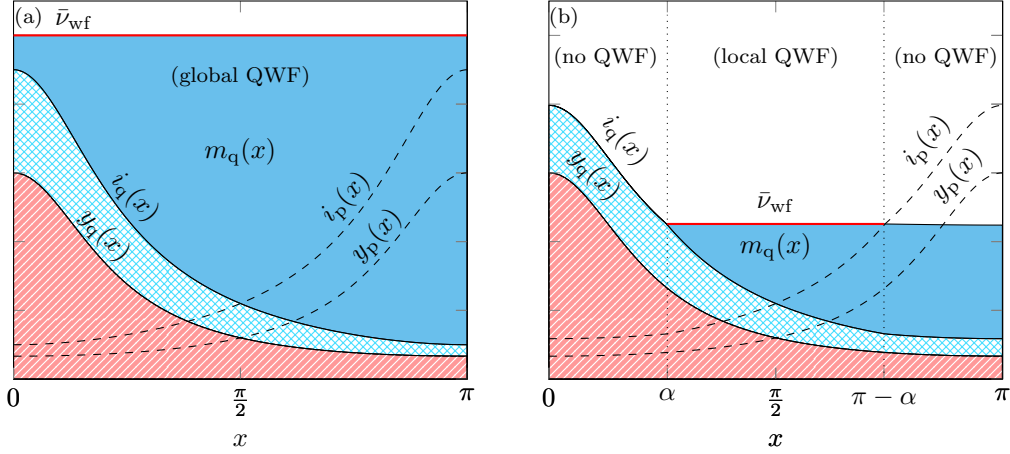


Figure 7.5.: Stacked area plot: optimal input and modulation eigenvalue spectra $i_q(x), m_q(x)$ and noise spectrum $y_q(x)$ ($y_p(x)$ and $i_p(x)$ are given by the lower and upper dashed curve, respectively) for particular, fixed ϕ and N . (a) Global quantum water-filling solution, where $\bar{N} > \bar{N}_{\text{glthr}}$. \bar{v}_{wff} (solid bar) denotes the water-filling level. (b) Below threshold ($\bar{N} < \bar{N}_{\text{glthr}}$): Modes with $x \in [\alpha, \pi - \alpha]$ belong to \mathcal{N}_3 with water-filling level \bar{v}_{wff} (solid bar). Modes with $x \in [0, \alpha]$ and $x \in [\pi - \alpha, \pi]$ belong to set \mathcal{N}_2 , where the modulation is below \bar{v}_{wff} .

are diagonal, the optimal input spectrum leads to the optimal input state given by a product of one-mode squeezed states. Recall that the CM \mathbf{Y} for the Markov correlated noise matrix [given in Eq. (7.75)] is Toeplitz (see Appendix A). Following our assumption that the Gaussian capacity of the given multi-mode channel is given by the sum (for $n \rightarrow \infty$ by an integral) of Gaussian capacities of one-mode channels it follows that the optimal input covariance matrix \mathbf{V}_{in} is diagonalized in the same basis as the total noise covariance matrix \mathbf{Y} . Thus, \mathbf{V}_{in} is asymptotically Toeplitz with quadrature spectra

$$i_{\text{q,p}}(x) = \sum_{k=0}^{\infty} i_{\text{q,p}k} e^{-ikx}, \quad x \in [0, 2\pi],$$

where $i_{\text{q,p}k}$ are here the k th diagonal of \mathbf{V}_{in} (and the Fourier coefficient of a Fourier series) in the original basis. Since $i_{\text{q,p}}(x)$ is Riemann integrable we conclude that

$$i_{\text{q,p}k} = \frac{1}{2\pi} \int_0^{2\pi} dx e^{ikx} i_{\text{q,p}}(x), \quad k = 0, 1, 2, \dots, \infty, \quad (7.99)$$

which provides the covariance matrix of the input state in the case of a global water-filling ($\bar{N} \geq \bar{N}_{\text{glthr}}$), which we consider for the rest of this subsection. In this case the

7. Multi-mode Gaussian channels

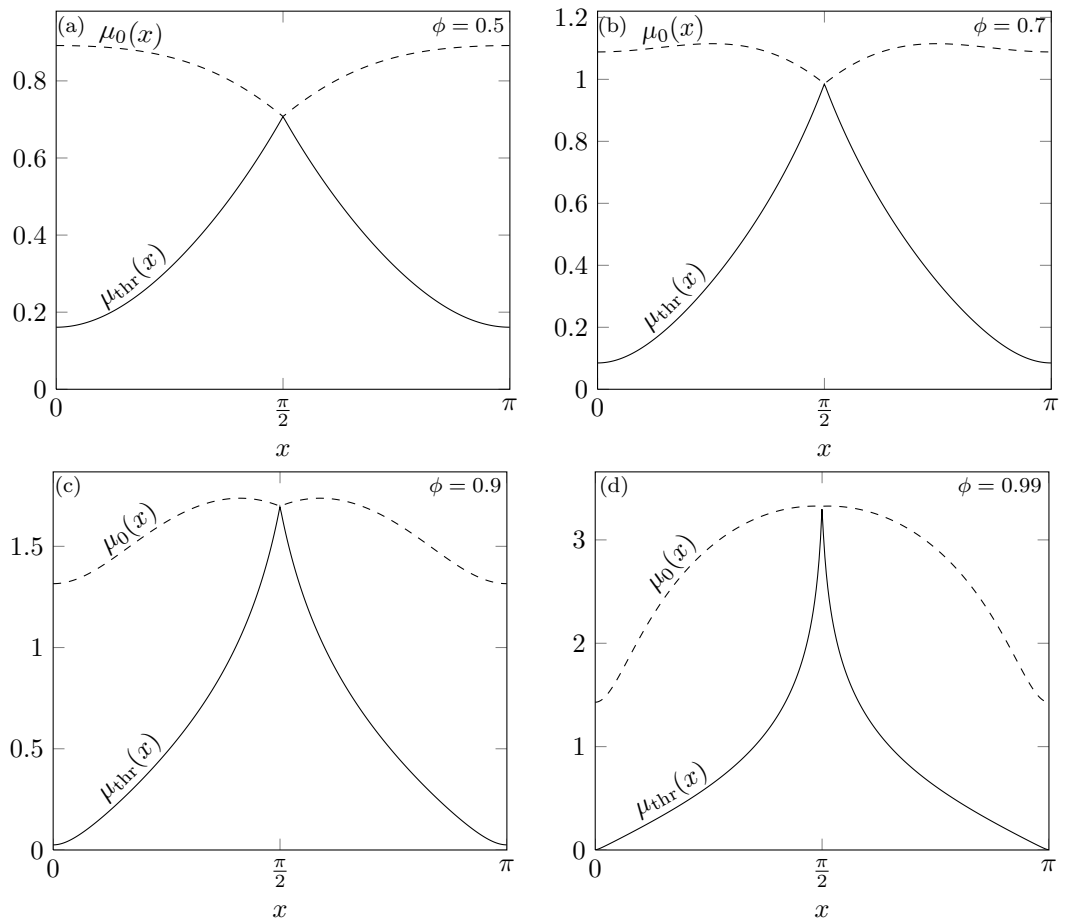


Figure 7.6.: Functions $\mu_0(x)$ (upper dashed curve) $\mu_{\text{thr}}(x)$ (lower solid curve) for (a) $\phi = 0.5$, (b) $\phi = 0.7$, (c) $\phi = 0.9$, (d) $\phi = 0.99$. For all plots we took $N = 1$.

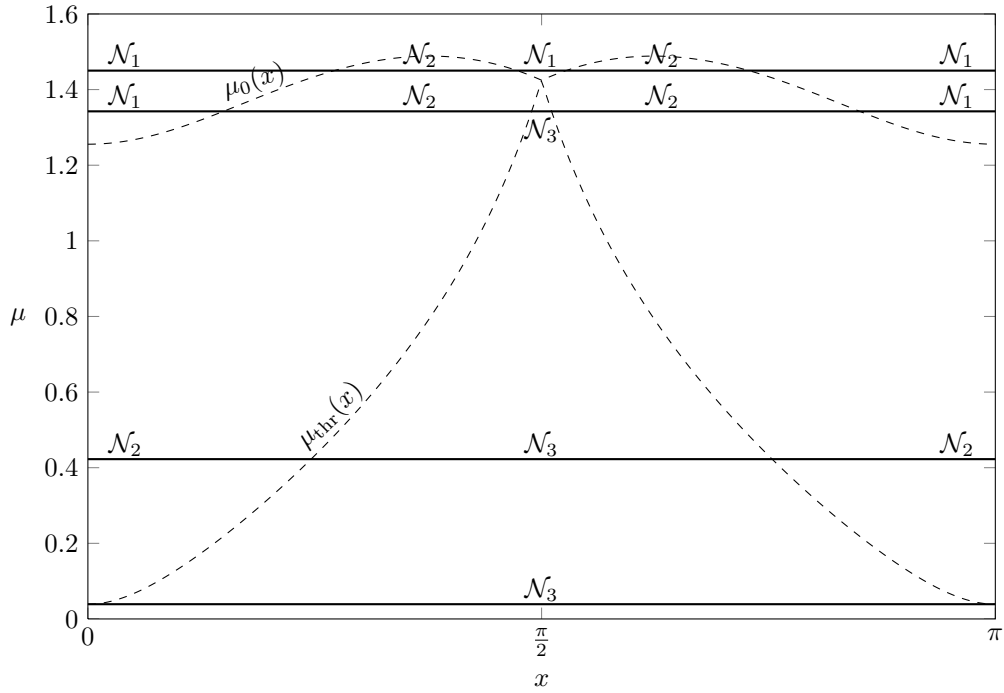


Figure 7.7.: Functions $\mu_{\text{thr}}(x)$ (lower dashed curve), $\mu_0(x)$ (upper dashed curve) and values for μ (solid bars) for different input energies $\bar{\lambda}$, and noise parameters $\phi = 0.85, N = 1$. From top to bottom the values are $\mu = 1.45(\bar{N} = 0.003), 1.34(\bar{N} = 0.02), 0.42(\bar{N} = 1), 0.04(\bar{N} = 17)$. The numbers indicate the intervals on the x -axis that belong to sets $\mathcal{N}_1, \mathcal{N}_2$ or \mathcal{N}_3 .

7. Multi-mode Gaussian channels

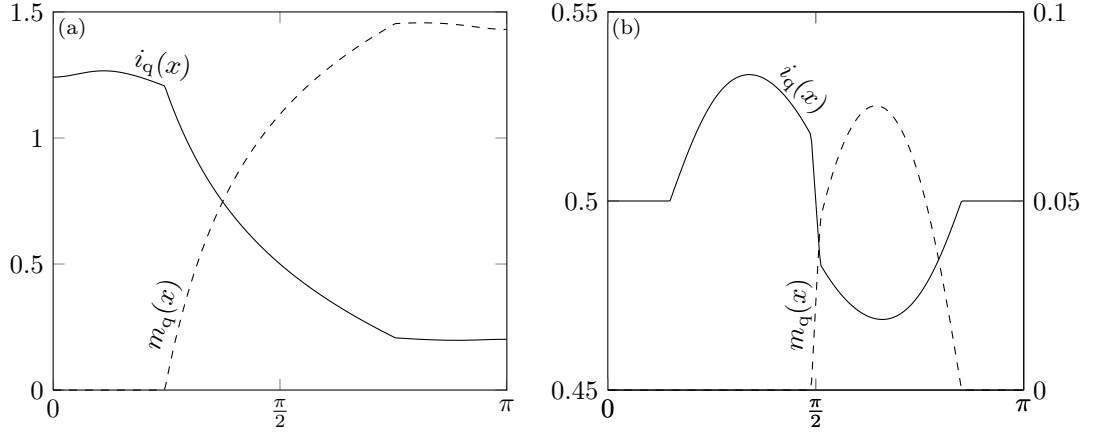


Figure 7.8.: Optimal input $i_q(x)$ (solid curve) and modulation $m_q(x)$ (dashed curve) eigenvalue spectra of the q -quadrature (p -quadrature spectra are the same but mirrored with respect to a vertical line at $\pi/2$) vs. spectral parameter x , for $\phi = 0.85$, $N = 1$ and $\bar{N} < \bar{N}_{\text{glthr}}$. The partitioning in sets is taken from Fig. 7.7. In (a): $\bar{N} = 1$ which corresponds to $\mu = 0.42$, in (b): $\bar{N} = 0.02$ which corresponds to $\mu = 1.34$.

optimal input spectra read

$$i_{q,p}(x) = \frac{1}{2} \sqrt{\frac{y_{q,p}(x)}{y_{p,q}(x)}}, \quad \forall x. \quad (7.100)$$

Inserting the noise spectra $y_{q,p}(x)$ of the Gauss-Markov channel given in Eq. (7.93) in the latter leads to the k -th diagonal of the input covariance matrix:

$$i_{q,pk} = \frac{1}{4\pi} \int_0^{2\pi} dx e^{ikx} \sqrt{\frac{1 + \phi^2 \pm 2\phi \cos(x)}{1 + \phi^2 \mp 2\phi \cos(x)}}, \quad (7.101)$$

where the upper sign is for q and the lower for p . In order to verify that the overall state is entangled we can check whether the reduced single mode states are mixed, i.e. whether the 2×2 covariance matrix (obtained by tracing out all other modes) of the reduced state satisfies

$$\det \mathbf{V}_{\text{in}} = i_{q_0} i_{p_0} > \frac{1}{4}, \quad \phi > 0. \quad (7.102)$$

Integration over the whole domain 0 to 2π leads to $i_{q_0} = i_{p_0}$. Then we find for $i_{q_0}(\phi = 0) = 1/2$, which means that in the absence of correlations the optimal input state is a set of coherent states and not entangled. In the limit $\phi \rightarrow 1$ each single mode state becomes a thermal state with its number of thermal photons tending to infinity. This corresponds to an overall maximally entangled state. It is easy to show that (7.102) is monotonically increasing from $\phi = 0$ to $\phi = 1$ and therefore we conclude that for all $\phi > 0$ the optimal input state is entangled.

7.4. Classical additive channel with Gauss-Markov correlated noise

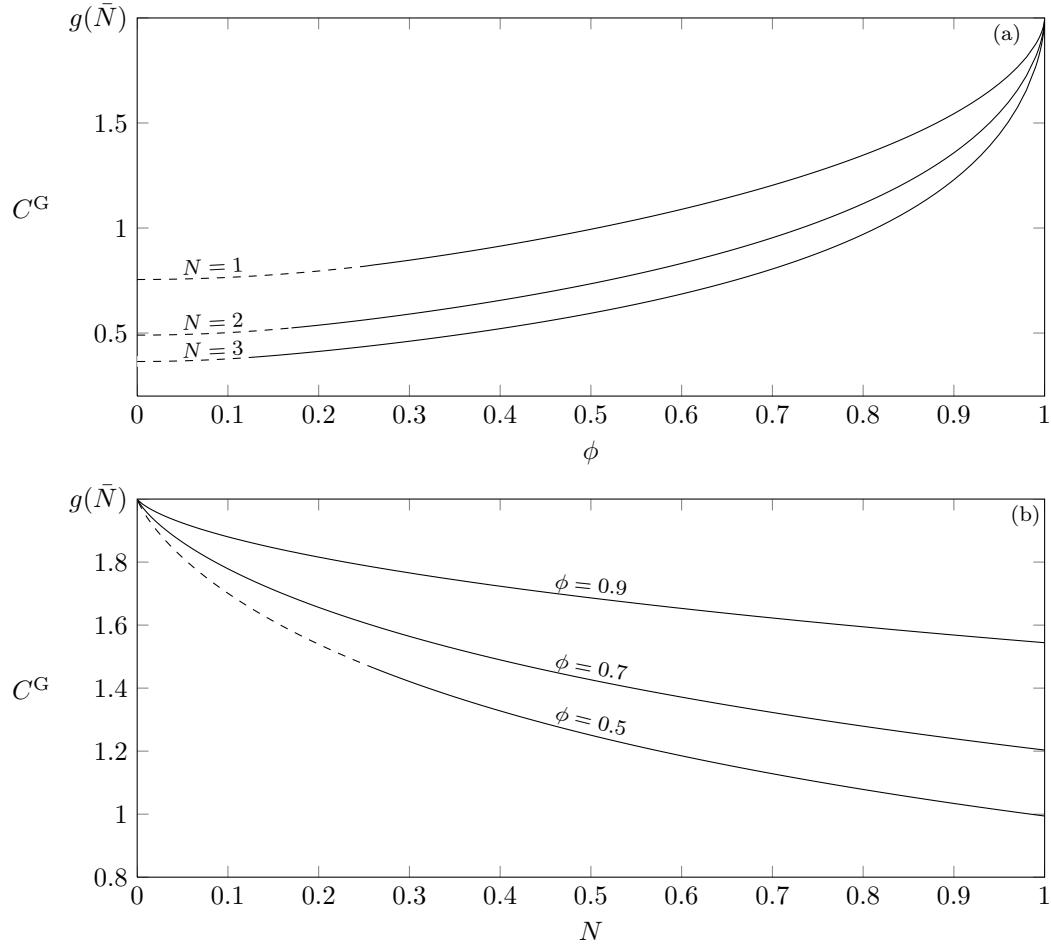


Figure 7.9.: (a) One-shot Gaussian capacity C^G_χ vs. correlation ϕ , where from top to bottom $N = 1, 2$ and 3 . (b) One-shot Gaussian capacity C^G_χ vs. noise variance N , where from top to bottom $\phi = 0.9, 0.7$ and 0.5 . The input energy is $\bar{N} = 1$ ($\bar{\lambda} = 3$) for both plots. The dashed part of the curves corresponds to the global water-filling solution with $\bar{N} \geq \bar{N}_{\text{gthr}}$. One observes that the capacity for full correlations $\phi \rightarrow 1$ tends to the capacity $C = g(\bar{N})$ of the noiseless channel $N = 0$.

7. Multi-mode Gaussian channels

7.4.4. Full correlations

We observe in Fig. 7.9 that for fixed N and \bar{N} the capacity increases monotonically with the correlation parameter ϕ . Furthermore, for $\phi \rightarrow 1$ the capacity tends to the capacity of the noiseless channel:

$$\lim_{\phi \rightarrow 1} C^G(\Phi_\Lambda^{(\infty)}, \bar{N}) = C = g(\bar{N}). \quad (7.103)$$

Equation (7.103) can be proven as follows. For any ϕ the classical capacity C is upper bounded by $g(\bar{N})$. In addition, C is lower bounded by the *coherent rate* R_{coh} [defined in Eq. (7.23)]. As shown in Sec. 7.2 the coherent rate is obtained by a classical water-filling solution. For the given Markovian noise the solution of the coherent rate is equivalent to the solution of the classical capacity of the classical Gaussian channel with Markovian noise (presented in Sec. 2.3.4). Namely, the solution is obtained by finding the position κ , such that

$$\frac{\pi - \kappa}{\pi} y_q(\kappa) = \frac{1}{\pi} \int_{\kappa}^{\pi} dx y_q(x) + \bar{N}, \quad (7.104)$$

where used the fact that $y_q(x) = y_p(\pi - x)$. Once κ is obtained the optimal modulation eigenvalue spectra read

$$\begin{aligned} m_q(x) &= \theta(x - \kappa) \left[\bar{\nu}_{\text{wf}} - y_q(x) - \frac{1}{2} \right], \\ m_p(x) &= \theta(\pi - \kappa - x) \left[\bar{\nu}_{\text{wf}} - y_p(x) - \frac{1}{2} \right], \end{aligned} \quad (7.105)$$

where the water-filling level reads $\bar{\nu}_{\text{wf}} = y_q(\kappa)$ and the coherent rate is given by

$$R_{\text{coh}}(\Phi_\Lambda^{(\infty)}, \bar{N}) = \frac{1}{\pi} \int_{\kappa}^{\pi} dx g \left(\bar{\nu}_{\text{out}}(x) - \frac{1}{2} \right) - g \left(\nu_{\text{out}}(x) - \frac{1}{2} \right). \quad (7.106)$$

In the case of a global water-filling solution the coherent rate becomes for the given noise spectrum

$$\begin{aligned} R_{\text{coh}}(\Phi_\Lambda^{(\infty)}, \bar{N}) &= g(\bar{N} + N) - \frac{1}{\pi} \int_0^{\pi} dx g \left(\frac{1}{2} \sqrt{\frac{(1 + \phi^2 + 2N(1 - \phi^2))^2 - 4\phi^2 \cos^2(x)}{1 + \phi^4 - 2\phi^2 \cos(2x)}} - \frac{1}{2} \right), \\ \bar{N} &\geq N \left(\frac{1 + \phi}{1 - \phi} - 1 \right), \end{aligned} \quad (7.107)$$

where \bar{N}_{cohtthr} is obtained by Eq. (7.96), substituting $i_q(0) = \frac{1}{2}$.

We showed in Sec. 2.3.4 that the noise spectrum $y_q(x)$ (and equivalently $y_p(x) = y_q(\pi - x)$) tends to 0 in the limit $\phi \rightarrow 0$ for all values of x except at $x = 0$ where it

diverges. Since the contribution to the integral of the value at $x = 0$ is infinitesimally small it can be neglected, and thus, in the limit $\phi \rightarrow 1$ the coherent rate is given by the solution for the global water-filling solution (stated in Eq. (7.107)) in this limit, which yields

$$\lim_{\phi \rightarrow 1} R_{\text{coh}}(\Phi_{\Lambda}^{(\infty)}, \bar{N}) = g(\bar{N}). \quad (7.108)$$

Since $R_{\text{coh}} \leq C \leq g(\bar{N})$ we proved Eq. (7.103).

7.4.5. Classical limit

In the classical limit we increase the input energy \bar{N} as well as the noise variance N while keeping the signal-to-noise $SNR = \bar{N}/N$ constant. In this limit the symplectic eigenvalue spectra entering in χ^{G} tend to infinity and therefore we can replace $g(x)$ by its asymptotic function $\log_2(x)$ (we used this simplification already in Sec. 6.4.6). In the case of a global water-filling $\bar{N} \geq \bar{N}_{\text{glthr}}$ the second term in Eq. (7.98) then simplifies to

$$\lim_{\substack{\bar{N} \rightarrow \infty \\ N \rightarrow \infty \\ \frac{\bar{N}}{N} = SNR}} \frac{1}{\pi} \int_0^{\pi} dx \log \left(\sqrt{y_q(x) y_p(x)} \right) = \log_2(N(1 - \phi^2)), \quad (7.109)$$

where the integral is taken from Ref. [GR80]. Thus, the Gaussian capacity in this limit is given by

$$\lim_{\bar{N}, N \rightarrow \infty, \frac{\bar{N}}{N} = c} C^{\text{G}}(\Phi_{\Lambda}^{(\infty)}, \bar{N}) = \log_2(\bar{N} + N) - \log_2(N(1 - \phi^2)), \quad \bar{N} \geq \bar{N}_{\text{glthr}}. \quad (7.110)$$

We conclude that

$$\lim_{\substack{\bar{N} \rightarrow \infty \\ N \rightarrow \infty \\ \frac{\bar{N}}{N} = SNR}} C^{\text{G}}(\Phi_{\Lambda}^{(\infty)}, \bar{N}) \rightarrow C_{\text{cl}} = \log_2 \left(\frac{1}{1 - \phi^2} \left(1 + \frac{\bar{N}}{N} \right) \right), \quad \bar{N} \geq \bar{N}_{\text{glthr}}, \quad (7.111)$$

where C_{Sh} is the classical capacity given in Eq. (2.44) of the classical Gaussian additive noise channel. Since $g(x) < \log(x)$ we reach this limit from below and hence, for finite $\bar{N} \geq \bar{N}_{\text{thr}}$ the classical capacity of the bosonic channel is always smaller than the capacity of the classical Gaussian additive channel. This is the expected result because for the bosonic channel (for $\phi \neq 0$) a certain amount of energy is needed to prepare the input squeezed state, which is not the case for the classical channel. In Fig. 7.10 we plotted the Gaussian capacity C^{G} versus the noise parameter N for different ϕ and fixed $SNR = 1$. For a large range of N we have that $\bar{N} < \bar{N}_{\text{glthr}}$ so C^{G} is obtained numerically by the algorithm stated in Sec. 7.3. We observe that for lower values of ϕ the Gaussian capacity converges faster to the corresponding classical capacity C_{Sh} .

7. Multi-mode Gaussian channels

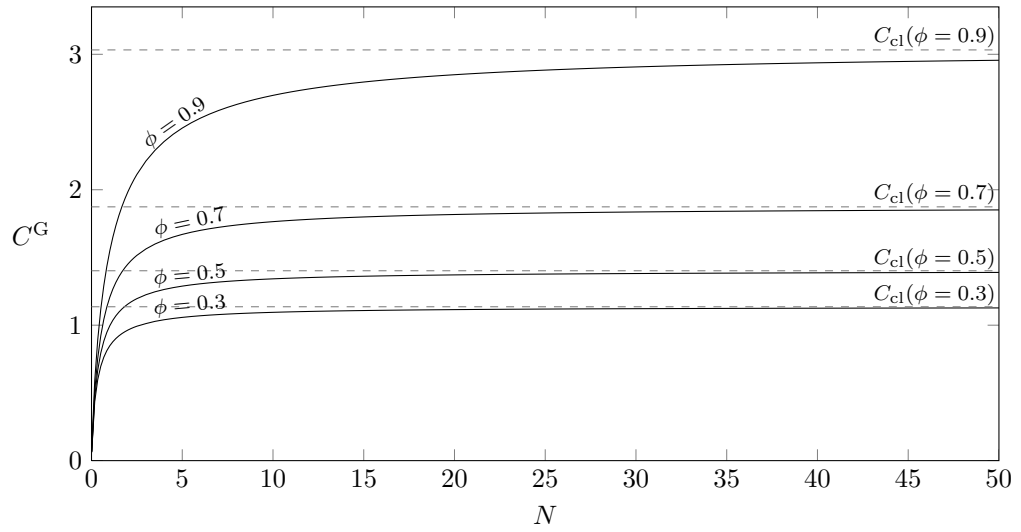


Figure 7.10.: Gaussian capacity C^G vs. noise variance N (solid lines) for fixed $SNR = \bar{N}/N = 1$, where from top to bottom we choose $\phi = \{0.9, 0.7, 0.5, 0.3\}$. The dashed horizontal lines correspond to (twice) the capacity C_{cl} of the classical Gaussian channel for the corresponding values of ϕ . For parameters $\phi = \{0.9, 0.7, 0.5\}$ in the entire domain of N we find that $\bar{N} < \bar{N}_{glthr}$. For the parameter $\phi = 0.3$ we find that $\bar{N} \geq \bar{N}_{glthr}$ for $N \leq 3$ and $\bar{N} < \bar{N}_{glthr}$ otherwise.

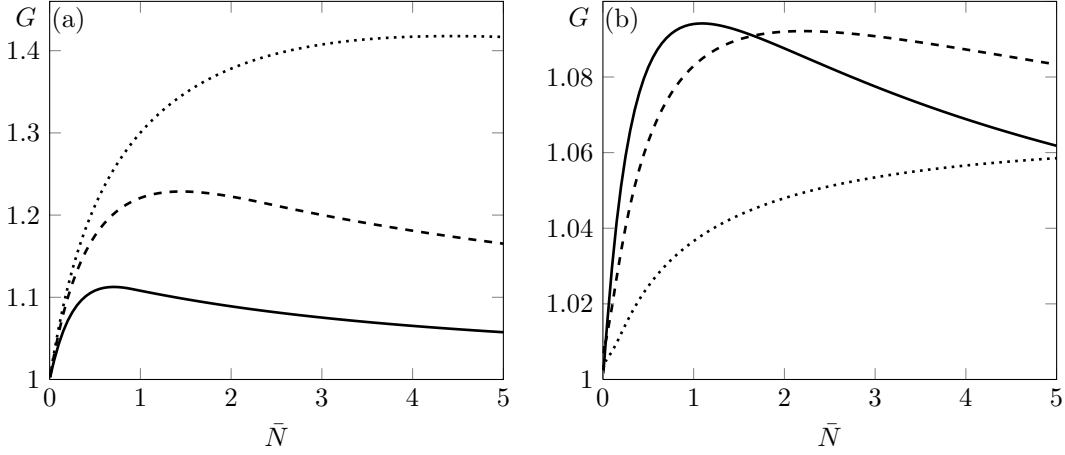


Figure 7.11.: Gain G vs. \bar{N} for (a) two modes and (b) an infinite number of modes, where $\phi = 0.7$ (solid curve), $\phi = 0.9$ (dashed curve), $\phi = 0.99$ (dotted curve). For both plots we took $SNR = 3$.

7.4.6. Symmetric correlations

Now we consider a modified, “symmetric” noise matrix, i.e. a CM with same correlations in both quadratures:

$$\mathbf{Y}_M = \begin{pmatrix} \mathbf{V}_{MK}(\phi) & 0 \\ 0 & \mathbf{V}_{MK}(\phi) \end{pmatrix}, \quad (7.112)$$

As both quadrature blocks have now identical spectra, we treat a set of independent thermal channels, when \mathbf{Y}_M is diagonalized. We recover from Eq. (7.20) immediately that in the asymptotic limit the optimal input spectra read

$$i_{q,p}(x) = \frac{1}{2} \sqrt{\frac{y_{q,p}(x)}{y_{p,q}(x)}} = \frac{1}{2}, \quad \forall x, \quad (7.113)$$

i.e. the overall optimal input state is a set of coherent states and entanglement does not improve the transmission rate. This is in agreement with previous investigations of the two-mode model discussed in [CCMR05]. The same observation was made independently in Ref. [LMM09].

7.4.7. How useful are the optimal input states?

In this subsection we evaluate the gain G by the use of the optimal input states compared to the use of coherent product states. We define the gain G as the ratio of the Gaussian capacity C^G and the coherent rate R_{coh} , i.e.

$$G \equiv \frac{C^G}{R_{\text{coh}}}. \quad (7.114)$$

7. Multi-mode Gaussian channels

Our motivation here is that the optimal input states are entangled and therefore may be not easy to generate. On the contrary, coherent states are easily accessible in the laboratory by standard tools of quantum optics.

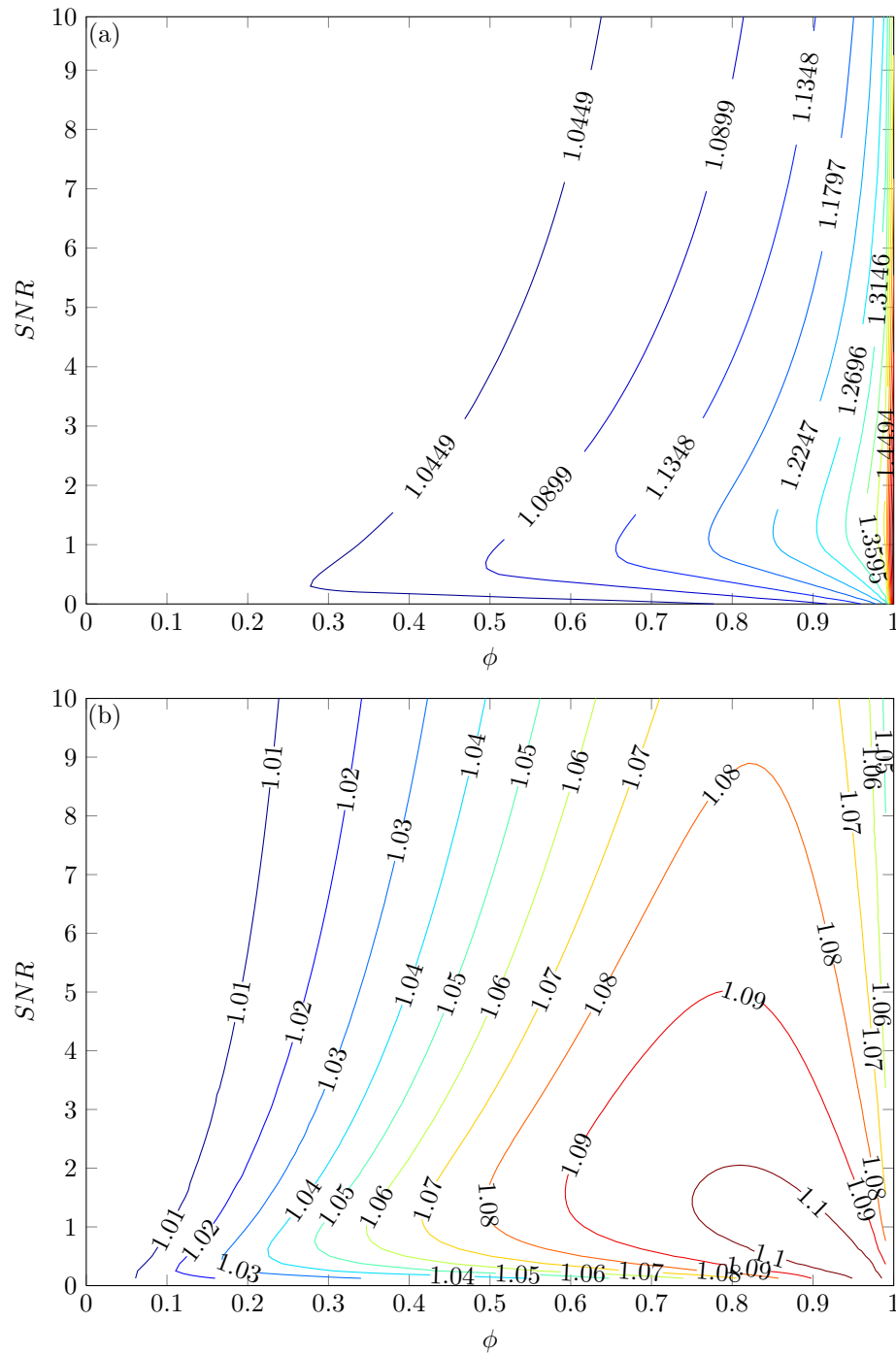
The gain was already discussed in [CCMR05] for the case of two modes, where it was shown that for such a channel G exhibits a maximum with respect to \bar{N} for fixed signal-to-noise ratio $SNR = \frac{\bar{N}}{N}$ and correlation ϕ . Furthermore, it was deduced that the gain increases with increasing correlations ϕ between the two modes.

In the case of an infinite number of modes, we know already that in the absence of correlations the optimal input states are coherent states, and therefore there is no gain ($G = 1$). For full correlations, the behavior is essentially different from the two-mode case: since the channel becomes effectively noiseless, coherent input states are optimal in this limit as well, whereas for two modes the highest available squeezing is best. Therefore, an interesting question is where we find the maximum gain with respect to the noise correlations in the limit of an infinite number of uses of the channel.

In Fig. 7.11 we plotted the gain G vs. \bar{N} for fixed SNR and different ϕ for an infinite number of modes and for two modes. We see that unlike in the case of two modes, where the gain with higher correlations is always higher, in the case of an infinite number of modes the maximum of the gain is found for some intermediate correlations. However, in this plot one does not see the dependency on the SNR . So the question that follows is: What is the dependence of the maximal gain (with respect to \bar{N}) on ϕ and the SNR ? In order to answer this question we make a contour plot of $\max_{\bar{N}} G$ vs. ϕ and SNR . In the case of two modes we see in Fig. 7.12 (a) that the optimal gain is obtained at $\phi = 1$ for a certain SNR . In addition, in this case, the increase in gain at high correlations is very strong compared to that at lower correlations. Furthermore, a low SNR seems to benefit from entanglement more than a higher SNR .

For an infinite number of modes the situation is different, as we can see in Fig. 7.12 (b): instead of a sharp edge toward high correlations we see an almost-flat area of maximal gain in the region of high correlations and low SNR . This holds, on one hand, for a high correlation and low SNR but, on the other hand, also for less correlated noise and a higher SNR . Furthermore, the enhancement is rather robust and does not drop as sharply with decreasing correlations as in the two-mode case. However, as the region of high gain has input energies below the global water-filling threshold, where the optimal input squeezing becomes quite complex [as depicted, e.g., in Fig. 7.8 (b)] a modulation of coherent states might be practically more favorable. We conclude that the gain due to entanglement does not exceed 10% and therefore, a coherent state encoding achieves at least 90% of the Gaussian capacity.

7.4. Classical additive channel with Gauss-Markov correlated noise



8. Gaussian matrix-product states for coding

8.1. Optical scheme for nearest-neighbor GMPS

We consider now a particular GMPS which only requires one finitely entangled state per site ($m = 1$). Namely, a pure, translationally invariant one-dimensional GMPS that was studied in [AE06, AE07]. Each GMPS mode i is obtained by performing two quantum teleportations of two halves of two TMS and a three-mode entangled state with CM \mathbf{V}_{BB} (also called “building block”, see [AE06, AE07] for details), such that the third mode of the building block collapses into the i th GMPS mode¹. We depicted the corresponding setup in Fig. 8.1 (a).

The resulting CM of the one-dimensional GMPS can be written as [AE06]

$$\mathbf{V}_{\text{GMPS}} = \frac{1}{2} \begin{pmatrix} \mathbf{T}^{(C)^{-1}} & 0 \\ 0 & \mathbf{T}^{(C)} \end{pmatrix}, \quad (8.1)$$

where $\mathbf{T}^{(C)}$ is a $n \times n$ circulant symmetric Toeplitz matrix (see Appendix A). Interestingly, the setup shown in Fig. 8.1 can be realized by the sequential application of the same optical transformation. We depict an alternative realization of the same setup in Fig. 8.2. Here, only one TMSV is used together with a delay line, followed by the above explained operations. One central difficulty is the connection of the very first half of the TMSV and the very last one, which then needs to be connected in a cyclic way and therefore would need to be stored in a delay line for a long time. In a practical scheme the first and last half may be replaced by vacua leading to an imperfect but still usable multi-mode entangled state. For the sake of completeness we depict the full optical scheme of a 1D-GMPS in Fig. 8.3 showing the explicit homodyne detections and teleportations (as introduced in Secs. 5.2.3 and 5.2.3).

Now let us focus furthermore on the restricted case of a *nearest-neighbor* correlated GMPS, i.e. the GMPS with the shortest entanglement range among one-dimensional

¹The fact that the state is translationally invariant implies here that the left half of the first TMS has to be used together with the right half of the TMS of the last mode in the setup depicted in Fig. 8.1 (a)

8. Gaussian matrix-product states for coding

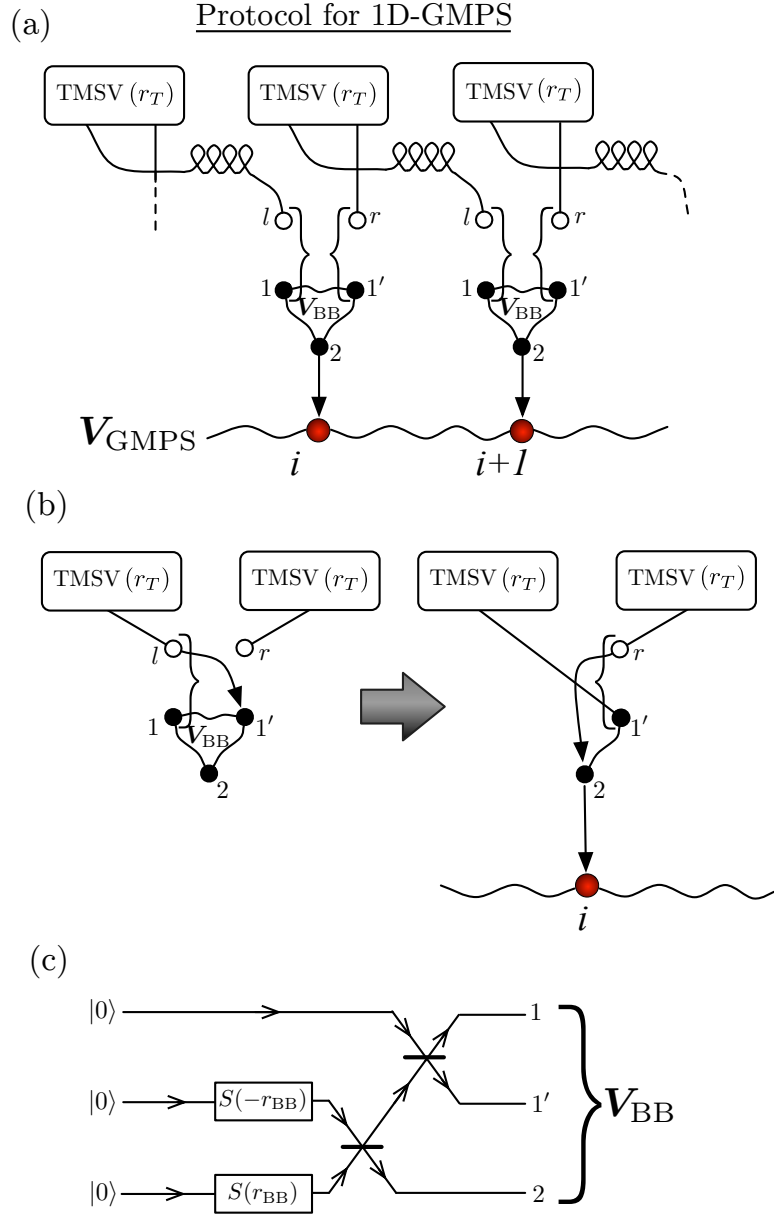


Figure 8.1.: (a) and (b): Modification of the optical scheme defined in [AE06]. $\text{TMSV}(r_T)$ is a two mode squeezed vacuum state with squeezing r_T . For the GMPS mode i , one half of the TMSV is used, the other half is sent to a delay line (to be used in use $i + 1$). After two EPR measurements (represented by curly brackets) involving the TMSV halves of uses i and $i - 1$ and the two identical modes \mathbf{V}_1 of the three-mode building block \mathbf{V}_{BB} , the mode \mathbf{V}_2 collapses into the i th GMPS mode. (c) Optical setup of the three-mode building block \mathbf{V}_{BB} that, when used as described in (a), generates a 1D-GMPS. $|0\rangle$ denote vacuum modes, $S(r_{\text{BB}})$ is a one mode squeezer with squeezing parameter r_{BB} and the bold horizontal lines represent 50 : 50 beamsplitters.

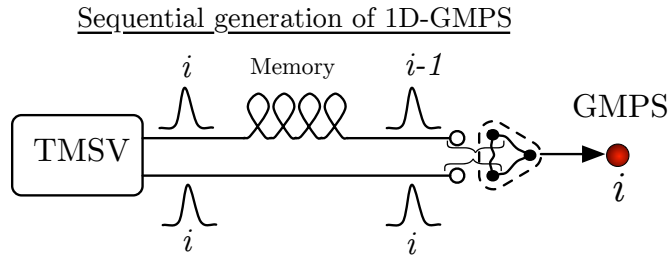


Figure 8.2.: Sequential generation of a 1D-GMPS: The same TMSV state is used repeatedly together with a delay line.

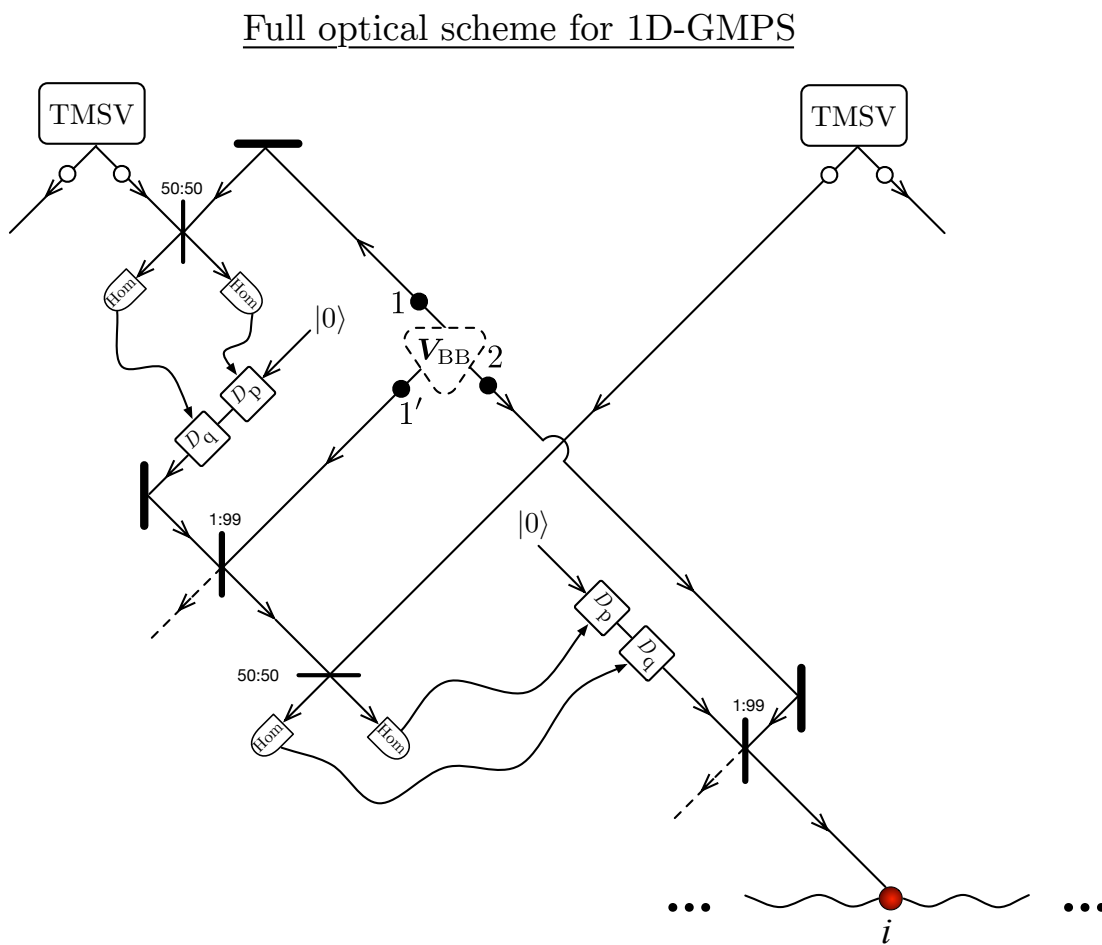


Figure 8.3.: Full optical scheme of the 1D-GMPS. Here D_q and D_p are short notations for displacements depending on homodyne measurement outcomes q_m and p_m (see Sec. 5.2.3) and bold vertical lines with label “1:99” correspond to highly unbalanced beam splitters needed for homodyne detection (see Fig. 5.7).

8. Gaussian matrix-product states for coding

GMPS. In this case the CM \mathbf{V}_{BB} of the building block is given by [AE07]

$$\mathbf{V}_{\text{BB}} = \frac{1}{2} \begin{pmatrix} w & v & u & 0 & 0 & 0 \\ v & w & u & 0 & 0 & 0 \\ u & u & t & 0 & 0 & 0 \\ 0 & 0 & 0 & w & v & -u \\ 0 & 0 & 0 & v & w & -u \\ 0 & 0 & 0 & -u & -u & t \end{pmatrix}, \quad (8.2)$$

with $w = (t+1)/2$, $v = (t-1)/2$ and $u = \sqrt{(t^2-1)/2}$, where $t \geq 1$. The optical scheme for the three-mode building block is depicted in Fig. 8.1 (b), where $\mathbf{S}(r_{\text{BB}})$ is a one-mode squeezing operation as defined in Eq. (5.24), and where $t = \cosh(2r_{\text{BB}})$ [AE07]. The resulting CM of the n -mode nearest-neighbor correlated GMPS is given by [AE06]

$$\mathbf{V}_{\text{GMPS,nn}} = \mathbf{\Gamma}_{\text{T}} - \mathbf{\Gamma}_{\text{WT}}^{\text{T}} (\mathbf{\Gamma}_{\text{WW}} + \mathbf{P} \mathbf{\Gamma}_{\text{TMSV}} \mathbf{P})^{-1} \mathbf{\Gamma}_{\text{WT}}, \quad (8.3)$$

with $\mathbf{P} = \mathbb{I} \oplus -\mathbb{I}$, where \mathbb{I} is the $n \times n$ identity matrix²,

$$\begin{aligned} \mathbf{\Gamma}_{\text{T}} &= \frac{1}{2} \bigoplus_{i=1}^n \text{diag}\{t, t\}, & \mathbf{\Gamma}_{\text{WT}}^{\text{T}} &= \frac{1}{2} \bigoplus_{i=1}^n \begin{pmatrix} u & u & 0 & 0 \\ 0 & 0 & -u & -u \end{pmatrix}, \\ \mathbf{\Gamma}_{\text{WW}} &= \frac{1}{2} \bigoplus_{i=1}^{2n} \begin{pmatrix} w & v \\ v & w \end{pmatrix}, \end{aligned} \quad (8.4)$$

where

$$\mathbf{V}_{\text{TMSV}} = \frac{1}{2} \mathbf{V}_{\text{TMSV}}(r_T) \oplus \mathbf{V}_{\text{TMSV}}(-r_T),$$

$$\mathbf{V}_{\text{TMSV}}(r_T) = \begin{pmatrix} \text{ch}(2r_T) & 0 & 0 & \cdots & \cdots & \cdots & 0 & \text{sh}(2r_T) \\ 0 & \text{ch}(2r_T) & \text{sh}(2r_T) & 0 & 0 & \cdots & \cdots & 0 \\ 0 & \text{sh}(2r_T) & \text{ch}(2r_T) & 0 & 0 & \cdots & \cdots & \vdots \\ \vdots & 0 & 0 & \text{ch}(2r_T) & \text{sh}(2r_T) & 0 & \cdots & \vdots \\ \vdots & 0 & 0 & \text{sh}(2r_T) & \text{ch}(2r_T) & 0 & \cdots & \vdots \\ \vdots & \vdots & \vdots & \ddots & \ddots & \ddots & \ddots & \vdots \\ 0 & \vdots & \vdots & \ddots & \ddots & \ddots & \ddots & 0 \\ \text{sh}(2r_T) & 0 & \cdots & \cdots & 0 & \cdots & 0 & \text{ch}(2r_T) \end{pmatrix}, \quad (8.5)$$

with $\text{ch}(2r_T) = \cosh(2r_T)$ and $\text{sh}(2r_T) = \sinh(2r_T)$, respectively. In order to further simplify the complexity we impose another restriction on the squeezing parameters, namely we choose to fix

$$r_T = r_{\text{BB}} \equiv r_{\text{in}}. \quad (8.6)$$

Even with this restriction the resulting GMPS will prove very useful for information transmission through Gaussian memory channels, as shown later in Section 8.2.

²We remark that the application of Θ on $\mathbf{\Gamma}_{\text{TMSV}}$ corresponds to a partial transpose $\hat{p}_i \rightarrow -\hat{p}_i$, which however has no effect here as $\mathbf{\Gamma}_{\text{TMSV}}$ does not contain any $q-p$ correlations.

8.2. Transmission rates using GMPS

We concluded in the previous section that for the Markov correlated classical additive noise channel the coherent states achieve (at least) 90% of the Gaussian capacity. For some applications it may be crucial to exploit the full potential of the given channel. For this reason we investigate in the following a more sophisticated encoding protocol which, though being suboptimal, may achieve a rate that is significantly closer to the Gaussian capacity. Namely, we use the nearest-neighbor (n.n.) GMPS (discussed above) as an input state. Since the GMPS is heavily entangled it is expected to be useful because we showed that the optimal input state exhibits multi-mode entanglement. In order to study the usefulness of GMPS we use it for two different noise models: the Markovian correlated noise discussed in Sec. 7.4 and a non-Markovian noise model, introduced in [PZM08]:

$$\mathbf{Y}_\Sigma = y_\Sigma \begin{pmatrix} e^{s\Sigma} & 0 \\ 0 & e^{-s\Sigma} \end{pmatrix}, \quad (8.7)$$

where $s \in \mathbb{R}$ and Σ is a $n \times n$ matrix defined as

$$\Sigma = \begin{pmatrix} 0 & 1 & 0 & 0 & \cdots \\ 1 & 0 & 1 & 0 & \cdots \\ 0 & 1 & 0 & 1 & \\ 0 & 0 & 1 & 0 & \ddots \\ \vdots & \vdots & \ddots & \ddots & \ddots \end{pmatrix}. \quad (8.8)$$

Recall that the effective noise matrix for the channels that we consider can be expressed as $\mathbf{Y} = |1 - \tau| \mathbf{V}_{\text{env}}$, $\tau \neq 1$ and $\mathbf{Y} = \mathbf{V}_{\text{env}}$, $\tau = 1$ and thus the parameter y_Σ can be expressed as

$$y = \begin{cases} |1 - \tau| (M_\Sigma + \frac{1}{2}), & \tau \neq 1, \\ M_\Sigma, & \tau = 1, \end{cases} \quad (8.9)$$

where M_Σ is the number of thermal photons of the noise state (if $\tau \neq 1$) and the (normalized) determinant of the classical added noise (if $\tau = 1$). We define the quadrature blocks equivalently to Eq. (7.78), i.e.

$$\mathbf{Y}_\Sigma^q = y_\Sigma \exp(s\Sigma), \quad \mathbf{Y}_\Sigma^p = y_\Sigma \exp(-s\Sigma). \quad (8.10)$$

Then, in the limit $n \rightarrow \infty$ the spectra of the quadrature blocks read

$$\begin{aligned} \bar{\lambda}(\mathbf{Y}_\Sigma^q)(x) &= y_\Sigma e^{2s \cos(x)} \equiv y_q^{(\Sigma)}(x), \\ \bar{\lambda}(\mathbf{Y}_\Sigma^p)(x) &= y_\Sigma e^{-2s \cos(x)} \equiv y_p^{(\Sigma)}(x), \quad x \in [0, 2\pi]. \end{aligned} \quad (8.11)$$

In order to distinguish the noise spectra $y_{q,p}^{(\Sigma)}$ from the Markovian noise we introduce the notations:

$$\begin{aligned} \lambda^{(\mathbf{V}_{\text{MK}}(\phi))}(x) &= N \frac{1 - \phi^2}{1 + \phi^2 - 2\phi \cos(x)} \equiv y_q^{(\text{MK})}(x), \\ \lambda^{(\mathbf{V}_{\text{MK}}(-\phi))}(x) &= N \frac{1 - \phi^2}{1 + \phi^2 - 2\phi \cos(x)} \equiv y_p^{(\text{MK})}(x), \quad x \in [0, 2\pi]. \end{aligned} \quad (8.12)$$

8. Gaussian matrix-product states for coding

where $\lambda^{(\mathbf{V}_{\text{MK}}(\pm\phi))}(x)$ was defined in Eq. (7.93). Note that noise spectra $y_{\text{q,p}}^{(\Sigma)}(x)$ [as well as $y_{\text{q,p}}^{(\text{MK})}(x)$] are mirror symmetric around $x = \pi$ and furthermore,

$$y_{\text{q}}^{(\Sigma)}(x) = y_{\text{p}}^{(\Sigma)}(\pi - x). \quad (8.13)$$

Therefore we consider in the following only the domain $x \in [0, \pi]$ for both noise spectra $y_{\text{q,p}}(x) = \{y_{\text{q,p}}^{(\Sigma)}(x), y_{\text{q}}^{(\text{MK})}(x)\}$ which both satisfy the equality

$$\int_0^\pi dx y_{\text{q}}(x) = \int_0^\pi dx y_{\text{p}}(x). \quad (8.14)$$

Let us now investigate the transmission rates that can be achieved by using a GMPS for Gaussian memory channels with noise CM \mathbf{Y}_{M} and \mathbf{Y}_{Σ} . Throughout this section we restrict ourself to an infinite number of uses of the channel and the input energy regime $\bar{N} \geq \bar{N}_{\text{glthr}}$. Due to the symmetry properties of both noise spectra and the fact that for both noises $y_{\text{q}}(x)$ is monotonically decreasing (for $x \in [0, \pi]$), the solution can be obtained in the same way as in Eq. (7.96), i.e.

$$|\tau| i_{\text{q}}(0) + y_{\text{q}}(0) = \bar{\nu}_{\text{wf}} = \frac{1}{\pi} \int_0^\pi dx y_{\text{q}}(x) + |\tau| \bar{N}_{\text{thr}} + \frac{|\tau|}{2}, \quad (8.15)$$

which simplifies for the particular noise spectra to

$$\bar{N}_{\text{thr}} = \begin{cases} \left(\frac{1+\phi}{1-\phi} - 1 \right) \left(N + \frac{1}{2} \right), & y_{\text{q,p}}(x) = y_{\text{q,p}}^{(\text{MK})}(x), \\ \frac{1}{2} (e^{2s} - 1) + y_{\Sigma} |\tau|^{-1} [e^{2s} - I_0(2s)], & y_{\text{q,p}}(x) = y_{\text{q,p}}^{(\Sigma)}(x), \end{cases} \quad (8.16)$$

where $I_0(x)$ is the modified Bessel function of first kind. Note that we use the (classical) noise spectra $y_{\text{q,p}}^{(\text{MK})}(x)$ only for the classical additive noise channel where $\tau = 1$.

Recall that the covariance matrix of the one-dimensional GMPS [see Eq. (8.1)] can be expressed as $\mathbf{V}_{\text{GMPS}} = \frac{1}{2} \mathbf{T}^{(C)-1} \oplus \mathbf{T}^{(C)}$. In [SWC08] it was proven that the correlations of one-dimensional GMPS decay exponentially. Therefore, in the limit $n \rightarrow \infty$ the spectrum of $\mathbf{T}^{(C)-1}$ reads (up to a change of variance) as the spectrum of the CM of the Markovian correlated noise $\mathbf{V}_{\text{MK}}(\phi)$ ³, i.e.

$$\frac{1}{2} \bar{\lambda}^{(\mathbf{T}^{(C)-1})}(x) \equiv i_{\text{q}}^{(\text{GMPS})}(x) = N_{\text{GMPS}} \left(\frac{1 - \phi_{\text{in}}^2}{1 + \phi_{\text{in}}^2 - 2\phi_{\text{in}} \cos(x)} + \Delta \right), \quad (8.17)$$

with $x \in [0, 2\pi]$, $N_{\text{GMPS}} \geq 0$, $0 \leq \phi_{\text{in}} < 1$, $\Delta \in \mathbb{R}$, and the additional condition $\Delta N_{\text{GMPS}} \geq -1/2$ ensuring the spectrum to correspond to a quantum state.

By comparison of the spectrum (8.17) with the optimal input spectra (7.20) (for $\bar{N} \geq \bar{N}_{\text{glthr}}$) for both noise spectra stated in Eqs. (8.11) and (8.12) one can directly

³We remark that in the limit of $n \rightarrow \infty$ the spectrum of a symmetric circulant matrix tends to the spectrum of its corresponding symmetric Toeplitz matrix (see Appendix A).

verify that for these noises the optimal input state is not a GMPS. Thus, the 1D-GMPS can only serve as an approximation to the optimal input state of both noise models. Then one can define [similarly to the coherent rate stated in Eq. (7.23)] the GMPS rate

$$R_{\text{GMPS}}\left(\Phi_M^{(\infty)}, \bar{N}\right) \equiv \lim_{n \rightarrow \infty} \frac{1}{n} \max_{\mathbf{V}_{\text{GMPS}}, \mathbf{V}_{\text{mod}}} \chi^G, \quad (8.18)$$

where we impose the additional energy restriction that the global quantum-water filling solution is fulfilled, i.e.

$$|\tau| i_q^{(\text{GMPS})}(x) + |\tau| m_q(x) + y_q(x) = \frac{|\tau|}{4i_q^{(\text{GMPS})}(x)} + |\tau| m_p(x) + y_p(x), \quad \forall x. \quad (8.19)$$

We find numerically that for both noise models the highest transmission rate is indeed achieved for the n.n. GMPS [defined in Eqs. (8.2)-(8.5)] with CM $\mathbf{V}_{\text{GMPS}, \text{nn}}$. The CM $\mathbf{V}_{\text{GMPS}, \text{nn}}$ can be expressed as in Eq. (8.1), i.e.

$$\mathbf{V}_{\text{GMPS}, \text{nn}} = \frac{1}{2} \begin{pmatrix} \mathbf{T}_{\text{nn}}^{(C)-1} & 0 \\ 0 & \mathbf{T}_{\text{nn}}^{(C)} \end{pmatrix}. \quad (8.20)$$

We observe that among all 1D-GMPS that can be generated with the setup defined in Fig. 8.1 only the n.n. GMPS has a mirror symmetric spectrum:

$$i_q^{(\text{nn})}(x) = i_p^{(\text{nn})}(\pi - x), \quad (8.21)$$

where $i_q^{(\text{nn})}(x)$ denotes the asymptotic spectrum of $\mathbf{T}_{\text{nn}}^{(C)-1}$ and $i_p^{(\text{nn})}(x)$ the asymptotic spectrum of $\mathbf{T}_{\text{nn}}^{(C)}$. Since the noise spectra of Markovian noise and non-Markovian noise [stated in Eqs. (8.11) and (8.12)] satisfy the same symmetry it is intuitively clear that this state is the most suitable for the given noise models. With relation (8.21) and the fact that the GMPS is a pure state, i.e., $\gamma_{\text{GMPS}}^q(x) \gamma_{\text{GMPS}}^p(x) = 1/4, \forall x$, we obtain the following equality

$$N_{\text{GMPS}}^2 \left(\frac{1 - \phi_{\text{in}}^2}{1 + \phi_{\text{in}}^2 - 2\phi_{\text{in}} \cos(x)} + \Delta \right) \left(\frac{1 - \phi_{\text{in}}^2}{1 + \phi_{\text{in}}^2 + 2\phi_{\text{in}} \cos(x)} + \Delta \right) = \frac{1}{4}, \quad \forall x. \quad (8.22)$$

The latter leads after a few algebraic steps to the solutions

$$\begin{aligned} N_{\text{GMPS}} &= \frac{1 + \phi_{\text{in}}^2}{1 - \phi_{\text{in}}^2}, \\ N_{\text{GMPS}} \Delta &= -\frac{1}{2}. \end{aligned} \quad (8.23)$$

Thus, the nearest-neighbor correlated GMPS has quadrature spectra

$$\begin{aligned} \frac{1}{2} \bar{\lambda}(\mathbf{T}_{\text{nn}}^{(C)-1})(x) &\equiv i_q^{(\text{nn})}(x) = \frac{1 + \phi_{\text{in}}^2}{1 + \phi_{\text{in}}^2 - 2\phi_{\text{in}} \cos(x)} - \frac{1}{2}, \\ \frac{1}{2} \bar{\lambda}(\mathbf{T}_{\text{nn}}^{(C)})(x) &\equiv i_p^{(\text{nn})}(x) = \frac{1 + \phi_{\text{in}}^2}{1 + \phi_{\text{in}}^2 + 2\phi_{\text{in}} \cos(x)} - \frac{1}{2}. \end{aligned} \quad (8.24)$$

8. Gaussian matrix-product states for coding

Therefore, when looking for the optimal transmission rate, one has to optimize only over the parameter ϕ_{in} which eventually can be linked to the squeezing parameter r_{in} [see Eq. (8.6)]. Together with the constraint of global water-filling the GMPS rate of the nearest-neighbor correlated state simplifies for both noise models to

$$R_{\text{nn}} \left(\Phi_{\text{M}}^{(\infty)}, \bar{N} \right) = \max_{\phi_{\text{in}}} g \left(|\tau| \bar{N} + \frac{1}{2\pi} \int_0^\pi dx [y_{\text{q}}(x) + y_{\text{p}}(x)] + \frac{|\tau| - 1}{2} \right) - \frac{1}{\pi} \int_0^\pi dx g \left(\sqrt{[|\tau| i_{\text{q}}^{(\text{nn})}(x) + y_{\text{q}}(x)] [|\tau| i_{\text{p}}^{(\text{nn})}(x) + y_{\text{p}}(x)]} - \frac{1}{2} \right), \quad (8.25)$$

$$\bar{N} \geq \bar{N}_{\text{nnthr}},$$

where \bar{N}_{nnthr} is the input energy required in order to fulfill the global quantum water-filling solution with the input spectra $i_{\text{q}}^{(\text{nn})}(x)$ and $i_{\text{p}}^{(\text{nn})}(x)$, respectively. Due to the fact that $i_{\text{q}}^{(\text{nn})}(x)$ is monotonically decreasing in x (for $x \in [0, \pi]$) (as well as both noise spectra) and that $i_{\text{q}}^{(\text{nn})}(x) = i_{\text{p}}^{(\text{nn})}(\pi - x)$ we obtain the threshold value \bar{N}_{nnthr} in the same way as in Eq. (8.15), i.e.

$$|\tau| i_{\text{q}}^{(\text{nn})}(0) + y_{\text{q}}(0) = \bar{\nu}_{\text{wf}} = \frac{1}{\pi} \int_0^\pi dx y_{\text{q}}(x) + |\tau| \bar{N}_{\text{nnthr}} + \frac{|\tau|}{2}, \quad (8.26)$$

which simplifies with Eq. (8.24) to

$$\bar{N}_{\text{nnthr}} = \frac{1 + \phi_{\text{in}}}{(1 - \phi_{\text{in}})^2} - 1 + \frac{1}{|\tau|} \left(y_{\text{q}}(0) - \frac{1}{\pi} \int_0^\pi dx y_{\text{q}}(x) \right). \quad (8.27)$$

For the two particular noise spectra the latter becomes

$$\bar{N}_{\text{nnthr}} = \frac{1 + \phi_{\text{in}}}{(1 - \phi_{\text{in}})^2} - 1 + \begin{cases} N \left(\frac{1+\phi}{1-\phi} - 1 \right), & y_{\text{q,p}}(x) = y_{\text{q,p}}^{(\text{MK})}(x), \\ y_{\Sigma} |\tau|^{-1} [e^{2s} - I_0(2s)], & y_{\text{q,p}}(x) = y_{\text{q,p}}^{(\Sigma)}(x). \end{cases} \quad (8.28)$$

Recall that we require the inequality $\bar{N} \geq \bar{N}_{\text{glthr}}$ to be fulfilled in order to satisfy the ‘‘ordinary’’ global quantum water-filling solution. In the case of equality $\bar{N} = \bar{N}_{\text{glthr}}$ we find an upper bound on the physically allowed ϕ_{in} such that at the same time $\bar{N} = \bar{N}_{\text{nnthr}}$ holds:

$$\begin{aligned} \bar{N}_{\text{glthr}} &= \bar{N}_{\text{nnthr}} \\ \Leftrightarrow i_{\text{q}}(0) &= i_{\text{q}}^{(\text{nn})}(0), \end{aligned} \quad (8.29)$$

which leads with Eq. (8.24) and the fact that $i_{\text{q}}(0) = \frac{1}{2} \sqrt{y_{\text{q}}(0)/y_{\text{p}}(0)}$ to the upper bound

$$\phi_{\text{in}} \leq \frac{\left(\frac{y_{\text{q}}(0)}{y_{\text{p}}(0)} \right)^{\frac{1}{4}} - 1}{\left(\frac{y_{\text{q}}(0)}{y_{\text{p}}(0)} \right)^{\frac{1}{4}} + 1}. \quad (8.30)$$

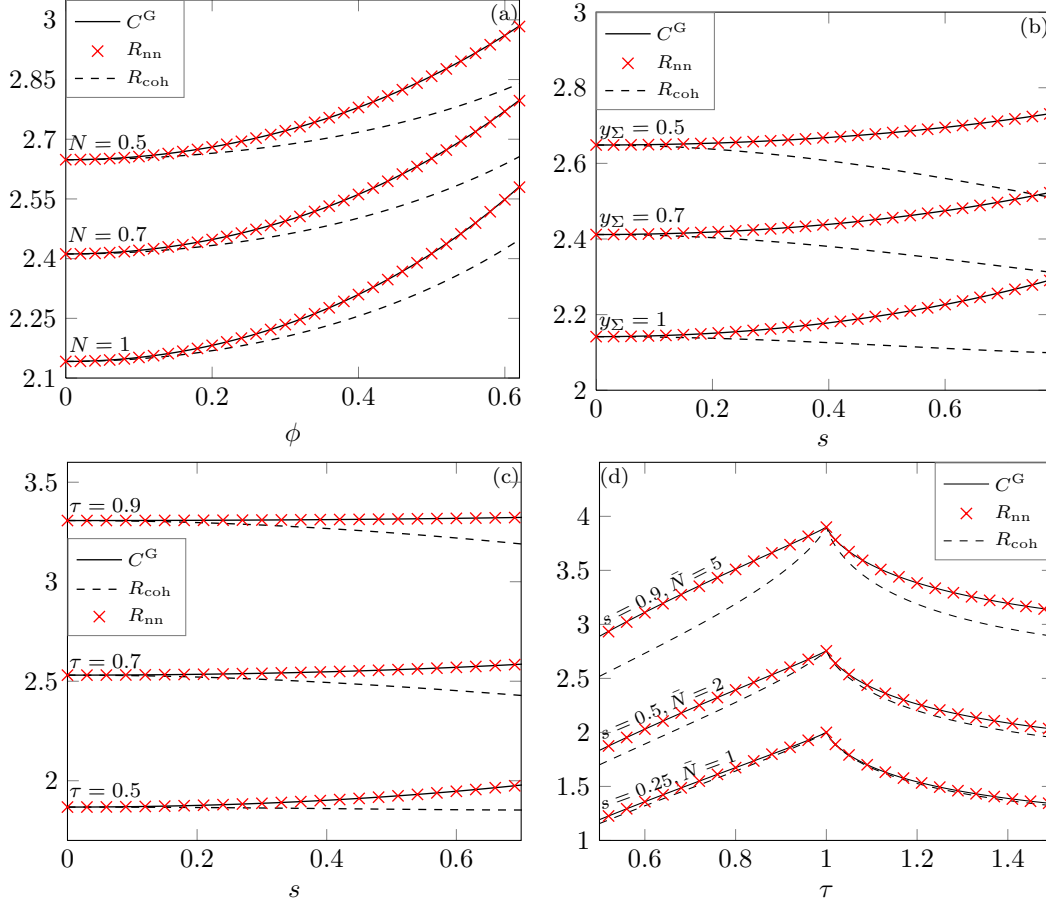


Figure 8.4.: Gaussian capacity C_χ^G (solid line), nearest-neighbor GMPS rate R_{nn} (\times markers) and coherent rate R_{coh} (dashed line) vs. correlation parameters and vs. τ (a) Classical additive noise channel ($\tau = 1$) with Markov noise, where from top to bottom $N = \{0.5, 0.7, 1\}$; in addition we choose $\bar{N} = 5$. (b) Classical additive noise channel ($\tau = 1$) and non-Markovian noise, where from top to bottom $y_\Sigma = \{0.5, 0.7, 1\}$; in addition we choose $\bar{N} = 5$. (c) Lossy channel where from bottom to top $\tau = \{0.5, 0.7, 0.9\}$. In addition we fixed $M_{env} = 1$ and $\bar{N} = 5$. (d) Lossy channel and amplification channel, where $\tau = 1$ corresponds to the perfect transmission channel. From top to bottom we choose the following combinations: $s = 0.9, \bar{N} = 5$, $s = 0.5, \bar{N}$ and $s = 0.25, \bar{N} = 1$. The other parameter was fixed to $M_{env} = 0.1$.

8. Gaussian matrix-product states for coding

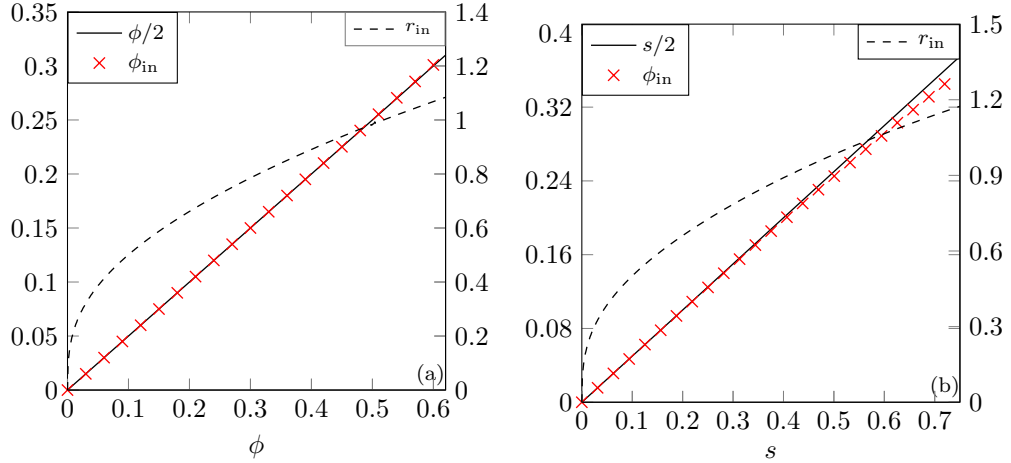


Figure 8.5.: Optimal input correlation ϕ_{in} (\times markers, left axis), corresponding squeezing r_{in} (dashed line, right axis) vs. correlation parameter for (a) the channel with additive Markov noise, where the solid line depicts $\phi/2$ (left axis); (b) the channel with non-Markovian noise (lossy and additive), where the solid line depicts $s/2$ (left axis). We took for both plots $N = y_{\Sigma} = 1$ and $\bar{N} = 5$ and for (b) $\tau = 0.7$.

For the two noise models this bound can be expressed in terms of the respective correlation parameters:

$$\phi_{\text{in}} \leq \begin{cases} \frac{\sqrt{1+\phi} - \sqrt{1-\phi}}{\sqrt{1+\phi} + \sqrt{1-\phi}}, & y_{\text{q,p}}(x) = y_{\text{q,p}}^{(\text{MK})}(x), \\ \tanh\left(\frac{|s|}{2}\right), & y_{\text{q,p}}(x) = y_{\text{q,p}}^{(\Sigma)}(x), \end{cases} \quad (8.31)$$

where at the same time $\bar{N} \geq \bar{N}_{\text{glthr}}$ is fulfilled. We plot for several parameters the Gaussian capacity C^{G} , the optimal rate R_{nn} and the coherent rate R_{coh} in Fig. 8.4. We see that for all examples the nearest-neighbor correlated GMPS is close-to-capacity achieving. Namely, in the plotted region we find $R_{\text{coh}}/C^{\text{G}} > 0.999$. At the same time we observe that the coherent rate becomes more distant from the Gaussian capacity for higher correlation/squeezing values which corresponds to stronger correlated/entangled noise. In this regime one expects input entanglement to play a stronger role and thus, the GMPS to be more useful.

The optimal input correlations ϕ_{in} for both presented noise models are approximately given by $\phi/2$ and $s/2$, respectively, as shown by Fig. 8.5 (a) and Fig. 8.5 (b). This can be verified as follows. Since the quantum water-filling solution holds for the GMPS (as well as for the optimal input state) only the second term depends on ϕ_{in} [see Eq. (8.25)] and we try to minimize it by minimizing the integrand, i.e.

$$\frac{\partial}{\partial \phi_{\text{in}}} g \left(\sqrt{[|\tau| i_{\text{q}}^{(\text{nn})}(x) + y_{\text{q}}(x)] [|\tau| i_{\text{p}}^{(\text{nn})}(x) + y_{\text{p}}(x)]} - \frac{1}{2} \right) = 0, \quad (8.32)$$

8.3. Optimal input state and ground state of quadratic Hamiltonian

which needs to hold for all x . We find the relation

$$\frac{y_q(x)}{y_p(x)} = \frac{(1 + \phi_{\text{in}}^2 + 2\phi_{\text{in}} \cos x)^2}{(1 + \phi_{\text{in}}^2 - 2\phi_{\text{in}} \cos x)^2}. \quad (8.33)$$

Since the optimal input correlation ϕ_{in} does not depend on x , Eq. (8.33) cannot be solved for all x . Therefore, we approximate both noise spectra [defined in Eqs. (8.11) and (8.12)] by dropping quadratic terms (and terms of higher order), i.e.

$$\frac{y_q(x)}{y_p(x)} \approx \frac{1 + 2\alpha \cos(x)}{1 - 2\alpha \cos(x)}, \quad (8.34)$$

where $\alpha = \phi$ for the Markovian noise and $\alpha = s$ for the non-Markovian noise, respectively. Assuming in addition $\phi_{\text{in}}^2 \ll 1$ we find the simple relations $\phi_{\text{in}} \approx \phi/2$ and $\phi_{\text{in}} \approx s/2$, respectively.

Finally, let us discuss the required optical squeezing strength to realize the optimal input correlation ϕ_{in} for both noise models: recall the construction of the covariance matrix of the nearest-neighbor GMPS presented in Sec. 5.4. We choose in Eq. (8.6) to simplify the dependence of the nearest-neighbor GMPS to a single squeezing parameter r_{in} , which is at the same time the squeezing parameter of the three-mode building block and the (finitely entangled) two-mode squeezed vacua (see Fig. 8.1). Interestingly, this restriction still allows us to generate all required input correlations ϕ_{in} . For a given ϕ_{in} we find numerically the best r_{in} by fitting the spectra of the (large) CM $\mathbf{V}_{\text{GMPS,nn}}$ to the spectra $i_q^{(\text{nn})}(x, \phi_{\text{in}})$, $i_p^{(\text{nn})}(x, \phi_{\text{in}})$, respectively. We show the corresponding curves in Fig. 8.5. For the Markov noise, in the plotted region, a maximal correlation of $\phi_{\text{in}} \approx 0.3$ is required, which can be realized by $r_{\text{in}} \approx 1.08$ (about 9.4 dB squeezing). For the non-Markovian noise, a maximal correlation of $\phi_{\text{in}} \approx 0.4$ is required, which corresponds to $r_{\text{in}} \approx 1.18$ (about 10.2 dB squeezing). This shows that the presented setup can be realized with accessible non-linear optics for a realistic assumption of noise correlations, since the maximal input squeezing values have recently been realized experimentally [VMC⁺08, MAE⁺11].

8.3. Optimal input state and ground state of quadratic Hamiltonian

We showed that the GMPS is not the optimal input state for the considered noise models. Let us consider a new, effective noise matrix with CM

$$\mathbf{Y}_{\text{nn}} = \begin{cases} |1 - \tau| \mathbf{V}_{\text{env,nn}}, & \tau \neq 1, \\ \mathbf{V}_{\text{env,nn}} & \tau = 1, \end{cases} \quad (8.35)$$

$$\mathbf{V}_{\text{env,nn}} = (\mathcal{N}_{\text{env}} \oplus \mathcal{N}_{\text{env}}) \frac{1}{2} \left(\mathbf{T}_{\text{nn}}^{(C)-1} \oplus \mathbf{T}_{\text{nn}}^{(C)} \right),$$

where \mathcal{N}_{env} is a $n \times n$ matrix that commutes with $\mathbf{T}_{\text{nn}}^{(C)}$ [given in (8.20)]. Then, for all noise matrices $\mathbf{Y} = \mathbf{Y}_{\text{nn}}$ the GMPS with CM $\mathbf{V}_{\text{GMPS,nn}}$ is the *exact* optimal input state,

8. Gaussian matrix-product states for coding

i.e.

$$R_{\text{nn}}\left(\Phi_{\text{M}}^{(\infty)}, \bar{N}\right) = C^{\text{G}}\left(\Phi_{\text{M}}^{(\infty)}, \bar{N}\right), \quad \bar{N} \geq \bar{N}_{\text{glthr}}, \quad (8.36)$$

where now trivially $\bar{N}_{\text{glthr}} = \bar{N}_{\text{nmthr}}$. This result follows directly from the fact that the optimal input state (for the quantum water-filling solution) is given by $i_{\text{q}}(x) = \frac{1}{2}\sqrt{y_{\text{q}}(x)/y_{\text{p}}(x)}$. Thus, if $y_{\text{q,p}}(x)$ are the spectra of matrix \mathbf{Y}_{nn} then it follows that $i_{\text{q}}(x) = i_{\text{q}}^{(\text{nn})}(x)$ which implies for $\bar{N} \geq \bar{N}_{\text{glthr}}$ Eq. (8.36).

Furthermore, as already mentioned in section 5.4, GMPS are known to be ground states of quadratic Hamiltonians [SWC08]. More precisely, $\mathbf{V}_{\text{GMPS,nn}}$ is the CM of the *exact* ground state of the translationally invariant Hamiltonian, given in natural units by

$$\hat{H} = \frac{1}{2} \left(\sum_i \hat{p}_i^2 + \sum_{i,j} \hat{q}_i V_{ij} \hat{q}_j \right), \quad (8.37)$$

where \hat{q}_i and \hat{p}_i are the position and momentum operators and where the potential matrix is simply given by $\mathbf{V} = \mathbf{T}_{\text{nn}}^{(C)2}$, where $\mathbf{T}_{\text{nn}}^{(C)}$ is defined in Eq. (8.20). This already hints to a connection between finding the channel capacity (for $\bar{N} \geq \bar{N}_{\text{thr}}$) and the thermodynamic energy minimum of a chain of harmonic oscillators.

A realistic example for a noise with CM $\mathbf{V}_{\text{env,nn}}$ is given by the (Gaussian) state of the system defined in Eq. (8.37) at a finite inverse temperature β . We assume the system to be described by a canonical ensemble, thus the density matrix of the oscillators is given by the Gibbs-state

$$\rho_{\text{Gibbs}} = \frac{\exp \beta \hat{H}}{\text{Tr}[\exp \beta \hat{H}]}, \quad (8.38)$$

The CM \mathbf{V}_{G} of Gaussian state ρ_{Gibbs} is given by Eq. (8.35) with (see Ref. [AEPW02] for details)

$$\mathcal{N}_{\text{env}} = \mathbb{I} + [2 \exp(\beta \mathbf{T}_{\text{nn}}^{(C)}) - \mathbb{I}]^{-1}, \quad (8.39)$$

where indeed $[\mathcal{N}_{\text{env}}, \mathbf{T}_{\text{nn}}^{(C)}] = 0$ (which is the requirement for the effective noise matrix to be diagonalizable by a symplectic passive transformation). Therefore, if we assume the noise of the channel to be given by a set of coupled harmonic oscillators at finite temperature as defined above, i.e. $\mathbf{V}_{\text{env,nn}} = \mathbf{V}_{\text{G}}$, then for $\bar{N} \geq \bar{N}_{\text{glthr}}$ the GMPS with CM $\mathbf{V}_{\text{GMPS,nn}}$ is the exact optimal input state and the ground state of the system given by (8.37).

9. Conclusions & Outlook

We studied optimal transmission rates of Gaussian quantum channels and the corresponding optimal input encodings. The central quantity of interest was the classical capacity C , which is the maximal number of bits that can be reliably transmitted through the channel per use of the channel and given a fixed number of photons \bar{N} at the input. The capacity C is given by $C = \lim_{n \rightarrow \infty} C_\chi/n$, where the one-shot capacity C_χ is the Holevo χ -quantity maximized over all possible encodings. Due to the difficulty of the optimization problem which needs to be treated in an infinite dimensional Hilbert space, we focused in particular on the one-shot Gaussian capacity C_χ^G and Gaussian capacity $C^G = \lim_{n \rightarrow \infty} C_\chi^G/n$, where C_χ^G corresponds to the Holevo χ -quantity maximized over Gaussian encodings: the classical information is encoded in so-called Gaussian states for which the mean field amplitudes are Gaussian distributed.

9.1. Single-mode Gaussian channel

First, we studied the single-mode case in depth. We introduced a new *fiducial* channel which consists of a beamsplitter, a two-mode squeezer and two identical single-mode squeezers and depends only on three parameters: an effective input transmissivity or gain τ , the effective added (thermal) noise y and the squeezing of the noise s . Depending on the range of the input transmissivity/gain the fiducial channel corresponds physically either to a lossy channel, a classical additive noise channel, an amplification channel or a phase-conjugating channel. Any single-mode Gaussian channel was then proven to be equivalent (up to displacements) to the fiducial channel, preceded by a passive Gaussian unitary transformation and followed by a general Gaussian unitary transformation. This equivalence implies that the fiducial channel may be used to calculate the classical capacity as well as the Gaussian capacity of any Gaussian channel (in particular cases this equivalence holds in the limit of infinite squeezing).

We studied then the Gaussian capacity of the fiducial channel and its dependency on the channel parameters. Above an input energy threshold \bar{N}_{thr} the optimal input encoding was found to be given by a *quantum water-filling solution*, which is equivalent to a classical water-filling solution known from Shannon Information Theory. The difference to the classical water-filling solution is that quantum states are used for information encoding and the energy spent on their generation (squeezing) needs to be taken into account. We showed that if $\bar{N} \geq \bar{N}_{\text{thr}}$ and if the noise is squeezed ($s \neq 0$) then the optimal input state is a squeezed state that matches exactly the squeezing of the noise. Furthermore, the optimal modulated output state is a thermal state. We proved additionally that if $\bar{N} \geq \bar{N}_{\text{thr}}$, the Gaussian capacity is additive, i.e. that $C_\chi^G = C^G$. For

9. Conclusions & Outlook

	$\bar{N} \geq \bar{N}_{\text{thr}}$		$\bar{N} < \bar{N}_{\text{thr}}$	
	known	if MOC holds	known	if MOC holds
$y \geq \frac{1+ \tau }{2}$ (EB)	$C = C_\chi \leq \frac{1}{\ln 2} + C_\chi^{\text{G}},$ $C_\chi^{\text{G}} = C^{\text{G}}$	$C = C_\chi = C_\chi^{\text{G}}$	$C = C_\chi$	$C = C_\chi$
$y < \frac{1+ \tau }{2}$	$C \leq \frac{1}{\ln 2} + C_\chi^{\text{G}},$ $C_\chi^{\text{G}} = C^{\text{G}}$?	?

Table 9.1.: Summary of results and open questions for one-mode Gaussian channels. Here, MOC stands for “minimum output entropy conjecture”. If $y \geq \frac{1+|\tau|}{2}$ then the one-mode Gaussian channel is known to be entanglement-breaking. Note that for the phase-conjugating channel ($\tau \leq 0$) $y \geq 1/2$ and thus, it is always entanglement-breaking. Note that for $\bar{N} < \bar{N}_{\text{thr}}$, even if MOC holds, no further conclusions can be made.

input energies $\bar{N} < \bar{N}_{\text{thr}}$ the solution was found to be given by a transcendental equation which needs to be solved numerically. We observed that the input state remains squeezed (if $s \neq 0$). However only the less noisy quadrature is modulated.

While we confirmed that the one-shot Gaussian capacity C_χ^{G} is a monotonous function of the transmissivity (or gain) and the added thermal noise, we observed that (for input energies below the input energy threshold) it is non-monotonous with respect to the squeezing of the noise. In particular, we showed that C_χ^{G} behaves as follows with respect to the noise squeezing: for the phase-conjugating channel ($\tau < 0$) it is a monotonously increasing function, for the classical additive noise channel ($\tau = 1$) and amplification channel ($\tau > 1$) it exhibits one maximum or is monotonically increasing and for the lossy channel ($0 \leq \tau \leq 1$) it can be a monotonous function, exhibit one maximum, a saddle point or a maximum and a minimum. All behaviors were distinguished by analytically obtained bounds on τ and y and thus, classified in the (τ, y) plane.

In addition, for the single-mode case, we derived useful bounds on the classical capacity. In particular, we proved that above the input energy threshold and for a wide range of parameters the classical capacity does not exceed the Gaussian capacity by more than $1/\ln 2$ bits.

We summarize in Table 9.1 all known results on the classical capacity and Gaussian capacity, as well as implications if the minimum output entropy conjecture (MOC) was proven to be true (those implications rely on Ref. [GPC13]). Unfortunately, although we can calculate the one-shot Gaussian capacity C_χ^{G} for $\bar{N} < \bar{N}_{\text{thr}}$, even if the MOC holds it does not imply that $C_\chi^{\text{G}} = C_\chi$. Therefore, in order to draw further conclusions, the much stronger equality $C_\chi^{\text{G}} = C_\chi$ needs to be proven. Then, at least in the entanglement-breaking regime $y \geq (1 + |\tau|)/2$ the classical capacity would be obtained even for input energies $\bar{N} < \bar{N}_{\text{thr}}$.

9.2. Multi-mode Gaussian memory channels

Second, we investigated the solution to the Gaussian capacity of multi-mode Gaussian *memory* channels where the noise exhibits correlations. Such an n -mode memory channel is equivalent to n uses of a single-mode channel where the noise of each use is correlated to the noise of previous uses. We restricted ourselves to correlations that can be unraveled by passive symplectic transformations, thus, reducing the study to the case of a collection of different, individual, *uncorrelated* single-mode Gaussian channels with a common input energy constraint \bar{N} . We proved that above a global input energy threshold \bar{N}_{glthr} the solution is obtained by a *global quantum water-filling solution*: the quantum water-filling solution is satisfied for each individual channel and furthermore, each modulated output state is the same thermal state. In addition, if for each single-mode channel the parameter τ is identical it follows that $C_{\chi}^{\text{G}} = C^{\text{G}}$. For input energies $\bar{N} < \bar{N}_{\text{glthr}}$ the solution was studied in detail for the (multi-mode) classical additive noise channel. We showed that in this case, each channel may belong to one out of three sets: i) it is fully excluded from information transmission, ii) only its less noisy quadrature is modulated or iii) it satisfies the quantum water-filling solution. The overall solution was obtained by the method of Lagrange multipliers, where a multiplier β is connected to the input energy constraint \bar{N} . We showed that the resulting equation can be expressed as a Bose-Einstein-statistics, such that β can be regarded as an inverse temperature. Then, the maximum is obtained when all channels are in *thermal equilibrium*.

We applied our solution to a particular Markov correlated noise model in the case of two channels (or uses) and in the limit of an infinite number of channels. We showed that the Gaussian capacity increases with the correlation parameter. In the limit of full correlations we proved that the Gaussian capacity coincides with the classical capacity of the noiseless channel. Additionally, we recovered the Shannon capacity in the classical limit and demonstrated that the optimal multi-mode input state is given (in the “unraveled basis”) by a collection of single-mode squeezed states. When rotated back to the original, correlated basis it corresponds to a massively entangled multi-mode state. We compared the performance of the optimal input state with a simple, coherent state encoding and showed that it can gain up to 10% with respect to this simple encoding.

The number of open questions for the case of multi-mode Gaussian channels is as expected much greater than in the one-mode case. First of all, the types of multi-mode channels we considered were very restricted, i.e. each channel had the same transmissivity/gain τ and the overall correlations could be “unraveled” by a passive symplectic transformation. Although for this collection of single-mode channels it follows that $C_{\chi}^{\text{G}} = C^{\text{G}}$, if $\bar{N} \geq \bar{N}_{\text{glthr}}$, generally, it is not known if the one-shot Gaussian capacity of a collection of (general) single-mode channels is additive. If the MOC was proven and the one-shot Gaussian capacity (of a collection of single-mode channels) was proven to be additive, one could prove straightforwardly (using the results of [GPC13]) that $C_{\chi}^{\text{G}} = C$ (for $\bar{N} \geq \bar{N}_{\text{glthr}}$) for the particular ensemble of channels that we considered.

9.3. **Gaussian matrix-product states as input states**

In general one may be interested in exploiting the full potential of a given Gaussian memory channel. Since in the case of the Markov correlated noise the optimal input state may be complicated to produce, we focused on a sub-optimal input state with a known generation scheme, namely, a Gaussian matrix product state (GMPS). In particular, we used a GMPS with nearest-neighbor correlations which can be generated sequentially. In order to study its performance we used it as an input state for the Markov correlated noise model as well as a non-Markov correlated noise model (additionally no longer restricting ourselves to the classical additive noise channel). We demonstrated that in a large range of channel parameters, the GMPS achieves more than 99.9% of the Gaussian capacity of both noise models, showing that it serves as a great resource for Gaussian memory channels.

Finally, we defined a new class of memory channels for which the GMPS is proven to be the exact optimal input state. Such noise physically corresponds to a many-body system of Harmonic oscillators that are heated to a certain temperature. Since the GMPS is known to be the exact ground state of such a system, we furthermore established a starting point to find further links between optimization problems in many-body physics and quantum communication.

A. Toeplitz matrices

In the following we present definitions and properties of Toeplitz and circulant matrices taken from [Gra05] and [SZ99]. Toeplitz matrices are often the covariance matrices of (weakly) stationary stochastic processes, which are used in signal processing theory, information theory (see e.g. [Gra05]), climate research (see e.g. [SZ99]) and many other cases. A matrix \mathbf{T} is called *Toeplitz matrix* if $\mathbf{T}_{n \times n} = [t_{k,j}; k, j = 0, 1, \dots, n-1]$, with $t_{k,j} = t_{k-j}$, i.e. it has the form

$$\mathbf{T}_{n \times n} = \begin{pmatrix} t_0 & t_{-1} & t_{-2} & \cdots & t_{-(n-1)} \\ t_1 & t_0 & t_{-1} & & \vdots \\ t_2 & t_1 & t_0 & t_{-1} & \vdots \\ \vdots & & & \ddots & \\ t_{n-1} & \cdots & & & t_0 \end{pmatrix}. \quad (\text{A.1})$$

A Toeplitz matrix \mathbf{T} belongs to the *Wiener class* if $\{t_k\}$ is absolutely convergent, that is

$$\sum_{k=-\infty}^{\infty} |t_k| < \infty. \quad (\text{A.2})$$

If (A.2) is fulfilled, then the Fourier series

$$f_t(x) = \sum_{k=-\infty}^{\infty} t_k e^{ikx}, \quad x \in [0, 2\pi], \quad (\text{A.3})$$

exists and $f(x)$ is Riemann integrable, with Fourier coefficients

$$t_k = \frac{1}{2\pi} \int_0^{2\pi} df(x) e^{-ikx}. \quad (\text{A.4})$$

For the given sequence $\{t_k\}$ or the function $f(x)$ the matrix \mathbf{T} is fully characterized, thus $\mathbf{T} = \mathbf{T}(f)$. The existence of the inverse of \mathbf{T} requires that the essential infimum¹ of f is greater than zero, that is

$$\text{ess inf } f > 0 \quad (\text{A.5})$$

If \mathbf{T} is furthermore Hermitian, i.e.

$$\mathbf{T} = \mathbf{T}^\dagger = (\mathbf{T}^\top)^*, \quad (\text{A.6})$$

¹The largest essential lower bound of f ; in (A.5) $f(x) \leq 0$ for only a negligible part of $x \in \mathbb{R}$.

A. Toeplitz matrices

and (A.2) and (A.5) are fulfilled, then the following statements hold: If the spectrum $\lambda(\mathbf{T}) = \{\lambda_1^{(\mathbf{T})}, \lambda_2^{(\mathbf{T})}, \dots, \lambda_n^{(\mathbf{T})}\}$ (i.e. the eigenvalues of \mathbf{T}) is strictly positive, then its inverse is asymptotically Toeplitz, i.e. $\mathbf{T}(f)^{-1} \sim \mathbf{T}(1/f)$.

$$t_k^{(\mathbf{T}^{-1})} = \frac{1}{2\pi} \int_{-\pi}^{\pi} d \frac{e^{-ikx}}{f(x)}, \quad n \rightarrow \infty. \quad (\text{A.7})$$

A particular case of a Toeplitz matrix is the *circulant matrix* $\mathbf{T}^{(C)}$, defined as $T_{ij}^{(C)} = t_{i-j \bmod n}$, i.e. it has the form

$$\mathbf{T}_{n \times n}^{(C)} = \begin{pmatrix} t_0 & t_{-1} & t_{-2} & \cdots & t_{-(n-1)} \\ t_{-(n-1)} & t_0 & t_{-1} & & \vdots \\ t_{-(n-2)} & t_{-(n-1)} & t_0 & t_{-1} & \vdots \\ \vdots & & & \ddots & \\ t_{-1} & & \cdots & & t_0 \end{pmatrix}. \quad (\text{A.8})$$

Then, we can introduce the notation

$$k = (i - j) \bmod n \quad (\text{A.9})$$

which indicates the k th diagonal of $\mathbf{T}^{(C)}$. The rotation matrix \mathbf{Q} that diagonalizes any circulant matrix \mathbf{C} reads [Ful96]

$$\mathbf{Q}^T = \sqrt{\frac{2}{n}} \times \begin{pmatrix} \frac{1}{\sqrt{2}} & \frac{1}{\sqrt{2}} & \frac{1}{\sqrt{2}} & \cdots & \frac{1}{\sqrt{2}} \\ 1 & \cos\left(\frac{2\pi}{n}\right) & \cos\left(\frac{4\pi}{n}\right) & \cdots & \cos\left(\frac{2\pi(n-1)}{n}\right) \\ 0 & \sin\left(\frac{2\pi}{n}\right) & \sin\left(\frac{4\pi}{n}\right) & \cdots & \sin\left(\frac{2\pi(n-1)}{n}\right) \\ 1 & \cos\left(\frac{4\pi}{n}\right) & \cos\left(\frac{8\pi}{n}\right) & \cdots & \cos\left(\frac{4\pi(n-1)}{n}\right) \\ \vdots & \vdots & \vdots & & \vdots \\ 0 & \sin\left(\frac{n-1}{2} \frac{2\pi}{n}\right) & \sin\left(\frac{n-1}{2} \frac{4\pi}{n}\right) & \cdots & \sin\left(\frac{n-1}{2} \frac{2\pi(n-1)}{n}\right) \end{pmatrix}. \quad (\text{A.10})$$

For even n the same pattern holds, except for a row $n^{-1/2}(1, -1, 1, \dots, -1)$ at $i = n/2$. The diagonal matrix $\mathbf{Q}^T \mathbf{T}^{(C)} \mathbf{Q}$ converges with increasing n to \mathbf{D} , where

$$\mathbf{D} = \text{diag}(d_1, d_2, \dots, d_n), \quad (\text{A.11})$$

where for odd n

$$\begin{aligned} d_1 &= f_T(0) \\ d_{2j} &= d_{2j+1} = f_T(2\pi kj/n), \end{aligned} \quad (\text{A.12})$$

$d_n = f_t(\pi)$ for even n , where $j = 1, 2, \dots, (n-1)/2$ and $f_t(x)$ as defined in (A.3). We remark that if a Toeplitz matrix \mathbf{T} belongs to the Wiener class, then $\mathbf{Q}^\top \mathbf{T} \mathbf{Q}$ also converges to \mathbf{D} . This means that $\mathbf{T}^{(C)}$ and \mathbf{T} can be asymptotically diagonalized in the same basis, and hence all Toeplitz matrices (which belong to the Wiener class) asymptotically commute. The spectrum $\lambda^{(\mathbf{T}^{(C)})} = \{\lambda_1^{(\mathbf{T}^{(C)})}, \lambda_2^{(\mathbf{T}^{(C)})}, \dots, \lambda_n^{(\mathbf{T}^{(C)})}\}$ of $\mathbf{T}^{(C)}$ reads

$$\lambda_m^{(\mathbf{T}^{(C)})} = \sum_{k=0}^{n-1} t_k e^{-i2\pi mk/n}, \quad m = 1, 2, \dots, n. \quad (\text{A.13})$$

In the limit $n \rightarrow \infty$ the $\lambda_m^{(\mathbf{T}^{(C)})}$ becomes the Fourier series stated in Eq. (A.3), i.e.

$$\lambda^{(\mathbf{T}^{(C)})}(x) = \sum_{k=-\infty}^{\infty} t_k e^{-ikx}, \quad x \in [0, 2\pi], \quad (\text{A.14})$$

where $x \in [0, 2\pi]$ is now a spectral parameter. In this limit, Eq. (A.14) is also the eigenvalue spectrum of all Toeplitz matrices that belong to the Wiener class.

B. Entropy of Gaussian states

In the following we derive the von Neumann entropy of Gaussian states. Let us first consider the thermal state $\hat{\rho}_{M_{\text{env}}}^{\text{th}}$ introduced in Sec. 5.1, which is a one-mode Gaussian state with covariance matrix

$$\mathbf{V}_{\text{th}} = \begin{pmatrix} M_{\text{env}} + \frac{1}{2} & 0 \\ 0 & M_{\text{env}} + \frac{1}{2} \end{pmatrix}. \quad (\text{B.1})$$

In the Fock basis the density operator reads [Hol98b]

$$\hat{\rho}_{M_{\text{env}}}^{\text{th}} = \frac{1}{M_{\text{env}} + 1} \sum_{m=0}^{\infty} \left(\frac{M_{\text{env}}}{M_{\text{env}} + 1} \right)^m |m\rangle \langle m|, \quad (\text{B.2})$$

where $\{|m\rangle\}$, $m = 0, 1, \dots, \infty$, are Fock states introduced in Sec. (4.3.1). Then, using Eq. (3.5)

$$\begin{aligned} & -\text{Tr}[\hat{\rho}^{\text{th}} \log_2 \hat{\rho}^{\text{th}}] \\ = & -\text{Tr} \left[\frac{1}{M_{\text{env}} + 1} \sum_{m=0}^{\infty} \left(\frac{M_{\text{env}}}{M_{\text{env}} + 1} \right)^m |m\rangle \langle m| \log_2 \left(\frac{1}{M_{\text{env}} + 1} \sum_{m=0}^{\infty} \left(\frac{M_{\text{env}}}{M_{\text{env}} + 1} \right)^m |m\rangle \langle m| \right) \right] \\ = & -\text{Tr} \left[\frac{1}{M_{\text{env}} + 1} \sum_{m=0}^{\infty} \left(\frac{M_{\text{env}}}{M_{\text{env}} + 1} \right)^m \log_2 \frac{1}{M_{\text{env}} + 1} \left(\frac{M_{\text{env}}}{M_{\text{env}} + 1} \right)^m |m\rangle \langle m| \right] \\ = & -\frac{1}{M_{\text{env}} + 1} \sum_{k,m=0}^{\infty} \left(\frac{M_{\text{env}}}{M_{\text{env}} + 1} \right)^m \log_2 \frac{1}{M_{\text{env}} + 1} \left(\frac{M_{\text{env}}}{M_{\text{env}} + 1} \right)^m \underbrace{\langle k|m\rangle}_{=\delta_{km}} \underbrace{\langle m|k\rangle}_{=\delta_{mk}} \\ = & -\frac{1}{M_{\text{env}} + 1} \log_2 \left(\frac{1}{M_{\text{env}} + 1} \right) \underbrace{\sum_{m=0}^{\infty} \left(\frac{M_{\text{env}}}{M_{\text{env}} + 1} \right)^m}_{=M_{\text{env}}+1} \\ = & -\frac{1}{M_{\text{env}} + 1} \log_2 \left(\frac{M_{\text{env}}}{M_{\text{env}} + 1} \right) \underbrace{\sum_{m=0}^{\infty} m \left(\frac{M_{\text{env}}}{M_{\text{env}} + 1} \right)^m}_{=M_{\text{env}}(M_{\text{env}}+1)} \\ = & (M_{\text{env}} + 1) \log_2 (M_{\text{env}} + 1) - M_{\text{env}} \log_2 (M_{\text{env}}), \end{aligned} \quad (\text{B.3})$$

we conclude that

$$S(\hat{\rho}_{M_{\text{env}}}^{\text{th}}) = g(M_{\text{env}}), \quad (\text{B.4})$$

B. Entropy of Gaussian states

where

$$g(x) = \begin{cases} (x+1) \log_2(x+1) - x \log_2(x), & x > 0, \\ 0, & x = 0. \end{cases} \quad (\text{B.5})$$

is a concave function. Let a state $\hat{\rho}^{\text{th}(n)}$ be an n -mode thermal state, i.e. a Gaussian state with CM

$$\mathbf{V}_{\text{th}}^{(n)} = \text{diag} \left(M_{\text{env}1} + \frac{1}{2}, M_{\text{env}2} + \frac{1}{2}, \dots, M_{\text{env}n} + \frac{1}{2}; M_{\text{env}1} + \frac{1}{2}, \dots, M_{\text{env}n} + \frac{1}{2} \right). \quad (\text{B.6})$$

This state can be decomposed as

$$\hat{\rho}^{\text{th}(n)} = \hat{\rho}_{M_{\text{env},1}}^{\text{th}} \otimes \hat{\rho}_{M_{\text{env},2}}^{\text{th}} \otimes \dots \otimes \hat{\rho}_{M_{\text{env},n}}^{\text{th}}, \quad (\text{B.7})$$

where $\hat{\rho}_{M_{\text{env},i}}^{\text{th}}$ is a one-mode thermal state with thermal photon number $M_{\text{env}i}$. Thus, its entropy is additive, i.e.

$$S \left(\hat{\rho}^{\text{th}(n)} \right) = \sum_{i=1}^n S \left(\hat{\rho}_{M_{\text{env},i}}^{\text{th}} \right) = \sum_{i=1}^n g \left(\nu_i - \frac{1}{2} \right), \quad (\text{B.8})$$

where $\nu_i = M_{\text{env}i} + 1/2$ are the symplectic eigenvalues [see Sec. 5.2.1] of each one-mode thermal state. It is straightforward to argue why Eq. (B.8) is valid for an arbitrary n -mode Gaussian state. We stated in Sec. 5.2.1 that there exists a symplectic transformation \mathbf{M} which realizes a symplectic diagonalization of a given covariance matrix \mathbf{V} , i.e.

$$\mathbf{M}\mathbf{V}\mathbf{M}^{\text{T}} = \text{diag}(\nu_1, \nu_2, \dots, \nu_n; \nu_1, \nu_2, \dots, \nu_n). \quad (\text{B.9})$$

Since a symplectic transformation \mathbf{V} corresponds to a unitary transformation \hat{U}_{G} on the density operator $\hat{\rho}^{\text{G}}$ of the Gaussian state its entropy is left invariant, i.e.

$$S \left(\hat{\rho}^{\text{G}}(\mathbf{M}\mathbf{V}\mathbf{M}) \right) = S \left(\hat{U}_{\text{G}} \hat{\rho}^{\text{G}} \hat{U}_{\text{G}} \right) = S \left(\hat{\rho}^{\text{G}}(\mathbf{V}) \right). \quad (\text{B.10})$$

Therefore, one can directly calculate the entropy of the Gaussian state with its CM in the diagonal symplectic form $\mathbf{M}\mathbf{V}\mathbf{M}^{\text{T}}$ which is then simply given by Eq. (B.8). An alternative proof using the definition of the g function can be found in [HSH99].

C. Gaussian Operations and Choi-Jamiolkowski Isomorphism

We discuss in the following the general form of Gaussian operations. The basic idea is to extend the Choi-Jamiolkowski isomorphism (recall Sec. 3.2) that was introduced in [Fiu02, GI02] for a finite sized Hilbert space to Gaussian states and operations that live in an infinite dimensional Hilbert space. It consists of replacing the positive operator stated in Eq. (3.19) by a Gaussian operator as well as the maximally entangled state of finite dimension⁹ by a maximally entangled Gaussian state. In this section we discuss the equivalence for the ordering $\hat{\mathbf{R}} = \hat{\mathbf{R}}^{(\text{qp})}$.

Let Φ be a completely positive map which maps n -mode Gaussian input states with quadratures $\hat{\mathbf{R}}_{\text{in}}^{(\text{qp})}$ and CM \mathbf{V}_{in} to n -mode Gaussian output states¹ with quadratures $\hat{\mathbf{R}}_{\text{out}}^{(\text{qp})}$ and CM \mathbf{V}_{out} , where furthermore $\mathbb{I} \otimes \Phi$ maps Gaussian states to Gaussian states. In order to formulate the Choi-Jamiolkowski isomorphism for Gaussian states one replaces in Eq. (3.23) the state $|\Phi^+\rangle$ by a tensor product of n EPR pairs (maximally entangled two-mode squeezed vacua) and the map Ψ by Φ so that the operator \hat{O}_{AB} becomes a Gaussian state \hat{O}_{AB}^G . Effectively, this states that Gaussian CP maps are Jamiolkowski-isomorphic (or Choi-isomorphic) to bipartite Gaussian quantum states \hat{O}_{AB}^G , where we group its quadratures in the vector $\hat{\mathbf{R}}_{AB}^{(\text{qp})} = (\hat{\mathbf{R}}_A^{(\text{qp})}, \hat{\mathbf{R}}_B^{(\text{qp})})^\top$. The bipartite Gaussian state \hat{O}_{AB}^G is completely characterized by its first moments \mathbf{d}_{AB} and its covariance matrix

$$\mathbf{\Gamma} = \begin{pmatrix} \mathbf{V}_A^{(\text{qp})} & \mathbf{C} \\ \mathbf{C}^\top & \mathbf{V}_B^{(\text{qp})} \end{pmatrix}, \quad (\text{C.1})$$

where $\mathbf{V}_A^{(\text{qp})}$ stands for the CM that maps the input modes, $\mathbf{V}_B^{(\text{qp})}$ for the CM that maps the output modes and \mathbf{C} contains the input-output correlations. Then, the output state of the Gaussian map Φ is given by the Wigner function

$$W(\mathbf{R}_{\text{out}}^{(\text{qp})}) = \frac{1}{(2\pi)^n} \int d^n \mathbf{R}_A^{(\text{qp})} W_\Phi(\mathbf{R}_{\text{in}}^{(\text{qp})}, \mathbf{R}_{\text{out}}^{(\text{qp})}) W(\tilde{\mathbf{X}} \mathbf{R}_{\text{in}}^{(\text{qp})}), \quad (\text{C.2})$$

where $\tilde{\mathbf{X}} = \text{diag}(1, -1, 1, -1, \dots, 1, -1)$ represent the transposition in phase-space ($q_j \rightarrow q_j, p_j \rightarrow -p_j$) and W_Φ is the Gaussian Wigner function with CM $\mathbf{\Gamma}$ associated to the state \hat{O}_{AB}^G . Then, after several simplifications one finds for a given input CM \mathbf{V}_{in} the CM of the output state

$$\mathbf{V}_{\text{out}}^{(\text{qp})} = \mathbf{V}_B^{(\text{qp})} - \mathbf{C}^\top (\mathbf{V}_A^{(\text{qp})} + \tilde{\mathbf{X}} \mathbf{V}_{\text{in}}^{(\text{qp})} \tilde{\mathbf{X}})^{-1} \mathbf{C}. \quad (\text{C.3})$$

¹In Sec. 5.3 we properly introduce completely positive trace-preserving maps for which we use the same symbol Φ .

C. Gaussian Operations and Choi-Jamiolkowski Isomorphism

For a more detailed derivation consider Refs. [[Fiu02](#), [GI02](#)].

D. Calculations with Lagrange multiplier method

D.1. Solution below input energy threshold

In the following we treat the Lagrange multiplier problem of Sec. 6.4.3. The Lagrangian is given by

$$\mathcal{L} = g(\bar{M}_{\text{out}}) - g(M_{\text{out}}) - \frac{\bar{\beta}}{\ln 2} \left(\frac{1}{2} \left(i_{\text{q}} + \frac{1}{4i_{\text{q}}} + m_{\text{q}} + m_{\text{p}} \right) - \bar{N} - \frac{1}{2} \right), \quad (\text{D.1})$$

and the gradient is given by

$$\nabla \mathcal{L} = 0, \quad \nabla = \left(\frac{\partial}{\partial i_{\text{q}}}, \frac{\partial}{\partial m_{\text{q}}}, \frac{\partial}{\partial m_{\text{p}}} \right)^{\text{T}}. \quad (\text{D.2})$$

Equation $\nabla \mathcal{L} = 0$ is equivalent to the system of equations

$$\frac{\partial \mathcal{L}}{\partial i_{\text{q}}} = g'(\bar{M}_{\text{out}}) \frac{\partial \bar{M}_{\text{out}}}{\partial i_{\text{q}}} - g'(M_{\text{out}}) \frac{\partial M_{\text{out}}}{\partial i_{\text{q}}} - \frac{\bar{\beta}}{2 \ln 2} \left(1 - \frac{1}{4i_{\text{q}}^2} \right) = 0, \quad (\text{D.3})$$

$$\frac{\partial \mathcal{L}}{\partial m_{\text{q}}} = g'(\bar{M}_{\text{out}}) \frac{\partial \bar{M}_{\text{out}}}{\partial m_{\text{q}}} - \frac{\bar{\beta}}{2 \ln 2} = 0, \quad (\text{D.4})$$

$$\frac{\partial \mathcal{L}}{\partial m_{\text{p}}} = g'(\bar{M}_{\text{out}}) \frac{\partial \bar{M}_{\text{out}}}{\partial m_{\text{p}}} - \frac{\bar{\beta}}{2 \ln 2} = 0., \quad (\text{D.5})$$

where $M_{\text{out}} = \sqrt{v_{\text{q}} v_{\text{p}}} - 1/2$, $\bar{M}_{\text{out}} = \sqrt{\bar{v}_{\text{q}} \bar{v}_{\text{p}}} - 1/2$ and

$$\begin{aligned} v_{\text{q}} &= |\tau| i_{\text{q}} + y e^{2s}, & v_{\text{p}} &= |\tau| \frac{1}{4i_{\text{q}}} + y e^{-2s}, \\ \bar{v}_{\text{q}} &= |\tau| (i_{\text{q}} + m_{\text{q}}) + y e^{2s}, & \bar{v}_{\text{p}} &= |\tau| \left(\frac{1}{4i_{\text{q}}} + m_{\text{p}} \right) + y e^{-2s}. \end{aligned} \quad (\text{D.6})$$

We can rewrite M_{out} and \bar{M}_{out} (given in Eq. (6.122)) as

$$\begin{aligned} M_{\text{out}} &= \sqrt{\frac{\tau^2}{4} + i_{\text{q}} |\tau| y e^{-2s} + i_{\text{p}} |\tau| y e^{2s} + y^2} - \frac{1}{2}, \\ \bar{M}_{\text{out}} &= \left[i_{\text{q}} (\tau^2 m_{\text{p}} + |\tau| y e^{-2s}) + \frac{1}{4i_{\text{q}}} (\tau^2 m_{\text{q}} + |\tau| y e^{2s}) \right. \\ &\quad \left. + m_{\text{q}} (\tau^2 m_{\text{p}} + |\tau| y e^{-2s}) + m_{\text{p}} |\tau| y e^{2s} + \frac{\tau^2}{4} + y^2 \right]^{\frac{1}{2}} - \frac{1}{2}. \end{aligned} \quad (\text{D.7})$$

D. Calculations with Lagrange multiplier method

Then, we find the following derivatives

$$\begin{aligned}
\frac{\partial \bar{M}_{\text{out}}}{\partial i_{\text{q}}} &= \frac{|\tau|}{2(\bar{M}_{\text{out}} + \frac{1}{2})} \left[|\tau| \left(m_{\text{p}} - \frac{m_{\text{q}}}{4i_{\text{q}}^2} \right) + y \left(e^{-2s} - \frac{e^{2s}}{4i_{\text{q}}^2} \right) \right] = \frac{|\tau|}{2(\bar{M}_{\text{out}} + \frac{1}{2})} \left(\bar{v}_{\text{p}} - \frac{\bar{v}_{\text{q}}}{4i_{\text{q}}^2} \right), \\
\frac{\partial M_{\text{out}}}{\partial i_{\text{q}}} &= \frac{|\tau|y}{2(M_{\text{out}} + \frac{1}{2})} \left(e^{-2s} - \frac{e^{2s}}{4i_{\text{q}}^2} \right), \\
\frac{\partial \bar{M}_{\text{out}}}{\partial m_{\text{q}}} &= \frac{|\tau|}{2(\bar{M}_{\text{out}} + \frac{1}{2})} \left[|\tau| \left(\frac{1}{4i_{\text{q}}} + m_{\text{p}} \right) + y e^{-2s} \right] = \frac{|\tau|\bar{v}_{\text{p}}}{2(\bar{M}_{\text{out}} + \frac{1}{2})}, \\
\frac{\partial \bar{M}_{\text{out}}}{\partial m_{\text{p}}} &= \frac{|\tau|}{2(\bar{M}_{\text{out}} + \frac{1}{2})} (|\tau|(i_{\text{q}} + m_{\text{q}}) + y e^{2s}) = \frac{|\tau|\bar{v}_{\text{q}}}{2(\bar{M}_{\text{out}} + \frac{1}{2})}.
\end{aligned} \tag{D.8}$$

Equalizing equations (D.4) and (D.5) yields the quantum water-filling solution [previously derived in Sec. 6.4.1]

$$\bar{v}_{\text{q}} = \bar{v}_{\text{p}}. \tag{D.9}$$

Then we can use Eq. (D.5) to obtain the Lagrange multiplier, that is

$$\bar{\beta} = \frac{g'(\bar{M}_{\text{out}}) \ln 2}{(\bar{M}_{\text{out}} + \frac{1}{2})} |\tau| \bar{v}_{\text{q}}. \tag{D.10}$$

We inject $\bar{\beta}$ in Eq. (D.3) which simplifies together with (D.8) to the equation

$$\frac{g'(\bar{M}_{\text{out}})}{(\bar{M}_{\text{out}} + \frac{1}{2})} (\bar{v}_{\text{p}} - \bar{v}_{\text{q}}) = \frac{g'(M_{\text{out}})}{(M_{\text{out}} + \frac{1}{2})} y \left(e^{-2s} - \frac{e^{2s}}{4i_{\text{q}}^2} \right). \tag{D.11}$$

Since $\bar{v}_{\text{p}} - \bar{v}_{\text{q}} = 0$ we find the solution

$$i_{\text{q}} = \frac{1}{2} e^{2s}. \tag{D.12}$$

We showed previously in Sec. 6.4.1 that this is the optimal squeezing that minimizes the second term of χ^{G} .

For $\bar{N} < \bar{N}_{\text{thr}}$ the Lagrange multiplier problem is modified where

$$\nabla = \left(\frac{\partial}{\partial i_{\text{q}}}, \frac{\partial}{\partial m_{\text{p}}} \right)^{\text{T}}. \tag{D.13}$$

In this case Eq. (D.4) is replaced by $m_{\text{q}} = 0$. We obtain $\bar{\beta}$ again by Eq. (D.10), and inserting it in Eq. (D.8) leads to Eq. (D.11). However, the quantum water-filling solution is no longer applicable to this equation (see discussion in Sec. 6.4.3).

D.2. Solution for frequency parametrization

Now we present the solution for the frequency parametrization introduced in Sec. 6.4.5 for $\bar{N} < \bar{N}_{\text{thr}}$.

D.2. Solution for frequency parametrization

In order to express the parameters M_{out} and \bar{M}_{out} in terms of the new variables we need to make the following substitutions:

$$e^{2s} = \omega_{\text{env}}^{-1}, \quad i_{\text{q}} = \frac{1}{2}\omega_{\text{in}}^{-1}, \quad i_{\text{q}} + m_{\text{q}} = \left(\bar{M}_{\text{in}} + \frac{1}{2}\right)\bar{\omega}_{\text{in}}^{-1}, \quad i_{\text{p}} + m_{\text{p}} = \left(\bar{M}_{\text{in}} + \frac{1}{2}\right)\bar{\omega}_{\text{in}}. \quad (\text{D.14})$$

Since for $\bar{N} < \bar{N}_{\text{thr}}$ we have $m_{\text{q}} = 0$ (where without loss of generality we choose here $s > 0$) it follows that

$$\left(\bar{M}_{\text{in}} + \frac{1}{2}\right) \frac{1}{\bar{\omega}_{\text{in}}} = \frac{1}{2\omega_{\text{in}}}, \quad \bar{N} < \bar{N}_{\text{thr}}. \quad (\text{D.15})$$

Then, we can express the number of thermal photons at the output and modulated output, respectively, as

$$\begin{aligned} M_{\text{out}} &= \sqrt{\frac{\tau^2}{4} + y^2 + \frac{y|\tau|}{2} \left(\frac{\omega_{\text{env}}^2 + \omega_{\text{in}}^2}{\omega_{\text{env}}\omega_{\text{in}}}\right)} - \frac{1}{2}, \\ \bar{M}_{\text{out}} &= \sqrt{\left(\frac{|\tau|}{2\omega_{\text{in}}} + \frac{y}{\omega_{\text{env}}}\right) \left(\frac{|\tau|\bar{\omega}_{\text{in}}^2}{2\omega_{\text{in}}} + y\omega_{\text{env}}\right)}, \quad \bar{N} < \bar{N}_{\text{thr}}. \end{aligned} \quad (\text{D.16})$$

Note, that furthermore

$$\begin{aligned} \omega_{\text{out}} &= \frac{1}{M_{\text{out}} + \frac{1}{2}} \left(\frac{|\tau|\omega_{\text{in}}}{2} + y\omega_{\text{env}}\right), \\ \omega_{\text{out}}^{-1} &= \frac{1}{M_{\text{out}} + \frac{1}{2}} \left(\frac{|\tau|}{2\omega_{\text{in}}} + \frac{y}{\omega_{\text{env}}}\right). \end{aligned} \quad (\text{D.17})$$

We choose as degrees of freedoms now ω_{in} and $\bar{\omega}_{\text{out}}$, i.e.

$$\nabla = \left(\frac{\partial}{\partial\omega_{\text{in}}}, \frac{\partial}{\partial\bar{\omega}_{\text{out}}}\right)^{\text{T}}. \quad (\text{D.18})$$

The Lagrangian [stated in Eq. (6.175)] reads

$$\mathcal{L} = g(\bar{M}_{\text{out}}) - g(M_{\text{out}}) - \frac{\bar{\beta}_{\text{out}}}{\ln 2} \left(\frac{1}{2} \left(\bar{M}_{\text{out}} + \frac{1}{2}\right) (\bar{\omega}_{\text{out}}^{-1} + \bar{\omega}_{\text{out}}) - \bar{N}_{\text{out}} - \frac{1}{2}\right), \quad (\text{D.19})$$

where \bar{N}_{out} is given by Eq. (6.176). Then, the system of equations $\nabla\mathcal{L} = 0$ simplifies with the help of Eqs. (D.16) and (D.17) to the two equations:

$$\begin{aligned} \frac{\partial\mathcal{L}}{\partial\omega_{\text{in}}} &= g'(\bar{M}_{\text{out}}) \frac{\partial\bar{M}_{\text{out}}}{\partial\omega_{\text{in}}} - g'(M_{\text{out}}) \frac{\partial M_{\text{out}}}{\partial\omega_{\text{in}}} \\ &\quad - \frac{\bar{\beta}_{\text{out}}}{2\ln 2} \left(\frac{1}{\bar{\omega}_{\text{out}}} + \bar{\omega}_{\text{out}}\right) \frac{\partial\bar{M}_{\text{out}}}{\partial\omega_{\text{in}}} = 0, \end{aligned} \quad (\text{D.20})$$

$$\begin{aligned} \frac{\partial\mathcal{L}}{\partial\bar{\omega}_{\text{out}}} &= g'(\bar{M}_{\text{out}}) \frac{\partial\bar{M}_{\text{out}}}{\partial\bar{\omega}_{\text{out}}} - \frac{\bar{\beta}_{\text{out}}}{2\ln 2} \left(\frac{\partial\bar{M}_{\text{out}}}{\partial\bar{\omega}_{\text{out}}}\right) \left(\frac{1}{\bar{\omega}_{\text{out}}} + \bar{\omega}_{\text{out}}\right) \\ &\quad + \frac{\bar{\beta}_{\text{out}}}{2\ln 2} \left[\bar{M}_{\text{out}} \left(1 - \frac{1}{\bar{\omega}_{\text{out}}^2}\right) + \frac{1}{2} \left(1 - \frac{1}{\bar{\omega}_{\text{out}}^2}\right)\right] = 0. \end{aligned} \quad (\text{D.21})$$

D. Calculations with Lagrange multiplier method

For the individual derivatives we find

$$\begin{aligned}\frac{\partial M_{\text{out}}}{\partial \omega_{\text{in}}} &= -\frac{|\tau|(\omega_{\text{out}}^2 - \omega_{\text{in}}^2)}{4\omega_{\text{in}}^2 \omega_{\text{out}}}, \\ \frac{\partial \bar{M}_{\text{out}}}{\partial \omega_{\text{in}}} &= -\frac{|\tau|\bar{\omega}_{\text{out}}}{2\omega_{\text{in}}^2}, \\ \frac{\partial \bar{M}_{\text{out}}}{\partial \bar{\omega}_{\text{out}}} &= \left(\bar{M}_{\text{out}} + \frac{1}{2}\right) \frac{1}{\bar{\omega}_{\text{out}}}.\end{aligned}\tag{D.22}$$

Then, Eq. (D.21) simplifies to the Bose-Einstein statistics

$$\bar{M}_{\text{out}} = \frac{1}{e^{\bar{\omega}_{\text{out}}\bar{\beta}_{\text{out}}} - 1},\tag{D.23}$$

and after a couple of algebraic simplifications of Eq. (D.20) one obtains the ‘‘resonance’’ equation given by

$$\bar{\omega}_{\text{out}} = \sqrt{1 - \frac{\beta_{\text{out}}}{\bar{\beta}_{\text{out}}} (\omega_{\text{in}}^2 - \omega_{\text{out}}^2)}.\tag{D.24}$$

In order to solve Eq. (D.24) one needs to express all parameters as functions of ω_{in} and the channel parameters $(\tau, y, \omega_{\text{env}}, \bar{N})$. Explicitly, those relations read:

$$\begin{aligned}\omega_{\text{in}} &= \frac{|\tau|}{2} \left(\frac{2\bar{N}_{\text{out}} + 1}{1 + \bar{\omega}_{\text{out}}^2} - \frac{y}{\omega_{\text{env}}} \right)^{-1}, \\ \omega_{\text{out}} &= \sqrt{\frac{|\tau|\omega_{\text{in}} + 2y\omega_{\text{env}}}{\frac{|\tau|}{\omega_{\text{in}}} + \frac{2y}{\omega_{\text{env}}}}}, \\ \bar{\omega}_{\text{out}} &= \sqrt{\frac{2\omega_{\text{in}}\omega_{\text{env}}[y\omega_{\text{env}} + |\tau|(2\bar{N} + 1)] - |\tau|\omega_{\text{env}}}{2y\omega_{\text{in}} + |\tau|\omega_{\text{env}}}}, \\ \bar{M}_{\text{out}} &= \frac{2\bar{N}_{\text{out}} + 1}{\bar{\omega}_{\text{out}} + \bar{\omega}_{\text{out}}^{-1}} - \frac{1}{2}.\end{aligned}\tag{D.25}$$

Now let us treat the extended problem where also an optimization over the noise frequency is performed, i.e.

$$\nabla = \left(\frac{\partial}{\partial \omega_{\text{in}}}, \frac{\partial}{\partial \bar{\omega}_{\text{out}}}, \frac{\partial}{\partial \omega_{\text{env}}} \right)^{\top}.\tag{D.26}$$

The Lagrangian reads as in (D.19) but since the output energy constraint \bar{N}_{out} also depends on ω_{env} we need to derive with respect to ω_{env} as well. We obtain the additional equation

$$\begin{aligned}\frac{\partial \mathcal{L}}{\partial \omega_{\text{env}}} &= \frac{\bar{\beta}_{\text{out}}\bar{\omega}_{\text{out}}}{\ln 2} \frac{\partial \bar{M}_{\text{out}}}{\partial \omega_{\text{env}}} - g'(M_{\text{out}}) \frac{\partial M_{\text{out}}}{\partial \omega_{\text{env}}} \\ &\quad - \frac{\bar{\beta}_{\text{out}}}{\ln 2} \left(\frac{1}{2}(\bar{\omega}_{\text{out}} + \bar{\omega}_{\text{out}}^{-1}) \frac{\partial \bar{M}_{\text{out}}}{\partial \omega_{\text{env}}} - \frac{\partial \bar{N}_{\text{out}}}{\partial \omega_{\text{env}}} \right) = 0.\end{aligned}\tag{D.27}$$

D.3. Proofs for the one-mode fiducial channel with $\tau = 1$

First, we find that

$$\begin{aligned}\frac{\partial M_{\text{out}}}{\partial \omega_{\text{env}}} &= -\frac{y\bar{\omega}_{\text{out}}}{\omega_{\text{env}}^2}, \\ \frac{\partial \bar{M}_{\text{out}}}{\partial \omega_{\text{env}}} &= \frac{1}{2(M_{\text{out}} + \frac{1}{2})} \frac{y|\tau|}{2\omega_{\text{in}}} \left(1 - \frac{\omega_{\text{in}}^2}{\omega_{\text{env}}^2}\right), \\ \frac{\partial \bar{N}_{\text{out}}}{\partial \omega_{\text{env}}} &= y(1 - \omega_{\text{env}}^{-2}).\end{aligned}\tag{D.28}$$

After injecting those relations in Eq. (D.27) and several simplifications we find the new transcendental equation stated in Eq. (6.191)

D.3. Proofs for the one-mode fiducial channel with $\tau = 1$

The following relations are derived for the one-mode fiducial channel with $\tau = 1$ and parametrization $\mathbf{Y} = \text{diag}(y_{\text{q}}, y_{\text{p}})$. We choose without loss of generality $y_{\text{q}} > y_{\text{p}}$. For the parametrization $\mathbf{Y} = \text{diag}(ye^{2s}, ye^{-2s})$ this choice corresponds to $s > 0$.

D.3.1. Bounds below the threshold

Lemma 6. *For the one-mode fiducial channel Φ^{F} with $\tau = 1$, $y_{\text{q}} > y_{\text{p}}$ and input energy $\lambda < \lambda_{\text{thr}}$ the solution to the optimization problem implies*

$$\bar{v}_{\text{p}} \geq 1/2.\tag{D.29}$$

Proof. For $\lambda < \lambda_{\text{thr}}$ (or equivalently $\bar{N} < \bar{N}_{\text{thr}}$) it follows that $m_{\text{q}} = 0$ and the solution is given by the solution of Eq. (D.11) which reads in the alternative parametrization

$$\frac{g'(\bar{\nu}_{\text{out}} - \frac{1}{2})}{\bar{\nu}_{\text{out}}} (\bar{v}_{\text{p}} - \bar{v}_{\text{q}}) = \frac{g'(\nu_{\text{out}} - \frac{1}{2})}{\nu_{\text{out}}} \left(y_{\text{p}} - \frac{y_{\text{q}}}{4i_{\text{q}}^2}\right).\tag{D.30}$$

Now, we recall inequalities (6.133) and (6.137):

$$|\bar{v}_{\text{p}} - \bar{v}_{\text{q}}| \geq \left|y_{\text{p}} - \frac{y_{\text{q}}}{4i_{\text{q}}^2}\right|,\tag{D.31}$$

$$\frac{1}{2} \leq i_{\text{q}} < \frac{1}{2} \sqrt{\frac{y_{\text{q}}}{y_{\text{p}}}}.\tag{D.32}$$

which imply that

$$\bar{v}_{\text{p}} < \bar{v}_{\text{q}}.\tag{D.33}$$

Furthermore, we can find a lower bound on \bar{v}_{p} . Suppose $\bar{v}_{\text{p}} < 1/2$, then we have

$$\begin{aligned}\frac{1}{\bar{\nu}_{\text{out}}} &= \frac{1}{\sqrt{\bar{v}_{\text{q}}\bar{v}_{\text{p}}}} > \frac{1}{\sqrt{\frac{1}{2}\bar{v}_{\text{q}}}} \\ \Rightarrow g'(\bar{\nu}_{\text{out}} - \frac{1}{2}) &> g'\left(\sqrt{\frac{1}{2}\bar{v}_{\text{q}}} - \frac{1}{2}\right),\end{aligned}\tag{D.34}$$

D. Calculations with Lagrange multiplier method

since $g'(x-1/2)$ is a monotonically decreasing function of x . Then can state the following bound on the left hand side of Eq. (D.30):

$$\frac{g'(\bar{\nu}_{\text{out}} - \frac{1}{2})}{\bar{\nu}_{\text{out}}} (\bar{v}_{\text{q}} - \bar{v}_{\text{p}}) > \frac{g'(\sqrt{\frac{1}{2}\bar{v}_{\text{q}}} - \frac{1}{2})}{\sqrt{\frac{1}{2}\bar{v}_{\text{q}}}} \left(\bar{v}_{\text{q}} - \frac{1}{2} \right) \quad (\text{D.35})$$

and by using (D.30) and the fact that below the threshold $\bar{v}_{\text{q}} = v_{\text{q}}$ we find

$$\frac{g'(\nu_{\text{out}} - \frac{1}{2})_{\Sigma}}{\nu_{\text{out}}} > \frac{g'(\sqrt{\frac{1}{2}v_{\text{q}}} - \frac{1}{2})}{\sqrt{\frac{1}{2}v_{\text{q}}}} \left(v_{\text{q}} - \frac{1}{2} \right) \quad (\text{D.36})$$

where

$$\Sigma = \frac{y_{\text{q}}}{4(i_{\text{q}})^2} - y_{\text{p}}. \quad (\text{D.37})$$

Thus, our assumption $\bar{v}_{\text{p}} < 1/2$ leads to an inequality which depends solely on $i_{\text{q}}, y_{\text{q}}, y_{\text{p}}$ with the constraints on i_{q} given by (D.32) and for the noise variances that $y_{\text{q}} > y_{\text{p}}, 0 \leq y_{\text{p}} \leq 1/2 - 1/(4i_{\text{q}})$. Since, inequality (D.36) is always violated for the given constraints, we come to a contradiction which proves the lemma. \square

D.3.2. Monotonicity of μ

Lemma 7. *The Lagrange multiplier μ of the Lagrangian defined in Eq. (7.33) with $n = 1$ is a monotonically decreasing function of the input energy λ on the solution, and moreover*

$$\frac{d\mu}{d\lambda} < 0. \quad (\text{D.38})$$

Proof. For $\lambda \geq \lambda_{\text{thr}}$ the quantum water-filling solution holds (see Eq. (6.86)) and μ is simply given by Eq. (7.43). Since $g'(x)$ is a monotonically decreasing function the lemma is proven for $\lambda \geq \lambda_{\text{thr}}$.

Now we prove the lemma for $\lambda < \lambda_{\text{thr}}$. Using Eq. (7.38) we can write

$$\frac{d\mu}{d\lambda} = g'' \left(\bar{\nu}_{\text{out}} - \frac{1}{2} \right) \frac{d\bar{\nu}}{d\lambda} \frac{\bar{v}_{\text{q}}}{2\bar{\nu}_{\text{out}}} + \frac{g'(\bar{\nu}_{\text{out}} - \frac{1}{2})}{2\bar{\nu}_{\text{out}}^2} \left(\frac{d\bar{v}_{\text{q}}}{d\lambda} \bar{\nu}_{\text{out}} - \bar{v}_{\text{q}} \frac{d\bar{\nu}_{\text{out}}}{d\lambda} \right). \quad (\text{D.39})$$

We can upper bound this quantity if we use the following property of $g(x)$:

$$-\frac{g'(\bar{\nu}_{\text{out}} - 1/2)}{\bar{\nu}_{\text{out}}} > g''(\bar{\nu}_{\text{out}} - 1/2). \quad (\text{D.40})$$

This leads to

$$\frac{d\mu}{d\lambda} < -\frac{g'(\bar{\nu}_{\text{out}} - \frac{1}{2})}{2\bar{\nu}_{\text{out}}^3} (\bar{v}_{\text{q}})^2 \frac{d\bar{v}_{\text{p}}}{d\lambda}. \quad (\text{D.41})$$

Since all factors in (D.41) except for $d\bar{v}_{\text{p}}/d\lambda$ are clearly positive the lemma will be proven if we show that

$$\frac{d\bar{v}_{\text{p}}}{d\lambda} = 1 - \frac{di_{\text{q}}}{d\lambda} > 0. \quad (\text{D.42})$$

D.3. Proofs for the one-mode fiducial channel with $\tau = 1$

This derivative can be expressed in terms of the function

$$F \equiv \frac{g'(\bar{\nu}_{\text{out}} - \frac{1}{2})}{2\bar{\nu}_{\text{out}}} (\bar{v}_{\text{p}} - \bar{v}_{\text{q}}) - \frac{g'(\nu_{\text{out}} - \frac{1}{2})}{2\nu_{\text{out}}} \left(v_{\text{p}} - \frac{i_{\text{p}}}{i_{\text{q}}} v_{\text{q}} \right). \quad (\text{D.43})$$

Indeed, when Eq. (D.30) holds then we have

$$\frac{di_{\text{q}}}{d\lambda} = -\frac{\frac{\partial F}{\partial \lambda}}{\frac{\partial F}{\partial i_{\text{q}}}}. \quad (\text{D.44})$$

We observe that

$$\begin{aligned} \frac{\partial F}{\partial \lambda} &= \frac{g''(\bar{\nu}_{\text{out}} - \frac{1}{2})}{4\bar{\nu}_{\text{out}}^2} \bar{v}_{\text{q}} (\bar{v}_{\text{p}} - \bar{v}_{\text{q}}) \\ &+ \frac{g'(\bar{\nu}_{\text{out}} - \frac{1}{2})}{4\bar{\nu}_{\text{out}}} \left(1 + \frac{(\bar{v}_{\text{q}})^2}{\bar{\nu}_{\text{out}}^2} \right) > 0, \end{aligned} \quad (\text{D.45})$$

because $g''(x) < 0$, $g'(x) > 0$ and $\bar{v}_{\text{q}} > \bar{v}_{\text{p}}$. Thus, in order to prove inequality Eq. (D.42) it suffices to prove that

$$\frac{\partial F}{\partial \lambda} + \frac{\partial F}{\partial i_{\text{q}}} < 0. \quad (\text{D.46})$$

By carrying out the partial derivatives we rewrite Eq. (D.46) in the form

$$-\frac{\eta}{4\bar{\nu}_{\text{out}}^3} \bar{v}_{\text{p}} (\bar{v}_{\text{q}} - \bar{v}_{\text{p}}) T_1 - \frac{1}{4\nu_{\text{out}}^3} T_2 < 0, \quad (\text{D.47})$$

where T_1 and T_2 denote the expressions

$$\begin{aligned} T_1 &= g''\left(\bar{\nu}_{\text{out}} - \frac{1}{2}\right) \frac{\bar{\nu}_{\text{out}}}{\eta} + g'\left(\bar{\nu}_{\text{out}} - \frac{1}{2}\right), \\ T_2 &= g''\left(\nu_{\text{out}} - \frac{1}{2}\right) \nu_{\text{out}} \zeta \\ &+ g'\left(\nu_{\text{out}} - \frac{1}{2}\right) \left(\frac{y_{\text{q}}}{(i_{\text{q}})^3} \nu_{\text{out}}^2 - \zeta \right), \end{aligned} \quad (\text{D.48})$$

and

$$\eta = \frac{\bar{v}_{\text{q}} + \bar{v}_{\text{p}}}{\bar{v}_{\text{q}} - \bar{v}_{\text{p}}}, \quad \zeta = \left(y_{\text{p}} - \frac{y_{\text{q}}}{4(i_{\text{q}})^2} \right)^2. \quad (\text{D.49})$$

Observe that all factors in front of T_1 and T_2 are positive, since $\bar{v}_{\text{p}}, \bar{\nu}_{\text{out}}, \nu_{\text{out}}, \bar{v}_{\text{q}} - \bar{v}_{\text{p}} > 0$. If we prove positivity of T_1 and T_2 , then inequality (D.47) will be proven as well as the lemma.

The positivity of T_1 can be verified via its partial derivatives with respect to $\bar{v}_{\text{q}}, \bar{v}_{\text{p}}$ which lead to:

$$\frac{\partial T_1}{\partial \bar{v}_{\text{q}}} = \{ \bar{v}_{\text{q}} + \bar{v}_{\text{p}} [3 - 4\bar{v}_{\text{p}}(\bar{v}_{\text{p}} + 3\bar{v}_{\text{q}})] \} T_{11}(\bar{v}_{\text{q}}, \bar{v}_{\text{p}}), \quad (\text{D.50})$$

D. Calculations with Lagrange multiplier method

$$\frac{\partial T_1}{\partial \bar{v}_p} = (\bar{v}_q - \bar{v}_p) T_{12}(\bar{v}_q, \bar{v}_p), \quad (\text{D.51})$$

where

$$\begin{aligned} T_{11}(\bar{v}_q, \bar{v}_p) &= \frac{4\sqrt{\bar{v}_q\bar{v}_p}}{(\bar{v}_q + \bar{v}_p)^3(1 - 4\bar{v}_q\bar{v}_p)^2} \\ T_{12}(\bar{v}_q, \bar{v}_p) &= \frac{4(\bar{v}_q)^2(1 + 4(\bar{v}_p)^2)}{\sqrt{\bar{v}_q\bar{v}_p}(\bar{v}_q + \bar{v}_p)^2(1 - 4\bar{v}_q\bar{v}_p)^2}. \end{aligned} \quad (\text{D.52})$$

Clearly the two functions $T_{11}(\bar{v}_q, \bar{v}_p)$ and $T_{12}(\bar{v}_q, \bar{v}_p)$ are positive for all $\bar{\gamma}^{q,p} > 0$. Then (D.51) is also positive since $\bar{v}_q - \bar{v}_p > 0$. From equations (D.33) and (D.29) we have that $\bar{v}_p \geq 1/2$, $\bar{v}_q \geq 1/2$. Then, for all these values of \bar{v}_q, \bar{v}_p it is easy to verify that the factor in front of $T_{11}(\bar{v}_q, \bar{v}_p)$ in Eq. (D.50) is negative. Thus,

$$\partial T_1 / \partial \bar{v}_q < 0, \quad \partial T_1 / \partial \bar{v}_p > 0 \quad (\text{D.53})$$

and T_1 takes its minimal value at the boundary of the allowed region for \bar{v}_q, \bar{v}_p , namely, at the point where \bar{v}_q is maximal and \bar{v}_p is minimal. Observe that for \mathcal{N}_2 using Eqs. (D.32), (D.33) and (D.29) we have

$$\frac{1}{2} < \bar{v}_p < \bar{v}_q < \frac{1}{2} \sqrt{\frac{y_q}{y_p}} + y_q. \quad (\text{D.54})$$

Then T_1 takes its minimal value for $\bar{v}_p^{\min} = 1/2$ and $\bar{v}_q^{\max} = \frac{1}{2} \sqrt{y_q/y_p} + y_q$. Therefore, if T_1 at this point is positive for all values of y_q, y_p then it is positive in the whole allowed region of \bar{v}_q and \bar{v}_p .

In order to evaluate T_1 at this point we derive it with respect to y_q, y_p and we find that

$$\begin{aligned} \frac{\partial}{\partial y_q} T_1|_{\bar{v}_q^{\max}, \bar{v}_p^{\min}} &< 0, \\ \frac{\partial}{\partial y_p} T_1|_{\bar{v}_q^{\max}, \bar{v}_p^{\min}} &> 0. \end{aligned} \quad (\text{D.55})$$

Then, again T_1 takes its minimal value at the point where y_q is maximal and y_p is minimal. At this limit point we find

$$T_1|_{y_q \rightarrow \infty, y_p \rightarrow 0} \rightarrow 0,$$

where the limit is reached from above. This proves that $T_1 > 0$.

Now we show that $T_2 > 0$ as well. We rewrite T_2 as

$$T_2 = \xi \left[(z^2 - 1)^2 \kappa(\nu_{\text{out}}) + \frac{8\nu_{\text{out}}^2 z}{\nu_{\text{env}}} \right] \quad (\text{D.56})$$

D.3. Proofs for the one-mode fiducial channel with $\tau = 1$

where

$$z = \frac{i_q}{\gamma_{\text{in(thr)}}, \quad \xi = \frac{g'(\nu_{\text{out}} - \frac{1}{2})(\gamma_{\text{env}}^p)^2}{z^4}, \quad (\text{D.57})$$

$$\kappa(\nu_{\text{out}}) = \frac{g''(\nu_{\text{out}} - \frac{1}{2})}{g'(\nu_{\text{out}} - \frac{1}{2})}\nu_{\text{out}} - 1,$$

where $\gamma_{\text{in(thr)}},^q$ was defined in Eq. (D.32) and therefore $0 \leq z < 1$. Using these notations we express

$$\nu_{\text{out}} = \sqrt{1/4 - \nu_{\text{env}}/2(z + 1/z) + \nu_{\text{env}}^2} \quad (\text{D.58})$$

and since $\xi > 0$ we can rewrite the desired inequality $T_2 > 0$ in the equivalent form

$$h(z, \nu_{\text{out}}) > -\frac{\kappa(\nu_{\text{out}})}{\nu_{\text{out}}^2}, \quad (\text{D.59})$$

where

$$h(z, \nu_{\text{out}}) = \frac{32z^2}{(\sqrt{(1-z^2)^2 + 16z^2\nu_{\text{out}}^2} - 1 - z^2)(1-z^2)^2}. \quad (\text{D.60})$$

We observe that

$$\lim_{z \rightarrow 0} h(z, \nu_{\text{out}}) = \frac{16}{4\nu_{\text{out}}^2 - 1}. \quad (\text{D.61})$$

It is easy to check that the inequality

$$\frac{16}{4\nu_{\text{out}}^2 - 1} > -\frac{\kappa(\nu_{\text{out}})}{\nu_{\text{out}}^2}, \quad (\text{D.62})$$

holds $\forall \nu_{\text{out}} \geq 1/2$. Thus, if $\partial h(z, \nu_{\text{out}})/\partial z > 0$ holds for all ν_{out} and z in the allowed region then the desired inequality (D.59) holds. We find that

$$\frac{\partial h(z, \nu_{\text{out}})}{\partial z} = 64z \frac{a(z, \nu_{\text{out}})}{b(z, \nu_{\text{out}})}, \quad (\text{D.63})$$

where

$$a(z, \nu_{\text{out}}) = -1 - 8z^2\nu_{\text{out}}^2 - 3z^4(8\nu_{\text{out}}^2 - 1) - 2z^6$$

$$+ l(z, \nu_{\text{out}})(1 + z^2 + 2z^4),$$

$$b(z, \nu_{\text{out}}) = (z^2 - 1)^3 l(z, \nu_{\text{out}})(1 + z^2 - l(z, \nu_{\text{out}}))^2, \quad (\text{D.64})$$

$$l(z, \nu_{\text{out}}) = \sqrt{1 + z^4 + 2z^2(8\nu_{\text{out}}^2 - 1)}.$$

Clearly $b(z, \nu_{\text{out}})$ is negative and therefore, if $a(z, \nu_{\text{out}})$ is negative as well then

$$\frac{\partial h(z, \nu_{\text{out}})}{\partial z} > 0. \quad (\text{D.65})$$

Since the first line in $a(z, \nu_{\text{out}})$ in Eq. (D.64) is negative in the allowed region of ν_{out} and z , and the second line is positive we can make a comparison of squares of the first and second line, which confirms that indeed $a(z, \nu_{\text{out}}) < 0$. Thus, $T_2 > 0$, as well as $T_1 > 0$ which proves (D.46) which means that (D.42) holds and thus, the Lemma is proven. \square

D. Calculations with Lagrange multiplier method

Since we proved that Eq. (D.46) holds it follows that

$$\frac{\partial F(i_q)}{\partial i_q} < 0, \quad (\text{D.66})$$

which implies that there is only one solution for the equation $F(i_q) = 0$. Additionally by combining Eqs. (D.44), (D.45) and (D.46) we conclude that

$$\frac{di_q}{d\lambda} > 0. \quad (\text{D.67})$$

This means that the anti-squeezing in the more noisy quadrature is always increasing until the squeezing value at $\lambda = \lambda_{\text{thr}}$ is reached.

D.3.3. Concavity of the Holevo χ^G -quantity in λ

Lemma 8. *The Holevo χ^G -quantity given by Eq. (5.90) with $\tau = 1$ and $n = 1$ is a concave function of λ , on the solution of the optimization problem.*

Proof. For $\lambda \geq \lambda_{\text{thr}}$ we find that i_q is given by (6.84) and independent of λ . Therefore, we conclude from Eq. (6.86) that χ^G is on the solution a function of only one variable λ . Then, at the extremum of \mathcal{L} the second partial derivative of χ^G with respect to λ is equal to the total second derivative, which reads

$$\frac{d^2\chi^G}{d\lambda^2} = \frac{\partial^2\chi^G}{\partial\lambda^2} = \frac{g''(\bar{\nu}_{\text{wf}} - \frac{1}{2})}{4} < 0. \quad (\text{D.68})$$

Thus, we have shown that above the threshold χ^G is a concave function of λ .

For an input energy λ below the threshold, i_q depends on λ via the implicit function given by Eq. (D.30). Therefore, the total second derivative of χ^G with respect to λ has to take into account this dependence. Now this reads

$$\begin{aligned} \frac{d^2\chi^G}{d\lambda^2} &= \frac{\partial^2\chi^G}{\partial\lambda^2} + \frac{\partial^2\chi^G}{\partial\lambda\partial i_q} \frac{di_q}{d\lambda} + \frac{\partial\chi^G}{\partial i_q} \frac{d^2i_q}{d\lambda^2} \\ &+ \left(\frac{\partial^2\chi^G}{\partial\lambda\partial i_q} + \frac{\partial^2\chi^G}{\partial(i_q)^2} \frac{di_q}{d\lambda} \right) \frac{di_q}{d\lambda}. \end{aligned} \quad (\text{D.69})$$

One can easily show using that $\partial\chi^G/\partial\lambda = \mu$ and by Eq. (D.43) it follows that $\partial\chi^G/\partial i_q = F$. Thus, Eq. (D.69) simplifies on the solution to

$$\frac{d^2\chi^G}{d\lambda^2} = \frac{d\mu}{d\lambda} < 0, \quad (\text{D.70})$$

as proven in Appendix D.3.2, which proves the lemma. \square

D.3.4. Optimal noise distribution for one-mode

Lemma 9. C_χ^G of the one-mode fiducial channel $\Phi_{(1,y,s)}^F$, with parametrization $y = \sqrt{y_q y_p}$ and $y_q = y e^{2s}, y_p = y e^{-2s}, \bar{N} > 0$ and noise constraint $y_p = 2N - y_q$ is monotonically increasing with y_q , i.e.

$$\frac{\partial C_\chi^G}{\partial y_q} > 0. \quad (\text{D.71})$$

Proof. We first consider the case $\bar{N} \geq \bar{N}_{\text{thr}}$. In this case we have [see Eq. (6.81)]

$$C_\chi^G = g(\bar{N} + N) - g(y_q[2N - y_q]). \quad (\text{D.72})$$

Since the first term is independent of y_q and the second term is monotonically decreasing with y_q the lemma is proven for $\bar{N} \geq \bar{N}_{\text{thr}}$. Now consider the case $\bar{N} < \bar{N}_{\text{thr}}$. We assume without loss of generality that $y_q > y_p$ which implies $m_q = 0$. The two symplectic eigenvalues with the above parametrization and noise constraint read

$$\begin{aligned} \nu_{\text{out}} &= \sqrt{(i_q + y_q) \left(\frac{1}{4i_q} + 2N - y_q \right)}, \\ \bar{\nu}_{\text{out}} &= \sqrt{(i_q + y_q)(\lambda - i_q + 2N - y_q)}, \end{aligned} \quad (\text{D.73})$$

where $\lambda = i_q + 1/(4i_q) + m_p$. Now we carry out the full derivate of χ^G with respect to y_q :

$$\begin{aligned} \frac{\partial \chi^G}{\partial y_q} &= \frac{g'(\bar{\nu}_{\text{out}} - 1/2)}{2\bar{\nu}_{\text{out}}} \left(\bar{v}_p \left(\frac{\partial i_q}{\partial y_q} + 1 \right) + \bar{v}_q \left(-\frac{\partial i_q}{\partial y_q} - 1 \right) \right) \\ &\quad - \frac{g'(\nu_{\text{out}} - 1/2)}{2\nu_{\text{out}}} \left(v_p \left(\frac{\partial i_q}{\partial y_q} + 1 \right) + v_q \left(-\frac{1}{4i_q^2} \frac{\partial i_q}{\partial y_q} - 1 \right) \right) \\ &= \frac{\partial i_q}{\partial y_q} \underbrace{\left(\frac{g'(\bar{\nu}_{\text{out}} - 1/2)}{2\bar{\nu}_{\text{out}}} (\bar{v}_p - \bar{v}_q) - \frac{g'(\nu_{\text{out}} - 1/2)}{2\nu_{\text{out}}} \left(v_p - \frac{v_q}{4i_q^2} \right) \right)}_{= \frac{\partial \chi^G}{\partial i_q}, \text{Eq. (7.37)}} \\ &\quad + \underbrace{\frac{g'(\bar{\nu}_{\text{out}} - 1/2)}{2\bar{\nu}_{\text{out}}} (\bar{v}_p - \bar{v}_q) - \frac{g'(\nu_{\text{out}} - 1/2)}{2\nu_{\text{out}}} (v_p - v_q)}_{= \frac{\partial \chi^G}{\partial i_q} + v_q \frac{g'(\nu_{\text{out}} - 1/2)}{2\nu_{\text{out}}} \left(1 - \frac{1}{4i_q^2} \right)} \\ &= \frac{\partial \chi^G}{\partial i_q} \left(\frac{\partial i_q}{\partial y_q} + 1 \right) + v_q \frac{g'(\nu_{\text{out}} - 1/2)}{2\nu_{\text{out}}} \left(1 - \frac{1}{4i_q^2} \right). \end{aligned} \quad (\text{D.74})$$

Now we evaluate the derivate of C_χ^G with respect to y_q . Since we are on the solution it follows that $\frac{\partial \chi^G}{\partial i_q} = 0$. Then we obtain

$$\frac{\partial C_\chi^G}{\partial y_q} = \underbrace{v_q \frac{g'(\nu_{\text{out}} - 1/2)}{2\nu_{\text{out}}}}_{>0} \underbrace{\left(1 - \frac{1}{4i_q^2} \right)}_{>0} > 0, \quad (\text{D.75})$$

D. Calculations with Lagrange multiplier method

where the second term is positive due to inequality $i_q > 1/2$ stated in Eq. (6.137) (it is strictly greater since we imposed $\bar{N} > 0$). Thus, we proved that for a noise constraint $2N = y_q + y_p$ it is optimal to put all noise to one quadrature. \square

Bibliography

- [AE06] Gerardo Adesso and Marie Ericsson. Entanglement in Gaussian matrix-product states. *Physical Review A*, 74(3):030305, September 2006. [arXiv:quant-ph/0602067](#), [doi:10.1103/PhysRevA.74.030305](#). 8.1, 8.1, 8.1
- [AE07] Gerardo Adesso and Marie Ericsson. Optical implementation and entanglement distribution in Gaussian valence bond states. *Optics and Spectroscopy*, 103(2):178–186, August 2007. [arXiv:0704.1580](#), [doi:10.1134/S0030400X07080024](#). 8.1, 8.1, 8.1
- [AEPW02] K. Audenaert, J. Eisert, M. Plenio, and R. Werner. Entanglement properties of the harmonic chain. *Physical Review A*, 66(4):042327, October 2002. [arXiv:quant-ph/0205025](#), [doi:10.1103/PhysRevA.66.042327](#). 8.3
- [AF97] Fady Alajaji and Nariman Farvardin. Quantization of memoryless and Gauss-Markov sources over binary Markov channels. *IEEE Transactions on Communications*, 45(6):668–675, June 1997. [doi:10.1109/26.592605](#). 1.1
- [ASW10] Guillaume Aubrun, Stanisław Szarek, and Elisabeth Werner. Hastings’s Additivity Counterexample via Dvoretzky’s Theorem. *Communications in Mathematical Physics*, 305(1):85–97, November 2010. [arXiv:1003.4925](#), [doi:10.1007/s00220-010-1172-y](#). 3.4
- [BaH10] Fernando G. S. L. Brandão and Michał Horodecki. On Hastings’ Counterexamples to the Minimum Output Entropy Additivity Conjecture. *Open Systems Information Dynamics*, 17(01):31–52, March 2010. [arXiv:0907.3210](#), [doi:10.1142/S1230161210000047](#). 3.4
- [BAS⁺12] Sergio Boixo, Tameem Albash, Federico M Spedalieri, Nicholas Chancellor, and Daniel A Lidar. Experimental signature of programmable quantum annealing. page 12, December 2012. [arXiv:1212.1739](#). 2
- [BB84] Charles H. Bennett and Gilles Brassard. Quantum Cryptography: Public key distribution and coin tossing. In *Proceedings of the IEEE International Conference on Computers, Systems, and Signal Processing*, page 175, Bangalore, 1984. 1

BIBLIOGRAPHY

- [BBC⁺93] Charles H Bennett, Gilles Brassard, Claude Crépeau, Richard Jozsa, Asher Peres, and William K Wootters. Teleporting an unknown quantum state via dual classical and Einstein-Podolsky-Rosen channels. *Physical Review Letters*, 70(13):1895–1899, March 1993. doi:10.1103/PhysRevLett.70.1895. 5.2.3
- [BDM05] Garry Bowen, Igor Devetak, and Stefano Mancini. Bounds on classical information capacities for a class of quantum memory channels. *Physical Review A*, 71(3):034310, March 2005. arXiv:quant-ph/0312216, doi:10.1103/PhysRevA.71.034310. 3.4
- [BFS97] Charles H Bennett, Christopher A Fuchs, and John A Smolin. Entanglement-Enhanced Classical Communication on a Noisy Quantum Channel. In O Hirota, A.S. Holevo, and C. Caves, editors, *Quantum communication and quantum measurement*, number 1, pages 79–88. Plenum Press, New York, 1997. arXiv:9611006v1. 3.4
- [BM04] Garry Bowen and Stefano Mancini. Quantum channels with a finite memory. *Physical Review A*, 69(1):012306, January 2004. arXiv:quant-ph/0305010, doi:10.1103/PhysRevA.69.012306. 3.4
- [BPM⁺97] Dik Bouwmeester, Jian-wei Pan, Klaus Mattle, Manfred Eibl, Harald Weinfurter, and Anton Zeilinger. Experimental quantum teleportation. *Nature*, 390:575–579, 1997. doi:10.1038/37539. 5.2.3
- [Bra98] Samuel L. Braunstein. Error Correction for Continuous Quantum Variables. *Physical Review Letters*, 80(18):4084–4087, May 1998. arXiv:quant-ph/9711049, doi:10.1103/PhysRevLett.80.4084. 5.2.2
- [Bra05a] Samuel Braunstein. Squeezing as an irreducible resource. *Physical Review A*, 71(5):055801, May 2005. arXiv:quant-ph/9904002, doi:10.1103/PhysRevA.71.055801. 5.2.2
- [Bra05b] Samuel L Braunstein. Quantum information with continuous variables. *Reviews of Modern Physics*, 77(2):513–577, June 2005. arXiv:quant-ph/0410100, doi:10.1103/RevModPhys.77.513. 1.1, 4, 4.5, 5.1, 5.2.1
- [Bra05c] Sergey Bravyi. Classical capacity of fermionic product channels. (4):1–12, July 2005. arXiv:quant-ph/0507282. 5.3, 5.6.1
- [BRI⁺13] Sergio Boixo, Troels F Rønnow, Sergei V Isakov, Zhihui Wang, David Wecker, Daniel A Lidar, John M Martinis, and Matthias Troyer. Quantum annealing with more than one hundred qubits. (1):20, April 2013. arXiv:1304.4595. 2
- [CC84] B.S. Choi and T.M. Cover. An information-theoretic proof of Burg’s maximum entropy spectrum. *Proceedings of the IEEE*, 72(8):1094–1096, 1984. doi:10.1109/PROC.1984.12981. 2.3.4

- [CCMR05] Nicolas Cerf, Julien Clavareau, Chiara Macchiavello, and Jérémie Roland. Quantum entanglement enhances the capacity of bosonic channels with memory. *Physical Review A*, 72(4):042330, October 2005. [arXiv:quant-ph/0412089](#), [doi:10.1103/PhysRevA.72.042330](#). 1.1, 3.4, 7.4, 7.4.1, 7.4.6, 7.4.7
- [CCRM06] Nicolas J. Cerf, Julien Clavareau, Jérémie Roland, and Chiara Macchiavello. Information Transmission via entangled quantum states in Gaussian channels with memory. *International Journal of Quantum Information*, 04(03):439–452, June 2006. [arXiv:quant-ph/0508197](#), [doi:10.1142/S021974990600189X](#). 1.1, 3.4, 7.4, 7.4.1
- [CD94] Carlton Caves and P. Drummond. Quantum limits on bosonic communication rates. *Reviews of Modern Physics*, 66(2):481–537, April 1994. [doi:10.1103/RevModPhys.66.481](#). 1.1, 5.3, 5.6
- [CGH06] F Caruso, V Giovannetti, and a S Holevo. One-mode bosonic Gaussian channels: a full weak-degradability classification. *New Journal of Physics*, 8(12):310–310, December 2006. [arXiv:quant-ph/0609013](#), [doi:10.1088/1367-2630/8/12/310](#). 5.3.1, 5.3.1, 6.1
- [Cho75] Man-Duen Choi. Completely positive linear maps on complex matrices. *Linear Algebra and its Applications*, 10(3):285–290, June 1975. [doi:10.1016/0024-3795\(75\)90075-0](#). 3.2
- [CIV02] N.J. Cerf, S. Iblisdir, and G. Van Assche. Cloning and cryptography with quantum continuous variables. *The European Physical Journal D - Atomic, Molecular and Optical Physics*, 18(2):211–218, February 2002. [arXiv:quant-ph/0107077](#), [doi:10.1140/epjd/e20020025](#). 5.5
- [CLA01] N. Cerf, M. Lévy, and G. Assche. Quantum distribution of Gaussian keys using squeezed states. *Physical Review A*, 63(5):052311, April 2001. [arXiv:quant-ph/0008058](#), [doi:10.1103/PhysRevA.63.052311](#). 5.5
- [CLP07] Nicolas J Cerf, Gerd Leuchs, and Eugene Polzik, editors. *Quantum Information with Continuous Variables of Atoms and Light*. Imperial College Press, London, 2007. 5.2.3
- [Con13] Wikipedia Contributors. Moore’s law. Wikipedia, The Free Encyclopedia., 2013. URL: http://en.wikipedia.org/wiki/Moore's_law. 3
- [CT05] Thomas M. Cover and Joy A. Thomas. *Elements of Information Theory*. John Wiley and Sons, New Jersey, 2005. 2, 2.1, 2.2, 2.3, 2.3.1, 2.3.4, 5.3.1, 5.3.1
- [Dae07] D. Daems. Entanglement-enhanced transmission of classical information in Pauli channels with memory: Exact solution. *Physical Review*

BIBLIOGRAPHY

- A, 76(1):012310, July 2007. [arXiv:quant-ph/0610165](#), [doi:10.1103/PhysRevA.76.012310](#). 3.4
- [DC01] S.N. Diggavi and T.M. Cover. The worst additive noise under a covariance constraint. *IEEE Transactions on Information Theory*, 47(7):3072–3081, 2001. [doi:10.1109/18.959289](#). 2.3.4, 2.3.4
- [DD07] Nilanjana Datta and Tony C Dorlas. The coding theorem for a class of quantum channels with long-term memory. *Journal of Physics A: Mathematical and Theoretical*, 40(28):8147–8164, July 2007. [arXiv:quant-ph/0610049](#), [doi:10.1088/1751-8113/40/28/S20](#). 3.4
- [DD09] Nilanjana Datta and Tony Dorlas. Classical Capacity of Quantum Channels with General Markovian Correlated Noise. *Journal of Statistical Physics*, 134(5-6):1173–1195, March 2009. [arXiv:0712.0722v1](#), [doi:10.1007/s10955-009-9726-0](#). 3.4
- [DM09] Tony Dorlas and Ciara Morgan. Classical capacity of quantum channels with memory. *Physical Review A*, 79(3):032320, March 2009. [arXiv:0902.2834](#), [doi:10.1103/PhysRevA.79.032320](#). 3.4, 3.4
- [DSS98] David DiVincenzo, Peter Shor, and John Smolin. Quantum-channel capacity of very noisy channels. *Physical Review A*, 57(2):830–839, February 1998. [arXiv:quant-ph/9706061](#), [doi:10.1103/PhysRevA.57.830](#). 3.5
- [EP03] J. Eisert and M. B. Plenio. Introduction to the basics of entanglement theory in continuous-variable systems. *International Journal of Quantum Information*, 01(04):479–506, December 2003. [arXiv:quant-ph/0312071](#), [doi:10.1142/S0219749903000371](#). 5.2.3
- [EPR35] A. Einstein, B. Podolsky, and N. Rosen. Can Quantum-Mechanical Description of Physical Reality Be Considered Complete? *Physical Review*, 47(10):777–780, May 1935. [arXiv:quant-ph/0701001](#), [doi:10.1103/PhysRev.47.777](#). 3.4, 5.1
- [EW05] J Eisert and M M Wolf. Gaussian Quantum Channels. In Nicolas J Cerf, Gerd Leuchs, and Eugene Polzik, editors, *Quantum Information with Continuous Variables of Atoms and Light*, pages 23–42. Imperial College Press, London, May 2005. [arXiv:quant-ph/0505151](#). 1.1, 5.3, 5.6, 5.7, 5.7
- [FCP04] Jaromír Fiurášek, Nicolas Cerf, and Eugene Polzik. Quantum Cloning of a Coherent Light State into an Atomic Quantum Memory. *Physical Review Letters*, 93(18):180501, October 2004. [arXiv:quant-ph/0404054](#), [doi:10.1103/PhysRevLett.93.180501](#). 5.2.2

- [Fiu02] Jaromír Fiurášek. Gaussian Transformations and Distillation of Entangled Gaussian States. *Physical Review Letters*, 89(13):137904, September 2002. [arXiv:quant-ph/0204069](#), [doi:10.1103/PhysRevLett.89.137904](#). C, C
- [FKM09] Motohisa Fukuda, Christopher King, and David Moser. Comments on Hastings’ Additivity Counterexamples. pages 1–38, May 2009. [arXiv:0905.3697](#). 3.4
- [FNW92] M Fannes, B Nachtergaele, and R F Werner. Physics Finitely Correlated States on Quantum Spin Chains. *Communications in Mathematical Physics*, 90:443–490, 1992. 5.4
- [FSB⁺98] A. Furusawa, J. L. Sørensen, S. L. Braunstein, C. A. Fuchs, H. J. Kimble, and E. S. Polzik. Unconditional Quantum Teleportation. *Science*, 282(5389):706–709, October 1998. [doi:10.1126/science.282.5389.706](#). 5.2.3
- [Ful96] W. A. Fuller. *Introduction to statistical time series*. Wiley, New York, 1996. A
- [GGL⁺04a] V Giovannetti, S Guha, S Lloyd, L Maccone, J. Shapiro, and H. Yuen. Classical Capacity of the Lossy Bosonic Channel: The Exact Solution. *Physical Review Letters*, 92(2):027902, January 2004. [arXiv:quant-ph/0308012](#), [doi:10.1103/PhysRevLett.92.027902](#). 1.1, 3.4, 3.4, 5.6, 5.6, 5.6
- [GGL⁺04b] Vittorio Giovannetti, Saikat Guha, Seth Lloyd, Lorenzo Maccone, and Jeffrey Shapiro. Minimum output entropy of bosonic channels: A conjecture. *Physical Review A*, 70(3):032315, September 2004. [arXiv:quant-ph/0404005](#), [doi:10.1103/PhysRevA.70.032315](#). 5.6.1, 5.6.1
- [GI02] Géza Giedke and J. Ignacio Cirac. Characterization of Gaussian operations and distillation of Gaussian states. *Physical Review A*, 66(3):032316, September 2002. [arXiv:quant-ph/0204085](#), [doi:10.1103/PhysRevA.66.032316](#). C, C
- [GLMS13] Vittorio Giovannetti, Seth Lloyd, Lorenzo Maccone, and Jeffrey H Shapiro. Electromagnetic channel capacity for practical purposes. *Nature Photonics*, (1):1–6, August 2013. [arXiv:1210.3300v1](#), [doi:10.1038/nphoton.2013.193](#). 6.4.1, 6.5, 6.5, 6.5
- [GM05] Vittorio Giovannetti and Stefano Mancini. Bosonic memory channels. *Physical Review A*, 71(6):062304, June 2005. [arXiv:quant-ph/0410176](#), [doi:10.1103/PhysRevA.71.062304](#). 3.4
- [GPC13] Raúl García-Patrón and Nicolas J. Cerf. To be published. 2013. 6.4.1, 9.1, 9.2

BIBLIOGRAPHY

- [GPNBL⁺12] Raúl García-Patrón, Carlos Navarrete-Benlloch, Seth Lloyd, Jeffrey H. Shapiro, and Nicolas J. Cerf. Majorization Theory Approach to the Gaussian Channel Minimum Entropy Conjecture. *Physical Review Letters*, 108(11):110505, March 2012. [arXiv:1111.1986](#), [doi:10.1103/PhysRevLett.108.110505](#). 6.1
- [GR80] I.S. Gradshteyn and I.M. Ryzhik. Table of Integrals, Series, and Products. Academic Press, New York, 1980. 7.4.5
- [Gra05] Robert M. Gray. Toeplitz and Circulant Matrices: A Review. *Foundations and Trends® in Communications and Information Theory*, 2(3):155–239, 2005. [doi:10.1561/0100000006](#). A
- [GVW⁺03] Frédéric Grosshans, Gilles Van Assche, Jérôme Wenger, Rosa Brouri, Nicolas J Cerf, and Philippe Grangier. Quantum key distribution using gaussian-modulated coherent states. *Nature*, 421(6920):238–241, January 2003. [doi:10.1038/nature01289](#). 5.2.3, 5.5
- [Has09] M B Hastings. Superadditivity of communication capacity using entangled inputs. *Nature Physics*, 5(4):255–257, March 2009. [doi:10.1038/nphys1224](#). 3.4, 3.4
- [HG12] A S Holevo and V Giovannetti. Quantum channels and their entropic characteristics. *Reports on progress in physics. Physical Society (Great Britain)*, 75(4):046001, April 2012. [arXiv:1202.6480](#), [doi:10.1088/0034-4885/75/4/046001](#). 3.4, 6.4.1
- [Hil00] Mark Hillery. Quantum cryptography with squeezed states. *Physical Review A*, 61(2):022309, January 2000. [arXiv:quant-ph/9909006](#), [doi:10.1103/PhysRevA.61.022309](#). 5.5
- [Hir06] Tohya Hiroshima. Additivity and multiplicativity properties of some Gaussian channels for Gaussian inputs. *Physical Review A*, 73(1):012330, January 2006. [arXiv:quant-ph/0511006](#), [doi:10.1103/PhysRevA.73.012330](#). 5.7, 3, 7.2
- [HJS⁺96] Paul Hausladen, Richard Jozsa, Benjamin Schumacher, Michael Westmoreland, and William Wootters. Classical information capacity of a quantum channel. *Physical Review A*, 54(3):1869–1876, September 1996. [doi:10.1103/PhysRevA.54.1869](#). 1, 3.4
- [HL06] Matthias Heid and Norbert Lütkenhaus. Efficiency of coherent-state quantum cryptography in the presence of loss: Influence of realistic error correction. *Physical Review A*, 73(5):052316, May 2006. [arXiv:quant-ph/0512013](#), [doi:10.1103/PhysRevA.73.052316](#). 5.5

- [Hol73] A S Holevo. Bounds for the Quantity of Information Transmitted by a Quantum Communication Channel. *Probl. Peredachi Inf.*, 9:3–11, 1973. [1](#), [3.3](#)
- [Hol98a] A S Holevo. Quantum coding theorems. *Russian Mathematical Surveys*, 53(6):1295–1331, December 1998. [arXiv:quant-ph/9809023](#), [doi:10.1070/RM1998v053n06ABEH000091](#). [5.1](#), [5.1](#), [6.4.1](#), [6.4.1](#)
- [Hol98b] Alexander S. Holevo. Coding Theorems for Quantum Channels. *Tamagawa University Research Review*, 4:41, September 1998. [arXiv:quant-ph/9809023](#). [B](#)
- [Hol98c] A.S. Holevo. The capacity of the quantum channel with general signal states. *IEEE Transactions on Information Theory*, 44(1):269–273, 1998. [arXiv:quant-ph/9611023](#), [doi:10.1109/18.651037](#). [1](#), [3.4](#)
- [Hol07] A S Holevo. One-mode quantum Gaussian channels. *Problems of Information Transmission*, 43:1–11, 2007. [arXiv:quant-ph/0607051](#). [1.1](#), [5.3.1](#), [5.3.1](#), [5.3.1](#), [6.1](#)
- [Hol08] A S Holevo. Entanglement-breaking channels in infinite dimensions. *Problems of Information Transmission*, 44(3):3–18, 2008. [arXiv:0802.0235](#). [6.1](#), [6.1](#)
- [HS04] A.S. Holevo and M.E. Shirokov. On Shor’s Channel Extension and Constrained Channels. *Communications in Mathematical Physics*, 249(2):1–19, May 2004. [arXiv:quant-ph/0306196](#), [doi:10.1007/s00220-004-1116-5](#). [3.4](#), [6.4.2](#)
- [HSH99] A. Holevo, M Sohma, and O Hirota. Capacity of quantum Gaussian channels. *Physical Review A*, 59(3):1820–1828, March 1999. [doi:10.1103/PhysRevA.59.1820](#). [5.1](#), [5.3.1](#), [5.6](#), [5.6](#), [1](#), [6.4.1](#), [B](#)
- [HW01] A. Holevo and R. Werner. Evaluating capacities of bosonic Gaussian channels. *Physical Review A*, 63(3):032312, February 2001. [arXiv:quant-ph/9912067](#), [doi:10.1103/PhysRevA.63.032312](#). [5.1](#), [5.3](#), [5.3](#), [5.3.1](#), [6.4.1](#)
- [ISS11] J. Solomon Ivan, Krishna Kumar Sabapathy, and R. Simon. Operator-sum representation for bosonic Gaussian channels. *Physical Review A*, 84(4):042311, October 2011. [arXiv:1012.4266](#), [doi:10.1103/PhysRevA.84.042311](#). [5.3.1](#), [6.1](#)
- [Jam72] A. Jamiołkowski. Linear transformations which preserve trace and positive semidefiniteness of operators. *Reports on Mathematical Physics*, 3(4):275–278, December 1972. [doi:10.1016/0034-4877\(72\)90011-0](#). [3.2](#)

BIBLIOGRAPHY

- [JKJL11] Paul Jouguet, Sébastien Kunz-Jacques, and Anthony Leverrier. Long-distance continuous-variable quantum key distribution with a Gaussian modulation. *Physical Review A*, 84(6):062317, December 2011. [arXiv:1110.0100](#), [doi:10.1103/PhysRevA.84.062317](#). 5.5
- [JKJL⁺13] Paul Jouguet, Sébastien Kunz-Jacques, Anthony Leverrier, Philippe Grangier, and Eleni Diamanti. Experimental demonstration of long-distance continuous-variable quantum key distribution. *Nature Photonics*, 7(5):378–381, April 2013. [arXiv:1210.6216](#), [doi:10.1038/nphoton.2013.63](#). 5.5
- [KDC06] E. Karpov, D. Daems, and N. J. Cerf. Entanglement-enhanced classical capacity of quantum communication channels with memory in arbitrary dimensions. *Physical Review A*, 74(3):032320, September 2006. [arXiv:quant-ph/0603286](#), [doi:10.1103/PhysRevA.74.032320](#). 3.4
- [Kin02] Christopher King. Additivity for unital qubit channels. *Journal of Mathematical Physics*, 43(10):4641, 2002. [arXiv:quant-ph/0103156](#), [doi:10.1063/1.1500791](#). 3.4
- [KL10] Pieter Kok and Brendon W. Lovett. *Introduction to Optical Quantum Information Processing*. Cambridge University Press, New York, 2010. 4, 4.5, 5.2.3
- [KM06] V Karimipour and L Memarzadeh. Transition behavior in the capacity of correlated noisy channels in arbitrary dimensions. *Physical Review A*, 74(3):032332, September 2006. [arXiv:quant-ph/0603223](#), [doi:10.1103/PhysRevA.74.032332](#). 3.4
- [KS13] Robert König and Graeme Smith. Classical Capacity of Quantum Thermal Noise Channels to within 1.45 Bits. *Physical Review Letters*, 110(4):040501, January 2013. [arXiv:1205.3409](#), [doi:10.1103/PhysRevLett.110.040501](#). 6.5, 2
- [KSZ91] A Klumper, A Schadschneider, and J Zittartz. Equivalence and solution of anisotropic spin-1 models and generalized t-J fermion models in one dimension. *Journal of Physics A: Mathematical and General*, 24(16):L955–L959, August 1991. [doi:10.1088/0305-4470/24/16/012](#). 5.4
- [KSZ93] A Klümper, A Schadschneider, and J Zittartz. Matrix Product Ground States for One-Dimensional Spin-1 Quantum Antiferromagnets. *European Physics Letters (EPL)*, 24(4):293–297, November 1993. [arXiv:9307028](#), [doi:10.1209/0295-5075/24/4/010](#). 5.4
- [KW05] Dennis Kretschmann and Reinhard Werner. Quantum channels with memory. *Physical Review A*, 72(6):062323, December 2005. [arXiv:quant-ph/0502106](#), [doi:10.1103/PhysRevA.72.062323](#). 3, 1, 3.2.2, 3.4

- [LDTBG05] Jérôme Lodewyck, Thierry Debuisschert, Rosa Tualle-Brouri, and Philippe Grangier. Controlling excess noise in fiber-optics continuous-variable quantum key distribution. *Physical Review A*, 72(5):050303, November 2005. [arXiv:quant-ph/0511104](#), [doi:10.1103/PhysRevA.72.050303](#). 5.2.3
- [LGM⁺09] S Lloyd, V Giovannetti, L Maccone, N J Cerf, S Guha, R. Garcia-Patron, S Mitter, S Pirandola, M B Ruskai, J H Shapiro, and H Yuan. The bosonic minimum output entropy conjecture and Lagrangian minimization. pages 1–6, June 2009. [arXiv:0906.2758](#). 5.6.1
- [LGM10] Cosmo Lupo, Vittorio Giovannetti, and Stefano Mancini. Capacities of Lossy Bosonic Memory Channels. *Physical Review Letters*, 104(3):030501, January 2010. [arXiv:0903.2764](#), [doi:10.1103/PhysRevLett.104.030501](#). 3, 3.4, 7.1, 7.1
- [LMM09] Cosmo Lupo, Laleh Memarzadeh, and Stefano Mancini. Forgetfulness of continuous Markovian quantum channels. *Physical Review A*, 80(4):042328, October 2009. [arXiv:0907.1544](#), [doi:10.1103/PhysRevA.80.042328](#). 3.4, 7.4.6
- [LPM09] Cosmo Lupo, Oleg V Pilyavets, and Stefano Mancini. Capacities of lossy bosonic channel with correlated noise. *New Journal of Physics*, 11(6):063023, June 2009. [arXiv:0901.4969](#), [doi:10.1088/1367-2630/11/6/063023](#). 3.4, 5.6, 6.4.1
- [LS11] M. S. Leifer and Robert W Spekkens. Formulating Quantum Theory as a Causally Neutral Theory of Bayesian Inference. page 43, July 2011. [arXiv:1107.5849](#). 3.2
- [MAE⁺11] Moritz Mehmet, Stefan Ast, Tobias Eberle, Sebastian Steinlechner, Henning Vahlbruch, and Roman Schnabel. Squeezed light at 1550 nm with a quantum noise reduction of 123 dB. *Optics Express*, 19(25):25763, December 2011. [doi:10.1364/OE.19.025763](#). 8.2
- [Man06] Stefano Mancini. Models for Quantum Memory Channels. *Journal of Physics: Conference Series*, 36:121–125, April 2006. [doi:10.1088/1742-6596/36/1/019](#). 3, 3.2.2
- [Moo65] Gordon E Moore. Cramming more components onto integrated circuits. *Electronics Magazineics*, 38(8):4, 1965. 3
- [MP02] Chiara Macchiavello and G. Palma. Entanglement-enhanced information transmission over a quantum channel with correlated noise. *Physical Review A*, 65(5):050301, April 2002. [arXiv:quant-ph/0107052](#), [doi:10.1103/PhysRevA.65.050301](#). 3.4

BIBLIOGRAPHY

- [MPV04] Chiara Macchiavello, G. Palma, and S. Virmani. Transition behavior in the channel capacity of two-qubit channels with memory. *Physical Review A*, 69(1):010303, January 2004. [doi:10.1103/PhysRevA.69.010303](https://doi.org/10.1103/PhysRevA.69.010303). 3.4
- [NC00] Michael A. Nielsen and Isaac L. Chuang. *Quantum Computation and Quantum Information*. Cambridge University Press, Cambridge, 2000. 3, 5.2.3
- [NH03] Ryo Namiki and Takuya Hirano. Security of quantum cryptography using balanced homodyne detection. *Physical Review A*, 67(2):022308, February 2003. [arXiv:quant-ph/0205191](https://arxiv.org/abs/quant-ph/0205191), [doi:10.1103/PhysRevA.67.022308](https://doi.org/10.1103/PhysRevA.67.022308). 5.5
- [NH04] Ryo Namiki and Takuya Hirano. Practical Limitation for Continuous-Variable Quantum Cryptography using Coherent States. *Physical Review Letters*, 92(11):117901, March 2004. [arXiv:quant-ph/0403115](https://arxiv.org/abs/quant-ph/0403115), [doi:10.1103/PhysRevLett.92.117901](https://doi.org/10.1103/PhysRevLett.92.117901). 5.5
- [PGVWC07] D Perez-Garcia, F Verstraete, M M Wolf, and J I Cirac. Matrix product state representations. *Quantum Information and Computation*, 7:401, 2007. [arXiv:quant-ph/0608197v2](https://arxiv.org/abs/quant-ph/0608197v2). 5.4
- [PLM12] Oleg V. Pilyavets, Cosmo Lupo, and Stefano Mancini. Methods for Estimating Capacities and Rates of Gaussian Quantum Channels. *IEEE Transactions on Information Theory*, 58(9):6126–6164, September 2012. [arXiv:0907.1532](https://arxiv.org/abs/0907.1532), [doi:10.1109/TIT.2012.2191475](https://doi.org/10.1109/TIT.2012.2191475). 3.4, 6.4, 6.4, 6.4.5, 6.4.6, 6.4.6
- [PZM08] Oleg Pilyavets, Vadim Zborovskii, and Stefano Mancini. Lossy bosonic quantum channel with non-Markovian memory. *Physical Review A*, 77(5):052324, May 2008. [arXiv:0802.3397](https://arxiv.org/abs/0802.3397), [doi:10.1103/PhysRevA.77.052324](https://doi.org/10.1103/PhysRevA.77.052324). 3.4, 8.2
- [Ral99] T. Ralph. Continuous variable quantum cryptography. *Physical Review A*, 61(1):010303, December 1999. [doi:10.1103/PhysRevA.61.010303](https://doi.org/10.1103/PhysRevA.61.010303). 5.5
- [Rei00] M. D. Reid. Quantum cryptography with a predetermined key, using continuous-variable Einstein-Podolsky-Rosen correlations. *Physical Review A*, 62(6):062308, November 2000. [arXiv:quant-ph/9909030](https://arxiv.org/abs/quant-ph/9909030), [doi:10.1103/PhysRevA.62.062308](https://doi.org/10.1103/PhysRevA.62.062308). 5.5
- [RSA78] R L Rivest, A Shamir, and L Adleman. A method for obtaining digital signatures and public-key cryptosystems. *Communications of the ACM*, 21(2):120–126, February 1978. [doi:10.1145/359340.359342](https://doi.org/10.1145/359340.359342). 1
- [SCS99] R. Simon, S. Chaturvedi, and V. Srinivasan. Congruences and canonical forms for a positive matrix: Application to the Schweinler–Wigner

- extremum principle. *Journal of Mathematical Physics*, 40(7):3632, 1999. [arXiv:9811003](#), [doi:10.1063/1.532913](#). 5.2.1
- [Sha48] Claude E. Shannon. A Mathematical Theory of Communication. *The Bell System Technical Journal*, 27:379–423, 623–656, 1948. 1, 2
- [Sho94] P.W. Shor. Algorithms for quantum computation: discrete logarithms and factoring. In *Proceedings 35th Annual Symposium on Foundations of Computer Science*, pages 124–134. IEEE Comput. Soc. Press, 1994. [doi:10.1109/SFCS.1994.365700](#). 1
- [Sho02] Peter W. Shor. Additivity of the classical capacity of entanglement-breaking quantum channels. *Journal of Mathematical Physics*, 43(9):4334, 2002. [arXiv:quant-ph/0201149](#), [doi:10.1063/1.1498000](#). 3.4, 3.4
- [SHW⁺07] C. Schön, K Hammerer, M. Wolf, J. Cirac, and E Solano. Sequential generation of matrix-product states in cavity QED. *Physical Review A*, 75(3):032311, March 2007. [arXiv:quant-ph/0612101](#), [doi:10.1103/PhysRevA.75.032311](#). 5.4
- [SL10] Denis Sych and Gerd Leuchs. Coherent state quantum key distribution with multi letter phase-shift keying. *New Journal of Physics*, 12(5):053019, May 2010. [arXiv:0902.1895](#), [doi:10.1088/1367-2630/12/5/053019](#). 5.5
- [Smi10] Graeme Smith. Quantum Channel Capacities. In *Information Theory Workshop (ITW)*, page 1. Proc. of IEEE, 2010. [arXiv:1007.2855v1](#). 3.4
- [SS] P W Shor and J A Smolin. Quantum Error-Correcting Codes Need Not Completely Reveal the Error Syndrome. pages 1–13. [arXiv:quant-ph/9604006v2](#). 3.5
- [SS07] Graeme Smith and John Smolin. Degenerate Quantum Codes for Pauli Channels. *Physical Review Letters*, 98(3):030501, January 2007. [arXiv:quant-ph/0604107](#), [doi:10.1103/PhysRevLett.98.030501](#). 3.5
- [SS13] John A Smolin and Graeme Smith. Classical signature of quantum annealing. page 8, May 2013. [arXiv:1305.4904](#). 2
- [SSV⁺05] C. Schön, E Solano, F Verstraete, J. Cirac, and M. Wolf. Sequential Generation of Entangled Multiqubit States. *Physical Review Letters*, 95(11):110503, September 2005. [arXiv:quant-ph/0501096](#), [doi:10.1103/PhysRevLett.95.110503](#). 5.4
- [ST91] Bahaa E. A. Saleh and Malvin Carl Teich. *Fundamentals of Photonics*, volume 5. John Wiley and Sons, New York, 1991. 4.4.4

BIBLIOGRAPHY

- [Ste01] Stefan M Stefanov. Convex Separable Minimization Subject to Bounded Variables. *Computational Optimization and Applications*, 18:27–48, 2001. [7.3](#)
- [SW97] Benjamin Schumacher and Michael Westmoreland. Sending classical information via noisy quantum channels. *Physical Review A*, 56(1):131–138, July 1997. [doi:10.1103/PhysRevA.56.131](#). [1](#), [3.4](#)
- [SWC08] Norbert Schuch, Michael M Wolf, and J Ignacio Cirac. Gaussian Matrix Product States. In Marie Ericsson and Simone Montangero, editors, *Proceedings on the conference on Quantum information and many body quantum systems*, page 129, Pisa, 2008. Edizioni della Normale. [arXiv:1201.3945](#). [1.1](#), [5.4](#), [8.2](#), [8.3](#)
- [SZ99] Hans Von Storch and Francis W Zwiers. *Statistical analysis in climate research*. Cambridge University Press, Cambridge, 1999. [2.3.4](#), [2.3.4](#), [A](#)
- [Vai94] Lev Vaidman. Teleportation of quantum states. *Physical Review A*, 49(2):1473–1476, February 1994. [arXiv:9305062](#), [doi:10.1103/PhysRevA.49.1473](#). [5.2.3](#)
- [Vid03] Guifré Vidal. Efficient Classical Simulation of Slightly Entangled Quantum Computations. *Physical Review Letters*, 91(14):147902, October 2003. [arXiv:quant-ph/0301063](#), [doi:10.1103/PhysRevLett.91.147902](#). [5.4](#)
- [VMC⁺08] Henning Vahlbruch, Moritz Mehmet, Simon Chelkowski, Boris Hage, Alexander Franzen, Nico Lastzka, Stefan Goßler, Karsten Danzmann, and Roman Schnabel. Observation of Squeezed Light with 10-dB Quantum-Noise Reduction. *Physical Review Letters*, 100(3):033602, January 2008. [arXiv:0706.1431](#), [doi:10.1103/PhysRevLett.100.033602](#). [8.2](#)
- [WGK⁺04] M. M. Wolf, G. Giedke, O. Krüger, R. F. Werner, and J. I. Cirac. Gaussian entanglement of formation. *Physical Review A*, 69(5):052320, May 2004. [arXiv:quant-ph/0306177](#), [doi:10.1103/PhysRevA.69.052320](#). [5.7](#), [5.7](#)
- [WHTH07] X.-B. Wang, T. Hiroshima, A. Tomita, and M. Hayashi. Quantum information with Gaussian states. *Physics Reports*, 448(1-4):1–111, August 2007. [arXiv:0801.4604](#), [doi:10.1016/j.physrep.2007.04.005](#). [5.3](#)
- [Wie83] Stephen Wiesner. Conjugate Coding. *ACM Sigact News*, 15:78–88, 1983. [1](#)
- [WM95] D. F. Walls and G. J. Milburn. *Quantum Optics*. Springer, 1995. [4](#)
- [WPGP⁺12] Christian Weedbrook, Stefano Pirandola, Raúl García-Patrón, Nicolas J. Cerf, Timothy C. Ralph, Jeffrey H. Shapiro, and Seth Lloyd. Gaussian quantum information. *Reviews of Modern Physics*, 84(2):621–669, May

BIBLIOGRAPHY

2012. [arXiv:1110.3234](#), [doi:10.1103/RevModPhys.84.621](#). 1.1, 5.1, 5.1, 5.2.1, 5.3
- [YO93] Horace Yuen and Masanao Ozawa. Ultimate information carrying limit of quantum systems. *Physical Review Letters*, 70(4):363–366, January 1993. [doi:10.1103/PhysRevLett.70.363](#). 5.6
- [ZVB04] Alessandro Zavatta, Silvia Viciani, and Marco Bellini. Tomographic reconstruction of the single-photon Fock state by high-frequency homodyne detection. *Physical Review A*, 70(5):053821, November 2004. [arXiv:quant-ph/0406090v1](#), [doi:10.1103/PhysRevA.70.053821](#). 5.2.3

Index

- Beamsplitter, 42
 - transformation, 53
- Bloch-Messiah decomposition, 53
- Canonical decomposition, 65
- Capacity
 - classical, 31, 73
 - Gaussian, 76
 - classical limit, 101, 171
 - classical signal, 137
 - multi-mode, 148, 157, 159, 164
 - one-mode, 98, 102, 111
 - single-quadrature classical noise, 134
 - one-shot classical, 30, 73
 - quantum, 33
 - Shannon, 12
- Channel
 - classical
 - Gauss-Markov, 17
 - Gaussian, 13
 - quantum, 26
 - entanglement-breaking, 32
 - Gauss-Markov, 160
 - Gaussian, *see* Gaussian channel
 - memory, 28
 - memoryless, 28
- Choi-Jamiolkowski isomorphism, 26
- Coherent state, 39, 49
- Conjecture
 - Holevo-Werner, 100
 - minimum output entropy, 75
- Displacement operator, 39, 43
- Entropy
 - Shannon, 9
 - conditional, 10
 - joint, 9
 - von Neumann, 24
 - conditional, 24
 - joint, 24
- EPR-state, 51
- Fock state, 38
- Gauss-Markov
 - process, 16
 - Shannon capacity, 19
- Gaussian channel, 62
 - multi-mode memory, 68, 145
 - one-mode, 64
 - canonical decomposition, 65
 - classical signal, 66, 137
 - entanglement breaking, 86
 - fiducial, 86
 - fiducial decomposition, 88, 93
 - general thermal channel, 83
 - input energy threshold, 98
 - single-quadrature classical noise, 67, 134
 - thermal amplification, 64
 - thermal classical additive noise, 65
 - thermal lossy, 64
 - thermal phase-conjugating, 65
- Gaussian operation
 - beamsplitter, 53
 - channels, *see* Gaussian channels
 - CV-CNOT gate, 56
 - displacement, 53
 - one-mode squeezer, 53
 - rotation, 52
 - two-mode squeezer, 55
 - unitary, 51

- Gaussian state, 47
 - coherent state, 49
 - matrix-product, 70, 177
 - squeezed state, 49
 - thermal state, 50
 - vacuum, 47
- Heterodyne detection, 60
- Holevo bound, 30
- Homodyne detection, 59
- Mutual information, 10
- Number of photons
 - mean, 50
 - thermal, 50
- Partial measurement, 57
- Partial trace, 25, 57
- Phase shift, 41, 52
- Quadrature operators, 37
- Quantum teleportation, 60
- Rate
 - coherent, 149, 186
 - Gaussian matrix-product state, 183, 184
- Squeezed state, 40, 44, 49
- Stinespring dilation, 26
- Symplectic transformation, 51
- Thermal equilibrium, 121, 158, 159
- Two-mode squeezed vacuum, 51
- Water-filling solution
 - classical, 14, 149
 - quantum, 97, 120
 - global, 147
- Wigner function, 44
 - Gaussian state, 47

